Impact of the Stiffness Characteristics of Wrapped Composite Joints on Eigenfrequencies of Wind Turbine Jacket Support Structures

Paul Mako

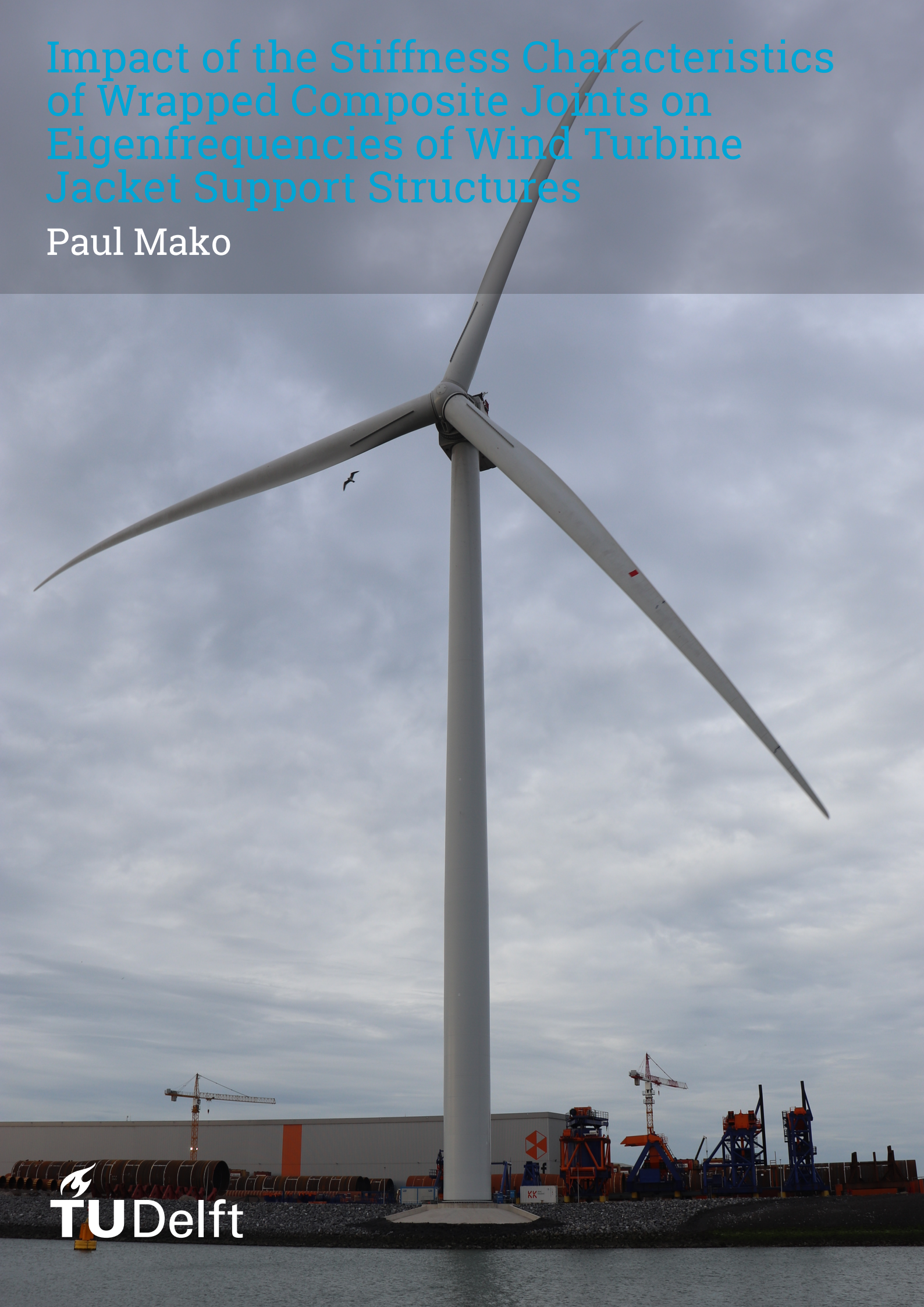

TU Delft

Impact of the Stiffness Characteristics of Wrapped Composite Joints on Eigenfrequencies of Wind Turbine Jacket Support Structures

by

Paul Mako

Student Number: 5046661

Project Duration: September, 2020 - September, 2021

Thesis Committee: Dr. M. (Marko) Pavlović, TU Delft CEG (Steel and Composite), Chair
Dr. ir. P. (Pim) van der Male, TU Delft CEG (Offshore Wind), Supervisor
Dr. M. (Maxim) Segeren, TU Delft CEG (Offshore Wind), Supervisor
Weikang Feng, TU Delft CEG (Steel and Composite), Daily Supervisor

Institution: Delft University of Technology

Place: Faculty of Civil Engineering, Delft

Cover Image: GE Haliade-X Wind Turbine, Maasvlakte 2, Photograph taken by Author, February 19th, 2021

TU Delft

Preface

It feels surreal to have finished. The thesis has been a part of my life for over a year. Through working on it I have learned a lot about the subject matter, but also I have learned a lot about myself and the people I have in my life. I know that I am a flawed man who, without the help of many, would not have completed this thesis.

I want to give a sincere thank you to my graduation chair, Marko Pavlović. You gave of your wisdom freely throughout the project, and you fostered within me a desire to seek for greater understanding. For this, I am greatly in your debt as your student and mentee.

Along with Marko, I would like to thank the entire graduation committee, my daily supervisor, Weikang Feng, and my other committee members, Pim van der Male, and Maxim Segeren. You were all so gracious in your provision of guidance and support throughout the thesis process. This was especially evident when times were difficult for me. I had many peculiar circumstances with my project including all things related to Covid-19, moving between countries, and starting a new job. As a committee, you were all patient with me, and were quick to encourage me to continue to work to create a project that represented the best of my ability. So, again, thank you.

No thesis student is able to complete his or her work without the help of friends and family. I want to sincerely thank all of my friends in the Netherlands and the United States who supported me and walked alongside me as I ventured on this journey. There are too many people to name, but you know who you all are. Your love and encouragement will be cherished. To my family, thank you for listening to me vent all of my frustrations and worries throughout my years in Delft. You believed in me even when I doubted. Thank you for your faithfulness and your unwavering support.

Most importantly, I dedicate this thesis to the loving God who sustained me in all ways and at all times during the thesis project. This piece of scripture has encouraged me many times over the course of the last year:

> The Lord is my shepherd,
> I lack nothing.
> He takes me to lush pastures,
> he leads me to refreshing water.
> He restores my strength.
> He leads me down the right paths
> for the sake of his reputation.
> Even when I must walk through the darkest valley,
> I fear no danger,
> for you are with me;
> your rod and your staff reassure me.
>
> Psalm 23 1:4 [NET]

Thank you to everyone who I know and would call a loved one. This thesis is mostly the product of your efforts to keep me encouraged, loved, and able to work. I am forever grateful.

Paul Mako
Delft, January 2022

Summary

This report investigates the influence of joint stiffness on the eigenfrequencies of offshore wind turbine supporting jacket structures. The joint is investigated individually, within the context of a jacket structure, and within the context of the entire offshore wind turbine structure. These analyses were specifically conducted for the case of a 10MW wind turbine jacket support structure. Eigenfrequencies of support structures for larger wind turbines are respectively lower than their counterparts which support smaller wind turbines. This causes issues to arise with overlap of the wave loading spectra and the lower eigenmodes of the structure. Due to this, it is of interest to be able to model the jacket structure with high accuracy and provide joints with sufficient stiffness that can accommodate the higher joint loads arising from the larger wind turbine.

This report aims to present an analysis method that can represent the joints of jacket support structures for offshore wind turbines with high fidelity while also ensuring low computational cost during the analyses. The joint stiffness is captured through an implementation of joint submodelling by applying the Craig-Bampton reduction technique. Along with this, the report serves to provide a comparison of innovative wrapped composite joints and traditional welded joints when applied to a 10MW wind turbine. The wrapped composite joint was developed by Dr. Marko Pavlović at the Delft University of Technology, and it was investigated due to its superior fatigue performance compared to welded joint alternatives.

The verification of the joint submodelling technique was done through conducting a natural frequency analysis of the different joint types, and through conducting a natural frequency analysis of the OC4 jacket. It was found that when analysing the two joint alternatives independently, the eigenmodes were of a similar shape, and the eigenfrequencies were of similar magnitude with the largest percent change between the two models found as 27.3%. When analysing the OC4 jackets with the joints applied, the percent change between the model with rigid joints and the model with wrapped joint submodels was found to be within the range of 2.1-3.7% for the first ten eigenfrequencies.

The joint submodelling technique was then applied to the context of a 10MW wind turbine jacket support structure. Two sets of analyses were conducted: the jacket analysed by itself, and the jacket analysed along with the tower, turbine, and piles (to be referred to as the "offshore wind turbine"). Natural frequency analyses were conducted for the jacket and for the offshore wind turbine for the different joint types. It was found that for the jacket and for the entire offshore wind turbine, the models with welded joints had the lowest natural frequencies, the models with wrapped composite joints had the second lowest natural frequencies, and the models with rigid joints had the highest natural frequencies when compared to their respective counterparts.

There were varying differences between the different models for the jacket and for the entire offshore wind turbine. The differences between the jacket models were greater than the differences found between the offshore wind turbine models. For the case of the jacket, when comparing the jacket modelled with rigid joints and the jacket modelled with wrapped composite joint submodels, the differences for the lower modes are smaller than the differences for the higher modes with an average change of 8.8% and 10.5% respectively, and a maximum change of 14.4% and 15.1% respectively. For the case of the entire offshore wind turbine, when comparing the offshore wind turbine modelled with rigid joints and the model with wrapped composite joints, the average percent change for the higher modes was 3.5% with a maximum of 9% for the first 20 modes. For the lower modes, the average percent change was 0.3% with a maximum of 1%.

Several limitations exist for the results presented during the course of the report. For results related to the joint submodels, the results should be limited to the global implications of the modelled joint stiffness for the jacket substructure. Local failure modes are not captured by the employed modelling

technique. Also, the soil stiffness, transition piece, RNA mass, and turbine blades were not modelled with a high degree of accuracy for the 10MW turbine. Due to this, it is only valid to draw conclusions from comparisons between the models with different joint submodels not when comparing the 10MW jacket modelled in Abaqus to the jacket shown in the INNWIND.EU report.

In conclusion, it was found that both the application of the wrapped composite joints and the application of the analysis method of submodelling joints of the jacket are beneficial for solving issues related to the construction of jacket support structures for large wind turbines.

Contents

Nomenclature

Abbreviations

Abbreviation	Definition
FRP	Fibre Reinforced Polymer
OWT	Offshore Wind Turbine
JSS	Jacket Support Structure
SE	Superelement
FE	Finite Element
FEA	Finite Element Analysis
FEM	Finite Element Method
GFRP	Glass Fibre-Reinforced Polymer
CHS	Circular Hollow Section
HSS	Hot Spot Stress
SCF	Stress Concentration Factor
SLS	Serviceability Limit State
ULS	Ultimate Limit State

Symbols

Symbol	Definition	Unit
v	Velocity	$[m/s]$
a	Acceleration	$[m/s^2]$
M	Mass Matrix	$[kg]$
K	Stiffness Matrix	$[N/m]$
C	Damping Matrix	$[N*s/m]$
ρ	Density	$[kg/m^3]$
ω_n	Natural Frequency	$[rad/s]$

List of Figures

List of Tables

I

Research Overview

1

Research Proposal

1.1. Introduction

Within the construction industry, specifically in the case of the structural engineering sector, there are often many drivers for why things are made. Whether that is a bridge connecting two cities and strengthening the transportation infrastructure, a residential building that functions as a home for hundreds of people, or any other useful structure that you can think of, there is always a reason why a structure is made. Additionally, there are many factors that influence how structures are made. Whether there are short deadlines, sustainability requirements, or fiscal constraints, all of these things lead to design choices that influence the creation of a structure.

This thesis report is specifically focused on structures within the context of the offshore wind industry. These structures are designed to support a wind turbine for a long service life while being subjected to harsh environmental conditions. Why these structures are built is self-evident. They generate power with a relatively low environmental impact when compared to other energy sources such as coal, oil, gas, and even other renewables. Due to the complex design scenarios associated with these structures, *how they are built* is often a better question. Because of the previously mentioned issues related to the harsh environmental conditions that offshore wind turbines experience, it is difficult to build these structures in a way that allows them to last for a long time. These structures are often susceptible to fatigue damage, which traditionally functions as the controlling load case. With the support structure being submerged in water, there is the requirement to use welded connections due to the likelihood of rust on bolted connections. Unfortunately, welded connections perform poorly in fatigue.

Promisingly, in previous research, the innovative wrapped composite joints developed by M. Pavlović offer a high performing alternative to traditional welded steel joints when considering common governing load cases for wind turbine structures (cyclic loads). The joints have been found to offer sufficient static resistance to allow the steel members to yield in case of failure. Even with a reduction of 40% of stiffness due to the fatigue loading, the joint is able to maintain a constant static resistance. In other research projects under the supervision of M. Pavlović, it was found that when applying wrapped composite joints to jacket support structures (JSS) for offshore wind turbines (OWT), many benefits were found. Because of the superior fatigue resistance, the members were now governed by buckling failure modes. This allowed smaller diameters and thinner members when compared to the welded alternative. The weight reduction for the case of a 5MW turbine was approximately 60%. This thesis project is concerned with the application of wrapped composite joints for offshore wind turbine jacket support structures because of these previous findings.

The field of wind energy is constantly pursuing bigger, more efficient, and more sustainable wind turbines. This thesis project is especially concerned with the application of wrapped composite joints to a jacket support structure for a large wind turbine (10MW). With the wind energy industry attempting to

make bigger turbines, the support structures for these turbines need to be designed to accommodate these larger turbines. The required material mass for a jacket support structure scales linearly with the depth of the shore. This is unlike the design alternative of a monopile support structure which mass scales quadratically with the depth of the shore in an offshore environment. Thus, due to cost restrictions, it is proposed that jacket support structures will likely be the preferred choice for the industry going forward for the cases of larger turbines and deeper waters.

When designing jacket support structures that are supporting large turbines, the need for accurate design methods is essential. Offshore wind turbine support structures are designed so that the first natural frequency lies within a certain range, called the ”soft-stiff frequency range”, which is between the 1P and 3P frequency of the turbine. With larger turbines, this frequency range is shifted to the left and contracts in magnitude. This is an issue because the frequency range then overlaps with the wave load spectrum, and the optimal design range is smaller. Both of these effects necessitate a higher degree of accuracy in the design phase. One promising method that provides this is through applying submodelling techniques when modelling the joints of the jacket support structure instead of modelling the joint through traditional beam models with local joint flexibility equations. Submodeling of the joint allows the joints to deform accurately, while also keeping the computational cost of the analysis low.

In summary, there is a strong demand for sustainable sources of energy. Offshore wind energy is a promising source of energy due to its environmental profile compared to other energy sources. The supporting structures for these turbines are difficult to analyse due to their nonlinear behaviour and harsh environmental conditions, and have been shown to perform poorly in fatigue with traditional construction methods. It is proposed that the fatigue life of jacket support structures can be greatly increased while also reducing the mass of steel required when applying innovative wrapped composite joints. It has also been proposed that when analysing jacket support structures, using the submodelling approach for the joints, the computational cost is kept low, while the accuracy of the numerical simulations is similar to a level equivalent to a shell model. Therefore, to best combine these ideas and validate them, it is desirable to analyse a jacket support structure with wrapped composite joints using the submodelling technique for a large offshore wind turbine (10MW).

1.2. Research question

When considering the application of the wrapped composite joint to the specific context of a jacket support structure for a 10MW offshore wind turbine, there are several important research questions to investigate. Due to the larger size of the wind turbine, the jacket structure’s tubular sections will have to be larger in diameter and thicker than the previously analysed members of the jacket for the 5MW turbine. It is desirable to know whether the wrapped composite joints will be a feasible option when compared to the welded alternative for these structures when considering issues of scale. Moreover, it is especially interesting to consider the effect of joint flexibility when analysing the jacket structure. This will further advance the argument for the benefits of applying the wrapped composite joint. Therefore, in summary, these areas of interest yield the following main research question for the thesis project:

“When considering stiffness characteristics of wrapped composite joints, what is the impact on the overall dynamic behaviour of a 10MW wind turbine jacket support structure?”

This research question is then further elaborated with the following subquestions:

- *What is the best way to calculate and represent the stiffness of the composite joint?*
- *How can the stiffness characteristics of the wrapped composite joint be implemented into the structural analysis of a jacket?*
- *What is the impact of joint characteristics on the eigenfrequencies of the jacket substructure?*
- *What is the influence of the joint characteristics of the jacket within the context of the entire offshore wind turbine (including piles, soil, tower, and wind turbine)?*

1.3. Report Structure

This thesis report serves to answer the previously stated research questions. The report is broken into three parts. Part I serves to motivate the basis for the research project with respect to the main research question and subquestions, along with providing an overview of the relevant research fields in the form of a literature study. Chapter 1 provides the motivation for the research questions and the questions themselves. In chapter 2, the previously mentioned relevant research fields will be presented and related to the research questions. These areas of research include fibre-reinforced polymer and its application to the wrapped composite joint, offshore wind turbine construction with a specific focus on jacket support structures, and the finite element method specifically focusing on the submodelling technique. An overview of the state-of-the-art for these research fields will be presented, along with links to the previously mentioned research questions.

In part II, the employed modelling strategy used to answer the research questions will be elaborated and verified. The purpose of this part of the report is to form the basis of the argument that the solution method proposed in this report can be applied to a problem with a context similar to the verification case. This part will be broken up into two chapters. In chapter 3, the solution method will be presented along with an overview of the analysis tools that are used in the project supported by the rationale for their use. In chapter 4, the steps taken to verify the modelling strategy against existing solution methods will be presented. This primarily entails verifying the original solution method used in this project with the work of another student previously under the supervision of Marko Pavlović using a more traditional solution method. The verification steps will be applied for the case of the 5MW OC4 jacket.

In part III, the solution method applied in part II will then be applied to a case study for a jacket support structure of a 10MW turbine. The chosen case study is the 10MW INNWIND.EU project which is a successor of the UpWind project. In the report, the fourth work package (WP4) was concerned with offshore support structures, and in this work package the main goal was to deliver an innovative jacket design for turbines of 10-20MW size. The research goal of the INNWIND.EU project aligns well with the purpose of this thesis report, which is why it was chosen as the basis for the application of the solution method. A brief overview of the case study and results from applying the previously proposed analysis method will be provided in chapter 5.

In part IV, the contribution of the thesis project will be summarised. This will be broken up into two parts. In chapter 6, there will be a discussion of the results of the verification process held in part II and the results of the case study held in part III. Chapter 7 will contain the conclusions of the thesis report along with recommendations for future work.

2

Literature

2.1. Introduction

This thesis project is concerned with several research fields. The first of these is concerned with the novel structural material of **Fibre Reinforced Polymer** (**FRP**), specifically within the context of its application in a wrapped composite joint. The second major research field is **offshore wind turbine** (**OWT**) construction, specifically in the context of supporting larger wind turbines (10MW+) with a **jacket support structure** (**JSS**). The third major research field is concerned with **Finite Element Method** (**FEM**) techniques, specifically focused on the application of **superelements** (**SE**) and submodels through the art of substructuring. In this literature review chapter, these research fields will be introduced and aspects that are pertinent to the thesis process will be elaborated. They will be introduced in the order presented in this paragraph.

2.2. Fibre-Reinforced Polymer (FRP)

In this section, the structural material FRP will be introduced with a specific focus on why it is significant in the field of structural engineering broken up into subsections. In these subsections, there will be a brief introduction of other structural engineering materials highlighting some key advantages and drawbacks of their use, a description of FRP's material characteristics and production processes, and an introduction into the specific application of wrapped composite joints.

2.2.1. Overview of structural engineering materials

The most conventional structural materials used in the civil engineering industry are steel and concrete. These traditional materials are ubiquitous and are found in all areas of the construction industry. This is due to many reasons besides solely tradition. Steel is a dense, high-strength material with isotropic material properties, lending it to be perceived as a reliable and trustworthy building material. Concrete, on the other hand, is a building material with a low weight and high compressive strength. Unlike steel, concrete is anisotropic due to its chemical makeup of cement, water, aggregate, and other additives. These two building materials are often combined to make reinforced concrete, and in harmony they can rely on each other's material advantages.

Despite the obvious advantages of these materials, they both give rise to significant consequences when using them in design applications. Concrete on its own has some distinct deficiencies for building purposes: it has a low tensile strength and a low strain at fracture. This is caused by concrete's propensity to hold microcracks at its conception. Additives such as fly ash and slag are the main combatants used against these microcracks because they increase the density of the concrete by filling

these microcracks (Narayanan & Mota, 2015). Similarly, steel has the significant drawback of corrosion from rust. This can be mitigated with the application of coatings, but applying coatings is costly and not always a permanent solution

Besides the disadvantages from a performance perspective, both concrete and steel have issues with respect to sustainability. Concrete is not a recyclable material, and in a best-case scenario it can be downcycled into a lower grade material after its first service life. It is also energy and water intensive to make. This is especially so for higher-strength concretes that require the use of more cement, which is the most energy intensive and toxic material in the composition of concrete. In addition, when considering aspects of longevity, concrete cracks, which reduces the service life.

Fortunately, steel can be recycled. This is an inherent advantage of using steel in construction. With that, it is important to to note that it is energy intensive to make at its conception, and if not maintained well and the rust levels kept low, then the service life of the steel will also be poor. This material is also costly and if not used in an intelligent way considering circular design methods, some of the structural steel will not be able to be reused and some may not even be able to be recycled (think for example rusted steel rebar embedded in concrete). Steel and concrete most likely will continue to be used in the construction industry, but the assumption that they are the best choice for every project will need to be addressed. They are often a costly choice regarding environmental impact (Thomas et al., 2017).

To avoid the potential negative impacts of climate change, there has been a shift towards more sustainable construction. Due to this, there has been an ongoing investigation within the field of civil engineering into other suitable and sustainable construction materials. One of these materials is FRP, which holds many advantages for structural engineering applications and is interchangeable with steel and concrete in many structural applications. Its advantages lie in its high strength to weight ratio, its customisable material properties that can yield excellent bending strength, and its ability to be shaped into any form. Along with this, using more sustainable materials, like FRP, will pay dividends, including emitting less greenhouse gases, releasing less toxic substances into the environment, using less water, and generating less waste.

2.2.2. FRP material overview

In its name, FRP indicates its composite nature. Essentially, FRP is a material that is composed of fibres that lie in resin. In many ways, FRP is analogous to timber in its chemical and mechanical makeup from the perspective of the structural engineer. The FRP fibres (conventionally glass or carbon) act similarly to the cellulose fibres in timber. These fibres carry the load along their longitudinal axis and have high tensile strength. The FRP resin acts similarly to the lignin in timber by keeping the fibres in their original position and carrying loads not aligned with the longitudinal axis of the fibres. This combination of the fibres and the resin lends FRP to be an anisotropic material similar to timber. Due to its composite nature, it can be shaped to fulfil any designer's desire and can be customised to have strength and stiffness properties that can fulfil the requirements of many design scenarios.

2.2.3. Material Composition

FRP can be made with many types of fibres, resins, and processes. With respect to fibres, there are three main types: glass, carbon, and aramid. Of the three main fibre types, glass is the most widely used, with a good combination of relatively high strength and stiffness, and low cost. Carbon fibres are the stiffest and the strongest fibres, but are prohibitively expensive in most cases. Aramid fibres lie in between the two other fibre types with respect to strength and stiffness. Unfortunately, aramid fibres are highly susceptible to moisture degradation. Considering that this project is concerned with the applications of FRP material in submerged water environments, there will be no further investigation into aramid fibres.

With respect to resin types, they are categorised as either thermoplastic or thermoset resins. The two differ in how they respond to heat. Thermoplastic resins are affected by temperature fluctuations and

will respond to an increase in temperature with a reduction in stiffness. As can be intuitively assumed, with the thermoset resin, below a certain threshold temperature known as the **Glass Transition Temperature** ($\mathbf{T_g}$), the stiffness properties of the resin remain unchanged. This is due to the fact that thermoset resins are cured, and after the curing process they have "set". After setting, the monomers that makeup the resin take on a rigid cross-linked form with a permanent shape. Due to the more consistent and reliable material properties of the thermoset resins, they are more widely used in the civil engineering practice. Due to this, only the applications of FRP with thermoset resins will be focused on in this thesis report henceforth.

In figure 2.1, you will see two subfigures representing some of the concepts previously mentioned. A stress-strain relationship for the individual components of FRP is shown in the subfigure to the left, and to the right is a representation of the fundamental difference between thermoset and thermoplastic resins. Referencing the left subfigure, it is important to notice the difference in stiffness between the fibre and the resin. Again, it is analogous to lignin and cellulose found in timber. The fibres are much stiffer with higher tensile strength, but they are relatively brittle when compared to the resin which has a lower maximum stress but experiences a more ductile failure mode. In the right subfigure, you can see the extra cross-links that are formed in the thermoset resins after processing. These crosslinks are a significant factor leading to thermosets being the most widely used resin in structural engineering applications of FRP.

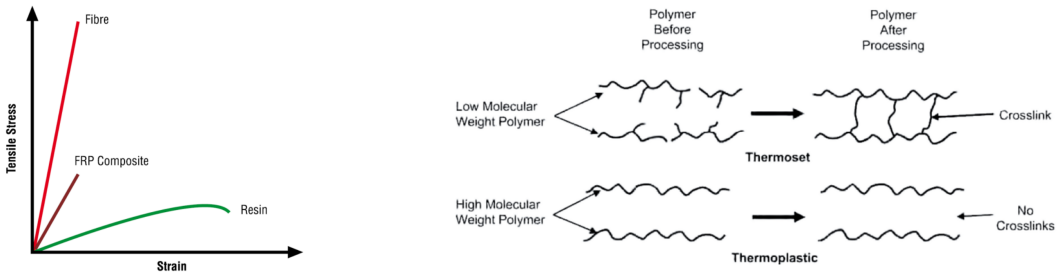

(a) Stress-Strain for FRP components (Cripps, 2020)

(b) Thermoset vs. thermoplastic resin, reprinted from (Abramovich, 2017)

Figure 2.1: FRP material characteristics

2.2.4. FRP production processes

With a basic understanding of the chemical makeup of FRP, it is important to examine how it is made. FRP has many different end products and respective production processes for these products. These different production processes yield widely varying material properties for the strength and stiffness of the material. Therefore, when deciding on a certain application of FRP, it is often associated with a specific product, with a specific production process. Some of the common end products include strands, yarn, rovings, reinforced mats, and fabrics. They differ in which way the fibres are combined, whether the fibres are grouped together compactly or loosely, and whether the fibres are aligned parallel, or perpendicular to each other. For further reference to the specific differences in the end products, you will find more information in the book "Structural Composite Materials" (Abramovich, 2017). In figure 2.2, you will see representations of some of the mentioned production processes.

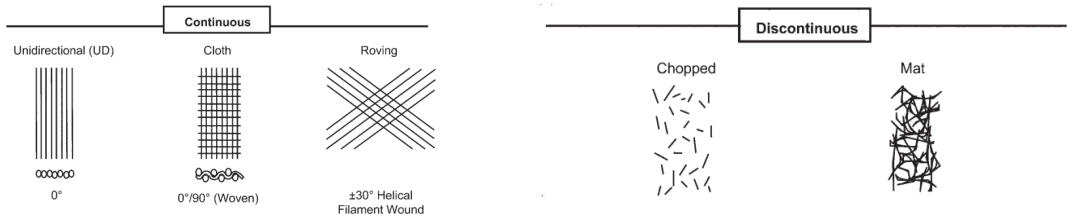

Figure 2.2: FRP reinforcement types, reprinted from (Abramovich, 2017)

What is important to know about FRP, and the many options available for different ways of production,

is that there is a very high level of control for the manufacturer. Regarding certain strength or stiffness requirements, shape or appearance, or any other desire of the designer, FRP can be made to fit those needs. This is an inherent advantage of the material, because it offers the ability to curtail the material to the design application, which is a unique attribute for a structural engineering material to have. It could be argued that this trait of the material is responsible for its wide use in mechanical and aerospace engineering applications as the material of choice. The only thing preventing FRP from its wide use in the field of civil engineering is that the material is novel, which inherently makes it less trustworthy in the eyes of the seasoned engineer. Due to the intended purpose of civil engineering projects to serve their function over a long period of time, safety is a key concern. This leads to the adoption of new materials to be traditionally slower in the civil engineering industry when compared to the aerospace or automotive industries.

2.2.5. Wrapped composite joint

As will be discussed later in section 2.3, welded joints are traditionally a necessary component of tubular structures due to the difficulty in designing, manufacturing, and installing common connections for their shape. This requirement for welded connections is a cause for concern in steel structures subjected to cyclic loads (like in the case of offshore wind turbines). Welds pose an issue to the structural health of these structures for several reasons. Because of the eccentricity of the weld and the geometric nonlinearity of the weld itself, there are stress concentrations in the welded connections. Moreover, during the welding process, the heat of the welding creates a heat affected zone (which leads to reduced fracture toughness). Both of these things lead to harsh reductions in strength in design codes, especially in cases of fatigue analysis. Fatigue analysis can be roughly summarised to be most affected by the number of cycles and the magnitude of stress ranges for those load cycles. When there are higher fluctuations of stress for a given load due to stress concentrations, a detail will always be prescribed a worse fatigue life (Zhao et al., 2001). In figure 2.3, the distribution of stress for a traditionally welded tubular joint is shown.

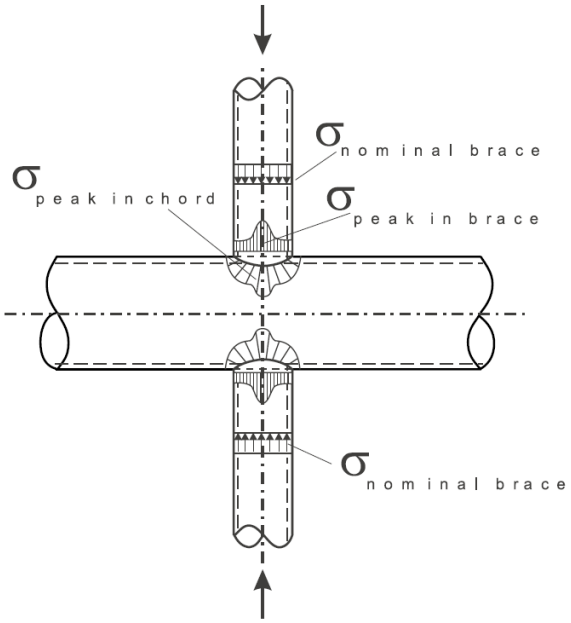

Figure 2.3: Geometrical non-uniform stress distribution for tubular joint (Zhao et al., 2001)

As previously mentioned, FRP can be manipulated into taking many forms with many different options for material characteristics. One specific application of interest for this thesis report is the application of FRP for wrapped composite joints. This joint type is under development and pending patent by Dr. M. Pavlović at Delft University of Technology. Its novel nature comes from the ability to join steel tubular members without welding. Through a wet lay-up process, the composite layers are placed

around the joining steel members with a method developed by Dr. M. Pavlović. A drawing depicting the wrapped composite joint is shown in figure 2.4. As can be seen in the figure, [1] represents the braces, [2] represents the chord, [3] the ”joint” itself, and [4] the composite wrap.

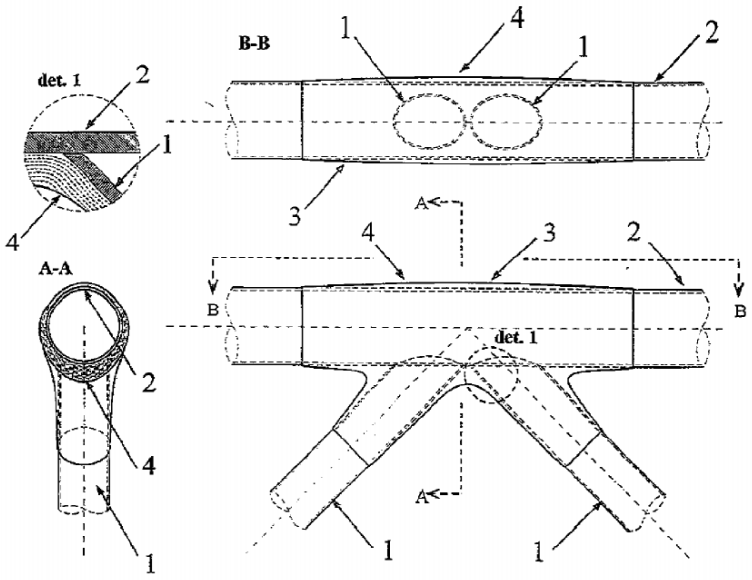

Figure 2.4: Wrapped composite joint drawing, reprinted from (Pavlović et al., 2021)

After curing, this joint offers superior fatigue resistance and joint stiffness than its welded alternative. This is due to many features of the joint. The FRP wrap material is optimised by placing it in areas where the joint experiences stress from common load scenarios. This functions as the antithesis to the problems provided by a welded joint. Instead of a geometric nonlinearity due to the presence of welds leading to a stress concentration in the case of a welded joint, the wrapped composite alternative is shaped in an optimal way to carry the load smoothly and evenly. In addition, because the wrap material acts as a transition piece transferring the loads, there is more ductility offered by the wrap material, and in the case of a X-joint or a KK-joint, the wrap material increases the joint stiffness approximately by a factor of three due to the ability of the wrap to reduce the ovalisation of the chord and brace members. All of these things lead to smaller variations in stress ranges, and in return yield superior fatigue life for the joint (Pavlović et al., 2021).

It is extremely beneficial in several ways to eliminate welds for a given building project. Firstly, the cost of welded structures is high, mostly due to the welds themselves. So eliminating them on a given building project will greatly reduce the project cost. Secondly, if the fatigue life can be extended for a given steel structure, for example, like a jacket support structure, the cost can further be reduced. If the need for replacement can be delayed 10 years, great cost savings would naturally follow from that. Additionally, the ability to use high strength steel in the application of jacket support structures is available and would help cost savings due to the weight reduction in the case of a wrapped composite alternative. The implementation of high strength steel is hindered by the weak point of the welds and causes the application of high strength steel to have less value because the welds are still the limiting factor in most design scenarios. As a bonus, the wrapped composite joints are not beneficial just because they are superior in fatigue load cases, but they also offer better corrosion resistance than the welded alternative. Welded locations at the joints traditionally represent the area most susceptible to damage through corrosion.

In the following figure 2.5, the wrapped composite joint is shown. In the left subfigure, a 3D render is shown of the wrapped composite joint applied to the case of a jacket structure. This is taken from Tree Composites website, which is showcasing the composite joint applied to its current project ”WrapNode-I” (Tree Composites, 2021). In the right subfigure, a wrapped composite joint is shown while undergoing a fatigue test. The joint is painted so that during the fatigue tests, through an application of Digital

Image Correlation (DIC) technique, any failure in the composite joint can be detected.

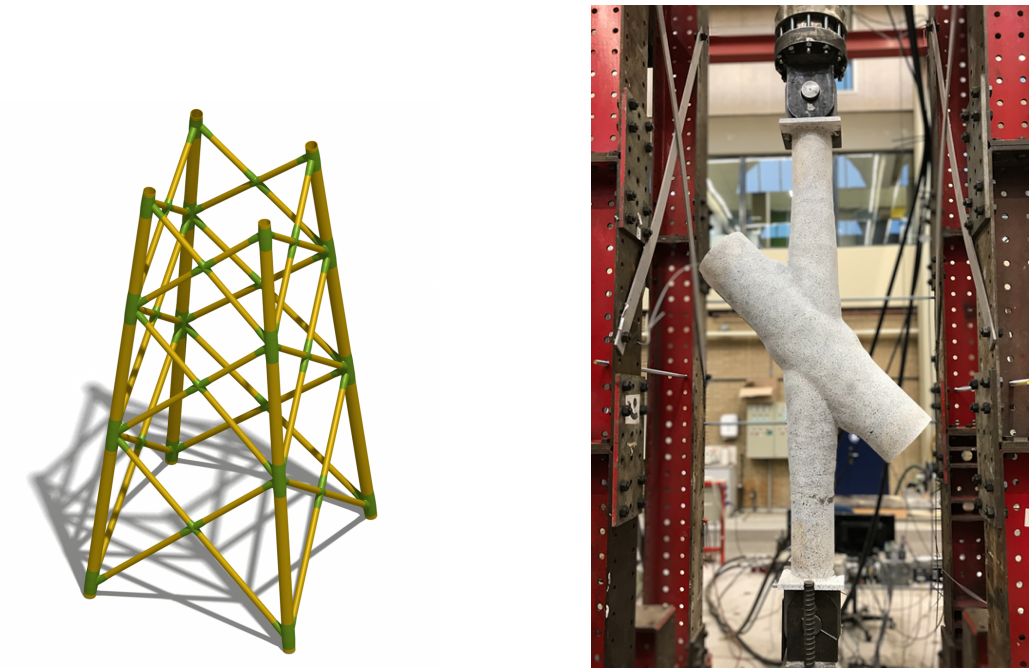

(a) Tower with wrapped composite joints (Tree Composites, 2021) **(b)** Wrapped composite joint specimen (Tree Composites, 2021)

Figure 2.5: Wrapped composite joint developed by Dr. M. Pavlović

2.2.6. Wrapped composite joint - Recent findings

A research team at TU Delft, under the advisement of Marko Pavlović, conducted monotonic tensile and cyclic loading cases on the innovative wrapped composite joint. Through the experiments, it was found that the wrapped composite joint had excellent performance for applications with high-strength and mild-strength steel, and for three different configurations of uni-axial, X45, and X30 joints. Some highlights from the experiments included the findings that the composite material would offer sufficient strength at the joint to let the steel yield during testing and that during fatigue testing of 7mil. cycles, the static resistance of the joint was not reduced even with a 40% reduction in stiffness. This gave the confirmation that the wrapped composite joint offers superior fatigue strength when compared to a welded alternative (He & Pavlovic, 2020).

In a previous master thesis project, it has been illustrated how when applying wrapped composite joints to a jacket support structure, the diameter and thickness of the tubular members for the braces and chords can be reduced. It was determined that in cases where you can assume that fatigue cases are not governing the design, as in the case of the application of wrapped composite joints, a reduction of over 50% can be seen for the weight of the jacket support structure. This is simply because the weight of a jacket support structure has to be increased to offer enough strength at the joints to be able to satisfy the fatigue load cases. Along with this, the fatigue life of the entire structure is also increased due to the removal of welds which are susceptible to fatigue damage (van Vliet, 2019).

2.3. Offshore wind turbine construction

As mentioned earlier, climate change is causing shifts in the civil engineering industry. Due to the many negative consequences related to the use of fossil fuels as energy sources, other sources of energy have been investigated. Some of the most popular alternative ”green” sources of energy include solar energy, tidal energy, and wind energy. These sustainable alternatives are all beneficial, but some of them are more beneficial from an environmental and economical perspective. Wind energy is often shown

to be superior regarding the return of investment in a fiscal sense and in evaluating the environmental profile holistically. This is even more clear when examining offshore wind turbines specifically. This is due to the increase in turbine size and of wind speeds available offshore which leads to more power generation (Intergovernmental Panel on Climate Change, 2015).

There are some common types of wind turbine structures that represent a majority share of existing wind turbine structures. These include monopiles, jackets, tripods, tripiles, gravity-based structures, and full truss towers. Of all these common types, this report is concerned specifically with jacket support structures.

2.3.1. Offshore wind turbine - support structure types

As mentioned previously, there are several different supporting structures for offshore wind turbines. The choice to focus on jacket support structures is due to several reasons. Because wind turbines are getting bigger, and the offshore wind turbine industry simultaneously grows in the market share of the energy sector, the supporting structures are also required to get bigger. For monopiles, currently the most common supporting structures for offshore wind turbines in the industry, issues arise when the wind farms are being placed farther away from shore. With an increase in water depth, there is a quadratic increase in diameter of the monopile due to the stiffness requirements for the supporting structure. In the case of jacket support structures, the diameter of the jacket legs increases linearly. This is due to the fact that jacket support structures are structurally more efficient due to the material that is contributing to the global bending stiffness being placed farther away from the centre. This is an inherent advantage for jacket support structures when compared to monopiles, and for water depths larger than 40m, it is proposed that jackets will represent the largest share of the market. (De Vries et al., 2011)

One potential disadvantage of using jacket support structures in the construction of offshore wind turbines is that there is a potential for an introduction of another mode. This new mode is called the ”rocking mode”, and it is a common phenomenon in the field of mechanical engineering for the manufacturing and use of helicopters. This mode is realised by the jacket moving up and down on either side, similar to the rocking motion of a rocking chair. Some researchers have found that this mode can act as the 1st bending mode. This is significant, because the frequency of the 1st mode of the offshore wind turbine supporting structure is used to determine the size of the supporting structure. It was shown in the research that there are ways to mitigate this phenomenon by altering the layout of the truss legs and by increasing the depth of the piles. It may not be significant for the case examined in this thesis project, but it should be mentioned because it is an inherent disadvantage respective to jackets as supporting structures for offshore wind turbines (Jalbi et al., 2019).

Larger wind turbines operate at lower frequencies than smaller wind turbines. These operating frequencies are referred to as ”1P”, ”3P”, and other multiples of 3. The ”P” represents the word pass, so the 1P frequency is the frequency of the passing of one specific blade of a three-bladed turbine, or rather the frequency of the operating turbine. The 3P frequency is the frequency of the passing 3 blades of the turbine. All wind turbine supporting structures are designed with certain frequency ranges. The ”soft-soft” range is the frequency range below the 1P operating frequency. The ”soft-stiff” range is the range in between the 1P and 3P frequencies of the turbine, and the ”stiff-stiff” range is the frequency range higher than 3P. These ranges and their relative shifts and contractions due to the increase in turbine size can be seen in figure 2.6.

The ”soft-stiff” range is often the preferred range for design. This is because it often is the most economical choice. The stiff-stiff range would offer the design alternative with the least concern for resonance, but would be the most costly regarding materials due to the requirement of more stiffness. The soft-soft range is avoided because there is a significant overlap with the wave and wind load spectra (this can be seen in figure 2.6). Therefore, jackets and other offshore wind turbine supporting structures are designed for the ”sweet spot” of the soft-stiff range. There have been theoretical investigations into designing large wind turbine supporting structures in the soft-soft region, but there are issues with designing the support structure to have the second natural frequency outside of the operating frequency

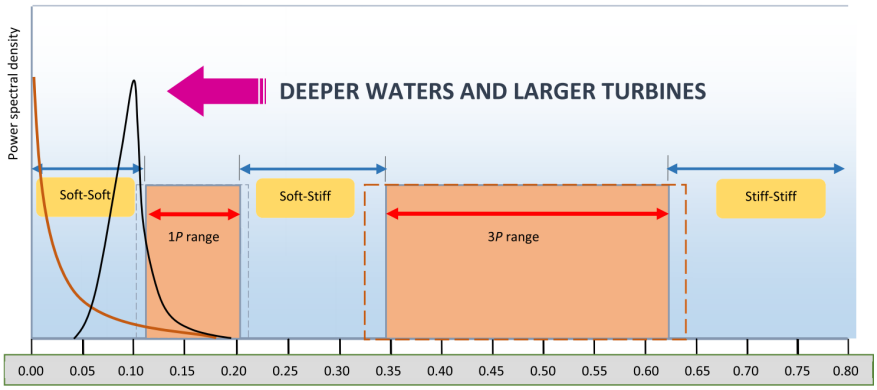

Figure 2.6: Turbine frequency spectrum shift with increase in turbine size, reprinted from (Amar Bouzid et al., 2018)

and the 3P frequency. Due to this, the traditional method of design for the offshore wind turbine in the soft-stiff region is the current norm for the industry (De Vries et al., 2011).

Again, to restate that the operating frequencies of the larger turbines are lower, this also means that the design range is shifting to the left and is contracting in size. This indicates that the design process must be more accurate because there is a larger overlap of the design frequency range with the loading spectrum, and the ideal range for the 1st natural frequency of the tower is smaller (Gaertner et al., 2020). To accommodate this stringent design constraint, the application of the Finite Element Method (FEM) technique of substructuring, with the use of submodels will be highlighted. This will be discussed in section 2.4. The benefit of this method is that a higher fidelity solution can be obtained, while keeping the computational cost low.

2.3.2. Jacket-supported offshore wind turbine modelling considerations

As previously mentioned, the offshore wind market is growing in size. With this growth in market size, there is also an increase in competition which is constraining designers to find ways to reduce costs. The areas of design that are traditionally optimised include reducing the the amount of material that is used, lowering fabrication costs, and improving analytical methods. The party responsible for the design of the substructure of the offshore wind turbine is often different than the party responsible for the design of the superstructure. This increases the complexity of the optimisation process and can cause errors in the design process due to the multiple parties working simultaneously with design changes that affect all other parties.

Although not directly responsible for the design of the tower and turbine, the jacket designer still must consider its effects. Some of these additional conditions include: the tower and turbine bring added mass and stiffness to the structure which affects the eigenfrequencies of the structure, the tower and turbine introduce a wind load case, and the turbine has operating frequencies and loads that must be considered. Due to the structure being subjected to simultaneously acting environmental loads with unknown direction and magnitude, the structure must be analysed in the time domain due to the time-sensitive dynamic interaction between the two load cases. This is an unfortunate reality because the designer is prohibited from using the more cost-effective method of analysing the structure in the frequency domain. In figure 2.7, the design process of an offshore wind turbine with a jacket support structure is presented. The substructure (jacket and foundation) is transformed into a superelement, with the interface point being at the bottom of the tower. This hand-off of the interface loads is an iterative process and will be elaborated upon later in the report in chapter 3.

Added to the complexity of the iterative design process, the jacket support structure itself has many complex structural elements that require special attention. Traditionally, any structural engineer would want to model a given structure with beam elements for the structural members and with either idealised rigid or pinned connections for the joints. This simplifies the design and poses as no problem

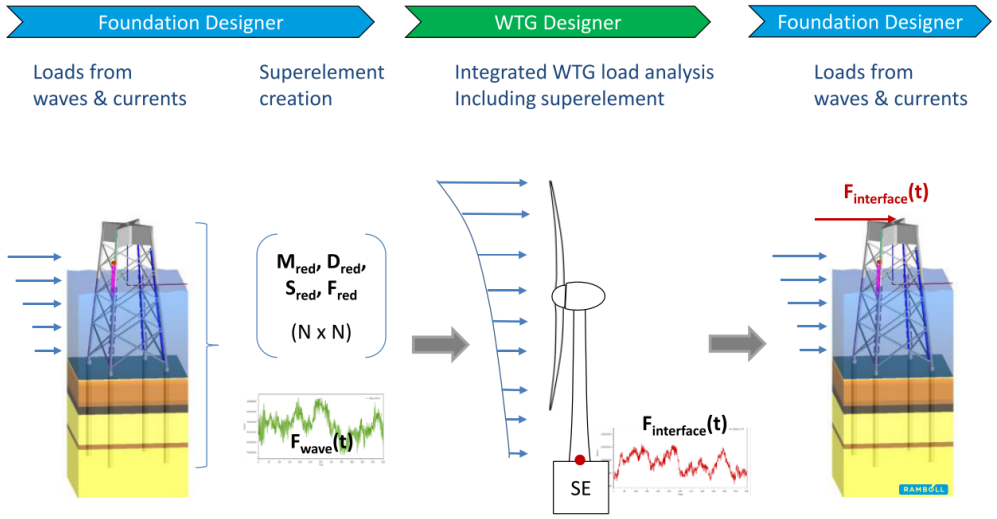

Figure 2.7: Visual representation of the superelement generation process, reprinted from (Stolpe et al., 2016)

for any structural analysis software to fully characterise the loads and response of the structural system. This cannot be done for the case of jacket support structures. The structural members are made primarily out of tubular elements which are joined with welds, and the **transition piece** (**TP**) often includes complex geometry. Both of these elements are susceptible to **hot spot stresses** (**HSS**). Along with these elements, the foundation piles often need to be analysed with nonlinear springs along the height of the piles to truly capture the stiffness behaviour of the soil. To accurately model the welded joints, transition piece, and soil piles, a highly accurate FEM is required. These FEM models, whether composed of shell elements or solid elements, dramatically increase the computational cost of the model.

To combat this, a design method has been developed in industry to analyse these nontrivial structural elements (welded joints, TP, soil piles, etc.) through a step-wise procedure, while keeping the degree of accuracy roughly equivalent to the use of a high fidelity solid element model and the computational cost equivalent to a beam model. This method is called ”substructuring” and will be elaborated in section 2.4.

2.4. Finite Element Method (FEM) - Substructuring

As mentioned previously, there is a FEM technique that is called substructuring. Essentially, substructuring is simplifying the model by keeping only the nodes of freedom that are of interest. These nodes are called the ”master” or ”leader” nodes, and the rest are called ”slave” or ”follower” nodes. This new sub-structured model is then used within a different model, but only the leader nodes are brought in. Then, in any given analysis, the reactions at the leader nodes for the kept degrees of freedom are then relayed to the follower nodes to find the reactions in post-processing. These substructured models are often called submodels.

2.4.1. Substructuring with the Craig-Bampton Method

The first step of this design method is to model the nontrivial structural elements in a computationally efficient way. This can be done with the **Craig-Bampton** (**CB**) reduction. The CB method’s main purpose is to reduce the **degrees of freedom** (**DOF**), while retaining the same level of accuracy after the reduction as before the reduction. During the process, a set of nodes are chosen to be kept, and a set of nodes are discarded. In literature, the set of nodes that are kept are given the synonymous names of retained, boundary, and master. The set of nodes that are discarded are given the synonymous names

of eliminated, internal, and slave, respectively. Going forward in this report, I will use the terms ”leader” and ”follower” in place of the terms ”master” and ”slave” (Craig & Bampton, 1968).

When making decisions on which nodes are to be retained, it is important to consider the intended purpose of the element and its relevant boundary conditions. In the case of the design of an offshore wind turbine with a jacket support structure, there are decisions that are traditionally made to reduce the complexity of the structure and the terms given to describe the reduced components. It can be said that the entire jacket support structure is made of three individual macrostructures: the turbine, tower, and substructure (also including the foundation). These macrostructures interact with each other at certain interface points which act as the previously mentioned boundary DOF. When reducing macrostructures with the CB method, and having the boundary conditions be at the interface point between the neighbouring macrostructures, the term **superelement** (**SE**) is used to describe the reduced macrostructure. The term that describes the reduction of a structure into macrostructures is called ”substructuring”.

Please note, there is an overlap in the terminology between ”substructure” and ”substructuring”. Henceforth, when using the term ”substructuring”, I will be referring to the CB reduction technique that generates a submodel. When using the term ”substructure”, I will be referring to the substructure of the offshore wind turbine, which is the jacket support structure and the foundation. In the literature, ”submodel” as the name for the end product of the CB reduction is preferred to ”superelement” in most cases, but due to the term submodel already being used to describe submodels for joints which will be discussed in section 2.4.3, I will continue with the use of the name of ”superelement” when referring to the foundation and jacket being transformed into a submodel. When discussing the generation of submodels and superelements, I will use the term ”substructuring” because there should be no ambiguity.

2.4.2. Mathematical Formulation of the Craig-Bampton Method

For a given structure, the equation of motion can be described by the following well-known equation:

$$\boldsymbol{M}\ddot{\boldsymbol{x}} + \boldsymbol{C}\dot{\boldsymbol{x}} + \boldsymbol{K}\boldsymbol{x} = \boldsymbol{f} \tag{2.1}$$

On the left-hand side of the equation, the structure is defined by its mass, damping, and stiffness matrix multiplied with the corresponding time derivative of the vector, ”$\boldsymbol{x}$”, representing the DOF of the system. The right-hand side of the equation is defined by the load vector, ”$\boldsymbol{f}$”. To apply the CB reduction, equation 2.1 is altered to yield the form found in equation 2.2. The previously mentioned terminology of leader and follower is used with ”ℓ” and ”f” notation.

$$\begin{bmatrix} M_{\ell\ell} & M_{\ell f} \\ M_{\ell f}^t & M_{ff} \end{bmatrix} \begin{bmatrix} \ddot{\boldsymbol{x}}_\ell \\ \ddot{\boldsymbol{x}}_f \end{bmatrix} + \begin{bmatrix} \boldsymbol{C}_{\ell\ell} & \boldsymbol{C}_{\ell f} \\ \boldsymbol{C}_{\ell f}^t & \boldsymbol{C}_{ff} \end{bmatrix} \begin{bmatrix} \dot{\boldsymbol{x}}_\ell \\ \dot{\boldsymbol{x}}_f \end{bmatrix} + \begin{bmatrix} \boldsymbol{K}_{\ell\ell} & \boldsymbol{K}_{\ell f} \\ \boldsymbol{K}_{\ell f}^t & \boldsymbol{K}_{ff} \end{bmatrix} \begin{bmatrix} \boldsymbol{x}_\ell \\ \boldsymbol{x}_f \end{bmatrix} = \begin{bmatrix} \boldsymbol{f}_\ell \\ \boldsymbol{f}_f \end{bmatrix} \tag{2.2}$$

The form of equation 2.2 is structured to describe the assumptions held in the CB reduction. The assumptions are that the motion of the follower DOF is described by the elastic response due to motion of the leader DOF when neglecting the effect of inertia of the follower DOF, and the forces applied to the follower DOF are neglected. This is equivalent to saying that $\boldsymbol{M}_{\ell f}$, $\boldsymbol{M}_{ff}$, and $\boldsymbol{f}_f$ are equal to zero. This leads to the following formula that describes the motion of the follower DOF.

$$\boldsymbol{x}_{f,\,\text{Guyan}} = -\boldsymbol{K}_{ff}^{-1}\boldsymbol{K}_{\ell f}^t\boldsymbol{x}_{\ell,\,\text{Guyan}} = \boldsymbol{\Phi}_1\boldsymbol{x}_{\ell,\,\text{Guyan}}\,, \quad \text{where} \quad \boldsymbol{\Phi}_1 \triangleq -\boldsymbol{K}_{ff}^{-1}\boldsymbol{K}_{\ell f}^t \tag{2.3}$$

This logically follows, because looking at the far-right term in equation 2.3, the variable $\boldsymbol{\Phi}_1$ describes the relationship between the follower displacements and the leader displacements as a linear transformation. These assumptions do have the cost of stating that the inertias of the follower DOF have no effect on the displacement of the follower DOF, which is only true in the case of a static regime. This form of reduction is equivalent to the Guyan reduction which is very popular and widely used, but only accurate for static cases or where inertial effects are deemed insignificant (Branlard et al., 2020).

The CB method introduces the inertial effects of the follower DOF by posing the undamped eigenvalue problem expressed as:

$$\left(\boldsymbol{K}_{ff} - \nu_i^2 \boldsymbol{M}_{\mathrm{ff}}\right) \phi_i = 0 \tag{2.4}$$

In equation 2.4, ν_i, and ϕ_i represent the frequency and mode shape of the eigenmodes, respectively. Traditionally, the eigenvalues are obtained for the first 20-30 modes of the jacket support structure. There are also some advantages to retain the first ten modes, and combining them with higher modes to ensure that the model is also able to capture the "true" response to higher-frequency loading. Whatever the choice, the retained modes are stored in a matrix $\boldsymbol{\Phi}_2$, then scaled with respect to their modal mass. The purpose of this effort is that the DOF is reduced from $10^3 - 10^5$ to 20-30 modes. This is shown elegantly through a coordinate transformation held in equation 2.5.

$$\begin{bmatrix} \boldsymbol{x}_l \\ \boldsymbol{x}_f \end{bmatrix} \approx \begin{bmatrix} \boldsymbol{I} & 0 \\ \boldsymbol{\Phi}_1 & \boldsymbol{\Phi}_2 \end{bmatrix} \begin{bmatrix} \boldsymbol{x}_{r1} \\ \boldsymbol{x}_{r2} \end{bmatrix} \quad \Leftrightarrow \quad \boldsymbol{x} \approx \boldsymbol{T}\boldsymbol{x}_r, \quad \text{with} \quad \boldsymbol{T} \triangleq \begin{bmatrix} \boldsymbol{I} & 0 \\ \boldsymbol{\Phi}_1 & \boldsymbol{\Phi}_2 \end{bmatrix} \tag{2.5}$$

The mass and stiffness matrix, along with the load vector can also be transformed with the $\boldsymbol{T}$ matrix from equation 2.5, yielding the new EOM for the undamped system.

$$\boldsymbol{M}_r \ddot{\boldsymbol{x}}_r + \boldsymbol{K}_r \boldsymbol{x}_r = \boldsymbol{f}_r \tag{2.6}$$

Which is expressed in matrix form in equation 2.7.

$$\begin{bmatrix} \boldsymbol{M}_{r11} & \boldsymbol{M}_{r12} \\ \boldsymbol{M}_{r12}^t & \boldsymbol{M}_{r22} \end{bmatrix} \begin{bmatrix} \ddot{\boldsymbol{x}}_{r1} \\ \ddot{\boldsymbol{x}}_{r2} \end{bmatrix} + \begin{bmatrix} \boldsymbol{K}_{r11} & 0 \\ 0 & \boldsymbol{K}_{r22} \end{bmatrix} \begin{bmatrix} \boldsymbol{x}_{r1} \\ \boldsymbol{x}_{r2} \end{bmatrix} = \begin{bmatrix} \boldsymbol{f}_{r1} \\ \boldsymbol{f}_{r2} \end{bmatrix} \tag{2.7}$$

With matrix entries defined as:

$$\begin{aligned} &\boldsymbol{M}_{r11} = \boldsymbol{M}_\ell + \boldsymbol{\Phi}_1^t \boldsymbol{M}_{f\ell} + \boldsymbol{M}_{\ell f}\boldsymbol{\Phi}_1 + \boldsymbol{\Phi}_1^t \boldsymbol{M}_{ff}\boldsymbol{\Phi}_1, \quad \boldsymbol{M}_{r22} = \mathbb{I}_2^t \boldsymbol{M}_{ff}\boldsymbol{\Phi}_2 = \boldsymbol{I} \\ &\boldsymbol{M}_{r12} = \left(\boldsymbol{M}_{\ell f} + \boldsymbol{\Phi}_1^t \boldsymbol{M}_{ff}\right)\boldsymbol{\Phi}_2, \quad \boldsymbol{f}_{r2} = \mathbb{I}_2^t \boldsymbol{f}_f, \quad \boldsymbol{f}_{r1} = \boldsymbol{f}_\ell + \boldsymbol{\Phi}_1^t \boldsymbol{f}_f \\ &\boldsymbol{K}_{r11} = \boldsymbol{K}_\ell + \boldsymbol{K}_{\ell f}\boldsymbol{\Phi}_1, \quad \boldsymbol{K}_{r22} = \boldsymbol{\Phi}_2^t \boldsymbol{K}_{ff}\boldsymbol{\Phi}_2 \end{aligned}$$

To obtain the damping matrix, it is common to use the Rayleigh damping assumption. This provides the ability to obtain the damping matrix with the previously defined mass and stiffness matrices multiplied by the α and β user-defined constants. Although the assumption that the damping is proportional to mass and stiffness is not perfectly accurate, due to the difficulty in accurately describing the damping in a given complex structural system, this method is treated as a useful approximation (Branlard et al., 2020).

2.4.3. Substructuring tubular joints of a jacket support structure

As mentioned in 2.3.2, certain structural elements in a jacket support structure are nontrivial and require higher fidelity modelling. One specific component of a jacket support structure that is of specific interest in this paper, are tubular joint connections. These usually take the form of double K-joints, X-joints, or Y-joints. These tubular joints, due to their geometric complexity, often attract high stress concentrations. To accurately model these joints, one alternative is to use **local joint flexibility equations** (**LJF**). These local joint flexibility equations are sufficient in static and fatigue cases. This is because LJF equations can effectively approximate the stiffness of a tubular joint connection. When considering dynamic load cases, inertial effects must be considered. The effect of inertial forces in a dynamic regime cannot be captured with these equations.

Therefore, an alternative to measure the effect of the joint on the overall structural performance in a dy-

namic regime is to use the substructuring method mentioned in the previous section. The leader DOFs are often taken as nodes centred along the longitudinal axes of the tubular members of the connection at a sufficient distance from the idealised joint centre. These leader DOFs are then connected to the joining members, which are modelled as traditional beam elements.

In figure 2.8, several strategies to model a jacket support structure are shown. The previously mentioned option of using submodeled joints is shown in the far-right subfigure. This method is compared to modelling the entire jacket support structure with beam elements (subfigure b), and modelling the joints with rigid beam elements that approximate the stiffness of the joint through the application of local joint flexibility equations.

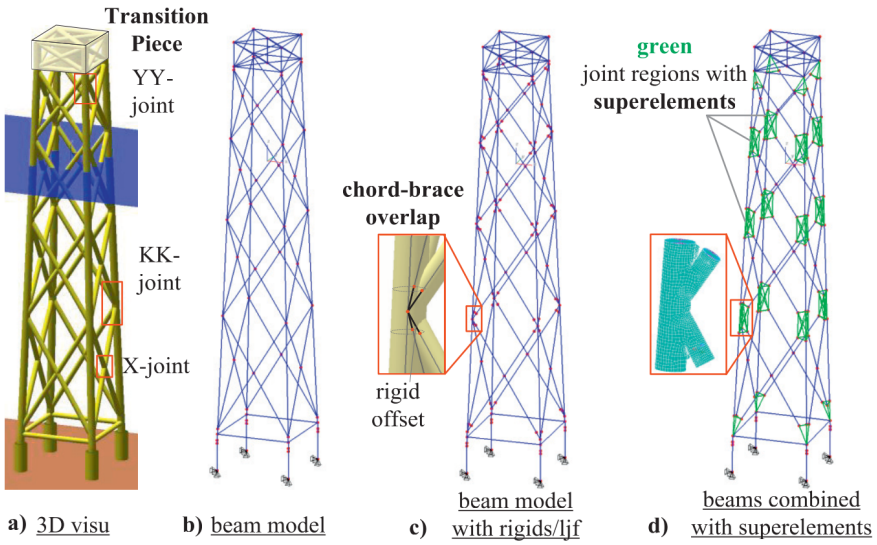

Figure 2.8: Tubular joint modelling strategies, reprinted from (Dubois et al., 2013)

By placing submodels at the joints for the case of a jacket-supported offshore wind turbine, the total degrees of freedom for the entire structure can be greatly reduced when compared to a shell model, and the added degrees of freedom when compared to a simple Euler-Bernoulli beam model is relatively small. Several researchers have investigated the effects of submodels applied to the joints of a jacket. When comparing the results of the jacket with submodeled joints with the case of a full shell model, and with a model composed of only beam elements and joints with stiffness derived from LJF equations, the model with submodeled joints yielded more accurate results. It was found that the model with submodeled joints, when compared to the model with joint stiffness represented by the LJF equations, gave a better representation of fatigue damage, dynamic amplification, and shear deformation when compared to the shell model. This was due to the fact that the substructuring approach changed the load distribution to correspond well with the shell model by more accurately modelling the joint flexibility while simultaneously being susceptible to inertial effects (Dubois et al., 2013).

In figure 2.9, the generated joint submodel is shown. The geometry of the local region affected by the joint was determined, which functioned as the starting point for the submodel. A shell model was then made for the joint, which was then substructured by keeping the leader DOFs as the centre point along the beam axis for the chord and braces. Simultaneously, the loading that would be acting on the joint is introduced in a separate model. This is done because the geometry of the joint that normally receives the distributed wave loading is now removed from the main model, so it must be added separately. The submodel is then fully defined and can be placed in the beam model.

Through this substructuring process, it was found that the local beam modes were more affected than the global modes. By the inclusion of submodelled joints, this logically follows because the addition of joint flexibility would have a large impact on the local brace modes, which are more susceptible to changes in the boundary conditions at the end of the beam span than the chord members due to the brace members having smaller section sizes and as a result being less stiff. On the contrary, the overall

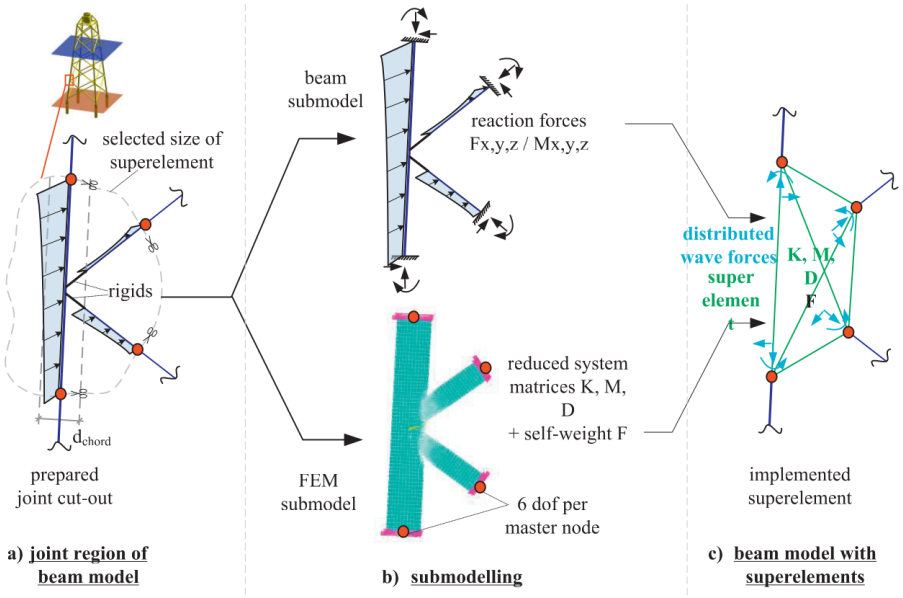

Figure 2.9: Steps of submodel creation for a tubular joint (Dubois et al., 2013)

stiffness of the jacket support structure is more affected by the stiffness of the layout of the entire jacket support structure, the stiffness of the foundation, and the mass and stiffness of the tower and turbine. The chords and braces individually do not contribute a large amount to the global stiffness of the jacket support structure. In the initial research done by the team, it was found that the higher global modes for the structure changed by 3% due to the submodeled joints, and for the bending modes that were predominantly local bending modes, there was a change of up to 7% when comparing the model with submodeled joints to the model with joint stiffness represented by LJF equations. With respect to fatigue damage, the submodeled joints gave a fatigue load reduction of 16% at the bottom YY-joint, 15% at the lowest X-joint, and 22% at the lowest KK-joint when compared to the model with joint stiffness given by LJF equations. These reductions of the fatigue damage through the use of submodeled joints would extend the fatigue life of the offshore wind turbine jacket by approximately 15% if a conservative estimate is desired (Dubois et al., 2013).

Another research group that is worth highlighting was also investigating the impact of the use of submodeled joints. In this study, there were two models (one with submodeled joints and one with beams with rigid joints). The two were compared for several load cases. Through the analysis, it was found that the damage equivalent loads for the model with submodeled joints were larger than for the model with beams and rigid joints. This phenomenon was exacerbated by higher wind speeds. By modelling the joint flexibility more accurately, larger displacements were obtained, and larger fatigue loads were measured (Popko et al., 2016).

In figure 2.10 for an applied stochastic wind load case, the **Damage Equivalent Loads** (**DELs**) for out-of-plane bending moments are shown with respect to different wind speeds. In subfigure 2.10a, the bending moments for the bottom X-joint for both models are shown, and in subfigure 2.10b, the bending moments for the bottom KK-joint for both models are shown. There are several important things to notice in these figures. The bending moments shown in subfigure 2.10a, can be used to approximate the impact of the submodeled joint on local dynamic effects, whereas the bending moments in subfigure 2.10b can be used to approximate the impact of the submodeled joint on the global dynamic behaviour of the offshore wind turbine.

For the case of the X-joint and KK-joint, in both models, an increase in wind speed led to an increase in DEL. The exception to the rule was for speeds greater than 24 m/s, but this is because the cut-off speed for the motor was set for 25 m/s wind speed. What is interesting to note is that for higher wind speeds (10-24 m/s), the X-joint experienced a steeper slope in DEL with respect to the wind speed

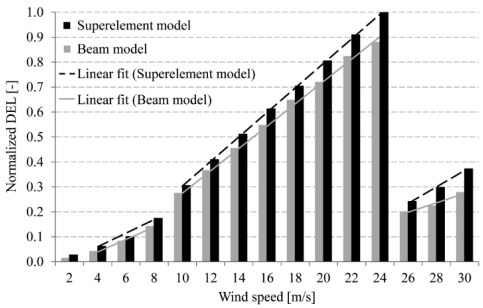

(a) DEL of out-of-plane bending moment at bottom X-joint, reprinted from (Popko et al., 2016)

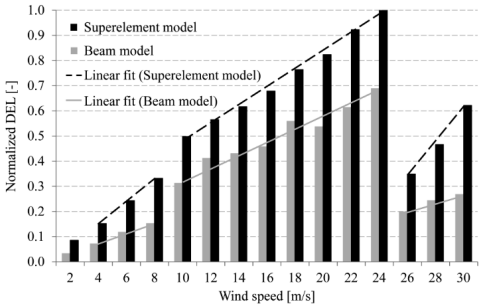

(b) DEL of out-of-plane bending moment for bottom KK-joint, reprinted from (Popko et al., 2016)

Figure 2.10: Effect of joint submodels on damage equivalent loads

for the model with submodeled joints. This relationship yields the conclusion that in the case of full loading, the jacket is more influenced by local dynamic effects. Most likely this can be attributed to the jacket receiving pure harmonic excitations at these higher wind speeds, which have a large effect on the local bending modes of the braces (Popko et al., 2016).

For the case of the KK-joint, the largest difference between the two models was found for the case of partial loading (4-8 m/s) and for idling conditions (>25 m/s). This indicates that the submodeled joints have a larger impact on the global behaviour of the offshore wind turbine for these loading conditions. In all cases, it can be seen that the inclusion of submodeled joints is necessary to obtain an accurate representation of fatigue loading (Popko et al., 2016).

As can be seen in figure 2.11, the local joint flexibility is affected by the implementation of joint submodels. Popko and his research group found that the out-of-plane displacements specifically were heavily affected by the submodeled joints. In subfigure 2.11a, what is meant by out-of-plane displacement with respect to the braces can be seen. In figure 2.11b, the maximum out-of-plane displacement and its standard deviation are shown for the beam and submodeled joint models. As can be seen, the model with submodeled joints had larger displacements for each height along the jacket support structure, with the largest difference between the two models at the highest point along the elevation of the jacket.

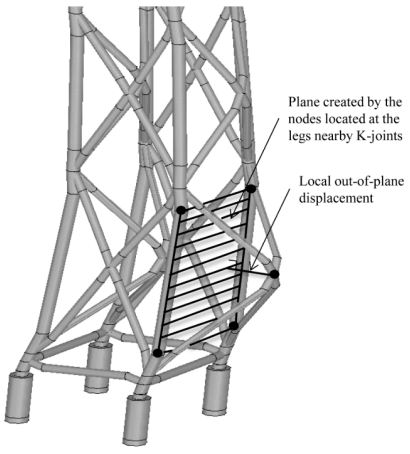

(a) Definition of "out-of-plane" displacement in context of JSS, reprinted from (Popko et al., 2016)

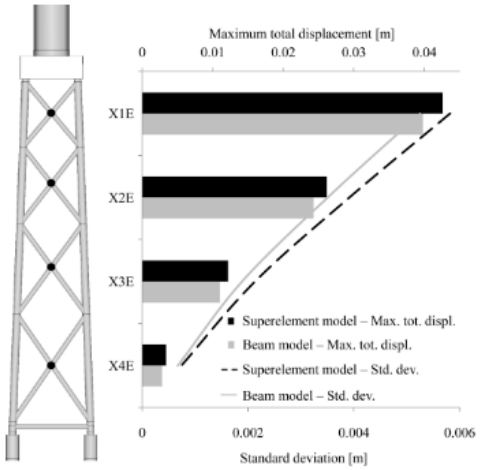

(b) Result of implementation of joint submodels, reprinted from (Popko et al., 2016)

Figure 2.11: Joint submodels and their effect on local joint flexibility

Please note, the jacket that was analysed in both of these research studies (Dubois and Popko) is the OC4 jacket. This jacket will be introduced in chapter 3, but what is important to know is the differences

found between the model with submodeled joints and a model with beams and joint stiffness given by LJF equations or with rigid joints should be larger for the case of a 10MW turbine. It is assumed that the loads imposed on the jacket would be higher for a 10MW turbine, leading to an increase in the resulting displacement and fatigue damage measured at the joints. This serves as a motivation to investigate the implementation of submodeled joints for the case of a larger turbine.

To summarise, the model with joint submodels better represents the true jacket support structure dynamic behaviour compared to the commonly used beam model, while also keeping similar computational efficiency to the beam model. Furthermore, the model with submodelled joints yields lower eigenfrequencies, higher structural flexibility, different load-bearing behaviour, and different fatigue damage effects on the support structure compared to the beam model. These differences can influence the design of the support structure. Therefore, the joint submodelling strategy should be used for this type of structure in the aero-hydro-servo-elastic simulations of offshore wind turbines when the above-mentioned differences play a significant role in the offshore wind turbine design.

II

Proof of Concept

3

Modelling Strategy and Methodology

3.1. Methodology Overview

The research questions being pursued were presented in chapter 1. To answer these questions, a certain solution strategy was employed utilising several tools that were available. The project workflow will be explained in section 3.2. Within this strategy, two specific programs were heavily relied upon: OpenFAST and Abaqus. OpenFAST was used to analyse the offshore wind turbine, and specifically the superstructure. This program will be introduced and related to the relevant research questions in section 3.3. Abaqus was used to create joint submodels and to conduct a wave load analysis on the jacket support structure. This program will be introduced and related to the relevant research questions in section 3.4.

The purpose of the modelling strategy that was employed was to isolate the impact of the submodeled joints. This was done by creating several models that have different strategies for modelling the joints. One model had only beam elements with the joints modelled as rigid joints. This model was to act as the control model. The other two models had submodeled joints, one with wrapped composite joints and one with welded joints.

These three models were analysed in the same way with respect to the input dimensions of structural members, boundary conditions, and load cases. This allowed the impact of the joint modelling strategy to be seen, with the different joint types set as independent variables. Dependent variables that were analysed included the natural frequencies and mode shapes, and member loads and displacements. The natural frequencies and mode shapes were obtained through a natural frequency analysis, with a specific focus on the individual joint, the jacket, and the entire offshore wind turbine structure. The loads and displacements were analysed through a time-history analysis.

Due to the nonlinear nature of an offshore wind turbine, the time-history analysis is necessary to get an accurate representation of the member displacements and member loads. These dependent variables that were measured were then used to evaluate the influence of the joint modelling strategy and argue for or against its necessity.

Moreover, through these analyses, a comparison between welded joints and wrapped composite joints was made. It was expected that the wrapped composite joints would be the stiffer joint type. This would then be reflected in the natural frequency analysis. It was also expected that the wrapped composite joints would have smaller damage equivalent loads than the welded alternative.

3.2. Modelling strategy

To sufficiently answer the research questions that were presented, and to align with the main purpose of the report, the following strategy was employed and can be explained in a series of steps:

1. A jacket support structure for supporting a 10MW turbine was modelled, including the foundation and transition piece - Model-A
2. Submodels of the X-joints and the KK-joints to be incorporated in the jacket model were created for the wrapped composite and welded alternatives
3. Three versions of Model-A were generated:
   (a) fitted with wrapped composite joints represented as submodels
   (b) fitted with welded joints represented as submodels
   (c) all beam elements with no submodels - joints modelled as rigid
4. A natural frequency analysis was conducted for the three versions of Model-A
5. A superelement of Model-A was created with the Craig-Bampton reduction including the first 20 eigenmodes - Model-B
6. Mass, stiffness, and damping matrices were extracted from Model-B
7. Model-B was analysed with a wave load time-history analysis
8. The results of the wave load analysis were stored in a load vector for the retained degrees of freedom (degrees of freedom at the interface point and the retained eigenmodes)
9. The tower and turbine were modelled - Model-C
10. An aero-hydro-servo-elastic analysis was conducted on Model-C with Model-B input as a boundary condition at the interface point
11. The results of the aero-hydro-servo-elastic time-history analysis at the interface point were exported from Model-C back to Model-A
12. A wave load time-history analysis was conducted on Model-A in combination with the load results from Model-C
13. Results of the analysis on the three version of Model-A were analysed and the differences between the versions were compared

The methodology can also be visualised in the flow chart held in figure 3.1.

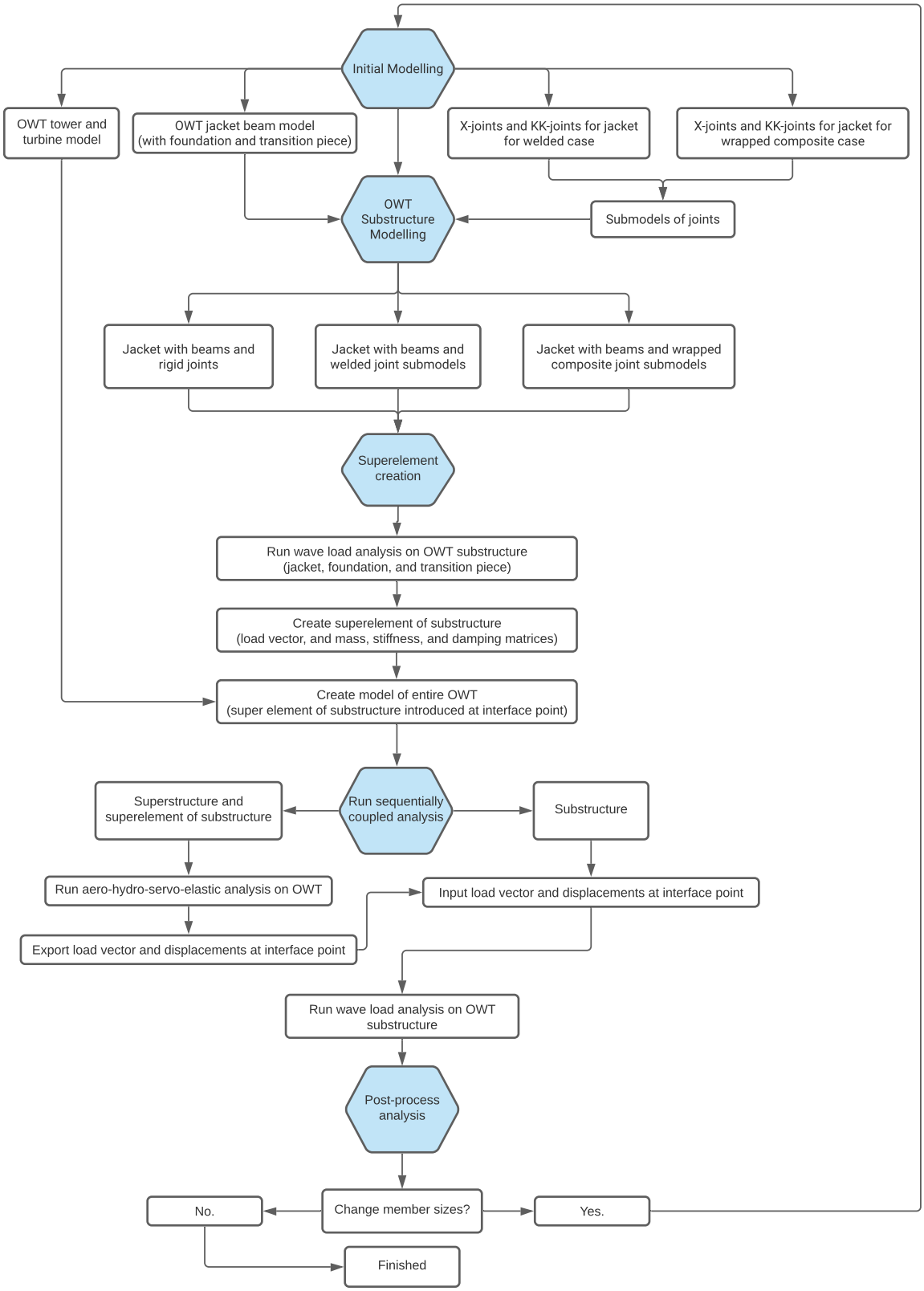

Figure 3.1: Flow chart of modelling strategy

A figure from an earlier chapter, figure 2.9, depicts the process of making a superelement. To visualise

the concept of running a sequentially coupled analysis, reference figure 3.2. The first stage is to model the jacket support structure and conduct a wave load analysis in FEM software (Abaqus). The second stage is to generate a SE of the jacket, including matrices that define the EOM and the wave load vector, and import it into a model including the tower and wind turbine (OpenFAST). The third stage is to conduct an aero-servo-elastic analysis and then export the results back to the original model. The fourth and last stage is then to conduct a reanalysis of the jacket support structure, by conducting another wave load time-history analysis.

The only step of the problem strategy that figure 3.2 does not include is the submodelled joints. Besides this step, the figure is beneficial in depicting the overall problem strategy of this report. This figure also depicts a module of OpenFAST, "ExtPtfm", which is elaborated in section A.1.2.

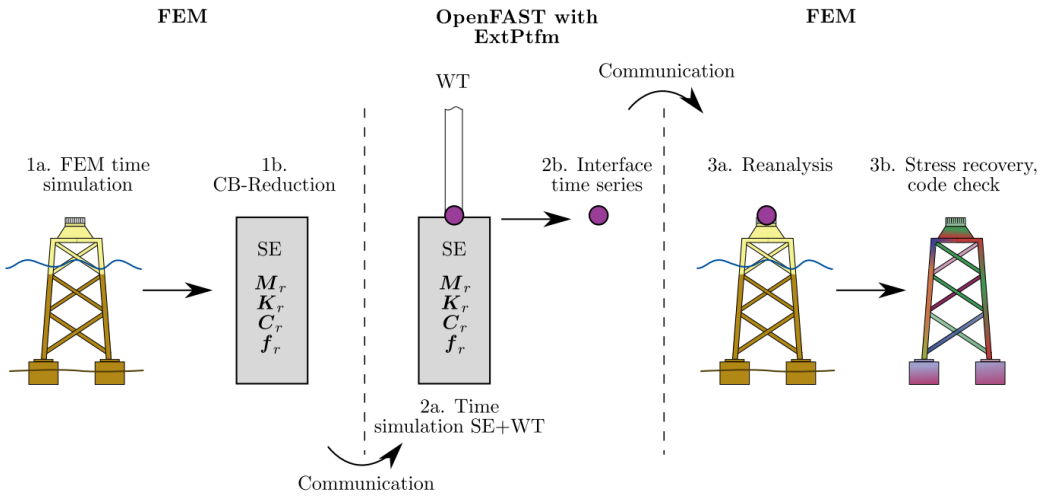

Figure 3.2: OpenFAST ExtPtfm (Branlard et al., 2020)

3.3. OpenFAST

OpenFAST is an open-source software tool that is used to simulate the response of wind turbines. It is composed of several modules that are focused on a specific part of the dynamic response of the wind turbine. What is beneficial about OpenFAST specifically is the goal that the creators share on their homepage (NREL, 2021):

> "It [OpenFAST] was created with the goal of being a community model developed and used by research laboratories, academia, and industry. It is managed by a dedicated team at the National Renewable Energy Lab. Our objective is to ensure that OpenFAST is a well-tested, well-documented, and self-sustaining software. To that end, we are continually improving the documentation and test coverage for existing code, and we expect that new capabilities will include adequate testing and documentation."

This ethos was inspiring for me as a young academic and led me to use their tool. Although using the tool was at times more difficult than using commercial software like Bladed, HAWC2, and Flex, the benefit of using a tool that is accessible to all, and actively developed by users around the world, outweighs the cost in my opinion. As shown in figure 3.3, OpenFAST, or "Fast 8", is the "glue code" that facilitates the nonlinear aero-hydro-servo-elastic simulations.

In the figure, two of the submodules are elaborated: HydroDyn and SubDyn. HydroDyn is the module that carries out the wave load analysis for the modelled substructure of a wind turbine. At a given time-step, HydroDyn takes as input the substructure's movement and gives as output the hydrodynamic loads at those given locations. SubDyn in a similar way is the module that carries out the response to the wave load analysis. As an input, SubDyn takes the hydrodynamic loads and the interface point

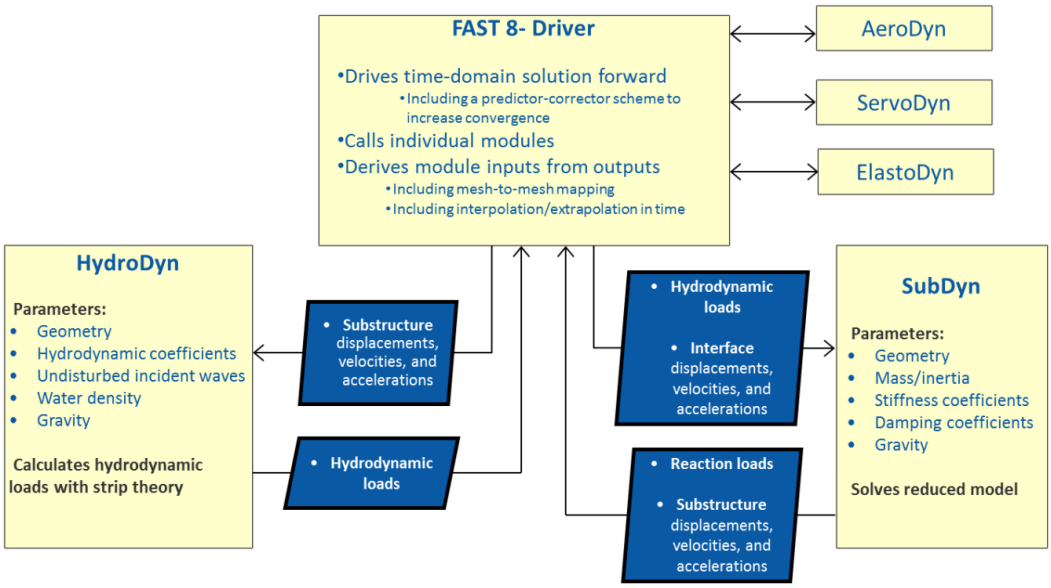

Figure 3.3: OpenFAST framework (NREL, 2021)

movement, and gives as output the reaction loads and the substructure's movement. In this way, these two modules are intrinsically coupled.

The other three modules: AeroDyn, ServoDyn, and ElastoDyn are focused more on the superstructure. They are coupled to each other, due to AeroDyn functioning as the module responsible for the wind loading, and ServoDyn and ElastoDyn responsible for the response of the turbine and tower to the loading respectively. As mentioned earlier, these modules interact with the substructure through the interface point (traditionally modelled as the base of the tower). This report is less focused on these superstructure modules, and most of the analysis efforts are focused on the SubDyn and ExtPtfm modules specifically. A further elaboration of these modules with information pertinent to this thesis project are included in appendix A. This elaboration is included for the interested reader and serves to give further background to the analyses done with OpenFAST in this thesis report. A further explanation of all modules in OpenFAST can be found in the documentation of OpenFAST (NREL, 2021).

3.4. Abaqus

Abaqus is a simulation program developed to solve engineering problems of all types. It is fundamentally based on FEM and can solve problems requiring linear and nonlinear analyses. Abaqus is capable of modelling an extensive list of materials, with an extensive list of element types. Within this thesis project, Abaqus was used to generate submodels of the joints for a jacket support structure and to conduct analyses of the jacket support structure subjected to wave loading. This was done through the application of several Abaqus products, specifically Abaqus/Standard, Abaqus/Explicit, and Abaqus/Aqua. A further elaboration on these analysis products for those interested is held in appendix A.

3.4.1. Substructuring with Abaqus

Substructuring in Abaqus is done with the Abaqus/Standard analysis product. As mentioned in section 2.4, the applied substructuring technique is the CB reduction, with the option to also apply the Guyan Reduction if the dynamic effects are not significant in the analysis. When substructuring with Abaqus, a substructure database is created, which is composed of several files that contain the mechanical and geometrical properties of the generated substructure. The files that make up the substructure database

must be located in the same directory as the working directory of the current project. Therefore, whenever a job is submitted, to analyse any model with substructures, the working directory must contain all substructure databases for all substructures in that model. Some significant and useful features of Abaqus substructures include the ability to export the stiffness and mass matrices. The load vectors for applied loads on the substructure can also be exported (Dassault Systèmes, 2019b).

In this thesis project, a structural distributing coupling constraint was used when generating the joint submodels for the wrapped and welded joints. This alternative was chosen over the kinematic coupling constraint for several reasons. When using a kinematic coupling constraint, the coupled nodes are constrained to the rigid body motion of the reference node. In the case of this project, this was undesired because artificial supplemental stiffness was added to the location of the reference node. The coupled nodes were unable to deform relative to each other, which led to a prevention of ovalisation in the case of the end of a tubular member.

The alternative to the kinematic coupling constraint is a distributing coupling constraint. With this constraint, a weight factor is applied to the coupled nodes with respect to the motion of the reference node. This weight factor can then allow load transfer by providing a distribution of force assigned to the coupled nodes. This distribution of nodal forces combines to a resultant force of an equivalent magnitude to the initial force at the reference node. This distributed constraint allows for relative displacement between the coupled nodes, which, in contrast to our previously mentioned example, allows the end of a tubular member to ovalise (Dassault Systèmes, 2019b).

The limitation to the distributed coupling constraint is that it can only be applied to axisymmetric elements when they are undergoing symmetric deformation. Therefore, the cases of traditional shear and bending are captured well, but for cases of asymmetric deformation the coupling constraint would not work. Moreover, for cases of imposed twist on the reference node, the imposed deformation is measured by displacement of the first two local degrees of freedom of the member. Both of these limitations do not apply to the thesis project but were shared for understanding of the reader (Dassault Systèmes, 2019b).

4

Verification

In this chapter, the results found by following the steps presented in section 3.2 will be shown. Through these steps, certain stages of the modelling strategy are verified. The reasoning for why the modelling strategy was verified was to establish that the modelling strategy was reliable, and that the proposed methodology can be applied to a different case study. In addition, the combination of the software being used for this specific application was novel, so having a portion of the work dedicated to verifying the validity of the modelling strategy would be beneficial for all future work. If the method of analysing the structure could be trusted, any differences that would be found between the models with different joint modelling strategies could be attributed to the joint and not the modelling strategy. The stages that were analysed independently for verification purposes include conducting aero-hydro-servo-elastic simulations on an OWT with and without modelling the foundation, submodelling of the joints through applying them to a jacket, and conducting a wave load analysis applied to a jacket structure.

All verification steps were done for the OC4 jacket, which was used as a case study. An introduction of the OC4 jacket will be given in section 4.1. The introduction will serve to give a brief overview of the jacket, including member sizes, environmental conditions, and loading conditions. This is to allow the reader to associate the results from the verification steps with a specific load case and given boundary conditions. The verification steps associated with the aero-hydro-servo-elastic simulations will be presented in section 4.2 and section 4.3.

Section 4.2 will summarise the efforts to verify OpenFAST, by comparing the obtained results from OpenFAST with the results given by Bladed DNV GL. A previous student, Marc van Vliet, under the advisement of Marko Pavlović analysed the OC4 jacket with Bladed DNV GL software in a previous thesis project. His work was focused on analysing the OC4 jacket for fatigue and ultimate limit states, and obtaining the natural frequencies for the jacket structure through a natural frequency analysis (van Vliet, 2019). The results of Marc's previous work were available to be used to verify OpenFAST capabilities of analysing an offshore jacket when compared to the proprietary software Bladed. This also served as a tutorial for the software through verifying the results obtained in OpenFAST.

In section 4.3, the OpenFAST module "ExtPtfm" will be verified. The ExtPtfm module allows the ability to model the foundation of an OWT with a superelement. By comparing a simulation done with a full model of an OWT to a simulation of an OWT with a superelement generated through the ExtPtfm module, the ExtPtfm module itself could be verified. This verification step was necessary to do because the submodelling technique could not be applied when modelling the jacket in OpenFAST. The jacket with submodelled joints can only be introduced to OpenFAST through this module.

The remaining verification steps were held in Abaqus. The first step was to verify the submodelling of the wrapped composite joint and the welded joint. This will be presented in section 4.4. The submodelled joints were applied to the OC4 jacket, and a natural frequency analysis was conducted on the model. This was then compared to the results of a different natural frequency analysis that was done

on the OC4 jacket with rigid joints. This verification was to ensure that the submodelling process was causing the anticipated changes to the overall structural behaviour of the jacket. The second stage of the modelling strategy that was verified in Abaqus was the verification of the Abaqus/Aqua module, which is held in section 4.5. The verification was done by conducting a wave load analysis on the OC4 jacket in Abaqus and comparing it to the previously conducted analyses done with OpenFAST. This verification step was necessary to establish that the method of wave load analysis done by the two software packages (Abaqus and OpenFAST) gave similar results regarding the wave loads imposed on the jacket.

4.1. OC4 jacket

Due to the many aero-hydro-servo-elastic tools available to analyse offshore wind turbines, there was an effort to verify and validate these different simulation tools. This was done in the OC4 project which was a joint effort of academia and industry with 10 countries participating in the project (Popko et al., 2012). The turbine used for the OC4 project is the NREL 5MW offshore baseline turbine. This turbine was made available to all, and had the capacity to work with many available simulation tools (Jonkman et al., 2009). The jacket for the OC4 project, henceforth called OC4 jacket, is a jacket that is inspired from the work of the UpWind project and finalised later by Vorpahl and Popko (Vorpahl et al., 2013).

To give a brief overview of the jacket, the jacket has four legs which are supported by piles. The piles are modelled as clamped at the seabed. The jacket legs are inclined and have four levels of X-braces, which then connect to a TP. The jacket is depicted in figure 4.1.

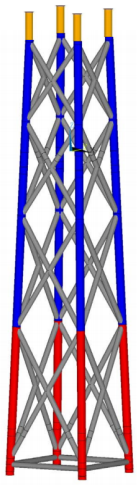

Figure 4.1: OC4 jacket geometry (Vorpahl et al., 2013)

Specific information about the geometry of the jacket is held in table 4.1. Further information about the OC4 jacket is held in appendix B. In this appendix, information about the jacket geometry, tower properties, and the turbine is provided. Along with this, site conditions regarding load cases and marine growth for the jacket members are provided.

Table 4.1: OC4 jacket properties (Vorpahl et al., 2013)

Property set	Component	Colour in figure	Outer diameter [m]	Thickness [mm]
1	X- and mud braces	Grey	0.8	20
2	Leg at lowest level	Red	1.2	50
3	Leg 2nd to 4th level	Blue	1.2	35
4	Leg crossing TP	Orange	1.2	40
5	Pile	Not shown	2.082	60

4.2. OC4 jacket - OpenFAST & Bladed Comparison

To model the OC4 OWT in OpenFAST, the jacket and foundation were modelled with the SubDyn module. The tower and turbine were modelled in the AeroDyn, ElastoDyn, and ServoDyn modules. The wind load was reflected in the AeroDyn module, and the wave loading was reflected in the HydroDyn module. These modules, along with the glue code, are held in the appendix C. In figure 4.2, a visualisation of the analysis conducted with OpenFAST is shown[1].

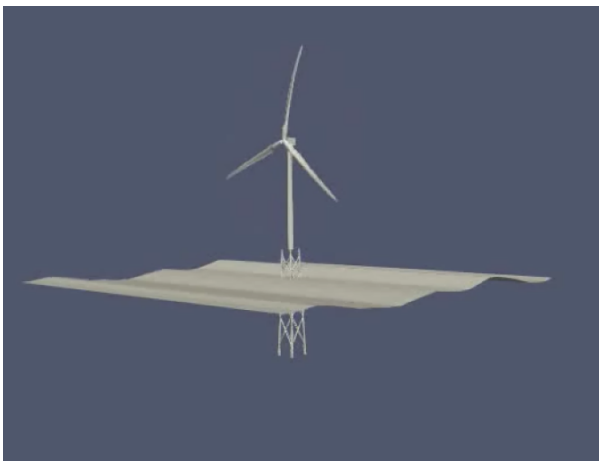

Figure 4.2: OC4 OWT modelled and visualised in OpenFAST

Figure 4.3 depicts the Campbell diagram produced by Popko in a previously mentioned research project that was investigating the effect of submodelling the joints of a jacket structure (Popko et al., 2016). The jacket that was used in the case study was the OC4 jacket. The figure shows the rotor harmonic frequencies for the turbine used with the OC4 jacket, and due to the fact that the turbine used in this thesis project was identical, it was included for clarity. These harmonic frequencies are plotted in figure 4.4 and used as a point of discussion when comparing the Bladed analyses to the OpenFAST analyses.

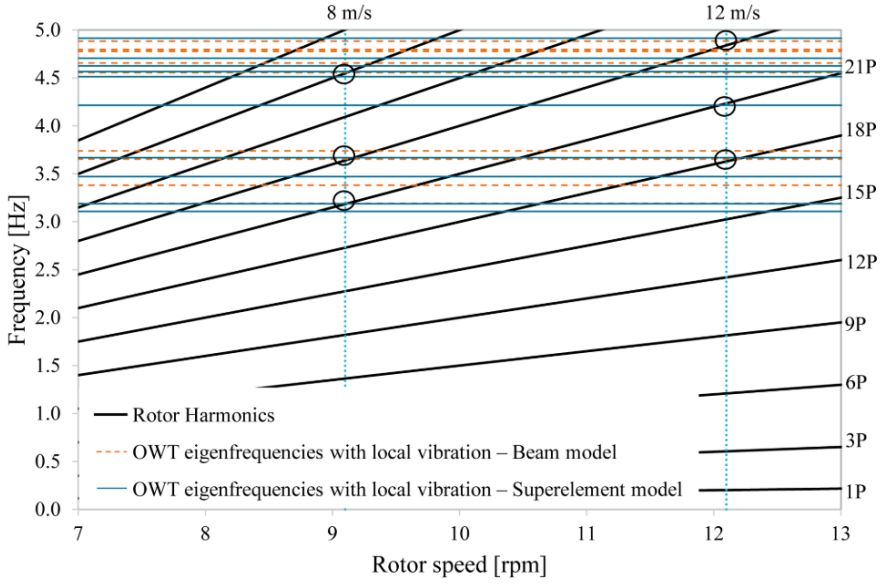

Figure 4.3: Campbell Diagram of OC4 jacket, copied from (Popko et al., 2016)

In Marc's previous work, Bladed was used to analyse the joint loads. Therefore, the joints were also

[1] This is done with the tool "ParaView", which opens the image files generated by the OpenFAST modules, glues them together, and plays a video file by moving through the frames generated by OpenFAST.

analysed with OpenFAST for verification purposes. Both the bottom KK-joint and the bottom X-joint of the OC4 jacket were used as the location to verify the two software packages. These two joints were chosen specifically because the bottom bay usually experiences higher loads, so it is often design critical because of this. Moreover, Marc did not have results for all joints throughout the structure, so the decision for these specific joints was also influenced by Marc's previous decision to analyse these specific joints. Due to the purpose of the analysis being concerned with verifying the software itself and not finding the location with the highest predicted member stress, the decision to analyse the same joints was deemed satisfactory.

In figure 4.4, the frequency response functions of the brace and chord that were analysed are shown for OpenFAST and Bladed. These frequency response functions were obtained through applying a Fourier transform to the results of the time-history analysis of the load case described in table B.4.

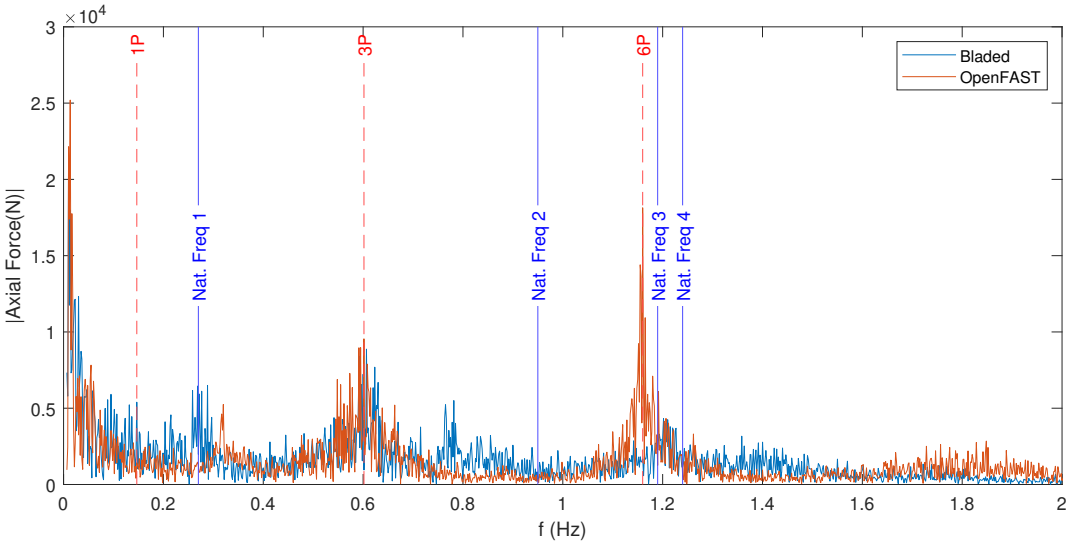

(a) Verification for lowest X-joint - FRF of fatigue load case

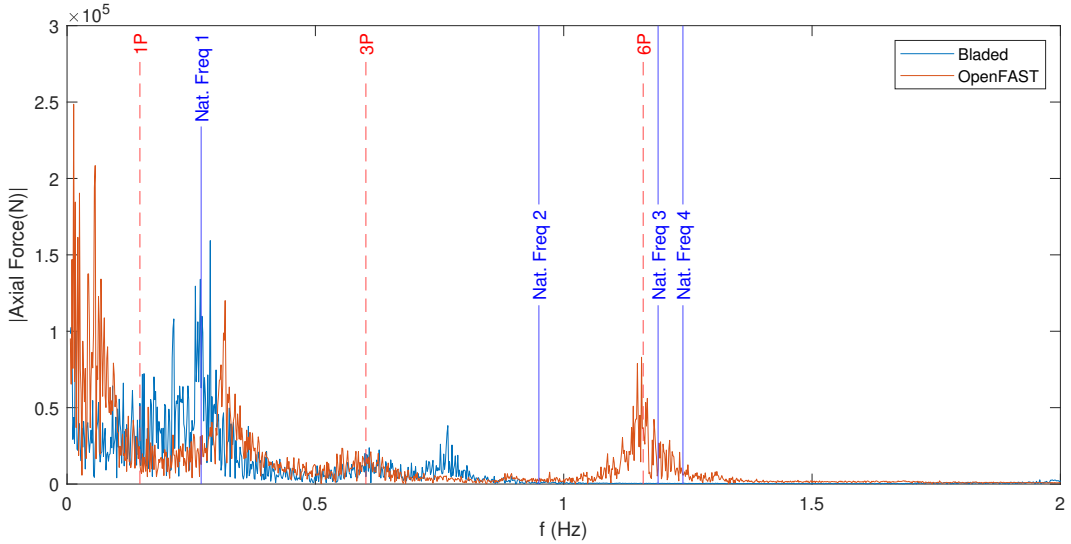

(b) Verification for the lowest KK-joint - FRF of fatigue load case

Figure 4.4: OpenFAST verification

In table 4.2, the first five natural frequencies obtained by Bladed and OpenFast are shown. The percent difference between the two software packages is held in the far right column of the table.

Table 4.2: Bladed and OpenFAST natural frequencies

Mode	Bladed [Hz]	OpenFAST [Hz]	Difference [%]
1	0.27	0.32	15%
2	0.95	0.90	-5%
3	1.16	1.17	1%
4	1.19	1.20	1%
5	1.24	1.31	6%

Overall, the two frequency response functions match quite well. Several phenomena are useful to analyse to evaluate the relative similarities between the two models. These are the natural frequencies, the response to rotor harmonics, and the amplitude of response for the brace and the chord.

Regarding the natural frequencies, the percent difference in the first five modes had an average percent difference of 5%. The percent difference would have been smaller in magnitude, if it were not for the relatively large difference in the first natural frequency. Reasons for this large difference are most likely due to the differences between the two models in how the soil was modelled. In Marc's analysis, he had made changes to the soil properties which lowered the first natural frequency when compared to the UpWind project. The first natural frequency that was obtained with OpenFAST corresponds well with the first natural frequency of the OC4 jacket found in other literature (Popko et al., 2012). So, the relatively large difference in the first natural frequency between the two models can be attributed to the changes made by Marc to the OC4 jacket model prior to the analyses conducted in Bladed, and not attributed to differences in the software packages.

Looking at the response of the jacket to the rotor harmonics, the 1P, 3P, and 6P frequencies are shown in figure 4.4. The 1P frequency for both models did not have a large effect on the amplitude of the response for either the brace or the chord. The peak due to the 3P frequency was found at the same point along the x-axis for both the brace and the chord, which indicated that the response of the OWT was calculated similarly between the two models. The two software packages also gave a similar response with respect to amplitude for the brace (reference figure 4.4a), and the chord (reference figure 4.4b). Taking into account that the y-axis for the chord is a factor of 10 larger, there is an approximate increase to a local maximum of $1 * 10^4[N]$ and $2.5 * 10^4[N]$ for the brace and chord respectively for both models. Due to the experienced similar amplitude in the frequency response function for the brace and the chord due to the rotor harmonic frequencies, and that the rotor harmonics were experienced at similar frequencies, the similarity between the two software packages was supported.

Regarding the 6P frequency, there were some significant differences between the two software packages. In the case of the chord, the differences are more pronounced. It can be seen clearly in figure 4.4b that there was no resulting response from the 6P rotor harmonic. However, for the case of OpenFAST, there was a resulting peak that was of similar magnitude to the peak found for the first natural frequency. Looking at the case of the brace, it can be seen that for both software packages the 6P rotor harmonic had an effect, but the amplitude obtained by OpenFAST was approximately four times larger than the force amplitude obtained by Bladed.

The large differences found for the 6P harmonic frequency between the two software packages could be due to several reasons. The 6P frequency aligns with three of the natural frequencies shown previously in table 4.2 (mode 3-5). The descriptions for the mode shapes were "support structure side-side rotational attachment mode", "support structure torsional rotational attachment mode", and "support structure fore-aft rotational attachment mode" (van Vliet, 2019). These mode shapes are more heavily influenced by the soil stiffness due to the "rocking phenomenon" experienced by jacket structures as mentioned in section 2.3.1.

Unlike monopiles, jacket structures primarily transfer the imposed environmental loads through axial forces carried by the piles to the foundation. A change in the stiffness of the soil has a large effect on this load transfer, which is seen by the development of a rocking mode. The rocking mode is usually found to have a natural frequency near other higher order bending modes of the tower (Bhattacharya,

2019). Because of this, it is assumed that the differences seen in the response to the 6P rotor harmonic between the two software packages can be attributed to the differences in soil modelling.

The Bladed model had highly detailed soil spring stiffnesses applied due to the piles. In the OpenFAST model, the jacket legs were modelled as fixed at the top of the soil or they were approximated with a 6x6 SSI matrix obtained from an OpenFAST example file. The soil stiffness modelling in OpenFAST was not done in a sophisticated way due to the desire to verify whether the two programs would offer a similar analysis, while at the same time being efficient with time. It was assumed that modelling the soil stiffness in a less sophisticated fashion in OpenFAST would still allow the two software packages to be compared in a fair manner regarding the overall prediction of the structural response for a given load case.

Other causes for the differences between the two software packages could be attributed to different magnitudes of applied structural damping and imposed wind loading. The damping in the Bladed model was higher, which could be the cause for the less pronounced peaks seen in the amplitude of the response for the higher frequencies (damping has a more pronounced effect on higher modes). Additionally, the wind loading was stochastically determined. In all cases, this leads to a nonlinear variation in the response spectrum due to unsteady rotor speeds due to the varying wind-speeds (Popko et al., 2016). The wind-speed and rotor speed of a typical OpenFAST analysis can be seen in figure 4.5. If interested in verifying the way the software packages incorporate rotor harmonics, the wind load must be applied with a steady wind speed. These analyses were not done in Bladed, so the stochastic wind load was used. This obscures the results and removes the ability to do a direct comparison between the two software packages.

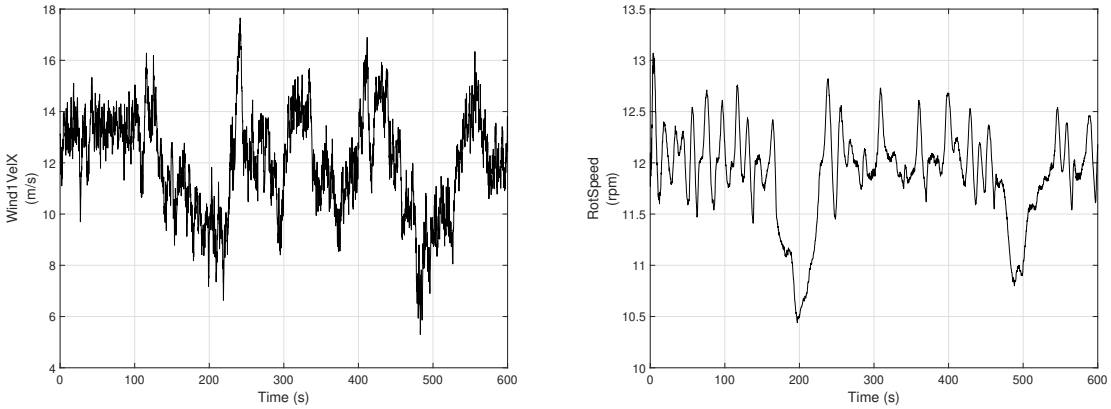

(a) Wind-speed during OpenFAST simulation

(b) Rotor Speed during OpenFAST simulation

Figure 4.5: OpenFAST results of stochastic wind loading

4.2.1. OpenFAST Verification - Summary

Taking the previously mentioned modelling differences into account, regarding the modelled soil properties, applied damping, and intrinsic irregularities respective to the stochastic wind load, the two software packages were deemed satisfactorily similar for this thesis project. This assumption is made primarily due to the similarities found with the natural frequencies, forcing amplitudes given by the frequency response function, and the structural response to the rotor harmonic frequencies (exempting the 6P frequency).

This assumption is also paired with a qualifier. The similarity between the two software packages is accepted because the primary intended use of the aero-hydro-servo-elastic simulations is to generate a time-history of the forcing and displacement found at the interface point. The main purpose of the analyses conducted in this project is to analyse the joints applied to the jacket. Therefore, a small difference between the two software packages is acceptable because there are already several levels

of abstraction in the analysis, and with these abstractions the degree of accuracy is reduced. Firstly, the load at the interface point of the aero-hydro-servo-elastic simulation of the jacket is an abstraction of the loads at the individual members of the jacket. The second abstraction is when transferring the joint loads to the submodel of the joint. Due to this multilevel abstraction, the desired level of accuracy of the interface forces and moments are deemed to be satisfied with OpenFAST.

4.3. ExtPtfm module verification

The next verification for OpenFAST was to apply the ExtPtfm module and ascertain if similar results were obtained with the ExtPtfm module when compared to an analysis with the full model in OpenFAST. This verification was desired due to the requirement to model the joints as submodels when modelling the jacket. This is not offered traditionally by OpenFAST, but can be done with the ExtPtfm module. A model was made, called the ”superelement model” henceforth, by taking the loading history from the full model case and combining it with the exported mass, stiffness, and damping matrix of the OC4 jacket. This was used to form the superelement with the ExtPtfm module, which was then used in a separate OpenFAST aero-hydro-servo-elastic simulation. The results of both time-history analyses at the interface point for the full model and the superelement model are plotted in figure 4.6 and 4.7.

Figure 4.6 holds the results of the time-history analysis with respect to forces at the interface point, and figure 4.7 holds the results with respect to moments at the interface point. In both figures, the model with the ExtPtfm module applied (superelement) is plotted against the original model with the entire substructure modelled (full model).

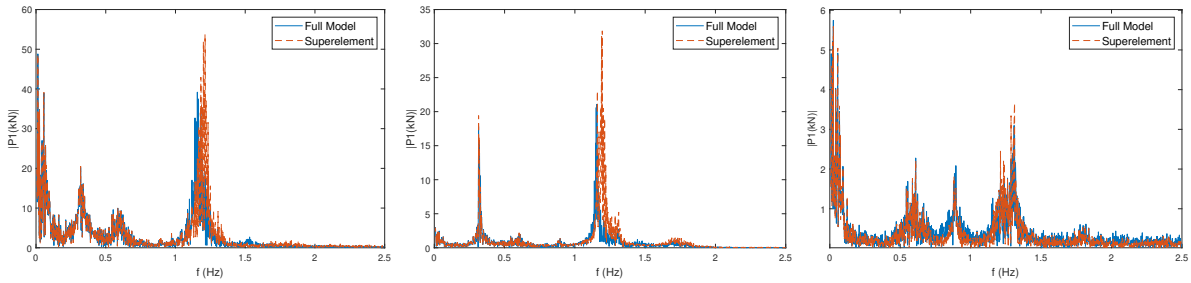

(a) Interface force in X-direction **(b)** Interface force in Y-direction **(c)** Interface force in Z-direction

Figure 4.6: OpenFAST verification of ExtPtfm - Interface point forces

As can be seen in figure 4.6, there is a good correspondence in all three force directions at the interface point for the superelement and the full model. The two match well with respect to natural frequencies, response to rotor harmonics, and relative amplitudes at these given frequencies. In table 4.3, the magnitudes of the frequency response functions for the different force directions for the first five modes are shown. The percent differences at these given frequencies are shown in the far right column of the table, with the average absolute percent difference shown for each force direction.

Across all force directions, there is a good correspondence with respect to natural frequencies. The difference was on average less than 1% for all three directions. If there was a change in the observed natural frequency, the superelement model would have higher natural frequencies than the full model. Regarding the magnitude of forcing, there were some differences observed. The superelement model would predict different magnitudes of forcing with an average absolute percent difference larger than 25% for the three force directions. One specific mode for a given direction had up to a difference of 80% (mode 3, x-direction).

Possible reasons for the differences in the interface forces between the two models could be due to the superelement being created through a Guyan reduction. This substructuring technique causes the superelement to be more susceptible to higher resonance peaks due to the lack of inertial damping. This loss of inertial damping makes the system stiffer with respect to its mass and leads to higher amplitudes resulting from the applied forcing and excitation due to rotor harmonics. This can be seen

Table 4.3: Full Model and Superelement frequency response function for interface force amplitudes for modes 1-5

Dir	Mode	Full Model		Superelement		Difference [%]	
		Freq [Hz]	Amp [kN]	Freq [Hz]	Amp [kN]	Freq [Hz]	Amp [kN]
X-Dir	1	0.32	17.81	0.32	19.42	0.0%	8.6%
	2	0.90	1.36	0.90	1.38	0.0%	1.0%
	3	1.17	9.82	1.17	23.02	0.0%	80.4%
	4	1.20	21.07	1.20	31.87	0.0%	40.8%
	5	1.31	2.75	1.31	5.26	0.0%	62.6%
					X-Dir Average:	**0.0%**	**38.7%**
Y-Dir	1	0.32	20.23	0.32	20.53	1.6%	1.5%
	2	0.90	2.26	0.90	3.66	0.0%	47.2%
	3	1.17	32.69	1.18	42.98	0.8%	27.2%
	4	1.20	39.19	1.21	53.74	1.4%	31.3%
	5	1.31	4.70	1.31	9.22	0.0%	65.0%
					Y-Dir Average:	**0.8%**	**34.4%**
Z-Dir	1	0.32	0.36	0.32	0.29	0%	-21%
	2	0.90	2.09	0.90	1.52	0%	-31%
	3	1.17	0.72	1.17	0.94	0%	26%
	4	1.20	1.74	1.21	2.46	1%	34%
	5	1.31	3.10	1.31	3.66	0%	17%
					Z-Dir Average:	**0.3%**	**25.7%**

visually in figure 4.6, with the interface force having a larger amplitude for the superelement at the first natural frequency (0.32 Hz) and at the 6P frequency (1.16 Hz).

For the first two modes in the z-direction, the force at the interface point was smaller for the superelement. For these two modes, the absolute difference in magnitude was small between the full model and the superelement, and the relative magnitude of the force with respect to the other two directions was small. Due to this, even though the percent difference is large for these two modes, the difference can be assumed to be negligible with respect to the entire structural response of the OWT because of the relatively small forcing magnitude respective to the z-direction when compared to the force respective to the x-direction and y-direction.

In figure 4.7, the results of the time-history analysis with respect to moments at the interface point are shown.

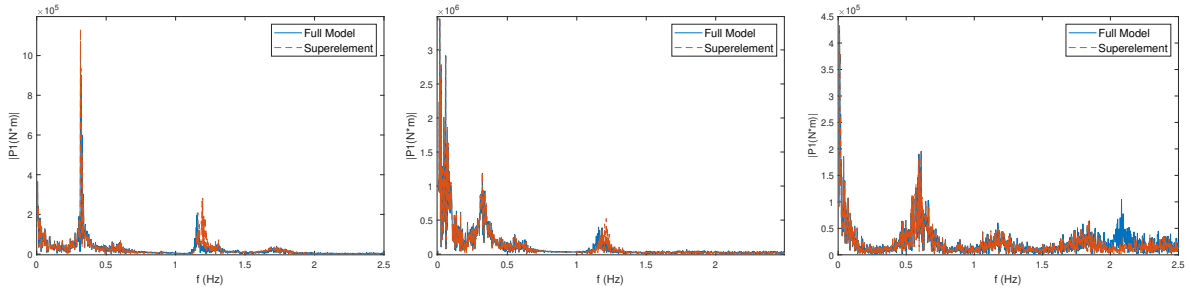

(a) Interface moment in X-direction **(b)** Interface moment in Y-direction **(c)** Interface moment in Z-direction

Figure 4.7: OpenFAST verification of ExtPtfm - Interface point moments

As can be seen in figure 4.7, there is a good correspondence in all three moment directions at the interface point for the superelement and the full model. The two match well with respect to natural frequencies, response to rotor harmonics, and relative amplitudes at these given frequencies. In table 4.4, the magnitudes of the frequency response functions for the different moment directions for the first five modes are shown. The percent differences at these given frequencies are shown in the far right column of the table, with the average absolute percent difference shown for each moment direction.

Across all moment directions, there is a good correspondence with respect to natural frequencies. The difference was on average less than 1% for all three directions. If there was a change in the observed natural frequency between the two models, the superelement model would have higher natural frequen-

Table 4.4: Full Model and Superelement frequency response function for interface moment amplitudes for modes 1-5

Dir	Mode	Full Model		Superelement		Difference [%]	
		Freq [Hz]	Amp [kN*m]	Freq [Hz]	Amp [kN*m]	Freq [Hz]	Amp [kN*m]
X-Dir	1	0.32	1039.0	0.32	1131.0	0.0%	8.5%
	2	0.90	15.5	0.90	10.9	0.0%	-35.0%
	3	1.17	79.9	1.17	148.9	0.2%	60.3%
	4	1.20	56.2	1.20	280.7	0.0%	133.2%
	5	1.31	57.2	1.31	72.7	0.0%	23.8%
					X-Dir Average:	**0.0%**	**52.2%**
Y-Dir	1	0.32	1184.0	0.32	1196.0	1.6%	1.0%
	2	0.90	42.0	0.90	34.5	0.0%	-19.7%
	3	1.17	349.2	1.18	346.8	0.8%	-0.7%
	4	1.20	212.1	1.21	522.9	1.4%	84.6%
	5	1.31	76.4	1.33	93.9	1.2%	20.5%
					Y-Dir Average:	**1.0%**	**25.3%**
Z-Dir	1	0.32	19.9	0.32	16.5	0%	-19%
	2	0.90	29.1	0.90	27.3	0%	-6%
	3	1.17	60.2	1.17	49.1	0%	-20%
	4	1.20	43.3	1.21	43.6	1%	1%
	5	1.31	31.2	1.31	21.6	0%	-36%
					Z-Dir Average:	**0.3%**	**16.5%**

cies than the full model. Regarding the magnitude of forcing, there were several differences observed. The superelement model predicted different magnitudes of moments than the full model for the three directions. The minimum average absolute percent difference was in the z-direction with a magnitude of 16.5%. The largest average absolute percent difference was in the x-direction with 52%. Certain modes for a given direction had up to a difference of 133% (mode 4, x-direction). Potential reasons for these differences are the same reasons stated for the interface point forces.

4.3.1. ExtPtfm Verification - Summary

Overall, the verification for the ExtPtfm module was satisfactory. The purpose of the verification was to determine if using the ExtPtfm module in OpenFAST would yield similar interface forces and moments for a given time-history analysis. The ExtPtfm module was able to capture the natural frequencies of the structure with small differences when compared to the full model. Regarding the magnitude of the interface forces and moments, ExtPtfm would most often overpredict the response, which yielded a conservative response. It is proposed that these conservative measurements predicted by the ExtPtfm module would be corrected through the use of the Craig-Bampton reduction method. In future analyses, the Craig-Bampton reduction will be used to include the internal DOF respective to the eigenmodes of the jacket. This would allow the analysis to consider inertial damping effects. Furthermore, efforts to model the foundation in a more accurate way will be taken in the 10MW model for the jacket.

Moreover, the intended purpose of the OpenFAST simulation is not to capture the structural response of the OWT with the highest degree of accuracy, but rather simulate the entire structural response and have it relate back to the jacket through the interface point. The point of interest would be a specific joint that controls the design with respect to imposed forces, moments, or displacements. Therefore, due to the main object of the analysis being the joint, the differences found at the interface point can be ruled to be acceptable.

4.4. Joint submodelling verification

An essential step of the overall modelling strategy (reference figure 3.1) is to create submodelled joints and include them in the analysis of the jacket. By submodelling the joint, a higher degree of accuracy can be introduced at the joint level of the structure. Furthermore, through applying this method, the individual effect of the joint stiffness on the structural response of the jacket, and the entire OWT, can be measured. To pursue this modelling strategy, there first must be a step to verify whether the inclusion

of joint submodels in the jacket model is possible, and that when the joint submodels are included that they are having the intended effect. This is essential to do in a step-by-step manner so that when the joint submodels are included in future analyses, they can be included with the intent to draw conclusions from their inclusion to the model. The certainty that the joint submodels can be trusted as a high fidelity option when modelling can be achieved through this verification.

The first verification will serve to evaluate how the submodelled joint for the wrapped and welded alternative affects the local joint stiffness. This will be done through conducting a natural frequency analysis on the individual joints for both joint alternatives and looking at the obtained eigenfrequencies and mode shapes. The second verification will include a second natural frequency analysis for the joints when applied to a jacket model. In this verification, a control jacket model will also be included that will have the joints modelled as rigid joints.

4.4.1. KK-joint submodel - natural frequency analysis

To carry out the first verification, the first step was to create the submodelled joint for both joint alternatives. This was done by generating the joint geometry in Autodesk Inventor and importing the geometry to Abaqus. Then, the contact pairs for the steel and FRP material were determined, and the mesh size was determined. The contact pairs were generated locally within the joint model in Abaqus. The faces of two materials making contact were associated as contact pairs. The mesh size was set to a refinement level that allowed accurate deformation when looking at the global joint behaviour. Other research members in the team under the advisement of Marko Pavlović have applied finer mesh sizes than were applied in this thesis project. The rougher mesh size used in this thesis project was selected because the conducted analyses were done in the linear regime, which led to no failure processes being dependent on stress or strain concentrations. Due to this, a mesh size of approximately 50-100 mm was determined to be acceptable. If an investigation was to be done into the failure modes of a specific joint, when pursuing an analogous analysis to the one conducted in this thesis project, the mesh would need to be refined.

Once the joint model properties were finalised, the submodels were created in a series of steps. First, the nodes lying on the longitudinal axes of the brace and chord members on the plane perpendicular to the end of the members were retained. This is shown in figure 4.8a, with the reference points being the previously mentioned nodes that were retained. These nodes would then be joined with beam members when placed in the jacket model. In figure 4.8b, the KK-joint submodel is shown for completeness.

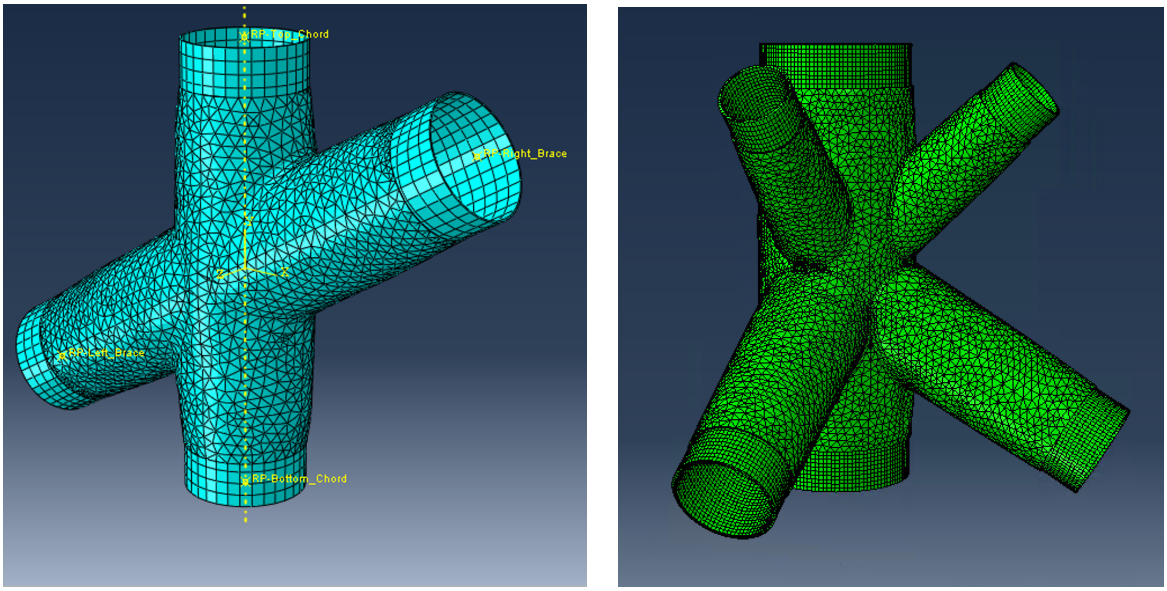

(a) X-joint submodel **(b)** KK-joint submodel

Figure 4.8: Joint submodels

After generating the joint submodels, the behaviour of the joint submodels was verified. This was especially important because the constraints that were used in earlier iterations of the submodelling process added artificial stiffness to the model. The ends of the members were not allowed to deform, so the chords and braces were not ovalising. Therefore, to verify that the joints were exhibiting the intended behaviour, a natural frequency analysis (NFA) was done for two cases: a wrapped joint alternative and a welded joint alternative. A screen capture of the results of these two cases are held in figure 4.9.

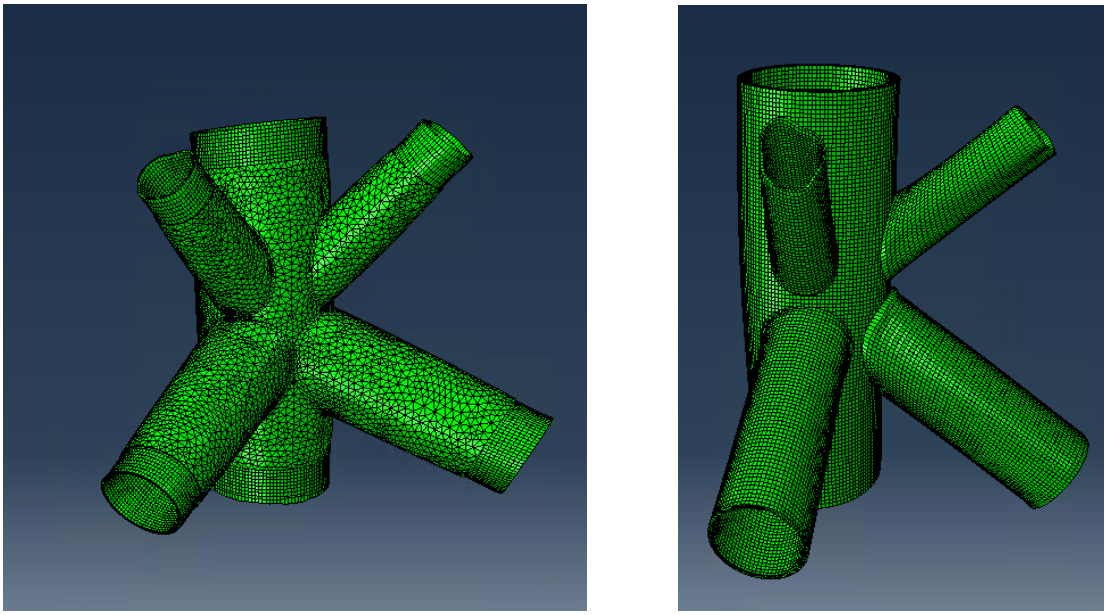

(a) Wrapped alternative KK-joint submodel - NFA **(b)** Welded alternative KK-joint submodel - NFA

Figure 4.9: Natural Frequency Analysis of submodelled joints

The two joint alternatives were analysed for the first ten modes. The results of the analysis are held in table 4.5. For the first ten modes, the eigenfrequency is reported along with the percent difference between the welded and wrapped alternatives. Mode shapes for modes 1-10 for both the welded and wrapped alternatives are held in Appendix D.

Table 4.5: KK-joint verification - mode 1-10

Mode	Wrapped [Hz]	Welded [Hz]	Difference [%]
1	40.6	41.3	-1.7%
2	41.4	41.6	-0.4%
3	49.8	45.7	8.9%
4	58.9	53.8	9.5%
5	62.1	55.6	11.5%
6	81.5	64.0	27.3%
7	91.8	79.2	16.0%
8	98.3	84.4	16.5%
9	102.0	85.4	19.4%
10	112.2	95.3	17.7%

The results of the NFA were promising. The joint submodels have similar mode shapes for the first ten modes, and the frequencies are similar in magnitude. Excluding the first natural frequency, the wrapped joint alternative of the KK-joint had higher natural frequencies. On average, the wrapped joint alternative had eigenfrequencies that were 11.7% higher than the welded joint alternative. This logically follows because the wrapped joint alternative is purportedly stiffer than the welded joint alternative. The magnitude of the increase in natural frequency was larger for the higher modes than for the lower modes. This behaviour was also expected because with the higher modes, there is a larger propensity for the steel members to have a mode shape with ovalisation. The wrap material present in the wrapped joint alternative reduces the ovalisation of the steel members due to the composite material functioning as a local stiffener to the steel members.

The two modes with the largest difference in eigenfrequency between the two joint alternatives were mode 6 and mode 9, with a difference of 27.3% and 19.4% respectively. These modes can be seen in figure 4.10 and figure 4.11. For both modes, the welded alternative is experiencing a relatively high degree of ovalisation when compared to the wrapped alternative.

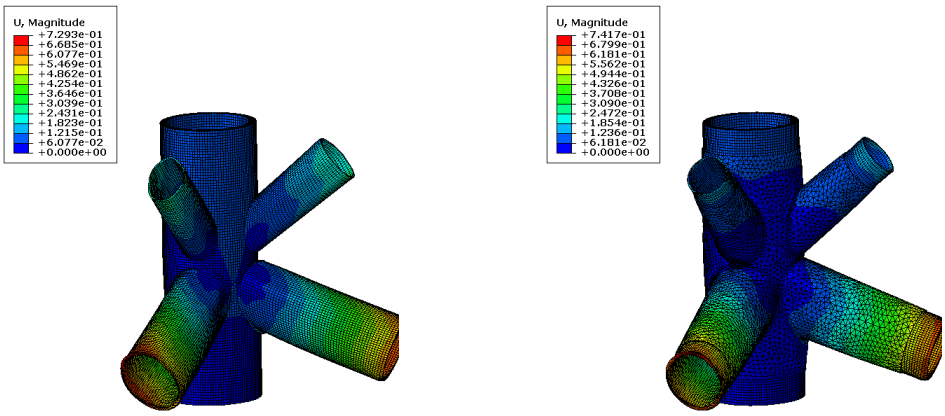

(a) Mode 6 - Welded

(b) Mode 6 - Wrapped

Figure 4.10: KK-Joint - Mode 6

Due to the high similarity in mode shapes between the two models for the first ten modes, and the similar range of magnitude for the obtained eigenfrequencies, it was determined that it was sufficient to claim that the submodelled joints were behaving as expected.

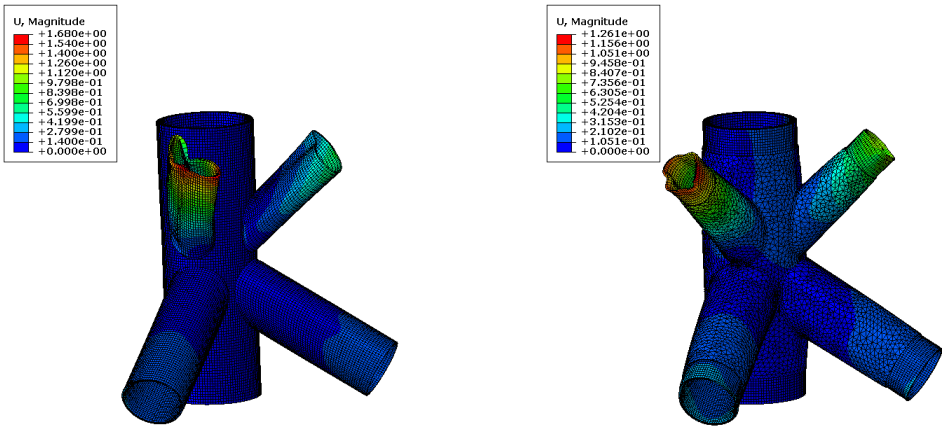

(a) Mode 9 - Welded **(b)** Mode 9 - Wrapped

Figure 4.11: KK-Joint - Mode 9

4.4.2. NFA of OC4 jacket - Wrapped and rigid joint alternatives

The second step for verifying the substructuring process was to apply the joints to the OC4 jacket. Two OC4 jacket models were made. The first model had wrapped joint submodels applied to all X-joints present in the jacket. The second model had the X-joints in the jacket modelled as rigid joints. Both models were then compared through conducting an NFA for both jackets. The eigenfrequencies obtained by the NFA for the modes that involved the largest local displacements of the braces are shown in table 4.6, and the mode shapes are shown in figure 4.12 and 4.13.

The results were promising for this verification. The wrapped joint submodels introduced more joint flexibility than rigid joints. This was reflected by the jacket that had the wrapped joint submodels having lower natural frequencies for all modes. When looking at the mode shapes, there was no mode switching between the two models. This was expected because the joint submodels should not have introduced such a large difference to the global stiffness of the jacket that there would be mode switching between the two OC4 jackets. This was a confirmation that the joints were deforming as expected. This served the purpose to verify the step of applying the wrapped composite joints to the jacket.

Table 4.6: NFA for OC4 jacket with submodelled joints and rigid joints

Mode	Wrapped [Hz]	Rigid [Hz]	Change [%]
1	2.6	2.7	2.1%
5	7.8	8.1	3.7%
10	9.7	10.0	2.8%

4.4.3. Joint submodel Verification - Summary

Joint submodels for both the wrapped and welded alternatives were created and verified in Abaqus. Through a natural frequency analysis, the wrapped and welded joint submodel alternatives for KK-joints were compared with respect to the obtained eigenfrequencies and mode shapes. The two were found to have similar mode shapes, with the welded alternative experiencing larger deformations and lower eigenfrequencies when compared to the wrapped joint alternative.

Two OC4 jackets were created, one with wrapped joint submodels and one with rigid joints. Through a natural frequency analysis, the two jackets were compared with respect to their eigenfrequencies and mode shapes. In this case, the jacket with wrapped joint submodels had lower eigenfrequencies for all

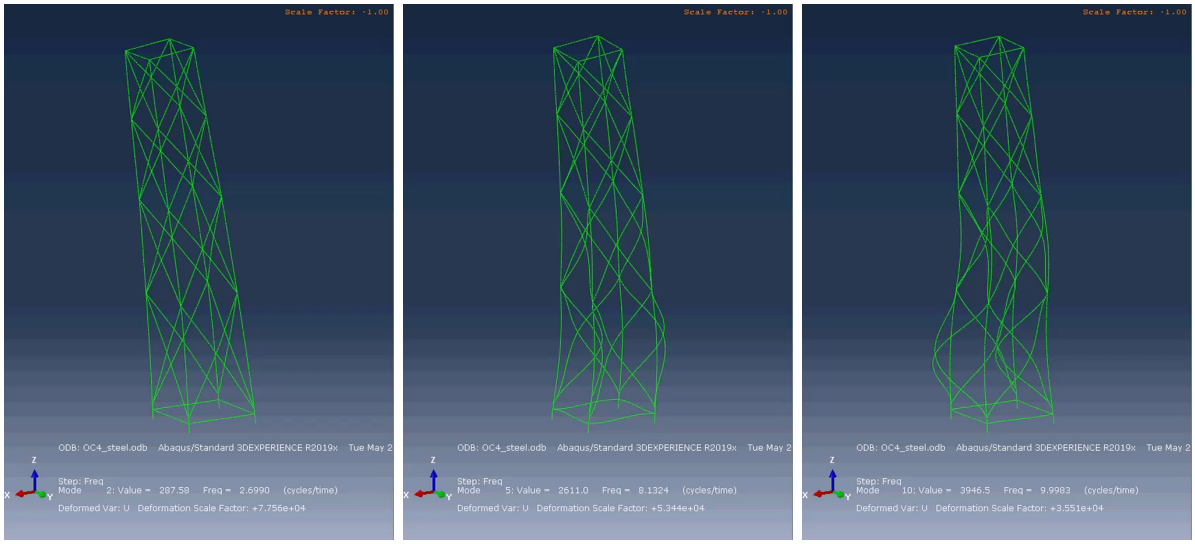

(a) OC4 jacket - Mode 1 **(b)** OC4 jacket - Mode 5 **(c)** OC4 jacket - Mode 10

Figure 4.12: OC4 mode shapes - welded alternative

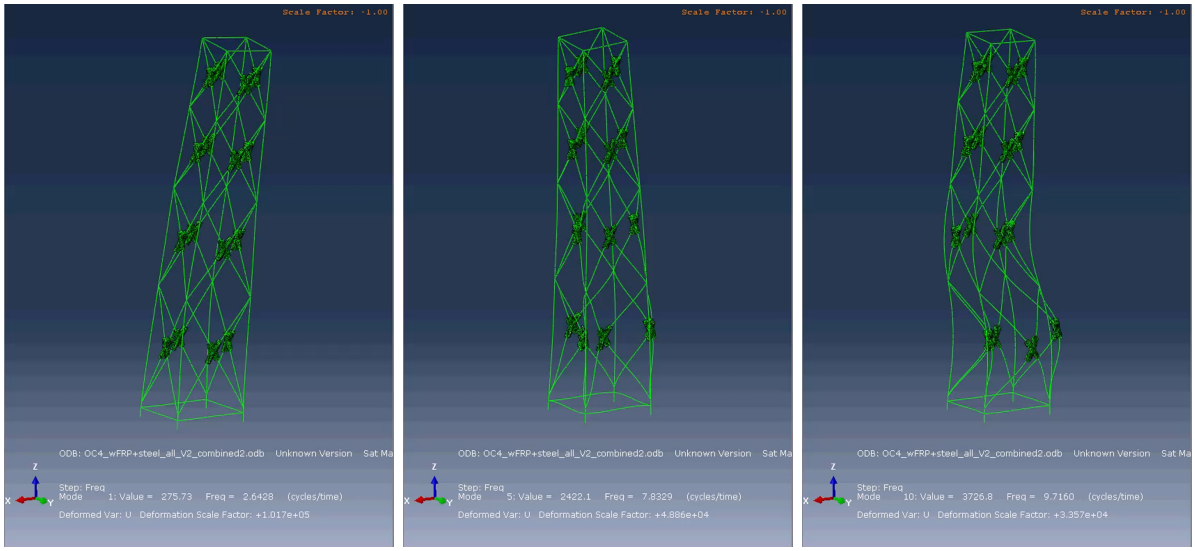

(a) OC4 jacket - Mode 1 **(b)** OC4 jacket - Mode 5 **(c)** OC4 jacket - Mode 10

Figure 4.13: OC4 mode shapes - wrapped composite alternative

modes when compared to the jacket with rigid joints. This confirmed that including joint submodels would have a perceivable effect, and that it would increase joint flexibility in an expected manner.

4.5. Wave load analysis verification

The last step of the verification process was to verify the use of Abaqus to conduct a dynamic wave load analysis. To conduct a sequentially coupled analysis on a jacket-supported OWT, the last step of the iterative process is to analyse the jacket with a wave load analysis. During the wave load analysis, a boundary condition at the interface point is imposed. The boundary condition includes the results from the aero-hydro-servo-elastic simulation. With this imposed boundary condition, a wave load analysis is conducted to analyse the jacket members.

As mentioned in appendix A.2.3, Abaqus/Aqua is an analysis product that allows the ability to model

wave loads. It was desirable to use this analysis product, because when using Abaqus, the joint sub-models could be incorporated in the jacket. Abaqus/Aqua was used to simulate a wave load case for the OC4 jacket. A snap-shot of the analysis is held in figure 4.14[2].

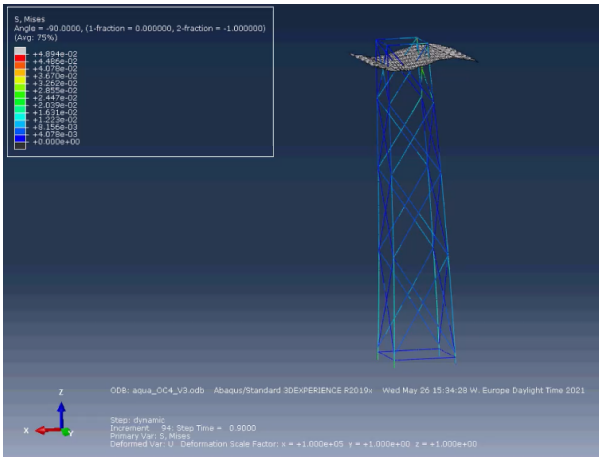

Figure 4.14: OC4 jacket modelled in Abaqus — wave loading applied with Aqua module

To verify the wave load analysis, the analysis conducted with Abaqus was compared with an analysis done with OpenFAST. Similar loading conditions were set for both programs, and the results were analysed at a specific point to compare the two software packages. A brace member in the third bay along the height of the jacket on the face pointing to the direction of the wave propagation was chosen to be the representative member.

The result of the comparison between the two programs is held in figure 4.15. Wave loading is traditionally composed of three types of loads: drag loads, fluid inertia loads, and buoyancy loads. The drag load was chosen to be compared for these analyses because it was the easiest to post-process. There is uncertainty of whether the other hydro-dynamic loads are also of the same magnitude between the two programs, but looking just at the drag load as shown in the figure, the two programs correspond well with respect to the force amplitude experienced at the brace.

One difference between the two software packages is the discrepancy between periods for the two loads. This was due to different significant digits being used to determine the wave period for the loading between the two programs, which led to a small difference growing with time as the analysis progressed. Within the analysis programs, there was no inherent difference. This overall served as confirmation that the Abaqus/Aqua module could be used to analyse a jacket as the first and last step of a sequentially coupled analysis of the OWT.

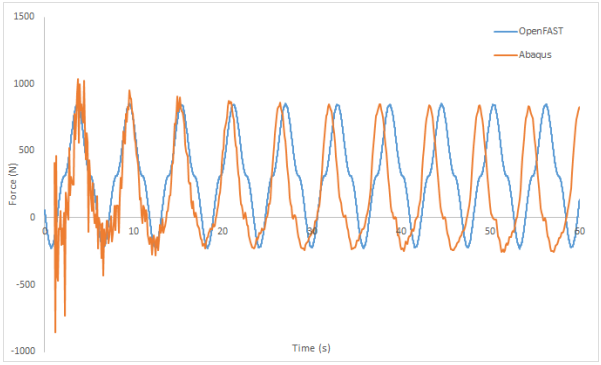

Figure 4.15: OpenFAST/HydroDyn compared to Abaqus/Aqua for X-Joint in OC4 jacket

[2]The surface at the top of the structure is representing the height and the shape of the wave loading. The axis in the direction of the wave propagation is scaled more than the vertical axis to visualise the deformation from the loading.

III

Analysis and Results

5

Case Study - 10MW INNWIND.EU

INNWIND.EU is a project that is a successor of the UpWind project. Its main goal was to accelerate the development of the offshore wind market. This was done through different work packages dedicated towards a certain aspect of the program. The fourth work package WP4, was concerned with offshore support structures. In this work package, the main goal was to deliver innovative jacket designs for turbines of 10-20MW size.

In figure 5.1, a conceptual drawing of the jacket is shown. Similar to the OC4 jacket, the jacket has X-joints for the braces, and KK-joints connecting the braces to the chords. The beams are tubular sections, and the joints are traditionally modelled with LJF equations approximating the joint stiffness. The jacket is supported by piles, and the piles are modelled with pile-soil interaction using p-y, t-z, and q-w soil load-deformation curves to represent the soil stiffness.

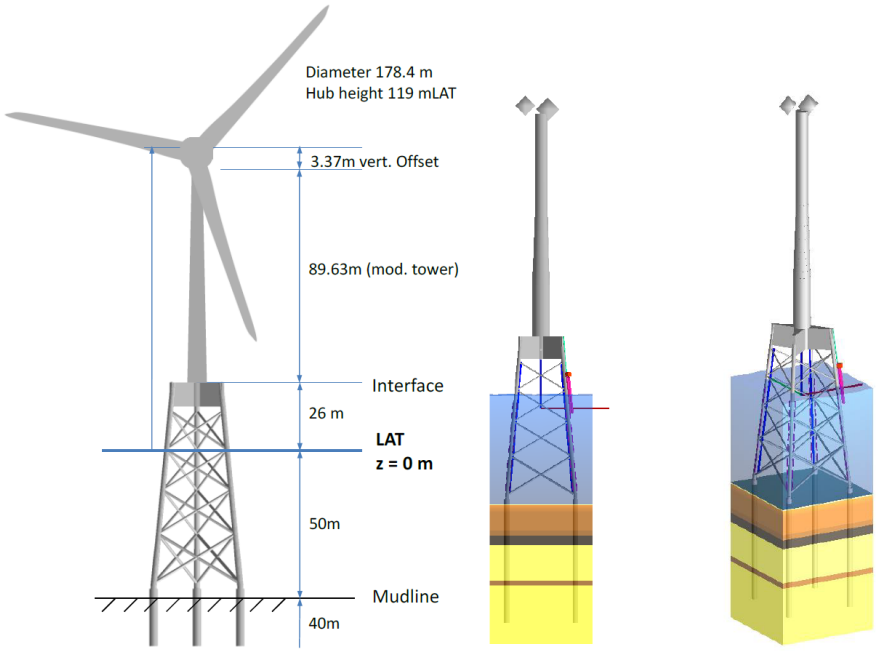

Figure 5.1: INNWIND 10MW jacket (Stolpe et al., 2016)

In the INNWIND.EU report, detailed information about the jacket, the tower, and the turbine is provided. These are reprinted in appendix E for clarity. These dimensions were used as a starting point for modelling the jacket in Abaqus.

5.1. INNWIND.EU, D4.34 - jacket - NFA

Using the previously mentioned annex in the INNWIND.EU report for the dimensions of the jacket, tower, and piles, the jacket support structure was modelled in Abaqus. Simultaneously, the KK-joints and X-joints of the jacket were created to have the same dimensions of the joining braces and chords to have alignment at the joint. With the submodels for the joints made, three versions of the jacket were made: one with welded joint submodels, one with wrapped joint submodels, and one with rigid joints. With these three versions of the jacket support structure, an NFA was done to analyse the effect of the joint submodels. The models are shown in figure 5.2. The submodelled joints are represented as a void, but they are present in the model. Because the submodels are represented as void, and because the jacket models are identical exempting the joint submodels, only one of the jackets with joint submodels is shown.

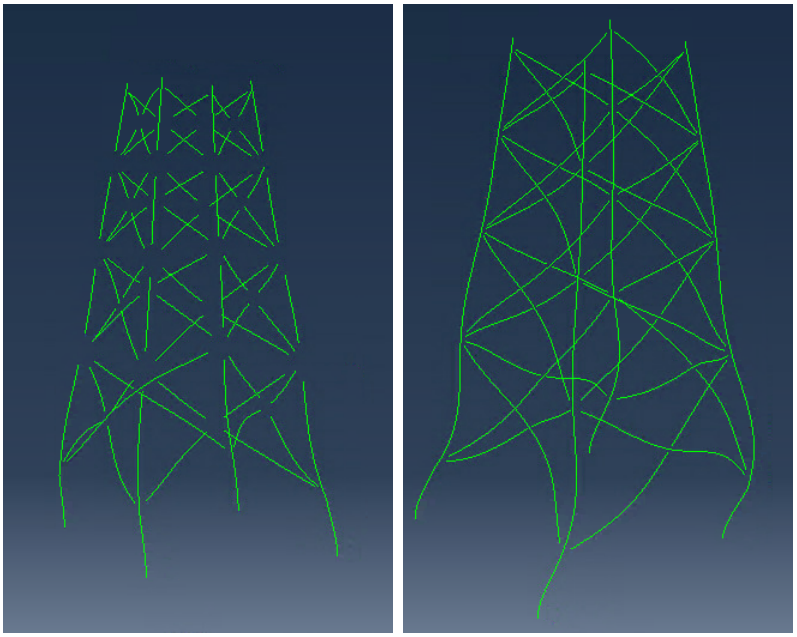

(a) INNWIND jacket - joint submodels **(b)** INNWIND jacket - Rigid joints

Figure 5.2: INNWIND Jacket

The jacket with submodelled joints is held in figure 5.3.

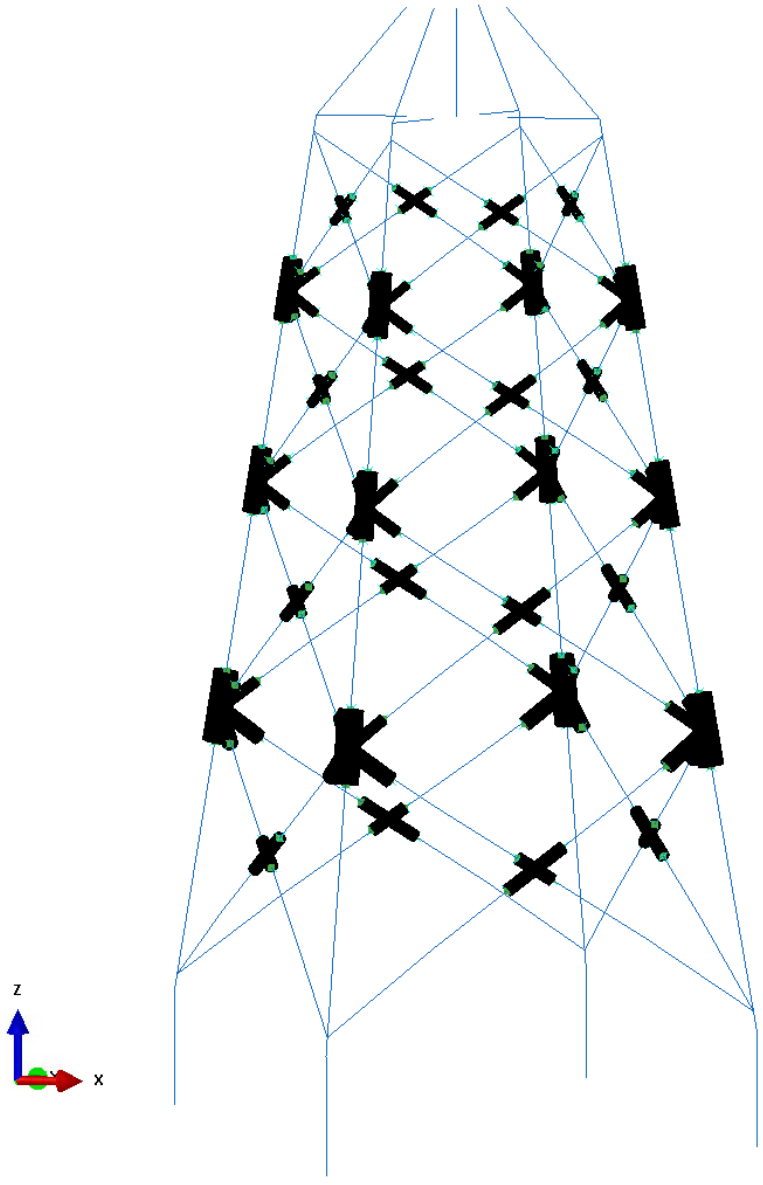

Figure 5.3: INNWIND jacket with submodelled joints

The results of the natural frequency analysis are held in table 5.1. Each version of the jacket is represented by a column, with the rigid model on the left, the welded model in the middle, and the wrapped model on the right. The natural frequencies respective to the first twenty modes are held in this table.

Table 5.1: 10MW jacket NFA for rigid, welded, and wrapped composite joints

Mode	Rigid [Hz]	Welded [Hz]	Wrapped [Hz]
1	2.79	2.63	2.61
2	2.79	2.65	2.63
3	2.83	2.65	2.63
4	3.49	3.30	3.27
5	3.84	3.65	3.65
6	4.84	4.15	4.20
7	4.84	4.34	4.38
8	4.94	4.60	4.63
9	5.58	4.70	4.80
10	6.00	5.00	5.14
11	6.00	5.10	5.23
12	6.29	5.27	5.49
13	6.71	5.60	5.70
14	6.82	5.95	6.11
15	6.82	5.98	6.13
16	7.05	6.40	6.73
17	7.97	6.75	6.79
18	7.97	7.19	7.32
19	8.18	7.20	7.33
20	8.22	7.61	7.72

Some important things to note for the results of the analysis for these three versions of the jacket. Firstly, the models with joint submodels (welded and wrapped) have lower eigenfrequencies than the model with rigid joints for all twenty modes. This logically follows, because the models with joint submodels are less stiff than the model with rigid joints. Moreover, when examining the differences in the natural frequencies for the three models, the differences between the model with rigid joints and the models with submodelled joints on average increases as you increase in mode number. Again, this logically follows because these higher modes are influenced more by the displacement of the braces. This supports the assumption that the added joint flexibility offered by the wrapped joints will have a larger effect on the brace dominant modes.

Table 5.2: 10MW jacket NFA - comparison of joint alternatives

(a) 10MW jacket NFA for welded and wrapped composite joints

Mode	Welded [Hz]	Wrapped [Hz]	Change [%]
1	2.63	2.61	-0.6%
2	2.65	2.63	-0.7%
3	2.65	2.63	-0.8%
4	3.30	3.27	-0.9%
5	3.65	3.65	0.0%
6	4.15	4.20	1.2%
7	4.34	4.38	1.0%
8	4.60	4.63	0.5%
9	4.70	4.80	2.0%
10	5.00	5.14	2.8%
11	5.10	5.23	2.5%
12	5.27	5.49	4.2%
13	5.60	5.70	1.8%
14	5.95	6.11	2.7%
15	5.98	6.13	2.6%
16	6.40	6.73	5.1%
17	6.75	6.79	0.5%
18	7.19	7.32	1.7%
19	7.20	7.33	1.7%
20	7.61	7.72	1.4%

(b) 10MW jacket NFA for rigid and wrapped composite joints

Mode	Rigid [Hz]	Wrapped [Hz]	Change [%]
1	2.79	2.61	-6.4%
2	2.79	2.63	-5.9%
3	2.83	2.63	-7.0%
4	3.49	3.27	-6.4%
5	3.84	3.65	-5.0%
6	4.84	4.20	-13.3%
7	4.84	4.38	-9.5%
8	4.94	4.63	-6.4%
9	5.58	4.80	-14.1%
10	6.00	5.14	-14.4%
11	6.00	5.23	-12.9%
12	6.29	5.49	-12.7%
13	6.71	5.70	-15.1%
14	6.82	6.11	-10.4%
15	6.82	6.13	-10.1%
16	7.05	6.73	-4.6%
17	7.97	6.79	-14.9%
18	7.97	7.32	-8.2%
19	8.18	7.33	-10.4%
20	8.22	7.72	-6.1%

To further expand upon the premise of higher modes being more affected by the joint submodelling, the percent change for each mode was calculated with respect to the jackets with welded and wrapped joint submodels, and with respect to the jackets with rigid joints and wrapped joint submodels. The calculated percent changes are held in table 5.2. When looking at table 5.2a, the differences for the lower modes, modes 1-10, are very small, with an average of 1.1% change. For the higher modes, modes 11-20, the average percent change increases to 2.4%. The two modes with the largest difference

between the two jackets with different joint submodel types were mode 12 and mode 16. These two modes are shown in figure 5.4 and in figure 5.5 respectively. As can be seen in the deflected shape of mode 12 and mode 16 for the jackets with the joint submodels, there is a large displacement of the braces. The braces are essentially the only members participating in the mode, which indicates that this is a local bending mode of the braces. This supports the premise that the joint submodels have a large effect on bending modes where the brace displacements are large.

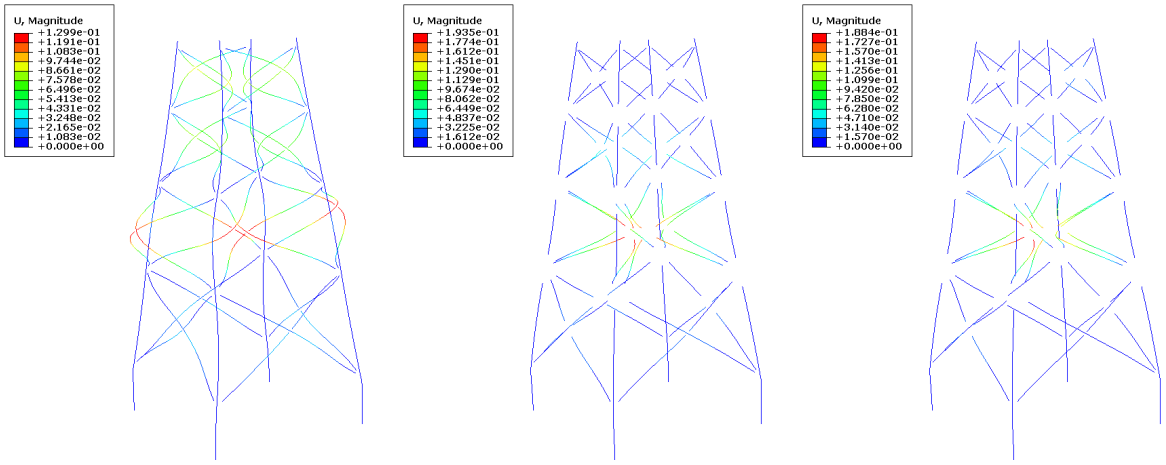

(a) Mode 12 - Rigid **(b)** Mode 12 - Welded **(c)** Mode 12 - Wrapped

Figure 5.4: Jacket - Mode 12

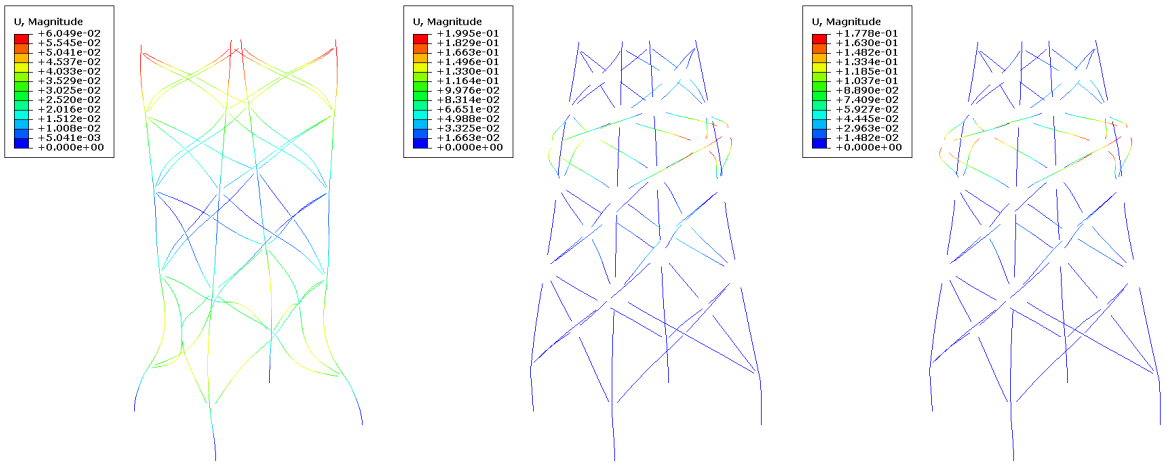

(a) Mode 16 - Rigid **(b)** Mode 16 - Welded **(c)** Mode 16 - Wrapped

Figure 5.5: Jacket - Mode 16

The comparison of the jacket with rigid joints and the jacket with wrapped joint submodels is held in table 5.2b. As can be seen in the table, the differences for the lower modes, modes 1-10, are smaller than the differences for the higher modes, modes 11-20, with an average of 8.8% change and 10.5% change respectively. For all modes, there was a larger difference between the jacket with joint submodels and the jacket with rigid joints than when comparing the two jackets with different joint submodel types. This was again, more obvious with the higher modes. The two modes with the largest difference between the two jackets were modes 13 and mode 17. These two modes are shown in figure 5.6 and in figure 5.7.

As can be seen in the deflected shape of mode 13 and mode 17 for the jackets, there is some mode switching between the jacket with rigid joints when compared to the jacket with wrapped joint submodels. When analysing mode 13 for the jacket with rigid joints (figure 5.6a), the deflected shape is similar

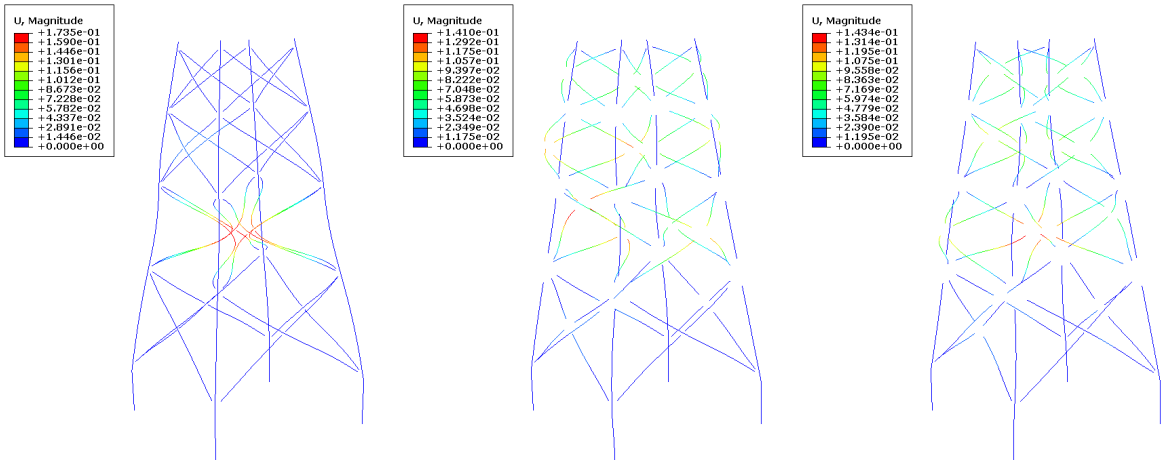

(a) Mode 13 - Rigid **(b)** Mode 13 - Welded **(c)** Mode 13 - Wrapped

Figure 5.6: Jacket - Mode 13

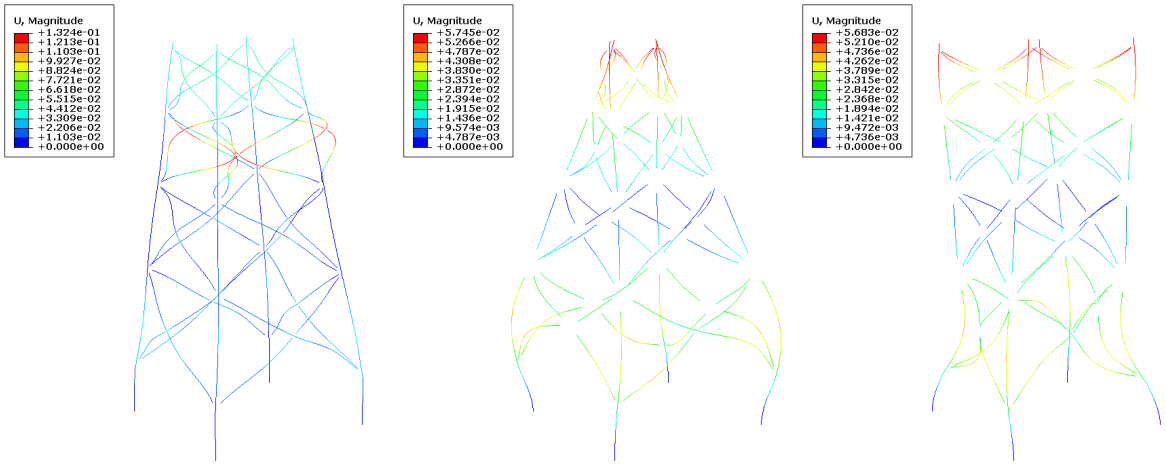

(a) Mode 17 - Rigid **(b)** Mode 17 - Welded **(c)** Mode 17 - Wrapped

Figure 5.7: Jacket - Mode 17

to mode 12 for the jacket with submodelled joints (figure 5.4c). Furthermore, when looking at the deflected shape of mode 17 for the jacket with submodelled joints (figure 5.7c and 5.7b), it matches well with the deflected shape of mode 16 for the jacket with rigid joints (figure 5.5a). The mode switching logically follows because the jackets with submodelled joints have less stiffness at the joints. This causes the bending modes that are most affected by the joint stiffness to have lower natural frequencies. This is highlighted by the jacket with rigid joints having the largest difference with the jacket with joint submodels for the brace-dominant modes.

5.2. INNWIND.EU, D4.34 - OWT - NFA

In figure 5.8, the different versions of the jacket are shown with the tower and piles also modelled. Again, an NFA was done to compare the three models. For this analysis, unlike the analysis of the jacket by itself, the obtained frequencies could also be compared to the INNWIND.EU jacket. The first nine modes were supplied in the report, and they acted as a benchmark to verify whether the model was built correctly (Stolpe et al., 2016).

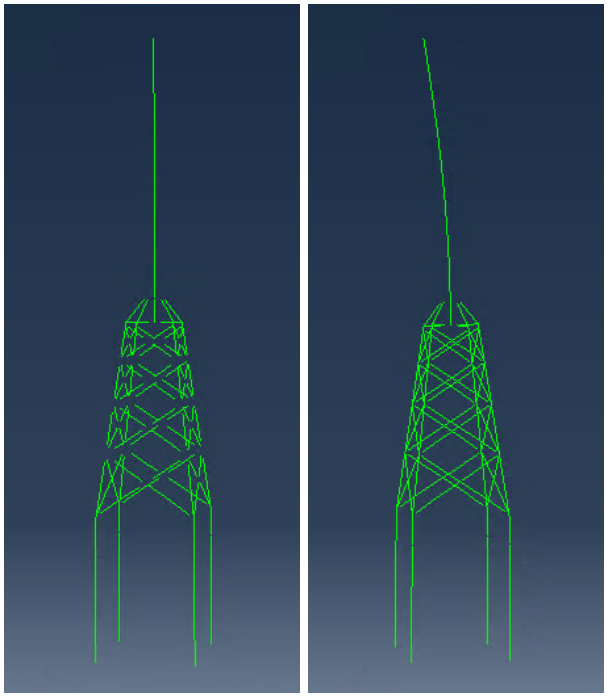

(a) Submodelled joint alternative **(b)** Rigid joint alternative

Figure 5.8: INNWIND Jacket with tower and foundation

The results of the INNWIND analysis are held in table 5.3a. The results from the Abaqus generated OWT models for the different joint modelling strategies are held in table 5.3b.

Table 5.3: 10MW OWT - INNWIND.EU and Abaqus comparison

(a) INNWIND 10MW OWT - Modes 1-9, (Stolpe et al., 2016)

Mode	Soft [Hz]	**Fatigue [Hz]**	Stiff [Hz]
1	0.26	**0.26**	0.26
2	0.26	**0.26**	0.27
3	0.94	**0.94**	0.95
4	1.19	**1.20**	1.37
5	1.21	**1.22**	1.45
6	1.60	**1.60**	1.88
7	1.71	**1.72**	1.94
8	1.84	**1.86**	2.43
9	1.93	**1.94**	2.44

(b) 10MW OWT - 3 joint alternatives - Modes 1-9

Mode	Rigid [Hz]	Welded [Hz]	Wrapped [Hz]
1	0.27	0.27	0.27
2	0.27	0.27	0.27
3	0.93	0.92	0.92
4	1.01	1.02	1.02
5	1.04	1.05	1.05
6	1.74	1.74	1.74
7	1.87	1.85	1.86
8	1.88	1.88	1.89
9	2.08	2.10	2.10

In the INNWIND.EU report, an NFA was done for three site conditions. These were labelled ”soft”, ”fatigue”, and ”stiff”. This was to account for the differences in site conditions regarding marine growth on the members, soil stiffness, and added mass due to miscellaneous elements attached to the operating offshore wind turbine. These three design scenarios offer a conservative way to evaluate the stiffness of the structure due to many uncertain aspects of the design from the engineer’s perspective (Stolpe et al., 2016).

When creating the models in Abaqus for the three different joint modelling strategies, the site conditions that were respective to the fatigue load case in the INNWIND.EU project were applied. The fatigue case is shown in bold in table 5.3a. This was the design target for the Abaqus generated OWT models. When comparing the eigenfrequencies obtained in the INNWIND.EU report, there is a good correspondence for the first three modes with an average percent difference of 2%. Thus, indicating that the models made in Abaqus were similar to what was made for the INNWIND.EU report. For modes 4-10, the differences between the Abaqus model and the INNWIND.EU model grew, with an average percent change of 9%.

When comparing the different OWT models made in Abaqus to each other, there is a good correspon-

dence between them. This is especially the case for the lower modes. The calculated percent changes for these modes are held in table table 5.4a and table 5.4b. When looking at table 5.4a, the differences for the lower modes when comparing the welded joint alternative to the rigid joint alternative are very small, with an average of 0.3% change. In table 5.4b, it can be seen that when comparing the model with welded joints to the model with wrapped joints, the average difference was 0.2%. This is essentially not a significant difference in either case.

Table 5.4: 10MW OWT - Lower mode comparison

(a) 10MW OWT - Rigid vs. Wrapped joint submodel - Mode 1-9

Mode	Rigid [Hz]	Wrapped [Hz]	Change [%]
1	0.27	0.27	0%
2	0.27	0.27	0%
3	0.93	0.92	0%
4	1.01	1.02	1%
5	1.04	1.05	0%
6	1.74	1.74	0%
7	1.87	1.86	0%
8	1.88	1.89	0%
9	2.08	2.10	1%

(b) 10MW OWT - Welded vs. Wrapped - Mode 1-9

Mode	Welded [Hz]	Wrapped [Hz]	Change [%]
1	0.27	0.27	0%
2	0.27	0.27	0%
3	0.92	0.92	1%
4	1.02	1.02	0%
5	1.05	1.05	0%
6	1.74	1.74	0%
7	1.85	1.86	1%
8	1.88	1.89	0%
9	2.10	2.10	0%

The results for the higher modes are held in table 5.5a. For these higher modes, modes 10-20, the average percent change increases to 3.5% and 2.7% for the comparison of rigid to wrapped and welded to wrapped respectively. The maximum percent change was 9% and 6% for the comparison of rigid to wrapped and welded to wrapped respectively. The two modes with the largest difference between the jacket with wrapped joints and the jacket with rigid joints were mode 20 and mode 17. Due to these two modes having the highest percent change between the model with rigid joints and the model with wrapped submodelled joints, they are shown along with modes 18 and 19. These four modes are shown in figure 5.9, figure 5.10, figure 5.11, and figure 5.12 respectively. As can be seen, for all four modes, unlike in the case of the jacket, there is no mode switching. Additionally, it can be said that all four of these bending modes are highly affected by brace out-of-plane displacements.

Table 5.5: 10MW OWT - Higher mode comparison

(a) 10MW OWT - Rigid vs. Wrapped joint submodel - Mode 10-20

Mode	Rigid [Hz]	Wrapped [Hz]	Change [%]
10	2.63	2.54	-4%
11	2.70	2.62	-3%
12	2.81	2.83	1%
13	3.09	3.10	0%
14	3.43	3.36	-2%
15	3.48	3.41	-2%
16	3.67	3.64	-1%
17	4.05	3.75	-8%
18	4.05	3.85	-5%
19	4.06	3.91	-4%
20	4.42	4.06	-9%

(b) 10MW OWT - Welded vs. Wrapped - Mode 10-20

Mode	Welded [Hz]	Wrapped [Hz]	Change [%]
10	2.50	2.54	2%
11	2.58	2.62	2%
12	2.82	2.83	0%
13	3.11	3.10	0%
14	3.33	3.36	1%
15	3.36	3.41	1%
16	3.51	3.64	4%
17	3.61	3.75	4%
18	3.68	3.85	5%
19	3.74	3.91	5%
20	3.83	4.06	6%

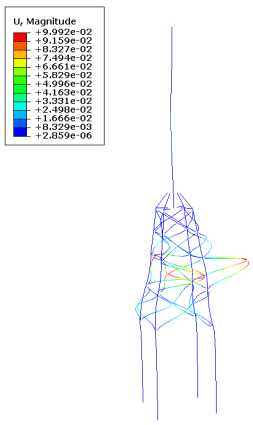

(a) Mode 17 - Rigid

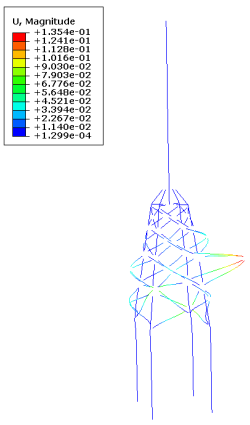

(b) Mode 17 - Welded

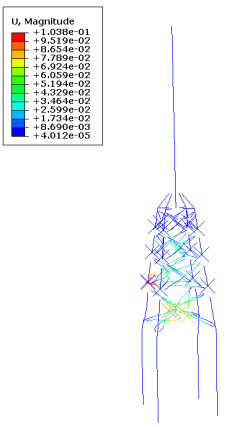

(c) Mode 17 - Wrapped

Figure 5.9: OWT - Mode 17

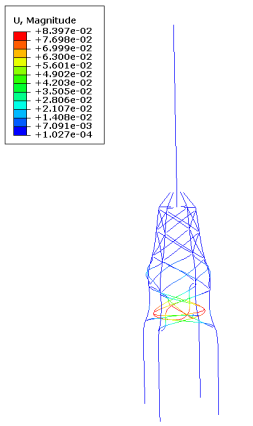

(a) Mode 18 - Rigid

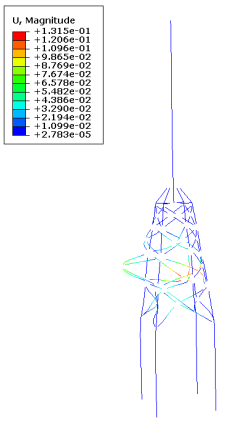

(b) Mode 18 - Welded

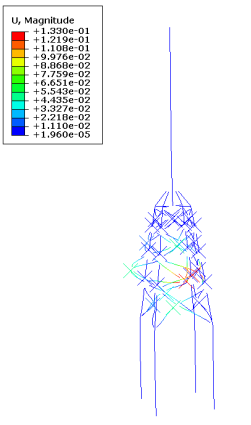

(c) Mode 18 - Wrapped

Figure 5.10: OWT - Mode 18

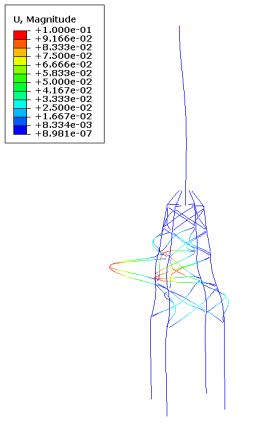

(a) Mode 19 - Rigid

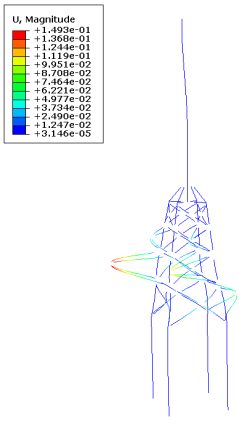

(b) Mode 19 - Welded

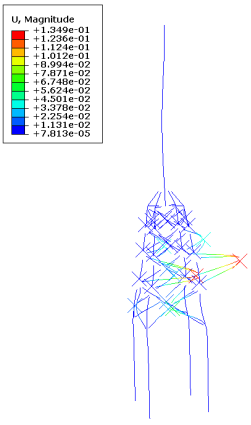

(c) Mode 19 - Wrapped

Figure 5.11: OWT - Mode 19

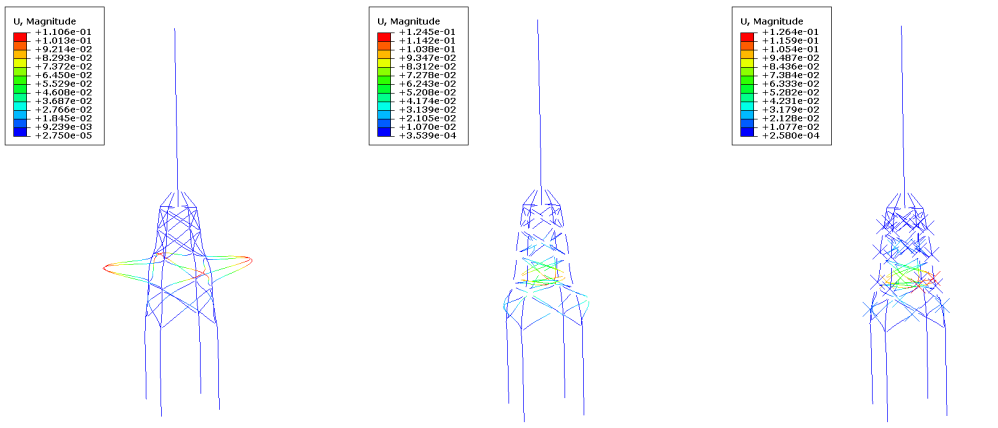

(a) Mode 20 - Rigid **(b)** Mode 20 - Welded **(c)** Mode 20 - Wrapped

Figure 5.12: OWT - Mode 20

5.3. Comparison of NFA to relevant literature

In previous analyses done by Popko (Popko et al., 2016), a natural frequency analysis was done comparing OC4 OWT models. The two that were compared included one modelled with beam elements and rigid joints, and the other with submodelled joints representing welded joints. It was found that for all modes, the OWT with submodelled joints had lower natural frequencies than the OWT with rigid joints. For some of the bending modes with larger local deflections of the x-braces, such as the 3rd global side-to-side mode, there were differences of approximately 5% between the two models. When comparing the same bending mode for the INNWIND OWT (mode 8) in this thesis project, a difference of approximately 7% was found between the two models (rigid and welded joint submodel).

This gives a good correspondence between previous literature and this work. The modelling assumptions used by Popko and the assumptions applied in this project were not the same. Moreover, the analysed OWT was different in size (5MW compared to 10MW). It is posed that due to a combination of these factors, a larger difference was found between the rigid and welded models for the INNWIND jacket. The results for all bending modes are held in table 5.6.

Table 5.6: 10MW OWT - Welded vs. Rigid - Mode 1-20

Mode	Rigid [Hz]	Welded	Change [%]
1	2.79	2.63	-5.8%
2	2.79	2.65	-5.3%
3	2.83	2.65	-6.2%
4	3.49	3.30	-5.5%
5	3.84	3.65	-4.9%
6	4.84	4.15	-14.3%
7	4.84	4.34	-10.4%
8	4.94	4.60	-6.9%
9	5.58	4.70	-15.7%
10	6.00	5.00	-16.7%
11	6.00	5.10	-15.0%
12	6.29	5.27	-16.2%
13	6.71	5.60	-16.6%
14	6.82	5.95	-12.8%
15	6.82	5.98	-12.4%
16	7.05	6.40	-9.2%
17	7.97	6.75	-15.3%
18	7.97	7.19	-9.8%
19	8.18	7.20	-11.9%
20	8.22	7.61	-7.4%

IV

Research Contribution

6

Discussion

In chapter 4 and chapter 5 the numerical analyses that were carried out for this thesis report were presented. With these numerical analyses, several important assumptions were made to efficiently conduct these analyses. Due to the scope of the work and the previously mentioned assumptions, there were certain limitations to the analyses. These assumptions and limitations will be presented in the following sections of this chapter of the report.

6.1. Assumptions

The solution strategy that was employed to answer the research questions of this thesis report involved generating several models. Due to each of these models being generated under different sets of assumptions, the assumptions will be grouped by each model: the individual joint submodel (wrapped and welded), the OWT substructure (jacket, foundation, and transition piece), and the OWT superstructure (tower and turbine).

6.1.1. Joint submodelling - assumptions

When generating the joint submodels, several assumptions were made. For the wrapped composite joint submodels, the geometry of the X-joints and KK-joints were imported from Autodesk Inventor. There is a parametric model for both the X-joint and KK-joint that was made in-house by the research team advised by Marko Pavlović. With this parametric model, most of the parameters of the joint were not altered. The only changes included setting the brace and chord diameters, and the angle of the joint. For the case of the X-joint, the edge thickness was set at the default limit of 3mm. For the case of the KK-joint, the edge thickness was increased to 20mm. This larger edge thickness for the KK-joint allowed ease of creation for the wrap material in Autodesk Inventor. Due to the relatively large mesh size used in Abaqus (50-100mm), and the relatively large section sizes analysed in the thesis report, the size of the edge thickness was deemed appropriate. If creating joint submodels for future analyses, and the individual failure modes of the joint are of interest, a finer mesh will be required.

Within Abaqus, as previously mentioned, a mesh size of 50-100mm was used depending on the specific joint. The mesh size was altered when the part experienced difficulties in meshing. The wrap material and the steel members were connected by tie constraints in Abaqus. Other contact conditions can be used to create a more sophisticated method of representing the contact between the two materials. When generating a substructure within Abaqus, certain contact conditions are not allowed in the same analysis due to the substructuring step being a linear perturbation step. Due to this, a simple tie constraint was chosen. This was assumed to be sufficient to model the differences between a welded and a wrapped joint when analysing the jacket on the global scale. Again, if interested in the individual

failure modes respective to the joint, then a different contact condition must be chosen.

Another assumption made with the wrapped composite joint was the tie constraint that tethered the outer perimeter of the ends of the braces and chords to a point coincident with the centreline of the steel members and the plane perpendicular to the end of the respective members. This floating point was assumed to be the retained degree of freedom that transferred the global displacement of the joint to the local joint deformation in the solid model. This tie constraint was chosen due to its allowance for ovalisation. This method does not capture local eccentricity effects due to the forces being transferred through the centrelines, but the consequences of this were deemed minor due to the analysis being more focused on the global behaviour of the jacket.

For the case of the welded joint submodel, there were also some significant assumptions. The welded submodels were created with the same steel members that are present in the wrapped joint submodels. The wrap material was removed from the model to generate the welded steel submodel. Although the model was referred to as the ”welded submodel” throughout the report, no welds were included in the model. The joining steel members were connected through tie constraints. Due to the large member diameters and member thicknesses, it was assumed that modelling the welds would not have a large effect on the local joint deformation of the joint submodel. This assumption causes the welded submodel to not be a perfect representation of a welded joint, but it was deemed appropriate for the thesis project.

For both joint submodels, when applying the substructuring method, the Craig-Bampton method was applied. With this method, 20 modes were kept in the generation of the joint submodels, because it was determined that the frequency of the 20th mode of the joint was sufficiently high to fully characterise the joint’s deformation in common load cases for the jacket support structure.

6.1.2. OWT substructure - assumptions

When generating the jacket model, several assumptions respective to the jacket were made. For the connection of the chord and braces, cans were not included in any models. This was done to primarily simplify the models, and in previous research it was shown that cans did not have a large impact on the jacket’s response. In addition, for the connections of the chords to the braces in the beam model, the length of the chords and braces that overlapped with the joint submodels was not meshed. Thus, this left the geometry of these members in the model, but at the mesh step they were not included. This generated jackets with joint submodels that had voids at the joint locations when analysing the results. To produce results with the joint submodels shown, a separate result file must be generated through combining the result files of all joint submodels and the main results file. This task is tedious and creates very large result files, so this was not always done for the results shown in the report.

Because the joint submodels were included in place of these voids, it was assumed that there was no change to the structure’s overall mass if you exclude the impact of the wrap material’s weight. Overall, this is not entirely true, because the joint submodels were included in the main jacket beam model by hand, and was not done with an automated process. This most likely led to user errors while accommodating the joint submodel geometry regarding the lengths of the braces and chords to ignore in the mesh, and with respect to the angle of alignment of the braces and chords. This would lead to inconsistencies in the model. It is assumed that these inconsistencies are minor, but in future analyses a more efficient way to accommodate the joint submodels should be found to reduce the propensity of the method to introduce errors into the analysis.

Regarding the other elements of the substructure of the OWT (soil, piles, and transition piece), there were other included assumptions. For the verification steps done for the OC4 jacket analysis, a transition piece, soil, and piles were not modelled. This was due to the lack of requirements to model these elements. For the INNWIND.EU case study, these elements were included in the analysis. In the D4.34 report, no detailed information was provided about the soil stiffness or dimensions of the transition piece. Only dimensions of the soil piles were given. Because there was no detailed information for the soil stiffness and the transition piece, they were both approximated until the eigenfrequencies of

the OWT aligned with the posted eigenfrequencies contained in the D4.34 report. This method is not accurate, but due to the scope of the project being more interested in the differences in the method of joint modelling by comparing different Abaqus models, the rough approximation of the transition piece and soil stiffness was accepted. If doing further analyses and hoping to compare with the INNWIND.EU report, further investigation into these structural elements will be required to model them with a higher degree of accuracy.

6.1.3. OWT superstructure - assumptions

When modelling the superstructure of the OWT, several assumptions were made. The superstructure of the OWT was modelled with OpenFAST for the case of the OC4 OWT, and with Abaqus for the INNWIND.EU jacket. For each program, different assumptions were made.

Regarding OpenFAST, the example files given during installation of the software were mostly left unchanged for the different modules used within OpenFAST. The default files align with the OC4 jacket regarding jacket and tower geometry, and turbine parameters. Therefore, the implicit assumption made is that these example files are accurate and that they correspond to the case study done by Mark van Vliet. Through the verification of OpenFAST by comparison with Bladed, this assumption was verified, but there were too many variables to know for certain which parts of OpenFAST were modelled correctly. The analyses were determined to be similar enough for the purposes of using OpenFAST to generate the loads at the interface point. For the case of this thesis project, this modelling uncertainty was accepted.

If there was a desire to use OpenFAST to generate and analyse results within OpenFAST, or OpenFAST was used to conduct more analyses for different jackets with different environmental conditions than conducted in this thesis project, it would be recommended to spend time to become familiar with OpenFAST to better understand what the individual modules do, and what the individual parameters do within those modules.

Regarding the modelling of the structure in Abaqus, there were several significant assumptions made. Abaqus was used to model the tower and turbine of the INNWIND.EU OWT. The tower dimensions were originally made to have a tapered diameter so that it smoothly transitioned from the base of the tower to the top. The tower diameter was modelled instead to have the average diameter for each segment, so that the diameter grew smaller in increments for each section when moving from the base of the tower to the top of the tower. The RNA was modelled by including point masses with rotational stiffness representing the different components of the RNA. These point masses and rotational stiffnesses were taken from the INNWIND.EU report. It was assumed that this modelling strategy would deliver a satisfactory representation of the dynamic behaviour of the superstructure. The downside to this method is the eigenfrequencies of the blades themselves are excluded with this method, and only the global structural eigenfrequencies can be captured. If in further analyses it is desired to analyse the resonance of the individual blades of the wind turbine, then the blades will have to be included in the model.

6.2. Limitations

Due to the previously mentioned assumptions, several limitations and qualifications should be mentioned in this thesis report. Regarding the joint submodels, the results should be limited to the global implications of the modelled joint stiffness. Due to the large mesh size, contact conditions between the materials of the composite wrap and steel, and the lack of modelled welds for the case of the welded joint submodel, the local failure modes of the joint cannot be characterised by these joint submodels. Instead, the impact of the joint stiffness on the global structural behaviour of the jacket should be analysed with a high degree of detail.

Regarding the OWT models generated with Abaqus, the soil stiffness and transition piece were not modelled with a high degree of accuracy. Due to this, it is not recommended to compare the results of

the modelled substructure of the OWT with the substructure of the INNWIND.EU report. Instead, it is recommended to compare the results between the Abaqus models that have different joint modelling alternatives. In a general sense, the INNWIND.EU results can be used as a sanity check for the eigen-frequencies of the structure, but a direct comparison is impossible without further detailing the soil stiffness and transition piece.

In a similar manner, regarding the RNA modelling strategy employed in Abaqus, because the blades of the turbine were not modelled, no information can be gleaned about resonance of the blades of the turbine and the rest of the jacket. This can only be done if the blades are modelled individually with beam or shell elements in the jacket model.

The last limitation worth mentioning is that in this report, the entire sequentially coupled analysis was not conducted. This was due to the incompatibility of the intended solution method with the utilised software. In Abaqus, when conducting a wave load analysis with the Abaqus/Aqua analysis product, it was not possible to create a superelement through substructuring. Due to the substructuring process in Abaqus being a linear perturbation step, there can be no dynamic analyses conducted at the same time. Therefore, a different strategy must be employed to export a superelement to be used in a software that can conduct aero-hydro-servo-elastic time-history simulations. Potential alternatives that are worth investigating include: using a different method to model the wave load analysis in Abaqus, using HAWC2 to analyse the substructure of the OWT, using proprietary software packages such as Bladed and Sesam, or using different FEM software to substructure the joints (such as Ansys). These solution method alternatives were not applied in this thesis report in the interest of time.

7

Conclusion and recommendations

In this chapter, conclusions regarding the main research question and subquestions will be provided. The conclusions will be separated by subquestion, with the main research question addressed last. In addition, recommendations for future work will be provided.

7.1. Conclusions

The main research question is restated below for convenience:

> ***When considering stiffness characteristics of wrapped composite joints, what is the impact on the overall dynamic behaviour of a 10MW wind turbine jacket support structure?***

- *Subconclusion regarding the representation of the stiffness of the wrapped composite joint*

  When modelling joint stiffness in jacket support structures for offshore wind turbines, using a submodeled joint offers the most detailed representation of the joint stiffness of the alternatives that were analysed. Through applying substructuring techniques in generating the joint submodels, such as the Craig-Bampton method, the joint is able to experience deformation that is similar to the true joint deformation behaviour. When comparing this alternative to other joint modelling alternatives that were referenced in the report (joint flexibility equations and rigid joints), the submodelled joint approach does not have the implicit errors respective to these alternatives when analysing in a dynamic regime.

  The rigid joint method adds artificial stiffness to the model. This artificial stiffness leads to incorrect load sharing between members connected at the joint and yields higher than expected local brace mode eigenfrequencies. When utilising the approach of the local joint flexibility equations, the stiffness of the joint is relatively accurate, but the effect of the mass at the joint is not included. This then leads to errors when analysing in a dynamic regime.

  The benefit gained from applying the joint submodelling approach is especially significant in the case of the wrapped composite joint. Because the wrap material is able to stiffen the chord and braces, the joining members do not experience ovalisation to the same extent as in the case of the welded joint. In the analyses presented earlier in the report, the wrapped composite joint experienced higher eigenfrequencies than the welded alternative for the brace dominant bending modes due to the phenomenon of the wrap material stiffening the steel members thus reducing the propensity for the steel members to ovalise. For the case of the modelled KK-joint, on average, the wrapped joint alternative had eigenfrequencies that were 11.7% higher than the welded

joint alternative. When stated in terms of stiffness, the wrapped joint alternative offered on average 28% higher joint stiffness than the welded joint alternative. This beneficial attribute of the wrapped composite joint can only be realised when analysing the joint with high fidelity, which is why the choice of the submodelling approach was chosen as the best alternative to represent the joint stiffness.

- *Subconclusion regarding the implementation of the stiffness characteristics of the wrapped composite joint into the structural analysis of a jacket*

  The best alternative to implement the joint stiffness into the structural analysis of the jacket is to conduct a sequentially coupled analysis of the jacket support structure and offshore wind turbine including the tower and turbine. Through this process, the entire OWT can be characterised, while simultaneously modelling the joint stiffness with high fidelity. This sequentially coupled analysis can be summarised in a four-step process. First, the jacket support structure model is created with the joint stiffness modelled with high fidelity (this can be done with FEM software such as Abaqus, Ansys, etc.). Second, a superelement of the substructure of the OWT (jacket and foundation) is exported along with a load vector respective to a wave load analysis conducted on the substructure. Thirdly, an aero-servo-elastic analysis is conducted on the superstructure of the OWT (tower and turbine), with the OWT substructure introduced at the interface point (top of the transition piece) by a superelement. Lastly, the results at the interface point are exported to the substructure and then combined with a separate wave load analysis.

- *Subconclusion regarding the impact of joint characteristics on the eigenfrequencies of the jacket substructure*

  The increased joint stiffness provided by the wrapped composite joint has a measurable impact on the eigenfrequencies of the jacket, with a larger impact found with the higher bending modes. For the three jackets that were analysed (the model with welded joint submodels, the model with wrapped joint submodels, and the model with rigid joints), the jacket with rigid joints had the highest natural frequencies, the model with wrapped joint submodels had the second highest natural frequencies, and the model with welded joint submodels had the lowest natural frequencies.

  The impact of the joint characteristics on the eigenfrequencies of the jacket can be quantitatively measured through analysing two comparisons. First, for the comparison of the two joint alternatives, welded and wrapped composite joints, the differences for the lower modes, modes 1-10, are small, with an average change of 1.1% and a maximum of 2.8%. For the higher modes, modes 11-20, the average percent change increases to 2.4% with a maximum of 5.1%. These changes in the eigenfrequencies for the jackets were lower than in the case of the KK-joint when analysed independently. For the comparison of the jacket modelled with rigid joints and the jacket modelled with wrapped composite joint submodels, the differences for the lower modes are smaller than the differences for the higher modes with an average change of 8.8% and 10.5% respectively, and a maximum change of 14.4% and 15.1% respectively.

  The larger change reflected in this second comparison argues for the necessity of modelling the joint stiffness with a submodelled joint approach. The shift to higher eigenfrequencies of the jacket for the case of rigid joints can lead to unconservative conclusions due to the loading frequencies being more present at lower frequencies. Artificially increasing the joint stiffness, leading to higher calculated eigenfrequencies, can give the designer a false sense of confidence that the jacket structure will not experience undesired resonance issues.

- *Subconclusion regarding the influence of the joint characteristics of the jacket within the context of the entire offshore wind turbine (including piles, soil, tower, and wind turbine)?*

  Similarly to the case of the jacket, the increased joint stiffness provided by the wrapped composite joint has a measurable impact on the eigenfrequencies of the offshore wind turbine, with

a larger impact found with the higher bending modes. For the three offshore wind turbines that were analysed (the model with welded joint submodels, the model with wrapped joint submodels, and the model with rigid joints), the jacket with rigid joints had the highest natural frequencies, the model with wrapped joint submodels had the second highest natural frequencies, and the model with welded joint submodels had the lowest natural frequencies.

The influence of the joint characteristics on the entire offshore wind turbine can be measured through analysing two comparisons. For the first comparison, when comparing the wrapped joint alternative to the welded joint alternative, the higher eigenfrequency modes, modes 10-20, had an average percent change of 2.7% with a maximum of 6%. For the lower modes, modes 1-9, the average percent change was 0.2% with a maximum of 1%. For the comparison of the wrapped joint alternative to the rigid joints, the average percent change for the higher modes was 3.5% with a maximum of 9% for the first 20 modes. For the lower modes, the average percent change was 0.3% with a maximum of 1%.

The obtained results for the eigenfrequencies of the OWT are counter intuitive for the comparison of the welded and wrapped joint alternatives. The differences in calculated eigenfrequencies between these two joint submodel alternatives are larger for the case of the OWT than for the case of the jacket. This is an interesting result that requires further study with specific attention applied to why the joint submodelling technique would have a larger impact for the case of the OWT than for the jacket when comparing different joint types to each other.

Final conclusion on main research question

Both the application of the wrapped composite joints and the application of the analysis method of submodelling joints of the jacket are beneficial for solving issues related to the construction of jacket support structures for large wind turbines. The wrapped composite joint, when applied to the context of an offshore wind turbine, has a manifold impact on the dynamic behaviour of the structure. When analysing the joint by itself, the wrapped composite joint stiffens the joining members and dissuades the joining steel members from ovalising. On a global scale, this stiffening of the joint leads to higher measured natural frequencies for the case of the jacket and for the case of the OWT when compared to the welded joint alternative. Moreover, the stiffening of the OWT support structure is significant for the case of a large turbine (10MW+), due to the inherent issues related to resonance of the large turbine with the operating frequency of the turbine and the natural frequencies of the structure.

7.2. Recommendations and future work

The presented work in this thesis report offers answers to some questions, but through the work, naturally more questions are brought up. These further issues that could be investigated will be presented in the following subsections.

7.2.1. Stiffness Degradation

Due to the use of composite material in the wrapped composite joint, it would be worthwhile to investigate the effects of stiffness degradation. This could entail determining what level of stiffness degradation would lead to resonance issues, given that the joint still satisfies the ultimate strength requirements. Paired with this, it would be valuable to investigate the effects of nonuniform stiffness degradation. This could be investigated in a global sense, assuming that certain joints have a higher rate of stiffness degradation over the lifetime of the jacket support structure, and it could be investigated in a local sense with respect to the joint, assuming that certain areas of the wrapped composite joint degrade at different rates. This could be posed to be related to certain joints within a jacket support structure, and certain areas within a given joint, attracting more load, and thus attracting more stress. This could lead to differential stiffness degradation of the composite material. Due to joint stiffness having a large effect on fatigue strength, and that the wrapped composite joint alternative is favourable due to its superiority in fatigue performance, it would be beneficial to conduct this investigation while

simultaneously relating it to fatigue limit states.

7.2.2. Impact of jacket layout on the dynamic behaviour of OWT

While investigating the impact of the joint stiffness on the overall dynamic behaviour of the jacket and the offshore wind turbine as a whole, it was evident that the impact of the joint stiffness was limited due to the global stiffness and mass of the structure being much larger than the joints themselves. When utilising wrapped composite joints in design, there is a larger allowance for flexibility in the design of the joints for the jacket support structure when compared to a welded alternative for the joints. Therefore, further research could investigate how the layout of the jacket could be optimised to avoid resonance issues through the use of wrapped composite joints. This could include unique joint configurations regarding the angles of joining members, spacing of the jacket legs, incline of the jacket legs, spacing of the intermediate bracing, etc. Through investigating this feature of wrapped composite joints, an argument could be made for their application to large wind turbine support structures.

7.2.3. Conducting a sequentially coupled analysis of a JSS of a 10MW+ OWT

The scope of this thesis project did not include the entire sequentially coupled design process. The analysis was carried out primarily in the frequency domain. A recommendation for further research would entail conducting a complete sequentially coupled analysis to obtain the member stresses and displacements given by a time-history analysis of the jacket. This future research could then be focused on obtaining the peak ultimate forces in the critical joints when analysing a jacket with wrapped composite joints, and comparing it to the case of a jacket with welded joints. Along with these peak ultimate forces, the member sizes and thicknesses could be obtained for the jacket for both of these two design cases.

7.2.4. Modal Assurance Criterion (MAC)

When analysing the dynamic behaviour of a given system, it is helpful to not only analyse the eigenfrequencies. Paired with the eigenfrequencies, a great understanding of a dynamic system can come from analysing the mode shapes. This can be done through the use of a MAC analysis. To better evaluate the wrapped composite joint's effect on the dynamic behaviour of an OWT, a specific effort should be made in analysing the mode shapes.

References

Abramovich, H. (2017). Introduction to composite materials. *Stability and Vibrations of Thin-Walled Composite Structures*, 1–47. https://doi.org/10.1016/B978-0-08-100410-4.00001-6

Amar Bouzid, D., Bhattacharya, S., & Otsmane, L. (2018). Assessment of natural frequency of installed offshore wind turbines using nonlinear finite element model considering soil-monopile interaction. *Journal of Rock Mechanics and Geotechnical Engineering*, *10*(2), 333–346. https://doi.org/10.1016/j.jrmge.2017.11.010

Bhattacharya, S. (2019). Design of Foundations for Offshore Wind Turbines. *Design of Foundations for Offshore Wind Turbines*, (March). https://doi.org/10.1002/9781119128137

Branlard, E., Shields, M., Anderson, B., Damiani, R., Wendt, F., Jonkman, J., Musial, W., & Foley, B. (2020). Superelement reduction of substructures for sequential load calculations in OpenFAST. *Journal of Physics: Conference Series*, *1452*(1). https://doi.org/10.1088/1742-6596/1452/1/012033

Cordle, A. (2013). *Final report for WP4.3: Enhancement of design methods and standards* (tech. rep. January 2013).

Craig, R., & Bampton, M. (1968). Coupling of Substructures for Dynamic Analyses. *AIAA Journal*, *6*(7), 1313–1319.

Cripps, D. (2020). Polymer Composites. https://netcomposites.com/guide/introduction/polymer-composites/

Damiani, R. R., Song, H., Robertson, A. N., & Jonkman, J. M. (2013). Assessing the importance of nonlinearities in the development of a substructure model for the wind turbine CAE tool fast. *Proceedings of the International Conference on Offshore Mechanics and Arctic Engineering - OMAE*, *8*(March). https://doi.org/10.1115/OMAE2013-11434

Dassault Systèmes. (2019a). Choosing between implicit and explicit analysis. *Abaqus Theory Manual 6.19*. https://abaqus-docs.mit.edu/2017/English/SIMACAEGSARefMap/simagsa-c-absadvexp.htm

Dassault Systèmes. (2019b). Substructuring and substructure analysis. *Abaqus Theory Manual 6.19*.

De Vries, W. E., Vemula, N. K., Passon, P., Fischer, T., Kaufer, D., Matha, D., Schmidt, B., & Vorpahl, F. (2011). Final report WP 4.2: Support Structure Concepts for Deep Water Sites: Deliverable D4.2.8 (WP4: offshore foundations and support structures). *Project UpWind*, 18–22.

Dubois, J., Muskulus, M., & Schaumann, P. (2013). Advanced representation of tubular joints in jacket models for offshore wind turbine simulation. *Energy Procedia*, *35*, 234–243. https://doi.org/10.1016/j.egypro.2013.07.176

Gaertner, E., Rinker, J., Sethuraman, L., Zahle, F., Anderson, B., Barter, G. E., Abbas, N. J., Meng, F., Bortolotti, P., Skrzypinski, W., Scott, G. N., Feil, R., Bredmose, H., Dykes, K., Shields, M., Allen, C., & Viselli, A. (2020). IEA Wind TCP Task 37: Definition of the IEA 15-Megawatt Offshore Reference Wind Turbine, 1–44. https://www.osti.gov/biblio/1603478%0Ahttps://www.osti.gov/servlets/purl/1603478

He, P., & Pavlovic, M. (2020). Feasibility of Wrapped FRP Circular Hollow Section Joints. (December), 292–299. https://doi.org/10.3850/978-981-11-0745-0{_}043-cd

Intergovernmental Panel on Climate Change. (2015). Technology-specific Cost and Performance Parameters. *Climate Change 2014 Mitigation of Climate Change*, 1329–1356. https://doi.org/10.1017/cbo9781107415416.025

Jalbi, S., Nikitas, G., Bhattacharya, S., & Alexander, N. (2019). Dynamic design considerations for offshore wind turbine jackets supported on multiple foundations. *Marine Structures*, *67*(May). https://doi.org/10.1016/j.marstruc.2019.05.009

Jonkman, J., Butterfield, S., Musial, W., & Scott, G. (2009). Definition of a 5-MW Reference Wind Turbine for Offshore System Development, NREL Technical Report No. TP-500-38060. *Nrel*, (February). http://www.osti.gov/servlets/purl/947422-nhrlni/

Narayanan, S., & Mota, M. (2015). Sustainability of steel reinforcement. *Green building with concrete: Sustainable design and construction, second edition* (pp. 373–394). CRC Press. https://doi.org/10.1201/b18613

NREL. (2021). OpenFAST Documentation Release v3.0.0, 1–101. https://openfast.readthedocs.io/en/latest/index.html

Pavlović, M., Bogers, P., & Veljkovic, M. (2021). Method for Making a Virgin Joint Between Two Separate Structural Hollow Sections, and Such a Virgin Joint, (United States Patent Application US20210079651A1). https://appft.uspto.gov/netacgi/nph-Parser?Sect1=PTO1&Sect2=HITOFF&p=1&u=/netahtml/PTO/srchnum.html&r=1&f=G&l=50&d=PG01&s1=20210079651.PGNR.

Popko, W., Georgiadou, S., Loukogeorgaki, E., & Vorpahl, F. (2016). Influence of joint flexibility on local dynamics of a jacket support structure. *Journal of Ocean and Wind Energy*, *3*(1), 1–9. https://doi.org/10.17736/jowe.2016.jcr45

Popko, W., Vorpahl, F., Zuga, A., Kohlmeier, M., Jonkman, J., Robertson, A., Larsen, T. J., Yde, A., Sætertrø, K., Okstad, K. M., Nichols, J., Nygaard, T. A., Gao, Z., Manolas, D., Kim, K., Yu, Q., Shi, W., Park, H., Vásquez-Rojas, A., … Von Waaden, H. (2012). Offshore code comparison collaboration continuation (OC4), phase I - Results of coupled simulations of an offshore wind turbine with jacket support structure. *Proceedings of the International Offshore and Polar Engineering Conference*, (March), 337–346.

Stolpe, M., Njomo Wandji, W., Natarajan, A., Shirzadeh, R., Kühn, M., & Kaufer, D. (2016). Innovative design of a hybrid-type jacket for 10MW turbines Document information. *308974*(308974), 67.

Thomas, N.-t., L., C. H., C., C. K., & W., Z. W. (2017). Environmental impacts of construction material production. *http://dx.doi.org/10.1680/jensu.15.00009*, *170*(3), 169–184. https://doi.org/10.1680/JENSU.15.00009

Tree Composites. (2021). Introducing the TC-joint. https://www.treecomposites.com/

van Vliet, M. (2019). Steel weight reduction in offshore wind jacket structures by wrapped FRP joints.

Vorpahl, F., Popko, W., & Kaufer, D. (2013). Technical Report Description of a basic model of the ' UpWind reference jacket ' for code comparison in the OC4 project under IEA Wind Annex 30. (November 2014).

Zhao, X. L., Herion, S., Packer, J. a., Puthli, R. S., Sedlacek, G., Wardenier, J., Weynand, K., Van Wingerde, a. M., & Yeomans, N. F. (2001). *Design guide for circular and rectangular hollow section welded joints under fatigue loading* (Vol. 8).

A

OpenFAST and Abaqus supplement

A.1. OpenFAST

A.1.1. OpenFAST - SubDyn Module

The SubDyn module is a time-domain structural dynamics module. It can be used to analyse fixed-bottom substructures such as monopiles, tripiles and jackets. The module is developed to function as a standalone program and couple with FAST. In this report, the module is used when coupled with FAST, but the standalone program has the capacity to calculate mode shapes, natural frequencies, and the time-domain response for the substructure given an interface point time series.

The SubDyn module employs two main engineering approaches to represent the substructure of an offshore wind turbine. The first is to use a **linear frame element model** (**LFEM**) to represent the substructure, and the second is to use the CB reduction method previously discussed in section 2.4. These two approaches were determined for several reasons. With respect to the choice of a LFEM, it has been seen in previous research that using a LFEM is suitable for analysing the substructures of offshore wind turbines. Through the analysis of several substructure types, with varying sizes of turbines, it was determined that the nonlinearities in the model were mostly due to the superstructure. This is due to the longer length of the tower and the heavier RNA mass.

The introduction of the nonlinearity is similar to the P-Delta effect, where small deviations from the undisturbed geometry have a large impact on the response of the structure. It was also seen that the substructure was made stiff enough to essentially behave linearly during these analyses (Damiani et al., 2013). Though not present in the SubDyn module, the ignored nonlinearities respective to the tower are captured in the ElastoDyn module. Within the SubDyn module, the choice of linear frame elements includes Euler-Bernoulli and Timoshenko beam elements. Regarding geometry of the cross-section, constant geometry or tapered geometry along the length of the beam are allowed.

With respect to the CB reduction, this method has previously been introduced in section 2.4. The reason for the use of this method in this submodule is to reduce the DOF of the substructure and to speed up the calculation of the time-history analysis of the offshore wind turbines. The lower frequency modes are kept because they are the most significant modes regarding the resonance due to the frequencies of the load spectrum. The higher frequency mode shapes characterised by large axial deformations normally would be ignored with this method. These mode shapes are often significant in the overall response of the substructure. SubDyn captures the contributions of these higher modes in a quasi-static way through the **static-improvement method** (**SIM**). To roughly explain the SIM, at each time step, the static solution of the full system stiffness matrix and the static solution of the CB reduced stiffness matrix are computed. The difference between the two solutions is retained and then summed with the dynamic solution at that given time step. This way, the otherwise ignored higher mode contributions

are now introduced to the solution at each time step.

SubDyn has several options to configure the boundary conditions of the substructure. The TP is forced to be treated as a rigid connection at the interface point. For the foundation, there is the choice of modelling the supports as fixed or through modelling **soil-stiffness interaction** (**SSI**). SSI is introduced through supplying a 6X6 matrix for the stiffness and mass of the foundation for each interface point. In this way, the soil response can be adjusted as an additional boundary condition. In figure A.1, the schematic of SubDyn is presented, highlighting some of the previously mentioned features of the module (NREL, 2021).

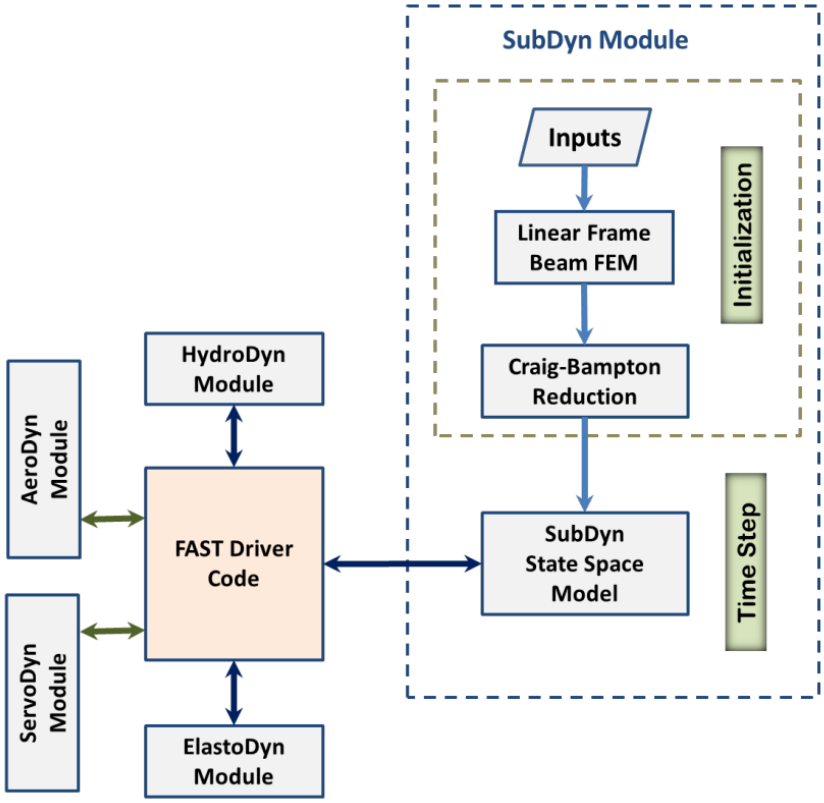

Figure A.1: SubDyn Layout (NREL, 2021)

A.1.2. OpenFAST - ExtPtfm Module

As previously shown in figure 3.2, OpenFAST has an ”ExtPtfm” module. The name comes from a shortened version of ”external platform”. This module acts as a substitute for the SubDyn module discussed in section A.1.1. By using ExtPtfm, instead of modelling the substructure in OpenFAST, the substructure is modelled with external software. This substructure is then imported into ExtPtfm in the form of system matrices and a loading vector due to the applied hydrodynamic loads. This then employs the superelement approach that was previously discussed in section 2.7. This option of analysis was utilised in this project due to the ability to model the jacket with high fidelity (specifically for joints). When using SubDyn, accounting for joint flexibility is limited. In figure A.2, the different options available to analyse the substructure with OpenFAST are shown (Branlard et al., 2020).

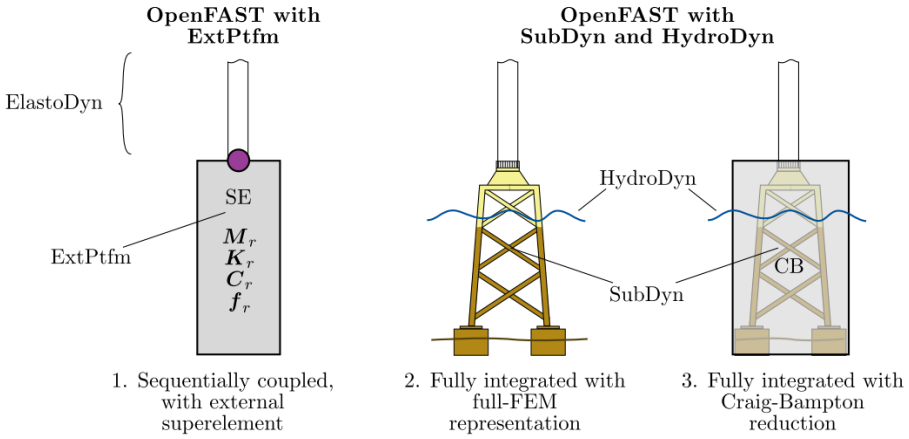

Figure A.2: SubDyn analysis options (Branlard et al., 2020)

A.2. Abaqus

A.2.1. Abaqus - Explicit vs. Implicit

Abaqus has two main analysis products. Abaqus/Standard and Abaqus/Explicit. Abaqus/Standard is an implicit solver that can be applied to many types of problems. This includes linear and nonlinear, and static and dynamic problems. The solution is obtained by solving the system of equations implicitly at each increment of the solver. This leads to this analysis product being unconditionally stable because it is a stiffness-based solution technique. Some of the drawbacks of the product are that it takes longer to solve the analyses, and the large number of iterations require a lot of memory.

Abaqus/Explicit is an explicit solver. This product is efficient for highly nonlinear analyses and contact simulations. This is because Abaqus/Explicit does not iterate between steps but rather solves for each time step explicitly through the use of an explicit central-difference time integration. Therefore, for each iteration, the acceleration, velocity, and displacement for all DOF are calculated, without solving the system of equations (like for the case of Abaqus/Standard). Unlike Abaqus/Standard, Abaqus/Explicit is conditionally stable and uses much less disk space while obtaining the solution (Dassault Systèmes, 2019a). To choose between the two products in an efficient manner, it requires an investigation into the DOF of the model that is being analysed. Figure A.3 highlights the relationship between computational cost for Abaqus/Standard and Abaqus/Explicit. A rough rule of thumb is that the computational cost for an implicit solver like Abaqus/Standard is proportional to the square of the number of DOF.

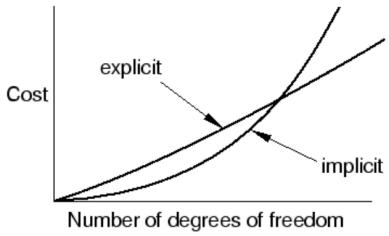

Figure A.3: Cost of analysis - explicit vs. implicit (Dassault Systèmes, 2019a)

When generating substructures, Abaqus/Standard is used, due to substructure generation being a linear perturbation procedure. A further elaboration is held in section 3.4.1. When applying a wave load analysis to the jacket support structure, this will be done with the Abaqus/Explicit analysis product, with the application of the Abaqus/Aqua module. This is discussed in section A.2.3

A.2.2. Abaqus - Modelling Options

With respect to the modelling itself, there are two main methods available: Abaqus/CAE and Abaqus keywords. Abaqus/CAE is the main method, with CAE being a backronymn for ”Complete Abaqus Environment”. With this environment, the model can be created regarding geometry, mesh size, material, load cases, boundary conditions, and desired results. When finished with the model, to start an analysis, Abaqus/CAE will submit jobs, which are called input files. Within the Abaqus/CAE environment, the user can monitor these jobs, and when complete, post-process the results.

The other modelling technique is to use Abaqus Keywords. The input files previously mentioned are text files that contain Abaqus Keywords that were generated internally with Abaqus/CAE. Instead of creating the model in the GUI of Abaqus/CAE, the user can generate the model through the application of Abaqus Keywords. There are syntax requirements, but the Keywords offer the ability to model faster than through the use of the GUI due to the ease of manipulating a text file compared to 3D simulated geometry. Some modules in Abaqus, like Abaqus/Aqua, require the user to submit the job with Abaqus Keywords. The Abaqus/Aqua module was used in this thesis project, so that is why the Abaqus Keywords were quickly mentioned.

A.2.3. Abaqus/Aqua analysis product

The Abaqus/Aqua analysis product can be used to apply steady current, wave, and wind loading. It can be used for cases of submerged or partially submerged structures. Within Abaqus/Aqua, static, direct-integration, and explicit dynamic analysis procedures can be used. In these analyses, the fluid particle velocity is determined through the sum of the gravity waves (depending on the applied theory), and the steady current (which can be set to be height dependent). The fluid particle velocities then determine the loads that are imposed on the elements in the model. These loads include drag, buoyancy, and fluid inertia loads.

As previously mentioned, the gravity waves that are employed in Abaqus/Aqua are defined by the user. Several options are available: Airy Wave theory, Stokes fifth-order wave theory, wave data read from a gridded mesh, or user-defined waves through subroutines. In this thesis project, Airy wave theory is used to shorten the duration of the analyses.

B

OC4 OWT - Project description

B.1. OC4 OWT supplementary information

B.1.1. OC4 - Transition piece overview

In the original version of the jacket, cans placed at the joint were present, but according to Cordle, the cans had a small impact on the overall dynamic behaviour, so they are not included in this project (Cordle, 2013). In the figure B.1, the jacket in combination with the tower and the TP are shown. The TP is made of concrete and is made to offer sufficient strength to act as a rigid piece on a macro-level.

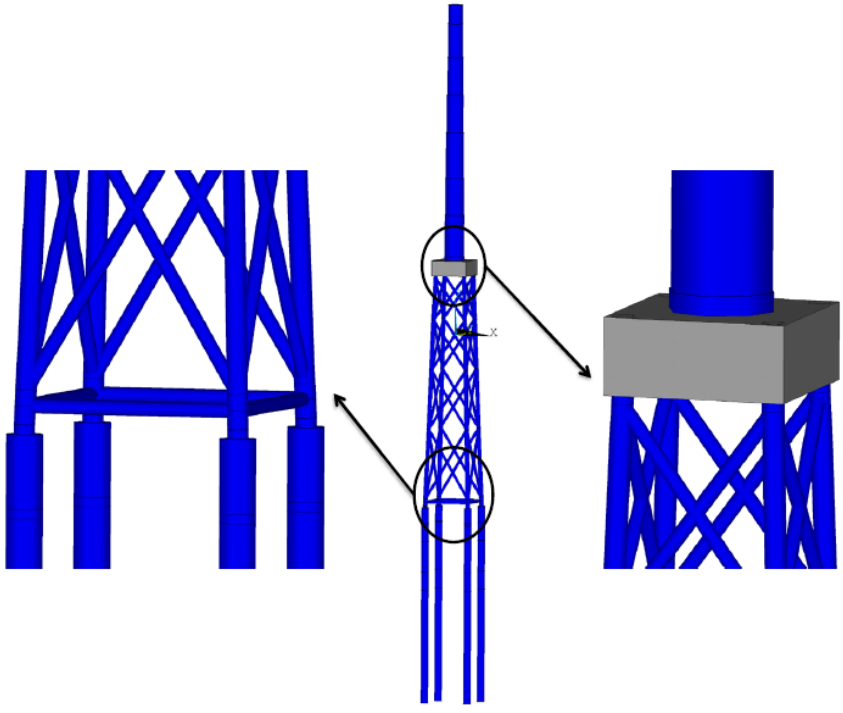

Figure B.1: OC4 tower and TP (Vorpahl et al., 2013)

B.1.2. OC4 - Tower properties

The tower geometrical properties are held in table B.1.

Table B.1: OC4 tower properties (Vorpahl et al., 2013)

Global height z [m]	Outer diameter [m]	Thickness [mm]	Point mass [t]
20.15	5.600	32	1.9
21.15	5.577	32	No
32.15	5.318	30	No
42.15	5.082	28	No
54.15	4.800	24	1.4
64.15	4.565	22	No
74.15	4.329	20	No
83.15	4.118	30	No
88.15	4.000	30	1.0

B.1.3. OC4 - Turbine properties

The turbine used in the OC4 OWT was the NREL 5MW turbine. Turbine information is held in table B.2.

Table B.2: NREL 5MW Baseline Wind Turbine (Jonkman et al., 2009)

Rating	5 MW
Rotor Orientation, Configuration	Upwind, 3 Blades
Control	Variable Speed, Collective Pitch
Drivetrain	High Speed, Multiple-Stage Gearbox
Rotor, Hub Diameter	126 m, 3 m
Hub Height	90 m
Cut-In, Rated, Cut-Out Wind Speed	3 m/s, 11.4 m/s, 25 m/s
Cut-In, Rated Rotor Speed	6.9 rpm, 12.1 rpm
Rated Tip Speed	80 m/s
Overhang, Shaft Tilt, Precone	5 m, 5º, 2.5º
Rotor Mass	110,000 kg
Nacelle Mass	240,000 kg
Tower Mass	347,460 kg
Coordinate Location of Overall CM	(-0.2 m, 0.0 m, 64.0 m)

B.1.4. OC4 - Marine growth properties

Lastly, it is important to mention that marine growth on the submerged members of the jacket was included in the analysis. This is because the marine growth was found to have a large impact on the dynamic response of the jacket in previous analyses done for the jacket (Popko et al., 2012). Information detailing this marine growth is held in table B.3.

Table B.3: Marine growth for OC4 jacket (Vorpahl et al., 2013)

Depth range:	40 $m \leq z_g \leq 2\ m$
Thickness:	t_g = 100 mm
Density:	ρ_g = 1100 kg/m^3

B.1.5. OC4 - Fatigue load case

The OC4 jacket was used to compare OpenFAST to Bladed. In the thesis previously published by Marc, there were several load cases applied to the offshore wind turbine to analyse the jacket support structure for fatigue and ultimate limit states. The load case to use as the verification was the 12 m/s fatigue load case. The details pertaining to the applied wind load and wave load are held in table B.4. The wind direction is 0 degrees from north, with no misalignment with the wave load. The simulation was run for 800 seconds, with the first 200 seconds ignored to remove the influence of start-up effects.

Table B.4: Fatigue load case information

Wind speed [m/s]	Turbulence Intensity [%]	H_s [m]	T_p [s]	Current speed [m/s]
11.4	14.78	1.63	5.84	0.6

C

OpenFAST files

Figure C.1: OpenFAST ”FAST glue code” for OC4 jacket analysis

```
------- OpenFAST EXAMPLE INPUT FILE -------------------------------------------
FAST Certification Test #21: NREL 5.0 MW Baseline Offshore Turbine with OC4 Jacket Configuration
---------------------- SIMULATION CONTROL --------------------------------------
True          Echo            - Echo input data to <RootName>.ech (flag)
"FATAL"       AbortLevel      - Error level when simulation should abort (string) {"WARNING", "SEVERE", "FATAL"}
        800   TMax            - Total run time (s)
       0.01   DT              - Recommended module time step (s)
          2   InterpOrder     - Interpolation order for input/output time history (-) {1=linear, 2=quadratic}
          1   NumCrctn        - Number of correction iterations (-) {0=explicit calculation, i.e., no corrections}
      99999   DT_UJac         - Time between calls to get Jacobians (s)
      1E+06   UJacSclFact     - Scaling factor used in Jacobians (-)
---------------------- FEATURE SWITCHES AND FLAGS ------------------------------
          1   CompElast       - Compute structural dynamics (switch) {1=ElastoDyn; 2=ElastoDyn + BeamDyn for blades}
          1   CompInflow      - Compute inflow wind velocities (switch) {0=still air; 1=InflowWind; 2=external from OpenFOAM}
          2   CompAero        - Compute aerodynamic loads (switch) {0=None; 1=AeroDyn v14; 2=AeroDyn v15}
          1   CompServo       - Compute control and electrical-drive dynamics (switch) {0=None; 1=ServoDyn}
          1   CompHydro       - Compute hydrodynamic loads (switch) {0=None; 1=HydroDyn}
          1   CompSub         - Compute sub-structural dynamics (switch) {0=None; 1=SubDyn; 2=External Platform MCKF}
          0   CompMooring     - Compute mooring system (switch) {0=None; 1=MAP++; 2=FEAMooring; 3=MoorDyn; 4=OrcaFlex}
          0   CompIce         - Compute ice loads (switch) {0=None; 1=IceFloe; 2=IceDyn}
---------------------- INPUT FILES ---------------------------------------------
"NRELOffshrBsline5MW_OC4Jacket_ElastoDyn.dat"    EDFile          - Name of file containing ElastoDyn input parameters (quoted string)
"../5MW_Baseline/NRELOffshrBsline5MW_BeamDyn.dat"    BDBldFile(1)    - Name of file containing BeamDyn input parameters for blade 1 (quoted string)
"../5MW_Baseline/NRELOffshrBsline5MW_BeamDyn.dat"    BDBldFile(2)    - Name of file containing BeamDyn input parameters for blade 2 (quoted string)
"../5MW_Baseline/NRELOffshrBsline5MW_BeamDyn.dat"    BDBldFile(3)    - Name of file containing BeamDyn input parameters for blade 3 (quoted string)
"../5MW_Baseline/NRELOffshrBsline5MW_InflowWind_12mps.dat"    InflowFile      - Name of file containing inflow wind input parameters (quoted string)
"NRELOffshrBsline5MW_OC4Jacket_AeroDyn15.dat"    AeroFile        - Name of file containing aerodynamic input parameters (quoted string)
"NRELOffshrBsline5MW_OC4Jacket_ServoDyn.dat"    ServoFile       - Name of file containing control and electrical-drive input parameters (quoted string)
"NRELOffshrBsline5MW_OC4Jacket_HydroDyn_Current.dat"    HydroFile       - Name of file containing hydrodynamic input parameters (quoted string)
"NRELOffshrBsline5MW_OC4Jacket_SubDyn_Dirty_SSI_Bot.dat"    SubFile         - Name of file containing sub-structural input parameters (quoted string)
"unused"      MooringFile     - Name of file containing mooring system input parameters (quoted string)
"unused"      IceFile         - Name of file containing ice input parameters (quoted string)
---------------------- OUTPUT --------------------------------------------------
True          SumPrint        - Print summary data to "<RootName>.sum" (flag)
          1   SttsTime        - Amount of time between screen status messages (s)
      99999   ChkptTime       - Amount of time between creating checkpoint files for potential restart (s)
       0.01   DT_Out          - Time step for tabular output (s) (or "default")
        200   TStart          - Time to begin tabular output (s)
          0   OutFileFmt      - Format for tabular (time-marching) output file (switch) {0: uncompressed binary [<RootName>.outb], 1: text file
[<RootName>.out], 2: binary file [<RootName>.outb], 3: both 1 and 2}
True          TabDelim        - Use tab delimiters in text tabular output file? (flag) {uses spaces if false}
"ES10.3E2"    OutFmt          - Format used for text tabular output, excluding the time channel.  Resulting field should be 10 characters. (quoted
string)
---------------------- LINEARIZATION -------------------------------------------
False         Linearize       - Linearization analysis (flag)
True         CalcSteady      - Calculate a steady-state periodic operating point before linearization? [unused if Linearize=False] (flag)
          3   TrimCase        - Controller parameter to be trimmed {1:yaw; 2:torque; 3:pitch} [used only if CalcSteady=True] (-)
      0.001   TrimTol         - Tolerance for the rotational speed convergence [used only if CalcSteady=True] (-)
       0.01   TrimGain        - Proportional gain for the rotational speed error (>0) [used only if CalcSteady=True] (rad/(rad/s) for yaw or pitch;
Nm/(rad/s) for torque)
       0.01   Twr_Kdmp        - Damping factor for the tower [used only if CalcSteady=True] (N/(m/s))
       0.01   Bld_Kdmp        - Damping factor for the blades [used only if CalcSteady=True] (N/(m/s))
          2   NLinTimes       - Number of times to linearize (-) [>=1] [unused if Linearize=False]
         30,         60    LinTimes        - List of times at which to linearize (s) [1 to NLinTimes] [used only when Linearize=True and
CalcSteady=False]
          1   LinInputs       - Inputs included in linearization (switch) {0=none; 1=standard; 2=all module inputs (debug)} [unused if Linearize=False]
          1   LinOutputs      - Outputs included in linearization (switch) {0=none; 1=from OutList(s); 2=all module outputs (debug)} [unused if
Linearize=False]
False         LinOutJac       - Include full Jacobians in linearization output (for debug) (flag) [unused if Linearize=False; used only if
LinInputs=LinOutputs=2]
False         LinOutMod       - Write module-level linearization output files in addition to output for full system? (flag) [unused if Linearize=False]
---------------------- VISUALIZATION -------------------------------------------
          0   WrVTK           - VTK visualization data output: (switch) {0=none; 1=initialization data only; 2=animation; 3=mode shapes}
          2   VTK_type        - Type of VTK visualization data: (switch) {1=surfaces; 2=basic meshes (lines/points); 3=all meshes (debug)} [unused if
WrVTK=0]
false         VTK_fields      - Write mesh fields to VTK data files? (flag) {true/false} [unused if WrVTK=0]
         15   VTK_fps         - Frame rate for VTK output (frames per second){will use closest integer multiple of DT} [used only if WrVTK=2 or WrVTK=3]
```

Figure C.2: OpenFAST ElastoDyn input file for OC4 jacket analysis P.1

```
------- ELASTODYN for OpenFAST INPUT FILE ----------------------------------------
OC4 TOWER+ NREL 5.0 MW Baseline Wind Turbine for Use in Offshore Analysis. Properties from Dutch Offshore Wind Energy Converter
(DOWEC) 6MW Pre-Design (10046_009.pdf) and REpower 5M 5MW (5m_uk.pdf);
---------------------- SIMULATION CONTROL --------------------------------------
False         Echo        - Echo input data to "<RootName>.ech" (flag)
          3   Method      - Integration method: {1: RK4, 2: AB4, or 3: ABM4} (-)
"DEFAULT"     DT          - Integration time step (s)
---------------------- ENVIRONMENTAL CONDITION ---------------------------------
    9.80665   Gravity     - Gravitational acceleration (m/s^2)
---------------------- DEGREES OF FREEDOM --------------------------------------
True          FlapDOF1    - First flapwise blade mode DOF (flag)
True          FlapDOF2    - Second flapwise blade mode DOF (flag)
True          EdgeDOF     - First edgewise blade mode DOF (flag)
False         TeetDOF     - Rotor-teeter DOF (flag) [unused for 3 blades]
True          DrTrDOF     - Drivetrain rotational-flexibility DOF (flag)
True          GenDOF      - Generator DOF (flag)
True          YawDOF      - Yaw DOF (flag)
True          TwFADOF1    - First fore-aft tower bending-mode DOF (flag)
True          TwFADOF2    - Second fore-aft tower bending-mode DOF (flag)
True          TwSSDOF1    - First side-to-side tower bending-mode DOF (flag)
True          TwSSDOF2    - Second side-to-side tower bending-mode DOF (flag)
True          PtfmSgDOF   - Platform horizontal surge translation DOF (flag)
True          PtfmSwDOF   - Platform horizontal sway translation DOF (flag)
True          PtfmHvDOF   - Platform vertical heave translation DOF (flag)
True          PtfmRDOF    - Platform roll tilt rotation DOF (flag)
True          PtfmPDOF    - Platform pitch tilt rotation DOF (flag)
True          PtfmYDOF    - Platform yaw rotation DOF (flag)
---------------------- INITIAL CONDITIONS --------------------------------------
          0   OoPDefl     - Initial out-of-plane blade-tip displacement (meters)
          0   IPDefl      - Initial in-plane blade-tip deflection (meters)
          0   BlPitch(1)  - Blade 1 initial pitch (degrees)
          0   BlPitch(2)  - Blade 2 initial pitch (degrees)
          0   BlPitch(3)  - Blade 3 initial pitch (degrees) [unused for 2 blades]
          0   TeetDefl    - Initial or fixed teeter angle (degrees) [unused for 3 blades]
          0   Azimuth     - Initial azimuth angle for blade 1 (degrees)
       12.1   RotSpeed    - Initial or fixed rotor speed (rpm)
          0   NacYaw      - Initial or fixed nacelle-yaw angle (degrees)
          0   TTDspFA     - Initial fore-aft tower-top displacement (meters)
          0   TTDspSS     - Initial side-to-side tower-top displacement (meters)
          0   PtfmSurge   - Initial or fixed horizontal surge translational displacement of platform (meters)
          0   PtfmSway    - Initial or fixed horizontal sway translational displacement of platform (meters)
    -0.00702  PtfmHeave   - Initial or fixed vertical heave translational displacement of platform (meters)
          0   PtfmRoll    - Initial or fixed roll tilt rotational displacement of platform (degrees)
          0   PtfmPitch   - Initial or fixed pitch tilt rotational displacement of platform (degrees)
          0   PtfmYaw     - Initial or fixed yaw rotational displacement of platform (degrees)
---------------------- TURBINE CONFIGURATION -----------------------------------
          3   NumBl       - Number of blades (-)
         63   TipRad      - The distance from the rotor apex to the blade tip (meters)
        1.5   HubRad      - The distance from the rotor apex to the blade root (meters)
       -2.5   PreCone(1)  - Blade 1 cone angle (degrees)
       -2.5   PreCone(2)  - Blade 2 cone angle (degrees)
       -2.5   PreCone(3)  - Blade 3 cone angle (degrees) [unused for 2 blades]
          0   HubCM       - Distance from rotor apex to hub mass [positive downwind] (meters)
          0   UndSling    - Undersling length [distance from teeter pin to the rotor apex] (meters) [unused for 3 blades]
          0   Delta3      - Delta-3 angle for teetering rotors (degrees) [unused for 3 blades]
          0   AzimB1Up    - Azimuth value to use for I/O when blade 1 points up (degrees)
    -5.0191   OverHang    - Distance from yaw axis to rotor apex [3 blades] or teeter pin [2 blades] (meters)
      1.912   ShftGagL    - Distance from rotor apex [3 blades] or teeter pin [2 blades] to shaft strain gages [positive for upwind
rotors] (meters)
         -5   ShftTilt    - Rotor shaft tilt angle (degrees)
        1.9   NacCMxn     - Downwind distance from the tower-top to the nacelle CM (meters)
          0   NacCMyn     - Lateral  distance from the tower-top to the nacelle CM (meters)
       1.75   NacCMzn     - Vertical distance from the tower-top to the nacelle CM (meters)
   -3.09528   NcIMUxn     - Downwind distance from the tower-top to the nacelle IMU (meters)
          0   NcIMUyn     - Lateral  distance from the tower-top to the nacelle IMU (meters)
    2.23336   NcIMUzn     - Vertical distance from the tower-top to the nacelle IMU (meters)
    1.96256   Twr2Shft    - Vertical distance from the tower-top to the rotor shaft (meters)
      88.15   TowerHt     - Height of tower above ground level [onshore] or MSL [offshore] (meters)
      20.15   TowerBsHt   - Height of tower base above ground level [onshore] or MSL [offshore] (meters)
          0   PtfmCMxt    - Downwind distance from the ground level [onshore] or MSL [offshore] to the platform CM (meters)
          0   PtfmCMyt    - Lateral distance from the ground level [onshore] or MSL [offshore] to the platform CM (meters)
      18.15   PtfmCMzt    - Vertical distance from the ground level [onshore] or MSL [offshore] to the platform CM (meters)
      18.15   PtfmRefzt   - Vertical distance from the ground level [onshore] or MSL [offshore] to the platform reference point
(meters)
---------------------- MASS AND INERTIA ----------------------------------------
          0   TipMass(1)  - Tip-brake mass, blade 1 (kg)
          0   TipMass(2)  - Tip-brake mass, blade 2 (kg)
          0   TipMass(3)  - Tip-brake mass, blade 3 (kg) [unused for 2 blades]
      56780   HubMass     - Hub mass (kg)
     115926   HubIner     - Hub inertia about rotor axis [3 blades] or teeter axis [2 blades] (kg m^2)
    534.116   GenIner     - Generator inertia about HSS (kg m^2)
     240000   NacMass     - Nacelle mass (kg)
2.60789E+06   NacYIner    - Nacelle inertia about yaw axis (kg m^2)
          0   YawBrMass   - Yaw bearing mass (kg)
     666000   PtfmMass    - Platform mass (kg)
6.00288E+06   PtfmRIner   - Platform inertia for roll tilt rotation about the platform CM (kg m^2)
6.00288E+06   PtfmPIner   - Platform inertia for pitch tilt rotation about the platform CM (kg m^2)
1.02298E+07   PtfmYIner   - Platform inertia for yaw rotation about the platform CM (kg m^2)
---------------------- BLADE ---------------------------------------------------
         17   BldNodes    - Number of blade nodes (per blade) used for analysis (-)
"../5MW_Baseline/NRELOffshrBsline5MW_Blade.dat"    BldFile(1)  - Name of file containing properties for blade 1 (quoted string)
"../5MW_Baseline/NRELOffshrBsline5MW_Blade.dat"    BldFile(2)  - Name of file containing properties for blade 2 (quoted string)
```

Figure C.3: OpenFAST ElastoDyn input file for OC4 jacket analysis P.2

```
"../5MW_Baseline/NRELOffshrBsline5MW_Blade.dat"    BldFile(3)  - Name of file containing properties for blade 3 (quoted string)
[unused for 2 blades]
---------------------- ROTOR-TEETER ---------------------------------------------
          0   TeetMod     - Rotor-teeter spring/damper model {0: none, 1: standard, 2: user-defined from routine UserTeet} (switch)
[unused for 3 blades]
          0   TeetDmpP    - Rotor-teeter damper position (degrees) [used only for 2 blades and when TeetMod=1]
          0   TeetDmp     - Rotor-teeter damping constant (N-m/(rad/s)) [used only for 2 blades and when TeetMod=1]
          0   TeetCDmp    - Rotor-teeter rate-independent Coulomb-damping moment (N-m) [used only for 2 blades and when TeetMod=1]
          0   TeetSStP    - Rotor-teeter soft-stop position (degrees) [used only for 2 blades and when TeetMod=1]
          0   TeetHStP    - Rotor-teeter hard-stop position (degrees) [used only for 2 blades and when TeetMod=1]
          0   TeetSSSp    - Rotor-teeter soft-stop linear-spring constant (N-m/rad) [used only for 2 blades and when TeetMod=1]
          0   TeetHSSp    - Rotor-teeter hard-stop linear-spring constant (N-m/rad) [used only for 2 blades and when TeetMod=1]
---------------------- DRIVETRAIN -----------------------------------------------
        100   GBoxEff     - Gearbox efficiency (%)
         97   GBRatio     - Gearbox ratio (-)
8.67637E+08   DTTorSpr    - Drivetrain torsional spring (N-m/rad)
  6.215E+06   DTTorDmp    - Drivetrain torsional damper (N-m/(rad/s))
---------------------- FURLING --------------------------------------------------
False         Furling     - Read in additional model properties for furling turbine (flag) [must currently be FALSE)
"unused"      FurlFile    - Name of file containing furling properties (quoted string) [unused when Furling=False]
---------------------- TOWER ----------------------------------------------------
         20   TwrNodes    - Number of tower nodes used for analysis (-)
"NRELOffshrBsline5MW_OC4Jacket_ElastoDyn_Tower.dat"    TwrFile     - Name of file containing tower properties (quoted string)
---------------------- OUTPUT ---------------------------------------------------
True          SumPrint    - Print summary data to "<RootName>.sum" (flag)
          2   OutFile     - Switch to determine where output will be placed: {1: in module output file only; 2: in glue code output
file only; 3: both} (currently unused)
True          TabDelim    - Use tab delimiters in text tabular output file? (flag) (currently unused)
"ES10.3E2"    OutFmt      - Format used for text tabular output (except time).  Resulting field should be 10 characters. (quoted
string) (currently unused)
         30   TStart      - Time to begin tabular output (s) (currently unused)
          1   DecFact     - Decimation factor for tabular output {1: output every time step} (-) (currently unused)
          0   NTwGages    - Number of tower nodes that have strain gages for output [0 to 9] (-)
          0   TwrGagNd    - List of tower nodes that have strain gages [1 to TwrNodes] (-) [unused if NTwGages=0]
          3   NBlGages    - Number of blade nodes that have strain gages for output [0 to 9] (-)
          5,          9,         13    BldGagNd    - List of blade nodes that have strain gages [1 to BldNodes] (-) [unused if
NBlGages=0]
              OutList     - The next line(s) contains a list of output parameters.  See OutListParameters.xlsx for a listing of
available output channels, (-)
"RotSpeed , GenSpeed"             - Low-speed shaft and high-speed shaft speeds
"TwrBsMxt , TwrBsMyt , TwrBsMzt"  - Side-to-side bending, fore-aft bending, and yaw moments at the mudline
END of input file (the word "END" must appear in the first 3 columns of this last OutList line)
---------------------------------------------------------------------------------------
```

Figure C.4: OpenFAST ElastoDyn tower input file for OC4 jacket analysis

```
------- ELASTODYN V1.00.* TOWER INPUT FILE ------------------------------------
NREL 5.0 MW offshore baseline OC4 tower with flexible Jacket SubStructure (however SS cantilevered at seabed).
---------------------- TOWER PARAMETERS ----------------------------------------
         22   NTwInpSt    - Number of input stations to specify tower geometry
          1   TwrFADmp(1) - Tower 1st fore-aft mode structural damping ratio (%)
          1   TwrFADmp(2) - Tower 2nd fore-aft mode structural damping ratio (%)
          1   TwrSSDmp(1) - Tower 1st side-to-side mode structural damping ratio (%)
          1   TwrSSDmp(2) - Tower 2nd side-to-side mode structural damping ratio (%)
---------------------- TOWER ADJUSTMUNT FACTORS --------------------------------
          1   FAStTunr(1) - Tower fore-aft modal stiffness tuner, 1st mode (-)
          1   FAStTunr(2) - Tower fore-aft modal stiffness tuner, 2nd mode (-)
          1   SSStTunr(1) - Tower side-to-side stiffness tuner, 1st mode (-)
          1   SSStTunr(2) - Tower side-to-side stiffness tuner, 2nd mode (-)
          1   AdjTwMa     - Factor to adjust tower mass density (-)
          1   AdjFASt     - Factor to adjust tower fore-aft stiffness (-)
          1   AdjSSSt     - Factor to adjust tower side-to-side stiffness (-)
---------------------- DISTRIBUTED TOWER PROPERTIES ----------------------------
HtFract    TMassDen      TwFAStif       TwSSStif
 (-)        (kg/m)        (Nm^2)         (Nm^2)
0.000    4900.472786      4.5556E+11     4.5556E+11
0.025    4900.472786      4.4419E+11     4.4419E+11
0.075    4200.272421      4.1707E+11     4.1707E+11
0.125    4057.180384      3.9120E+11     3.9120E+11
0.175    3915.575049      3.6655E+11     3.6655E+11
0.225    3770.476234      3.4234E+11     3.4234E+11
0.275    3626.859482      3.1932E+11     3.1932E+11
0.325    3477.860118      2.9733E+11     2.9733E+11
0.375    3291.027294      2.7214E+11     2.7214E+11
0.425    3102.11339       2.4846E+11     2.4846E+11
0.475    3123.48485       2.2622E+11     2.2622E+11
0.525    2969.643543      2.0732E+11     2.0732E+11
0.575    2639.437112      1.9143E+11     1.9143E+11
0.625    2517.768961      1.7644E+11     1.7644E+11
0.675    2398.659195      1.6232E+11     1.6232E+11
0.725    2282.133754      1.4902E+11     1.4902E+11
0.775    2173.8144        1.3653E+11     1.3653E+11
0.825    2344.181633      1.4213E+11     1.4213E+11
0.875    2687.066514      1.5659E+11     1.5659E+11
0.925    2971.054769      1.6870E+11     1.6870E+11
0.975    3260.985159      1.5955E+11     1.5955E+11
1.000    3260.985159      1.5481E+11     1.5481E+11
---------------------- TOWER FORE-AFT MODE SHAPES ------------------------------
     1.0221    TwFAM1Sh(2) - Mode 1, coefficient of x^2 term
     0.0483    TwFAM1Sh(3) -       , coefficient of x^3 term
    -0.0948    TwFAM1Sh(4) -       , coefficient of x^4 term
     0.2283    TwFAM1Sh(5) -       , coefficient of x^5 term
    -0.2039    TwFAM1Sh(6) -       , coefficient of x^6 term
     0.6197    TwFAM2Sh(2) - Mode 2, coefficient of x^2 term
     0.5380    TwFAM2Sh(3) -       , coefficient of x^3 term
    -0.4478    TwFAM2Sh(4) -       , coefficient of x^4 term
     0.7483    TwFAM2Sh(5) -       , coefficient of x^5 term
    -0.4582    TwFAM2Sh(6) -       , coefficient of x^6 term
---------------------- TOWER SIDE-TO-SIDE MODE SHAPES --------------------------
     1.0034    TwSSM1Sh(2) - Mode 1, coefficient of x^2 term
     0.0700    TwSSM1Sh(3) -       , coefficient of x^3 term
    -0.1377    TwSSM1Sh(4) -       , coefficient of x^4 term
     0.2943    TwSSM1Sh(5) -       , coefficient of x^5 term
    -0.2300    TwSSM1Sh(6) -       , coefficient of x^6 term
     0.5250    TwSSM2Sh(2) - Mode 2, coefficient of x^2 term
     0.6536    TwSSM2Sh(3) -       , coefficient of x^3 term
    -0.6967    TwSSM2Sh(4) -       , coefficient of x^4 term
     1.1231    TwSSM2Sh(5) -       , coefficient of x^5 term
    -0.6049    TwSSM2Sh(6) -       , coefficient of x^6 term
```

Figure C.5: OpenFAST ElastoDyn blade input file for OC4 jacket analysis

```
------- ELASTODYN V1.00.* INDIVIDUAL BLADE INPUT FILE --------------------------
NREL 5.0 MW offshore baseline blade input properties.
---------------------- BLADE PARAMETERS ----------------------------------------
         49   NBlInpSt    - Number of blade input stations (-)
   0.477465   BldFlDmp(1) - Blade flap mode #1 structural damping in percent of critical (%)
   0.477465   BldFlDmp(2) - Blade flap mode #2 structural damping in percent of critical (%)
   0.477465   BldEdDmp(1) - Blade edge mode #1 structural damping in percent of critical (%)
---------------------- BLADE ADJUSTMENT FACTORS --------------------------------
          1   FlStTunr(1) - Blade flapwise modal stiffness tuner, 1st mode (-)
          1   FlStTunr(2) - Blade flapwise modal stiffness tuner, 2nd mode (-)
    1.04536   AdjBlMs     - Factor to adjust blade mass density (-)  !bjj: value for AD14=1.04536; value for AD15=1.057344 (it would be nice
to enter the requested blade mass instead of a factor here)
          1   AdjFlSt     - Factor to adjust blade flap stiffness (-)
          1   AdjEdSt     - Factor to adjust blade edge stiffness (-)
---------------------- DISTRIBUTED BLADE PROPERTIES ----------------------------
    BlFract      PitchAxis      StrcTwst       BMassDen        FlpStff        EdgStff
      (-)            (-)          (deg)          (kg/m)         (Nm^2)         (Nm^2)
0.0000000E+00  2.5000000E-01  1.3308000E+01  6.7893500E+02  1.8110000E+10  1.8113600E+10
3.2500000E-03  2.5000000E-01  1.3308000E+01  6.7893500E+02  1.8110000E+10  1.8113600E+10
1.9510000E-02  2.5049000E-01  1.3308000E+01  7.7336300E+02  1.9424900E+10  1.9558600E+10
3.5770000E-02  2.5490000E-01  1.3308000E+01  7.4055000E+02  1.7455900E+10  1.9497800E+10
5.2030000E-02  2.6716000E-01  1.3308000E+01  7.4004200E+02  1.5287400E+10  1.9788800E+10
6.8290000E-02  2.7941000E-01  1.3308000E+01  5.9249600E+02  1.0782400E+10  1.4858500E+10
8.4550000E-02  2.9167000E-01  1.3308000E+01  4.5027500E+02  7.2297200E+09  1.0220600E+10
1.0081000E-01  3.0392000E-01  1.3308000E+01  4.2405400E+02  6.3095400E+09  9.1447000E+09
1.1707000E-01  3.1618000E-01  1.3308000E+01  4.0063800E+02  5.5283600E+09  8.0631600E+09
1.3335000E-01  3.2844000E-01  1.3308000E+01  3.8206200E+02  4.9800600E+09  6.8844400E+09
1.4959000E-01  3.4069000E-01  1.3308000E+01  3.9965500E+02  4.9368400E+09  7.0091800E+09
1.6585000E-01  3.5294000E-01  1.3308000E+01  4.2632100E+02  4.6916600E+09  7.1676800E+09
1.8211000E-01  3.6519000E-01  1.3181000E+01  4.1682000E+02  3.9494600E+09  7.2716600E+09
1.9837000E-01  3.7500000E-01  1.2848000E+01  4.0618600E+02  3.3865200E+09  7.0817000E+09
2.1465000E-01  3.7500000E-01  1.2192000E+01  3.8142000E+02  2.9337400E+09  6.2445300E+09
2.3089000E-01  3.7500000E-01  1.1561000E+01  3.5282200E+02  2.5689600E+09  5.0489600E+09
2.4715000E-01  3.7500000E-01  1.1072000E+01  3.4947700E+02  2.3886500E+09  4.9484900E+09
2.6341000E-01  3.7500000E-01  1.0792000E+01  3.4653800E+02  2.2719900E+09  4.8080200E+09
2.9595000E-01  3.7500000E-01  1.0232000E+01  3.3933300E+02  2.0500500E+09  4.5014000E+09
3.2846000E-01  3.7500000E-01  9.6720000E+00  3.3000400E+02  1.8282500E+09  4.2440700E+09
3.6098000E-01  3.7500000E-01  9.1100000E+00  3.2199000E+02  1.5887100E+09  3.9952800E+09
3.9350000E-01  3.7500000E-01  8.5340000E+00  3.1382000E+02  1.3619300E+09  3.7507600E+09
4.2602000E-01  3.7500000E-01  7.9320000E+00  2.9473400E+02  1.1023800E+09  3.4471400E+09
4.5855000E-01  3.7500000E-01  7.3210000E+00  2.8712000E+02  8.7580000E+08  3.1390700E+09
4.9106000E-01  3.7500000E-01  6.7110000E+00  2.6334300E+02  6.8130000E+08  2.7342400E+09
5.2358000E-01  3.7500000E-01  6.1220000E+00  2.5320700E+02  5.3472000E+08  2.5548700E+09
5.5610000E-01  3.7500000E-01  5.5460000E+00  2.4166600E+02  4.0890000E+08  2.3340300E+09
5.8862000E-01  3.7500000E-01  4.9710000E+00  2.2063800E+02  3.1454000E+08  1.8287300E+09
6.2115000E-01  3.7500000E-01  4.4010000E+00  2.0029300E+02  2.3863000E+08  1.5841000E+09
6.5366000E-01  3.7500000E-01  3.8340000E+00  1.7940400E+02  1.7588000E+08  1.3233600E+09
6.8618000E-01  3.7500000E-01  3.3320000E+00  1.6509400E+02  1.2601000E+08  1.1836800E+09
7.1870000E-01  3.7500000E-01  2.8900000E+00  1.5441100E+02  1.0726000E+08  1.0201600E+09
7.5122000E-01  3.7500000E-01  2.5030000E+00  1.3893500E+02  9.0880000E+07  7.9781000E+08
7.8376000E-01  3.7500000E-01  2.1160000E+00  1.2955500E+02  7.6310000E+07  7.0961000E+08
8.1626000E-01  3.7500000E-01  1.7300000E+00  1.0726400E+02  6.1050000E+07  5.1819000E+08
8.4878000E-01  3.7500000E-01  1.3420000E+00  9.8776000E+01  4.9480000E+07  4.5487000E+08
8.8130000E-01  3.7500000E-01  9.5400000E-01  9.0248000E+01  3.9360000E+07  3.9512000E+08
8.9756000E-01  3.7500000E-01  7.6000000E-01  8.3001000E+01  3.4670000E+07  3.5372000E+08
9.1382000E-01  3.7500000E-01  5.7400000E-01  7.2906000E+01  3.0410000E+07  3.0473000E+08
9.3008000E-01  3.7500000E-01  4.0400000E-01  6.8772000E+01  2.6520000E+07  2.8142000E+08
9.3821000E-01  3.7500000E-01  3.1900000E-01  6.6264000E+01  2.3840000E+07  2.6171000E+08
9.4636000E-01  3.7500000E-01  2.5300000E-01  5.9340000E+01  1.9630000E+07  1.5881000E+08
9.5447000E-01  3.7500000E-01  2.1600000E-01  5.5914000E+01  1.6000000E+07  1.3788000E+08
9.6260000E-01  3.7500000E-01  1.7800000E-01  5.2484000E+01  1.2830000E+07  1.1879000E+08
9.7073000E-01  3.7500000E-01  1.4000000E-01  4.9114000E+01  1.0080000E+07  1.0163000E+08
9.7886000E-01  3.7500000E-01  1.0100000E-01  4.5818000E+01  7.5500000E+06  8.5070000E+07
9.8699000E-01  3.7500000E-01  6.2000000E-02  4.1669000E+01  4.6000000E+06  6.4260000E+07
9.9512000E-01  3.7500000E-01  2.3000000E-02  1.1453000E+01  2.5000000E+05  6.6100000E+06
1.0000000E+00  3.7500000E-01  0.0000000E+00  1.0319000E+01  1.7000000E+05  5.0100000E+06
---------------------- BLADE MODE SHAPES ---------------------------------------
     0.0622   BldFl1Sh(2) - Flap mode 1, coeff of x^2
     1.7254   BldFl1Sh(3) -             , coeff of x^3
    -3.2452   BldFl1Sh(4) -             , coeff of x^4
     4.7131   BldFl1Sh(5) -             , coeff of x^5
    -2.2555   BldFl1Sh(6) -             , coeff of x^6
    -0.5809   BldFl2Sh(2) - Flap mode 2, coeff of x^2
     1.2067   BldFl2Sh(3) -             , coeff of x^3
   -15.5349   BldFl2Sh(4) -             , coeff of x^4
    29.7347   BldFl2Sh(5) -             , coeff of x^5
   -13.8255   BldFl2Sh(6) -             , coeff of x^6
     0.3627   BldEdgSh(2) - Edge mode 1, coeff of x^2
     2.5337   BldEdgSh(3) -             , coeff of x^3
    -3.5772   BldEdgSh(4) -             , coeff of x^4
      2.376   BldEdgSh(5) -             , coeff of x^5
    -0.6952   BldEdgSh(6) -             , coeff of x^6
```

Figure C.6: OpenFAST BeamDyn input file for OC4 jacket analysis

```
--------- BEAMDYN with OpenFAST INPUT FILE -------------------------------------------
NREL 5MW blade
---------------------- SIMULATION CONTROL --------------------------------------
False         Echo             - Echo input data to "<RootName>.ech"? (flag)
True          QuasiStaticInit  - Use quasi-static pre-conditioning with centripetal accelerations in initialization? (flag) [dynamic solve
only]
          0   rhoinf           - Numerical damping parameter for generalized-alpha integrator
          2   quadrature       - Quadrature method: 1=Gaussian; 2=Trapezoidal (switch)
"DEFAULT"     refine           - Refinement factor for trapezoidal quadrature (-) [DEFAULT = 1; used only when quadrature=2]
"DEFAULT"     n_fact           - Factorization frequency for the Jacobian in N-R iteration(-) [DEFAULT = 5]
"DEFAULT"     DTBeam           - Time step size (s)
"DEFAULT"     load_retries     - Number of factored load retries before quitting the simulation [DEFAULT = 20]
"DEFAULT"     NRMax            - Max number of iterations in Newton-Raphson algorithm (-) [DEFAULT = 10]
"DEFAULT"     stop_tol         - Tolerance for stopping criterion (-) [DEFAULT = 1E-5]
"DEFAULT"     tngt_stf_fd      - Use finite differenced tangent stiffness matrix? (flag)
"DEFAULT"     tngt_stf_comp    - Compare analytical finite differenced tangent stiffness matrix? (flag)
"DEFAULT"     tngt_stf_pert    - Perturbation size for finite differencing (-) [DEFAULT = 1E-6]
"DEFAULT"     tngt_stf_difftol - Maximum allowable relative difference between analytical and fd tangent stiffness (-); [DEFAULT = 0.1]
True          RotStates        - Orient states in the rotating frame during linearization? (flag) [used only when linearizing]
---------------------- GEOMETRY PARAMETER --------------------------------------
          1   member_total    - Total number of members (-)
         49   kp_total        - Total number of key points (-) [must be at least 3]
     1     49                 - Member number; Number of key points in this member
   kp_xr         kp_yr         kp_zr        initial_twist
   (m)             (m)          (m)            (deg)
0.0000000E+00  0.0000000E+00  0.0000000E+00  1.3308000E+01
0.0000000E+00  0.0000000E+00  1.9987500E-01  1.3308000E+01
0.0000000E+00  0.0000000E+00  1.1998650E+00  1.3308000E+01
0.0000000E+00  0.0000000E+00  2.1998550E+00  1.3308000E+01
0.0000000E+00  0.0000000E+00  3.1998450E+00  1.3308000E+01
0.0000000E+00  0.0000000E+00  4.1998350E+00  1.3308000E+01
0.0000000E+00  0.0000000E+00  5.1998250E+00  1.3308000E+01
0.0000000E+00  0.0000000E+00  6.1998150E+00  1.3308000E+01
0.0000000E+00  0.0000000E+00  7.1998050E+00  1.3308000E+01
0.0000000E+00  0.0000000E+00  8.2010250E+00  1.3308000E+01
0.0000000E+00  0.0000000E+00  9.1997850E+00  1.3308000E+01
0.0000000E+00  0.0000000E+00  1.0199775E+01  1.3308000E+01
0.0000000E+00  0.0000000E+00  1.1199765E+01  1.3181000E+01
0.0000000E+00  0.0000000E+00  1.2199755E+01  1.2848000E+01
0.0000000E+00  0.0000000E+00  1.3200975E+01  1.2192000E+01
0.0000000E+00  0.0000000E+00  1.4199735E+01  1.1561000E+01
0.0000000E+00  0.0000000E+00  1.5199725E+01  1.1072000E+01
0.0000000E+00  0.0000000E+00  1.6199715E+01  1.0792000E+01
0.0000000E+00  0.0000000E+00  1.8200925E+01  1.0232000E+01
0.0000000E+00  0.0000000E+00  2.0200290E+01  9.6720000E+00
0.0000000E+00  0.0000000E+00  2.2200270E+01  9.1100000E+00
0.0000000E+00  0.0000000E+00  2.4200250E+01  8.5340000E+00
0.0000000E+00  0.0000000E+00  2.6200230E+01  7.9320000E+00
0.0000000E+00  0.0000000E+00  2.8200825E+01  7.3210000E+00
0.0000000E+00  0.0000000E+00  3.0200190E+01  6.7110000E+00
0.0000000E+00  0.0000000E+00  3.2200170E+01  6.1220000E+00
0.0000000E+00  0.0000000E+00  3.4200150E+01  5.5460000E+00
0.0000000E+00  0.0000000E+00  3.6200130E+01  4.9710000E+00
0.0000000E+00  0.0000000E+00  3.8200725E+01  4.4010000E+00
0.0000000E+00  0.0000000E+00  4.0200090E+01  3.8340000E+00
0.0000000E+00  0.0000000E+00  4.2200070E+01  3.3320000E+00
0.0000000E+00  0.0000000E+00  4.4200050E+01  2.8900000E+00
0.0000000E+00  0.0000000E+00  4.6200030E+01  2.5030000E+00
0.0000000E+00  0.0000000E+00  4.8201240E+01  2.1160000E+00
0.0000000E+00  0.0000000E+00  5.0199990E+01  1.7300000E+00
0.0000000E+00  0.0000000E+00  5.2199970E+01  1.3420000E+00
0.0000000E+00  0.0000000E+00  5.4199950E+01  9.5400000E-01
0.0000000E+00  0.0000000E+00  5.5199940E+01  7.6000000E-01
0.0000000E+00  0.0000000E+00  5.6199930E+01  5.7400000E-01
0.0000000E+00  0.0000000E+00  5.7199920E+01  4.0400000E-01
0.0000000E+00  0.0000000E+00  5.7699915E+01  3.1900000E-01
0.0000000E+00  0.0000000E+00  5.8201140E+01  2.5300000E-01
0.0000000E+00  0.0000000E+00  5.8699905E+01  2.1600000E-01
0.0000000E+00  0.0000000E+00  5.9199900E+01  1.7800000E-01
0.0000000E+00  0.0000000E+00  5.9699895E+01  1.4000000E-01
0.0000000E+00  0.0000000E+00  6.0199890E+01  1.0100000E-01
0.0000000E+00  0.0000000E+00  6.0699885E+01  6.2000000E-02
0.0000000E+00  0.0000000E+00  6.1199880E+01  2.3000000E-02
0.0000000E+00  0.0000000E+00  6.1500000E+01  0.0000000E+00
---------------------- MESH PARAMETER ------------------------------------------
          5   order_elem     - Order of interpolation (basis) function (-)
---------------------- MATERIAL PARAMETER --------------------------------------
"NRELOffshrBsline5MW_BeamDyn_Blade.dat"    BldFile - Name of file containing properties for blade (quoted string)
---------------------- PITCH ACTUATOR PARAMETERS -------------------------------
False         UsePitchAct - Whether a pitch actuator should be used (flag)
        200   PitchJ      - Pitch actuator inertia (kg-m^2) [used only when UsePitchAct is true]
      2E+07   PitchK      - Pitch actuator stiffness (kg-m^2/s^2) [used only when UsePitchAct is true]
     500000   PitchC      - Pitch actuator damping (kg-m^2/s) [used only when UsePitchAct is true]
---------------------- OUTPUTS -------------------------------------------------
True          SumPrint        - Print summary data to "<RootName>.sum" (flag)
"ES10.3E2"    OutFmt          - Format used for text tabular output, excluding the time channel.
          0   NNodeOuts       - Number of nodes to output to file [0 - 9] (-)
          1,          2,          3,          4,          5,          6    OutNd          - Nodes whose values will be output  (-)
          OutList        - The next line(s) contains a list of output parameters. See OutListParameters.xlsx for a listing of available
output channels, (-)
"RootFxr, RootFyr, RootFzr"
"RootMxr, RootMyr, RootMzr"
"TipTDxr, TipTDyr, TipTDzr"
"TipRDxr, TipRDyr, TipRDzr"
END of input file (the word "END" must appear in the first 3 columns of this last OutList line)
---------------------------------------------------------------------------------------
```

Figure C.7: OpenFAST InflowWind input file for OC4 jacket analysis

```
------- InflowWind INPUT FILE ------------------------------------------------------------------------
12 m/s turbulent winds on 31x31 FF grid and tower for FAST CertTests #18, #19, #21, #22, #23, and #24
---------------------------------------------------------------------------------------------------------
False         Echo           - Echo input data to <RootName>.ech (flag)
          3   WindType       - switch for wind file type (1=steady; 2=uniform; 3=binary TurbSim FF; 4=binary Bladed-style FF; 5=HAWC format;
6=User defined; 7=native Bladed FF)
          0   PropagationDir - Direction of wind propagation (meteorological rotation from aligned with X (positive rotates towards -Y) --
degrees) (not used for native Bladed format WindType=7)
          0   VFlowAng       - Upflow angle (degrees) (not used for native Bladed format WindType=7)
          1   NWindVel       - Number of points to output the wind velocity    (0 to 9)
          0   WindVxiList    - List of coordinates in the inertial X direction (m)
          0   WindVyiList    - List of coordinates in the inertial Y direction (m)
         90   WindVziList    - List of coordinates in the inertial Z direction (m)
================== Parameters for Steady Wind Conditions [used only for WindType = 1] =========================
          0   HWindSpeed     - Horizontal wind speed                           (m/s)
         90   RefHt          - Reference height for horizontal wind speed      (m)
        0.2   PLExp          - Power law exponent                              (-)
================== Parameters for Uniform wind file   [used only for WindType = 2] ============================
"unused"      Filename_Uni   - Filename of time series data for uniform wind field.      (-)
         90   RefHt_Uni      - Reference height for horizontal wind speed               (m)
     125.88   RefLength      - Reference length for linear horizontal and vertical sheer (-)
================== Parameters for Binary TurbSim Full-Field files   [used only for WindType = 3] ==============
"Wind/90m_12mps_twr.bts"    FileName_BTS   - Name of the Full field wind file to use (.bts)
================== Parameters for Binary Bladed-style Full-Field files   [used only for WindType = 4 or WindType = 7] =========
"unused"      FileNameRoot   - WindType=4: Rootname of the full-field wind file to use (.wnd, .sum); WindType=7: name of the intermediate
file with wind scaling values
False         TowerFile      - Have tower file (.twr) (flag) ignored when WindType = 7
================== Parameters for HAWC-format binary files  [Only used with WindType = 5] =====================
"wasp\Output\basic_5u.bin"    FileName_u     - name of the file containing the u-component fluctuating wind (.bin)
"wasp\Output\basic_5v.bin"    FileName_v     - name of the file containing the v-component fluctuating wind (.bin)
"wasp\Output\basic_5w.bin"    FileName_w     - name of the file containing the w-component fluctuating wind (.bin)
         64   nx             - number of grids in the x direction (in the 3 files above) (-)
         32   ny             - number of grids in the y direction (in the 3 files above) (-)
         32   nz             - number of grids in the z direction (in the 3 files above) (-)
         16   dx             - distance (in meters) between points in the x direction    (m)
          3   dy             - distance (in meters) between points in the y direction    (m)
          3   dz             - distance (in meters) between points in the z direction    (m)
         90   RefHt_Hawc     - reference height; the height (in meters) of the vertical center of the grid (m)
  -------------   Scaling parameters for turbulence   ---------------------------------------------------------
          2   ScaleMethod    - Turbulence scaling method   [0 = none, 1 = direct scaling, 2 = calculate scaling factor based on a desired
standard deviation]
          1   SFx            - Turbulence scaling factor for the x direction (-)   [ScaleMethod=1]
          1   SFy            - Turbulence scaling factor for the y direction (-)   [ScaleMethod=1]
          1   SFz            - Turbulence scaling factor for the z direction (-)   [ScaleMethod=1]
        1.2   SigmaFx         - Turbulence standard deviation to calculate scaling from in x direction (m/s)    [ScaleMethod=2]
        0.8   SigmaFy         - Turbulence standard deviation to calculate scaling from in y direction (m/s)    [ScaleMethod=2]
        0.2   SigmaFz         - Turbulence standard deviation to calculate scaling from in z direction (m/s)    [ScaleMethod=2]
  -------------   Mean wind profile parameters (added to HAWC-format files)   ---------------------------------
         12   URef           - Mean u-component wind speed at the reference height (m/s)
          2   WindProfile    - Wind profile type (0=constant;1=logarithmic,2=power law)
        0.2   PLExp_Hawc     - Power law exponent (-) (used for PL wind profile type only)
       0.03   Z0             - Surface roughness length (m) (used for LG wind profile type only)
          0   XOffset         - Initial offset in +x direction (shift of wind box)
====================== OUTPUT ==================================================
False         SumPrint       - Print summary data to <RootName>.IfW.sum (flag)
              OutList        - The next line(s) contains a list of output parameters.  See OutListParameters.xlsx for a listing of available
output channels, (-)

END of input file (the word "END" must appear in the first 3 columns of this last OutList line)
---------------------------------------------------------------------------------------
```

Figure C.8: OpenFAST AeroDyn input file for OC4 jacket analysis

```
------- AERODYN v15 for OpenFAST INPUT FILE -------------------------------------------
NREL 5.0 MW offshore baseline aerodynamic input properties with OC4 jacket tower
======  General Options  ============================================================================
False          Echo                 - Echo the input to "<rootname>.AD.ech"?  (flag)
"default"      DTAero               - Time interval for aerodynamic calculations {or "default"} (s)
          1    WakeMod              - Type of wake/induction model (switch) {0=none, 1=BEMT, 2=DBEMT, 3=OLAF} [WakeMod cannot be 2 or 3 when linearizing]
          2    AFAeroMod            - Type of blade airfoil aerodynamics model (switch) {1=steady model, 2=Beddoes-Leishman unsteady model} [AFAeroMod must be 1 when linearizing]
          1    TwrPotent            - Type tower influence on wind based on potential flow around the tower (switch) {0=none, 1=baseline potential flow, 2=potential flow with Bak
correction}
False          TwrShadow            - Calculate tower influence on wind based on downstream tower shadow? (flag)
True           TwrAero              - Calculate tower aerodynamic loads? (flag)
False          FrozenWake           - Assume frozen wake during linearization? (flag) [used only when WakeMod=1 and when linearizing]
False          CavitCheck           - Perform cavitation check? (flag) [AFAeroMod must be 1 when CavitCheck=true]
False          CompAA               - Flag to compute AeroAcoustics calculation [used only when WakeMod = 1 or 2]
"unused"       AA_InputFile         - AeroAcoustics input file [used only when CompAA=true]
======  Environmental Conditions  ===================================================================
      1.225    AirDens              - Air density (kg/m^3)
  1.464E-05    KinVisc              - Kinematic air viscosity (m^2/s)
        335    SpdSound             - Speed of sound (m/s)
     103500    Patm                 - Atmospheric pressure (Pa) [used only when CavitCheck=True]
       1700    Pvap                 - Vapour pressure of fluid (Pa) [used only when CavitCheck=True]
        0.5    FluidDepth           - Water depth above mid-hub height (m) [used only when CavitCheck=True]
======  Blade-Element/Momentum Theory Options  ====================================================== [unused when WakeMod=0 or 3]
          2    SkewMod              - Type of skewed-wake correction model (switch) {1=uncoupled, 2=Pitt/Peters, 3=coupled} [unused when WakeMod=0 or 3]
"default"      SkewModFactor        - Constant used in Pitt/Peters skewed wake model {or "default" is 15/32*pi} (-) [used only when SkewMod=2; unused when WakeMod=0 or 3]
True           TipLoss              - Use the Prandtl tip-loss model? (flag) [unused when WakeMod=0 or 3]
True           HubLoss              - Use the Prandtl hub-loss model? (flag) [unused when WakeMod=0 or 3]
True           TanInd               - Include tangential induction in BEMT calculations? (flag) [unused when WakeMod=0 or 3]
False          AIDrag               - Include the drag term in the axial-induction calculation? (flag) [unused when WakeMod=0 or 3]
False          TIDrag               - Include the drag term in the tangential-induction calculation? (flag) [unused when WakeMod=0,3 or TanInd=FALSE]
"Default"      IndToler             - Convergence tolerance for BEMT nonlinear solve residual equation {or "default"} (-) [unused when WakeMod=0 or 3]
        100    MaxIter              - Maximum number of iteration steps (-) [unused when WakeMod=0]
======  Dynamic Blade-Element/Momentum Theory Options  ============================================== [used only when WakeMod=2]
          2    DBEMT_Mod            - Type of dynamic BEMT (DBEMT) model {1=constant tau1, 2=time-dependent tau1} (-) [used only when WakeMod=2]
          4    tau1_const           - Time constant for DBEMT (s) [used only when WakeMod=2 and DBEMT_Mod=1]
======  OLAF -- cOnvecting LAgrangian Filaments (Free Vortex Wake) Theory Options  ================== [used only when WakeMod=3]
"unused"       OLAFInputFileName    - Input file for OLAF [used only when WakeMod=3]
======  Beddoes-Leishman Unsteady Airfoil Aerodynamics Options  ===================================== [used only when AFAeroMod=2]
          3    UAMod                - Unsteady Aero Model Switch (switch) {1=Baseline model (Original), 2=Gonzalez's variant (changes in Cn,Cc,Cm), 3=Minnema/Pierce variant (changes
in Cc and Cm)} [used only when AFAeroMod=2]
True           FLookup              - Flag to indicate whether a lookup for f' will be calculated (TRUE) or whether best-fit exponential equations will be used (FALSE); if FALSE S1-S4
must be provided in airfoil input files (flag) [used only when AFAeroMod=2]
======  Airfoil Information =========================================================================
          1    AFTabMod             - Interpolation method for multiple airfoil tables {1=1D interpolation on AoA (first table only); 2=2D interpolation on AoA and Re; 3=2D
interpolation on AoA and UserProp} (-)
          1    InCol_Alfa           - The column in the airfoil tables that contains the angle of attack (-)
          2    InCol_Cl             - The column in the airfoil tables that contains the lift coefficient (-)
          3    InCol_Cd             - The column in the airfoil tables that contains the drag coefficient (-)
          4    InCol_Cm             - The column in the airfoil tables that contains the pitching-moment coefficient; use zero if there is no Cm column (-)
          0    InCol_Cpmin          - The column in the airfoil tables that contains the Cpmin coefficient; use zero if there is no Cpmin column (-)
          8    NumAFfiles           - Number of airfoil files used (-)
"../5MW_Baseline/Airfoils/Cylinder1.dat"    AFNames              - Airfoil file names (NumAFfiles lines) (quoted strings)
"../5MW_Baseline/Airfoils/Cylinder2.dat"
"../5MW_Baseline/Airfoils/DU40_A17.dat"
"../5MW_Baseline/Airfoils/DU35_A17.dat"
"../5MW_Baseline/Airfoils/DU30_A17.dat"
"../5MW_Baseline/Airfoils/DU25_A17.dat"
"../5MW_Baseline/Airfoils/DU21_A17.dat"
"../5MW_Baseline/Airfoils/NACA64_A17.dat"
======  Rotor/Blade Properties  =====================================================================
True           UseBlCm              - Include aerodynamic pitching moment in calculations?  (flag)
"../5MW_Baseline/NRELOffshrBsline5MW_AeroDyn_blade.dat"     ADBlFile(1)        - Name of file containing distributed aerodynamic properties for Blade #1 (-)
"../5MW_Baseline/NRELOffshrBsline5MW_AeroDyn_blade.dat"     ADBlFile(2)        - Name of file containing distributed aerodynamic properties for Blade #2 (-) [unused if NumBl < 2]
"../5MW_Baseline/NRELOffshrBsline5MW_AeroDyn_blade.dat"     ADBlFile(3)        - Name of file containing distributed aerodynamic properties for Blade #3 (-) [unused if NumBl < 3]
======  Tower Influence and Aerodynamics ============================================================ [used only when TwrPotent/=0, TwrShadow=True, or TwrAero=True]
          9    NumTwrNds            - Number of tower nodes used in the analysis  (-) [used only when TwrPotent/=0, TwrShadow=True, or TwrAero=True]
TwrElev        TwrDiam        TwrCd
(m)              (m)           (-)
2.0150000E+01  5.6000000E+00  1.0000000E+00
2.1150000E+01  5.5770000E+00  1.0000000E+00
3.2150000E+01  5.3180000E+00  1.0000000E+00
4.2150000E+01  5.0820000E+00  1.0000000E+00
5.4150000E+01  4.8000000E+00  1.0000000E+00
6.4150000E+01  4.5650000E+00  1.0000000E+00
7.4150000E+01  4.3290000E+00  1.0000000E+00
8.3150000E+01  4.1180000E+00  1.0000000E+00
8.8150000E+01  4.0000000E+00  1.0000000E+00
======  Outputs  ====================================================================================
True           SumPrint             - Generate a summary file listing input options and interpolated properties to "<rootname>.AD.sum"?  (flag)
          0    NBlOuts              - Number of blade node outputs [0 - 9] (-)
          1,             9,         19    BlOutNd              - Blade nodes whose values will be output  (-)
          0    NTwOuts              - Number of tower node outputs [0 - 9]  (-)
          1,          2,          3,          4,          5    TwOutNd              - Tower nodes whose values will be output  (-)
                OutList              - The next line(s) contains a list of output parameters.  See OutListParameters.xlsx for a listing of available output channels, (-)
END of input file (the word "END" must appear in the first 3 columns of this last OutList line)
---------------------------------------------------------------------------------------
```

Figure C.9: OpenFAST ServoDyn input file for OC4 jacket analysis

```
------- SERVODYN v1.05.* INPUT FILE -------------------------------------------
OC4 Jacket+NREL 5.0 MW Baseline Wind Turbine for Use in Offshore Analysis. Properties from Dutch Offshore Wind Energy Converter (DOWEC) 6MW Pre-Design
(10046_009.pdf) and REpower 5M 5MW (5m_uk.pdf);
---------------------- SIMULATION CONTROL --------------------------------------
False         Echo          - Echo input data to <RootName>.ech (flag)
"DEFAULT"     DT            - Communication interval for controllers (s) (or "default")
---------------------- PITCH CONTROL -------------------------------------------
          5   PCMode        - Pitch control mode {0: none, 3: user-defined from routine PitchCntrl, 4: user-defined from Simulink/Labview, 5: user-defined from
Bladed-style DLL} (switch)
          0   TPCOn         - Time to enable active pitch control (s) [unused when PCMode=0]
     9999.9   TPitManS(1)   - Time to start override pitch maneuver for blade 1 and end standard pitch control (s)
     9999.9   TPitManS(2)   - Time to start override pitch maneuver for blade 2 and end standard pitch control (s)
     9999.9   TPitManS(3)   - Time to start override pitch maneuver for blade 3 and end standard pitch control (s) [unused for 2 blades]
          8   PitManRat(1)  - Pitch rate at which override pitch maneuver heads toward final pitch angle for blade 1 (deg/s)
          8   PitManRat(2)  - Pitch rate at which override pitch maneuver heads toward final pitch angle for blade 2 (deg/s)
          8   PitManRat(3)  - Pitch rate at which override pitch maneuver heads toward final pitch angle for blade 3 (deg/s) [unused for 2 blades]
         90   BlPitchF(1)   - Blade 1 final pitch for pitch maneuvers (degrees)
         90   BlPitchF(2)   - Blade 2 final pitch for pitch maneuvers (degrees)
         90   BlPitchF(3)   - Blade 3 final pitch for pitch maneuvers (degrees) [unused for 2 blades]
---------------------- GENERATOR AND TORQUE CONTROL ----------------------------
          5   VSContrl      - Variable-speed control mode {0: none, 1: simple VS, 3: user-defined from routine UserVSCont, 4: user-defined from
Simulink/Labview, 5: user-defined from Bladed-style DLL} (switch)
          2   GenModel      - Generator model {1: simple, 2: Thevenin, 3: user-defined from routine UserGen} (switch) [used only when VSContrl=0]
       94.4   GenEff        - Generator efficiency [ignored by the Thevenin and user-defined generator models] (%)
True          GenTiStr      - Method to start the generator {T: timed using TimGenOn, F: generator speed using SpdGenOn} (flag)
True          GenTiStp      - Method to stop the generator {T: timed using TimGenOf, F: when generator power = 0} (flag)
     9999.9   SpdGenOn      - Generator speed to turn on the generator for a startup (HSS speed) (rpm) [used only when GenTiStr=False]
          0   TimGenOn      - Time to turn on the generator for a startup (s) [used only when GenTiStr=True]
     9999.9   TimGenOf      - Time to turn off the generator (s) [used only when GenTiStp=True]
---------------------- SIMPLE VARIABLE-SPEED TORQUE CONTROL --------------------
     9999.9   VS_RtGnSp     - Rated generator speed for simple variable-speed generator control (HSS side) (rpm) [used only when VSContrl=1]
     9999.9   VS_RtTq       - Rated generator torque/constant generator torque in Region 3 for simple variable-speed generator control (HSS side) (N-m) [used
only when VSContrl=1]
     9999.9   VS_Rgn2K      - Generator torque constant in Region 2 for simple variable-speed generator control (HSS side) (N-m/rpm^2) [used only when
VSContrl=1]
     9999.9   VS_SlPc       - Rated generator slip percentage in Region 2 1/2 for simple variable-speed generator control (%) [used only when VSContrl=1]
---------------------- SIMPLE INDUCTION GENERATOR ------------------------------
     9999.9   SIG_SlPc      - Rated generator slip percentage (%) [used only when VSContrl=0 and GenModel=1]
     9999.9   SIG_SySp      - Synchronous (zero-torque) generator speed (rpm) [used only when VSContrl=0 and GenModel=1]
     9999.9   SIG_RtTq      - Rated torque (N-m) [used only when VSContrl=0 and GenModel=1]
     9999.9   SIG_PORt      - Pull-out ratio (Tpullout/Trated) (-) [used only when VSContrl=0 and GenModel=1]
---------------------- THEVENIN-EQUIVALENT INDUCTION GENERATOR -----------------
     9999.9   TEC_Freq      - Line frequency [50 or 60] (Hz) [used only when VSContrl=0 and GenModel=2]
       9998   TEC_NPol      - Number of poles [even integer > 0] (-) [used only when VSContrl=0 and GenModel=2]
     9999.9   TEC_SRes      - Stator resistance (ohms) [used only when VSContrl=0 and GenModel=2]
     9999.9   TEC_RRes      - Rotor resistance (ohms) [used only when VSContrl=0 and GenModel=2]
     9999.9   TEC_VLL       - Line-to-line RMS voltage (volts) [used only when VSContrl=0 and GenModel=2]
     9999.9   TEC_SLR       - Stator leakage reactance (ohms) [used only when VSContrl=0 and GenModel=2]
     9999.9   TEC_RLR       - Rotor leakage reactance (ohms) [used only when VSContrl=0 and GenModel=2]
     9999.9   TEC_MR        - Magnetizing reactance (ohms) [used only when VSContrl=0 and GenModel=2]
---------------------- HIGH-SPEED SHAFT BRAKE ----------------------------------
          0   HSSBrMode     - HSS brake model {0: none, 1: simple, 3: user-defined from routine UserHSSBr, 4: user-defined from Simulink/Labview, 5: user-
defined from Bladed-style DLL} (switch)
     9999.9   THSSBrDp      - Time to initiate deployment of the HSS brake (s)
        0.6   HSSBrDT       - Time for HSS-brake to reach full deployment once initiated (sec) [used only when HSSBrMode=1]
    28116.2   HSSBrTqF      - Fully deployed HSS-brake torque (N-m)
---------------------- NACELLE-YAW CONTROL --------------------------------------
          0   YCMode        - Yaw control mode {0: none, 3: user-defined from routine UserYawCont, 4: user-defined from Simulink/Labview, 5: user-defined from
Bladed-style DLL} (switch)
     9999.9   TYCOn         - Time to enable active yaw control (s) [unused when YCMode=0]
          0   YawNeut       - Neutral yaw position--yaw spring force is zero at this yaw (degrees)
9.02832E+09   YawSpr        - Nacelle-yaw spring constant (N-m/rad)
  1.916E+07   YawDamp       - Nacelle-yaw damping constant (N-m/(rad/s))
     9999.9   TYawManS      - Time to start override yaw maneuver and end standard yaw control (s)
        0.3   YawManRat     - Yaw maneuver rate (in absolute value) (deg/s)
          0   NacYawF       - Final yaw angle for override yaw maneuvers (degrees)
---------------------- TUNED MASS DAMPER ---------------------------------------
False         CompNTMD      - Compute nacelle tuned mass damper {true/false} (flag)
"unused"      NTMDfile      - Name of the file for nacelle tuned mass damper (quoted string) [unused when CompNTMD is false]
False         CompTTMD      - Compute tower tuned mass damper {true/false} (flag)
"unused"      TTMDfile      - Name of the file for tower tuned mass damper (quoted string) [unused when CompTTMD is false]
---------------------- BLADED INTERFACE ---------------------------------------- [used only with Bladed Interface]
"../5MW_Baseline/ServoData/DISCON.dll"    DLL_FileName - Name/location of the dynamic library {.dll [Windows] or .so [Linux]} in the Bladed-DLL format (-)
[used only with Bladed Interface]
"DISCON.IN"   DLL_InFile    - Name of input file sent to the DLL (-) [used only with Bladed Interface]
"DISCON"      DLL_ProcName  - Name of procedure in DLL to be called (-) [case sensitive; used only with DLL Interface]
"default"     DLL_DT        - Communication interval for dynamic library (s) (or "default") [used only with Bladed Interface]
false         DLL_Ramp      - Whether a linear ramp should be used between DLL_DT time steps [introduces time shift when true] (flag) [used only with Bladed
Interface]
     9999.9   BPCutoff      - Cutoff frequency for low-pass filter on blade pitch from DLL (Hz) [used only with Bladed Interface]
          0   NacYaw_North  - Reference yaw angle of the nacelle when the upwind end points due North (deg) [used only with Bladed Interface]
          0   Ptch_Cntrl    - Record 28: Use individual pitch control {0: collective pitch; 1: individual pitch control} (switch) [used only with Bladed
Interface]
          0   Ptch_SetPnt   - Record  5: Below-rated pitch angle set-point (deg) [used only with Bladed Interface]
          0   Ptch_Min      - Record  6: Minimum pitch angle (deg) [used only with Bladed Interface]
          0   Ptch_Max      - Record  7: Maximum pitch angle (deg) [used only with Bladed Interface]
          0   PtchRate_Min  - Record  8: Minimum pitch rate (most negative value allowed) (deg/s) [used only with Bladed Interface]
          0   PtchRate_Max  - Record  9: Maximum pitch rate  (deg/s) [used only with Bladed Interface]
          0   Gain_OM       - Record 16: Optimal mode gain (Nm/(rad/s)^2) [used only with Bladed Interface]
          0   GenSpd_MinOM  - Record 17: Minimum generator speed (rpm) [used only with Bladed Interface]
          0   GenSpd_MaxOM  - Record 18: Optimal mode maximum speed (rpm) [used only with Bladed Interface]
          0   GenSpd_Dem    - Record 19: Demanded generator speed above rated (rpm) [used only with Bladed Interface]
          0   GenTrq_Dem    - Record 22: Demanded generator torque above rated (Nm) [used only with Bladed Interface]
          0   GenPwr_Dem    - Record 13: Demanded power (W) [used only with Bladed Interface]
---------------------- BLADED INTERFACE TORQUE-SPEED LOOK-UP TABLE -------------
          0   DLL_NumTrq    - Record 26: No. of points in torque-speed look-up table {0 = none and use the optimal mode parameters; nonzero = ignore the optimal
mode PARAMETERs by setting Record 16 to 0.0} (-) [used only with Bladed Interface]
 GenSpd_TLU   GenTrq_TLU
 (rpm)          (Nm)
---------------------- OUTPUT --------------------------------------------------
True          SumPrint      - Print summary data to <RootName>.sum (flag) (currently unused)
          2   OutFile       - Switch to determine where output will be placed: {1: in module output file only; 2: in glue code output file only; 3: both}
(currently unused)
True          TabDelim      - Use tab delimiters in text tabular output file? (flag) (currently unused)
"ES10.3E2"    OutFmt        - Format used for text tabular output (except time).  Resulting field should be 10 characters. (quoted string) (currently unused)
         30   TStart        - Time to begin tabular output (s) (currently unused)
              OutList       - The next line(s) contains a list of output parameters.  See OutListParameters.xlsx for a listing of available output channels, (-)
"GenPwr"                   - Electrical generator power and torque
"GenTq"                    - Electrical generator power and torque
END of input file (the word "END" must appear in the first 3 columns of this last OutList line)
---------------------------------------------------------------------------------------
```

Figure C.10: OpenFAST HydroDyn input file for OC4 jacket analysis - P.1

```
------- HydroDyn v2.03.* Input File ---------------------------------------------
NREL 5.0 MW offshore fixed-bottom HydroDyn input properties for the OC4 Jacket.
False            Echo           - Echo the input file data (flag)
---------------------- ENVIRONMENTAL CONDITIONS -------------------------------
         1025   WtrDens        - Water density (kg/m^3)
           50   WtrDpth        - Water depth (meters)
            0   MSL2SWL        - Offset between still-water level and mean sea level (meters) [positive upward; unused when WaveMod = 6; must be zero if PotMod=1 or
2]
---------------------- WAVES --------------------------------------------------
            2   WaveMod        - Incident wave kinematics model {0: none=still water, 1: regular (periodic), 1P#: regular with user-specified phase, 2:
JONSWAP/Pierson-Moskowitz spectrum (irregular), 3: White noise spectrum (irregular), 4: user-defined spectrum from routine UserWaveSpctrm (irregular), 5: Externally
generated wave-elevation time series, 6: Externally generated full wave-kinematics time series [option 6 is invalid for PotMod/=0]} (switch)
            0   WaveStMod      - Model for stretching incident wave kinematics to instantaneous free surface {0: none=no stretching, 1: vertical stretching, 2:
extrapolation stretching, 3: Wheeler stretching} (switch) [unused when WaveMod=0 or when PotMod/=0]
         3630   WaveTMax       - Analysis time for incident wave calculations (sec) [unused when WaveMod=0; determines WaveDOmega=2Pi/WaveTMax in the IFFT]
         0.25,          0.1    WaveDT         - Time step for incident wave calculations     (sec) [unused when WaveMod=0; 0.1<=WaveDT<=1.0 recommended; determines
WaveOmegaMax=Pi/WaveDT in the IFFT]
         1.63   WaveHs         - Significant wave height of incident waves (meters) [used only when WaveMod=1, 2, or 3]
         5.84   WaveTp         - Peak-spectral period of incident waves       (sec) [used only when WaveMod=1 or 2]
"DEFAULT"        WavePkShp      - Peak-shape parameter of incident wave spectrum (-) or DEFAULT (string) [used only when WaveMod=2; use 1.0 for Pierson-Moskowitz]
            0   WvLowCOff      - Low  cut-off frequency or lower frequency limit of the wave spectrum beyond which the wave spectrum is zeroed (rad/s) [unused when
WaveMod=0, 1, or 6]
          500   WvHiCOff       - High cut-off frequency or upper frequency limit of the wave spectrum beyond which the wave spectrum is zeroed (rad/s) [unused when
WaveMod=0, 1, or 6]
            0   WaveDir        - Incident wave propagation heading direction                 (degrees) [unused when WaveMod=0 or 6]
            0   WaveDirMod     - Directional spreading function {0: none, 1: COS2S}          (-)       [only used when WaveMod=2,3, or 4]
            1   WaveDirSpread  - Wave direction spreading coefficient ( > 0 )                (-)       [only used when WaveMod=2,3, or 4 and WaveDirMod=1]
            1   WaveNDir       - Number of wave directions                                   (-)       [only used when WaveMod=2,3, or 4 and WaveDirMod=1; odd
number only]
           90   WaveDirRange   - Range of wave directions (full range: WaveDir +/- 1/2*WaveDirRange) (degrees) [only used when WaveMod=2,3,or 4 and WaveDirMod=1]
    123456789   WaveSeed(1)    - First  random seed of incident waves [-2147483648 to 2147483647]    (-)       [unused when WaveMod=0, 5, or 6]
       RANLUX   WaveSeed(2)    - Second random seed of incident waves [-2147483648 to 2147483647] for intrinsic pRNG, or an alternative pRNG: "RanLux"    (-)
[unused when WaveMod=0, 5, or 6]
False            WaveNDAmp      - Flag for normally distributed amplitudes                    (flag)    [only used when WaveMod=2, 3, or 4]
""               WvKinFile      - Root name of externally generated wave data file(s)       (quoted string)    [used only when WaveMod=5 or 6]
            1   NWaveElev      - Number of points where the incident wave elevations can be computed (-)       [maximum of 9 output locations]
            0   WaveElevxi     - List of xi-coordinates for points where the incident wave elevations can be output (meters) [NWaveElev points, separated by commas or
white space; usused if NWaveElev = 0]
            0   WaveElevyi     - List of yi-coordinates for points where the incident wave elevations can be output (meters) [NWaveElev points, separated by commas or
white space; usused if NWaveElev = 0]
---------------------- 2ND-ORDER WAVES ----------------------------------------- [unused with WaveMod=0 or 6]
False            WvDiffQTF      - Full difference-frequency 2nd-order wave kinematics (flag)
False            WvSumQTF       - Full summation-frequency  2nd-order wave kinematics (flag)
            0   WvLowCOffD     - Low  frequency cutoff used in the difference-frequencies (rad/s) [Only used with a difference-frequency method]
          3.5   WvHiCOffD      - High frequency cutoff used in the difference-frequencies (rad/s) [Only used with a difference-frequency method]
          0.1   WvLowCOffS     - Low  frequency cutoff used in the summation-frequencies  (rad/s) [Only used with a summation-frequency  method]
          3.5   WvHiCOffS      - High frequency cutoff used in the summation-frequencies  (rad/s) [Only used with a summation-frequency  method]
---------------------- CURRENT ------------------------------------------------ [unused with WaveMod=6]
            1   CurrMod        - Current profile model {0: none=no current, 1: standard, 2: user-defined from routine UserCurrent} (switch)
            0   CurrSSV0       - Sub-surface current velocity at still water level  (m/s) [used only when CurrMod=1]
          180   CurrSSDir      - Sub-surface current heading direction (degrees) or DEFAULT (string) [used only when CurrMod=1]
           20   CurrNSRef      - Near-surface current reference depth           (meters) [used only when CurrMod=1]
          0.6   CurrNSV0       - Near-surface current velocity at still water level (m/s) [used only when CurrMod=1]
          180   CurrNSDir      - Near-surface current heading direction         (degrees) [used only when CurrMod=1]
            0   CurrDIV        - Depth-independent current velocity                (m/s) [used only when CurrMod=1]
            0   CurrDIDir      - Depth-independent current heading direction    (degrees) [used only when CurrMod=1]
---------------------- FLOATING PLATFORM --------------------------------------- [unused with WaveMod=6]
            0   PotMod         - Potential-flow model {0: none=no potential flow, 1: frequency-to-time-domain transforms based on WAMIT output, 2: fluid-impulse
theory (FIT)} (switch)
""              PotFile        - Root name of potential-flow model data; WAMIT output files containing the linear, nondimensionalized, hydrostatic restoring matrix
(.hst), frequency-dependent hydrodynamic added mass matrix and damping matrix (.1), and frequency- and direction-dependent wave excitation force vector per unit wave
amplitude (.3) (quoted string) [MAKE SURE THE FREQUENCIES INHERENT IN THESE WAMIT FILES SPAN THE PHYSICALLY-SIGNIFICANT RANGE OF FREQUENCIES FOR THE GIVEN PLATFORM;
THEY MUST CONTAIN THE ZERO- AND INFINITE-FREQUENCY LIMITS!]
            1   WAMITULEN     - Characteristic body length scale used to redimensionalize WAMIT output (meters) [only used when PotMod=1]
            0   PtfmVol0      - Displaced volume of water when the platform is in its undisplaced position (m^3) [only used when PotMod=1; USE THE SAME VALUE
COMPUTED BY WAMIT AS OUTPUT IN THE .OUT FILE!]
            0   PtfmCOBxt      - The xt offset of the center of buoyancy (COB) from the platform reference point (meters)  [only used when PotMod=1]
            0   PtfmCOByt      - The yt offset of the center of buoyancy (COB) from the platform reference point (meters)  [only used when PotMod=1]
            0   ExctnMod       - Wave Excitation model {0: None, 1: DFT, 2: state-space} (switch) [only used when PotMod=1; STATE-SPACE REQUIRES *.ssexctn INPUT FILE]
            0   RdtnMod        - Radiation memory-effect model {0: no memory-effect calculation, 1: convolution, 2: state-space} (switch) [only used when PotMod=1;
STATE-SPACE REQUIRES *.ss INPUT FILE]
            0   RdtnTMax       - Analysis time for wave radiation kernel calculations (sec) [only used when PotMod=1 and RdtnMod>0; determines RdtnDOmega=Pi/RdtnTMax
in the cosine transform; MAKE SURE THIS IS LONG ENOUGH FOR THE RADIATION IMPULSE RESPONSE FUNCTIONS TO DECAY TO NEAR-ZERO FOR THE GIVEN PLATFORM!]
            0   RdtnDT         - Time step for wave radiation kernel calculations (sec) [only used when PotMod=1 and RdtnMod=1; DT<=RdtnDT<=0.1 recommended;
determines RdtnOmegaMax=Pi/RdtnDT in the cosine transform]
---------------------- 2ND-ORDER FLOATING PLATFORM FORCES ---------------------- [unused with WaveMod=0 or 6, or PotMod=0 or 2]
            0   MnDrift        - Mean-drift 2nd-order forces computed                              {0: None; [7, 8, 9, 10, 11, or 12]: WAMIT file to use}
[Only one of MnDrift, NewmanApp, or DiffQTF can be non-zero]
            0   NewmanApp      - Mean- and slow-drift 2nd-order forces computed with Newman's approximation {0: None; [7, 8, 9, 10, 11, or 12]: WAMIT file to use}
[Only one of MnDrift, NewmanApp, or DiffQTF can be non-zero. Used only when WaveDirMod=0]
            0   DiffQTF        - Full difference-frequency 2nd-order forces computed with full QTF         {0: None; [10, 11, or 12]: WAMIT file to use}
[Only one of MnDrift, NewmanApp, or DiffQTF can be non-zero]
            0   SumQTF         - Full summation -frequency 2nd-order forces computed with full QTF         {0: None; [10, 11, or 12]: WAMIT file to use}
-------------------- FLOATING PLATFORM FORCE FLAGS  ------------------------- [unused with WaveMod=6]
True             PtfmSgF        - Platform horizontal surge translation force (flag) or DEFAULT
True             PtfmSwF        - Platform horizontal sway translation force (flag) or DEFAULT
True             PtfmHvF        - Platform vertical heave translation force (flag) or DEFAULT
True             PtfmRF         - Platform roll tilt rotation force (flag) or DEFAULT
True             PtfmPF         - Platform pitch tilt rotation force (flag) or DEFAULT
True             PtfmYF         - Platform yaw rotation force (flag) or DEFAULT
---------------------- PLATFORM ADDITIONAL STIFFNESS AND DAMPING  --------------
            0             0             0             0             0             0   AddF0    - Additional preload (N, N-m)
            0             0             0             0             0             0   AddCLin  - Additional linear stiffness (N/m, N/rad, N-m/m, N-m/rad)
            0             0             0             0             0             0
            0             0             0             0             0             0
            0             0             0             0             0             0
            0             0             0             0             0             0
            0             0             0             0             0             0
            0             0             0             0             0             0
            0             0             0             0             0             0   AddBLin  - Additional linear damping(N/(m/s), N/(rad/s), N-m/(m/s), N-m/(rad/s))
            0             0             0             0             0             0
            0             0       1066100             0             0             0
            0             0             0             0             0             0
            0             0             0             0             0             0
            0             0             0             0             0             0
            0             0             0             0             0             0   AddBQuad - Additional quadratic drag(N/(m/s)^2, N/(rad/s)^2, N-m(m/s)^2, N-
m/(rad/s)^2)
            0             0             0             0             0             0
            0             0             0             0             0             0
            0             0             0             0             0             0
            0             0             0             0             0             0
            0             0             0             0             0             0
---------------------- AXIAL COEFFICIENTS -------------------------------------
            1   NAxCoef        - Number of axial coefficients (-)
AxCoefID  AxCd     AxCa     AxCp
   (-)    (-)      (-)      (-)
    1     0.00     1.00     1.00
---------------------- MEMBER JOINTS ------------------------------------------
```

Figure C.11: OpenFAST HydroDyn input file for OC4 jacket analysis - P.2

```
          64   NJoints        - Number of joints (-)   [must be exactly 0 or at least 2]
JointID   Jointxi     Jointyi     Jointzi  JointAxID   JointOvrlp   [JointOvrlp= 0: do nothing at joint, 1: eliminate overlaps by calculating super member]
   (-)     (m)         (m)         (m)       (-)       (switch)
    1     6.00000     6.00000   -45.50000      1           0
    2     6.00000     6.00000   -45.00000      1           0
    3     5.96700     5.96700   -44.00100      1           0
    4     5.93900     5.93900   -43.12700      1           0
    5     5.33300     5.33300   -24.61400      1           0
    6    -6.00000     6.00000   -45.50000      1           0
    7    -6.00000     6.00000   -45.00000      1           0
    8    -5.96700     5.96700   -44.00100      1           0
    9    -5.93900     5.93900   -43.12700      1           0
   10    -5.33300     5.33300   -24.61400      1           0
   11    -6.00000    -6.00000   -45.50000      1           0
   12    -6.00000    -6.00000   -45.00000      1           0
   13    -5.96700    -5.96700   -44.00100      1           0
   14    -5.93900    -5.93900   -43.12700      1           0
   15    -5.33300    -5.33300   -24.61400      1           0
   16     6.00000    -6.00000   -45.50000      1           0
   17     6.00000    -6.00000   -45.00000      1           0
   18     5.96700    -5.96700   -44.00100      1           0
   19     5.93900    -5.93900   -43.12700      1           0
   20     5.33300    -5.33300   -24.61400      1           0
   21     4.82000     4.82000    -8.92200      1           0
   22     4.38500     4.38500     4.37800      1           0
   23     4.01600     4.01600    15.65100      1           0
   24     4.00000     4.00000    16.15000      1           0
   25    -4.82000     4.82000    -8.92200      1           0
   26    -4.38500     4.38500     4.37800      1           0
   27    -4.01600     4.01600    15.65100      1           0
   28    -4.00000     4.00000    16.15000      1           0
   29    -4.82000    -4.82000    -8.92200      1           0
   30    -4.38500    -4.38500     4.37800      1           0
   31    -4.01600    -4.01600    15.65100      1           0
   32    -4.00000    -4.00000    16.15000      1           0
   33     4.82000    -4.82000    -8.92200      1           0
   34     4.38500    -4.38500     4.37800      1           0
   35     4.01600    -4.01600    15.65100      1           0
   36     4.00000    -4.00000    16.15000      1           0
   37     5.62000     0.00000   -33.37300      1           0
   38    -5.62000     0.00000   -33.37300      1           0
   39     0.00000     5.62000   -33.37300      1           0
   40     0.00000    -5.62000   -33.37300      1           0
   41     5.06400     0.00000   -16.37100      1           0
   42    -5.06400     0.00000   -16.37100      1           0
   43     0.00000     5.06400   -16.37100      1           0
   44     0.00000    -5.06400   -16.37100      1           0
   45     4.59200     0.00000    -1.95800      1           0
   46    -4.59200     0.00000    -1.95800      1           0
   47     0.00000     4.59200    -1.95800      1           0
   48     0.00000    -4.59200    -1.95800      1           0
   49     4.19300     0.00000    10.26200      1           0
   50    -4.19300     0.00000    10.26200      1           0
   51     0.00000     4.19300    10.26200      1           0
   52     0.00000    -4.19300    10.26200      1           0
   53     4.00000     4.00000    20.15000      1           0
   54    -4.00000     4.00000    20.15000      1           0
   55     4.00000    -4.00000    20.15000      1           0
   56    -4.00000    -4.00000    20.15000      1           0
   57     6.00000    -6.00000   -49.50000      1           0
   58     6.00000     6.00000   -49.50000      1           0
   59    -6.00000    -6.00000   -49.50000      1           0
   60    -6.00000     6.00000   -49.50000      1           0
   61     6.00000    -6.00000   -50.00100      1           0
   62     6.00000     6.00000   -50.00100      1           0
   63    -6.00000    -6.00000   -50.00100      1           0
   64    -6.00000     6.00000   -50.00100      1           0
---------------------- MEMBER CROSS-SECTION PROPERTIES -------------------------
            6   NPropSets      - Number of member property sets (-)
PropSetID    PropD          PropThck
   (-)        (m)             (m)
    1        0.80000        0.02000
    2        1.20000        0.05000
    3        1.20000        0.03500
    4        1.20000        0.04000
    5        2.08200        0.49100
    6        2.08200        0.06000
---------------------- SIMPLE HYDRODYNAMIC COEFFICIENTS (model 1) --------------
     SimplCd     SimplCdMG    SimplCa    SimplCaMG    SimplCp    SimplCpMG   SimplAxCa  SimplAxCaMG  SimplAxCp   SimplAxCpMG
       (-)         (-)         (-)         (-)         (-)         (-)         (-)         (-)         (-)         (-)
      1.00        1.00        1.00        1.00        1.00        1.00        1.00        1.00        1.00        1.00
---------------------- DEPTH-BASED HYDRODYNAMIC COEFFICIENTS (model 2) ---------
            0   NCoefDpth      - Number of depth-dependent coefficients (-)
Dpth       DpthCd   DpthCdMG   DpthCa   DpthCaMG       DpthCp   DpthCpMG   DpthAxCa   DpthAxCaMG       DpthAxCp   DpthAxCpMG
(m)         (-)      (-)        (-)      (-)            (-)      (-)        (-)        (-)              (-)        (-)
---------------------- MEMBER-BASED HYDRODYNAMIC COEFFICIENTS (model 3) --------
            0   NCoefMembers      - Number of member-based coefficients (-)
MemberID    MemberCd1     MemberCd2    MemberCdMG1   MemberCdMG2    MemberCa1     MemberCa2    MemberCaMG1   MemberCaMG2    MemberCp1     MemberCp2    MemberCpMG1
MemberCpMG2   MemberAxCa1   MemberAxCa2  MemberAxCaMG1 MemberAxCaMG2  MemberAxCp1  MemberAxCp2   MemberAxCpMG1   MemberAxCpMG2
   (-)          (-)          (-)          (-)          (-)          (-)          (-)          (-)          (-)          (-)          (-)
(-)          (-)          (-)          (-)          (-)          (-)          (-)          (-)          (-)
---------------------- MEMBERS -------------------------------------------------
          112   NMembers       - Number of members (-)
MemberID  MJointID1  MJointID2  MPropSetID1  MPropSetID2  MDivSize   MCoefMod  PropPot   [MCoefMod=1: use simple coeff table, 2: use depth-based coeff table, 3: use
member-based coeff table] [ PropPot/=0 if member is modeled with potential-flow theory]
  (-)        (-)        (-)          (-)          (-)        (m)      (switch)   (flag)
    1          1          2            2            2        1.0000      1        FALSE
    2          2          3            2            2        1.0000      1        FALSE
    3          3          4            2            2        1.0000      1        FALSE
    4          4          5            2            2        1.0000      1        FALSE
    5          6          7            2            2        1.0000      1        FALSE
    6          7          8            2            2        1.0000      1        FALSE
    7          8          9            2            2        1.0000      1        FALSE
    8          9         10            2            2        1.0000      1        FALSE
    9         11         12            2            2        1.0000      1        FALSE
   10         12         13            2            2        1.0000      1        FALSE
   11         13         14            2            2        1.0000      1        FALSE
   12         14         15            2            2        1.0000      1        FALSE
   13         16         17            2            2        1.0000      1        FALSE
   14         17         18            2            2        1.0000      1        FALSE
   15         18         19            2            2        1.0000      1        FALSE
   16         19         20            2            2        1.0000      1        FALSE
   17          5         21            3            3        1.0000      1        FALSE
   18         21         22            3            3        1.0000      1        FALSE
   19         22         23            3            3        1.0000      1        FALSE
   20         23         24            3            3        1.0000      1        FALSE
   21         10         25            3            3        1.0000      1        FALSE
   22         25         26            3            3        1.0000      1        FALSE
```

Figure C.12: OpenFAST HydroDyn input file for OC4 jacket analysis - P.3

```
   23        26         27          3           3         1.0000     1        FALSE
   24        27         28          3           3         1.0000     1        FALSE
   25        15         29          3           3         1.0000     1        FALSE
   26        29         30          3           3         1.0000     1        FALSE
   27        30         31          3           3         1.0000     1        FALSE
   28        31         32          3           3         1.0000     1        FALSE
   29        20         33          3           3         1.0000     1        FALSE
   30        33         34          3           3         1.0000     1        FALSE
   31        34         35          3           3         1.0000     1        FALSE
   32        35         36          3           3         1.0000     1        FALSE
   33         3          8          1           1         1.0000     1        FALSE
   34         8         13          1           1         1.0000     1        FALSE
   35        13         18          1           1         1.0000     1        FALSE
   36        18          3          1           1         1.0000     1        FALSE
   37         4         37          1           1         1.0000     1        FALSE
   38        37         20          1           1         1.0000     1        FALSE
   39        19         37          1           1         1.0000     1        FALSE
   40        37          5          1           1         1.0000     1        FALSE
   41         9         38          1           1         1.0000     1        FALSE
   42        38         15          1           1         1.0000     1        FALSE
   43        14         38          1           1         1.0000     1        FALSE
   44        38         10          1           1         1.0000     1        FALSE
   45         4         39          1           1         1.0000     1        FALSE
   46        39         10          1           1         1.0000     1        FALSE
   47         9         39          1           1         1.0000     1        FALSE
   48        39          5          1           1         1.0000     1        FALSE
   49        19         40          1           1         1.0000     1        FALSE
   50        40         15          1           1         1.0000     1        FALSE
   51        14         40          1           1         1.0000     1        FALSE
   52        40         20          1           1         1.0000     1        FALSE
   53         5         41          1           1         1.0000     1        FALSE
   54        41         33          1           1         1.0000     1        FALSE
   55        20         41          1           1         1.0000     1        FALSE
   56        41         21          1           1         1.0000     1        FALSE
   57        10         42          1           1         1.0000     1        FALSE
   58        42         29          1           1         1.0000     1        FALSE
   59        15         42          1           1         1.0000     1        FALSE
   60        42         25          1           1         1.0000     1        FALSE
   61         5         43          1           1         1.0000     1        FALSE
   62        43         25          1           1         1.0000     1        FALSE
   63        10         43          1           1         1.0000     1        FALSE
   64        43         21          1           1         1.0000     1        FALSE
   65        20         44          1           1         1.0000     1        FALSE
   66        44         29          1           1         1.0000     1        FALSE
   67        15         44          1           1         1.0000     1        FALSE
   68        44         33          1           1         1.0000     1        FALSE
   69        21         45          1           1         1.0000     1        FALSE
   70        45         34          1           1         1.0000     1        FALSE
   71        33         45          1           1         1.0000     1        FALSE
   72        45         22          1           1         1.0000     1        FALSE
   73        25         46          1           1         1.0000     1        FALSE
   74        46         30          1           1         1.0000     1        FALSE
   75        29         46          1           1         1.0000     1        FALSE
   76        46         26          1           1         1.0000     1        FALSE
   77        21         47          1           1         1.0000     1        FALSE
   78        47         26          1           1         1.0000     1        FALSE
   79        25         47          1           1         1.0000     1        FALSE
   80        47         22          1           1         1.0000     1        FALSE
   81        33         48          1           1         1.0000     1        FALSE
   82        48         30          1           1         1.0000     1        FALSE
   83        29         48          1           1         1.0000     1        FALSE
   84        48         34          1           1         1.0000     1        FALSE
   85        22         49          1           1         1.0000     1        FALSE
   86        49         35          1           1         1.0000     1        FALSE
   87        34         49          1           1         1.0000     1        FALSE
   88        49         23          1           1         1.0000     1        FALSE
   89        26         50          1           1         1.0000     1        FALSE
   90        50         31          1           1         1.0000     1        FALSE
   91        30         50          1           1         1.0000     1        FALSE
   92        50         27          1           1         1.0000     1        FALSE
   93        22         51          1           1         1.0000     1        FALSE
   94        51         27          1           1         1.0000     1        FALSE
   95        26         51          1           1         1.0000     1        FALSE
   96        51         23          1           1         1.0000     1        FALSE
   97        34         52          1           1         1.0000     1        FALSE
   98        52         31          1           1         1.0000     1        FALSE
   99        30         52          1           1         1.0000     1        FALSE
  100        52         35          1           1         1.0000     1        FALSE
  101        24         53          4           4         1.0000     1        FALSE
  102        28         54          4           4         1.0000     1        FALSE
  103        32         56          4           4         1.0000     1        FALSE
  104        36         55          4           4         1.0000     1        FALSE
  105         1         58          5           5         1.0000     1        FALSE
  106        16         57          5           5         1.0000     1        FALSE
  107         6         60          5           5         1.0000     1        FALSE
  108        11         59          5           5         1.0000     1        FALSE
  109        58         62          6           6         1.0000     1        FALSE
  110        57         61          6           6         1.0000     1        FALSE
  111        60         64          6           6         1.0000     1        FALSE
  112        59         63          6           6         1.0000     1        FALSE
---------------------- FILLED MEMBERS ---------------------------------------------
            0   NFillGroups      - Number of filled member groups (-) [If FillDens = DEFAULT, then FillDens = WtrDens; FillFSLoc is related to MSL2SWL]
FillNumM FillMList             FillFSLoc     FillDens
(-)      (-)                   (m)           (kg/m^3)
---------------------- MARINE GROWTH ----------------------------------------------
            2   NMGDepths       - Number of marine-growth depths specified (-)
MGDpth     MGThck       MGDens
(m)        (m)          (kg/m^3)
  -2.00     0.100    1100
 -40.00     0.100    1100
---------------------- MEMBER OUTPUT LIST -----------------------------------------
            0   NMOutputs       - Number of member outputs (-) [must be < 10]
MemberID   NOutLoc    NodeLocs [NOutLoc < 10; node locations are normalized distance from the start of the member, and must be >=0 and <= 1] [unused if NMOutputs=0]
  (-)      (-)          (-)
---------------------- JOINT OUTPUT LIST ------------------------------------------
            0   NJOutputs       - Number of joint outputs [Must be < 10]
   0          JOutLst       - List of JointIDs which are to be output (-)[unused if NJOutputs=0]
---------------------- OUTPUT -----------------------------------------------------
True            HDSum          - Output a summary file [flag]
False           OutAll         - Output all user-specified member and joint loads (only at each member end, not interior locations) [flag]
            2   OutSwtch       - Output requested channels to: [1=Hydrodyn.out, 2=GlueCode.out, 3=both files]
"ES11.4e2"      OutFmt         - Output format for numerical results (quoted string) [not checked for validity!]
"A11"           OutSFmt        - Output format for header strings (quoted string) [not checked for validity!]
---------------------- OUTPUT CHANNELS --------------------------------------------
END of output channels and end of file. (the word "END" must appear in the first 3 columns of this line)
```

Figure C.13: OpenFAST SubDyn input file for OC4 jacket analysis - P.1

```
---------- SubDyn v1.01.x MultiMember Support Structure Input File ------------
OC4 'Jacket' SubStructure Input File. The grouted connection is simulated with an equivalent tubular beam of enhanced properties. RRD 10/15/2013
------------------------- SIMULATION CONTROL  --------------------------------
False            Echo        - Echo input data to "<rootname>.SD.ech" (flag)
"DEFAULT"        SDdeltaT    - Local Integration Step. If "default", the glue-code integration step will be used.
             3   IntMethod   - Integration Method [1/2/3/4 = RK4/AB4/ABM4/AM2].
True             SttcSolve   - Solve dynamics about static equilibrium point
-------------------- FEA and CRAIG-BAMPTON PARAMETERS----------------------------
             3   FEMMod      - FEM switch: element model in the FEM. [1= Euler-Bernoulli(E-B);  2=Tapered E-B (unavailable);  3= 2-node Timoshenko;  4= 2-node
tapered Timoshenko (unavailable)]
             2   NDiv        - Number of sub-elements per member
True             CBMod       - [T/F] If True perform C-B reduction, else full FEM dofs will be retained. If True, select Nmodes to retain in C-B reduced
system.
            20   Nmodes      - Number of internal modes to retain (ignored if CBMod=False). If Nmodes=0 --> Guyan Reduction.
             1   JDampings   - Damping Ratios for each retained mode (% of critical) If Nmodes>0, list Nmodes structural damping ratios for each retained mode
(% of critical), or a single damping ratio to be applied to all retained modes. (last entered value will be used for all remaining modes).
---- STRUCTURE JOINTS: joints connect structure members (~Hydrodyn Input File)---
            64   NJoints     - Number of joints (-)
JointID          JointXss              JointYss              JointZss  [Coordinates of Member joints in SS-Coordinate System]
  (-)               (m)                   (m)                   (m)
   1              6.00000               6.00000             -45.50000
   2              6.00000               6.00000             -45.00000
   3              5.96700               5.96700             -44.00100
   4              5.93900               5.93900             -43.12700
   5              5.33300               5.33300             -24.61400
   6             -6.00000               6.00000             -45.50000
   7             -6.00000               6.00000             -45.00000
   8             -5.96700               5.96700             -44.00100
   9             -5.93900               5.93900             -43.12700
  10             -5.33300               5.33300             -24.61400
  11             -6.00000              -6.00000             -45.50000
  12             -6.00000              -6.00000             -45.00000
  13             -5.96700              -5.96700             -44.00100
  14             -5.93900              -5.93900             -43.12700
  15             -5.33300              -5.33300             -24.61400
  16              6.00000              -6.00000             -45.50000
  17              6.00000              -6.00000             -45.00000
  18              5.96700              -5.96700             -44.00100
  19              5.93900              -5.93900             -43.12700
  20              5.33300              -5.33300             -24.61400
  21              4.82000               4.82000              -8.92200
  22              4.38500               4.38500               4.37800
  23              4.01600               4.01600              15.65100
  24              4.00000               4.00000              16.15000
  25             -4.82000               4.82000              -8.92200
  26             -4.38500               4.38500               4.37800
  27             -4.01600               4.01600              15.65100
  28             -4.00000               4.00000              16.15000
  29             -4.82000              -4.82000              -8.92200
  30             -4.38500              -4.38500               4.37800
  31             -4.01600              -4.01600              15.65100
  32             -4.00000              -4.00000              16.15000
  33              4.82000              -4.82000              -8.92200
  34              4.38500              -4.38500               4.37800
  35              4.01600              -4.01600              15.65100
  36              4.00000              -4.00000              16.15000
  37              5.62000               0.00000             -33.37300
  38             -5.62000               0.00000             -33.37300
  39              0.00000               5.62000             -33.37300
  40              0.00000              -5.62000             -33.37300
  41              5.06400               0.00000             -16.37100
  42             -5.06400               0.00000             -16.37100
  43              0.00000               5.06400             -16.37100
  44              0.00000              -5.06400             -16.37100
  45              4.59200               0.00000              -1.95800
  46             -4.59200               0.00000              -1.95800
  47              0.00000               4.59200              -1.95800
  48              0.00000              -4.59200              -1.95800
  49              4.19300               0.00000              10.26200
  50             -4.19300               0.00000              10.26200
  51              0.00000               4.19300              10.26200
  52              0.00000              -4.19300              10.26200
  53              4.00000               4.00000              20.15000
  54             -4.00000               4.00000              20.15000
  55              4.00000              -4.00000              20.15000
  56             -4.00000              -4.00000              20.15000
  57              6.00000              -6.00000             -49.50000
  58              6.00000               6.00000             -49.50000
  59             -6.00000              -6.00000             -49.50000
  60             -6.00000               6.00000             -49.50000
  61              6.00000              -6.00000             -50.00100
  62              6.00000               6.00000             -50.00100
  63             -6.00000              -6.00000             -50.00100
  64             -6.00000               6.00000             -50.00100
------------------- BASE REACTION JOINTS: 1/0 for Locked/Free DOF @ each Reaction Node ---------------------
             4   NReact      - Number of Joints with reaction forces; be sure to remove all rigid motion DOFs of the structure  (else det([K])=[0])
RJointID   RctTDXss     RctTDYss     RctTDZss     RctRDXss     RctRDYss     RctRDZss     SSIfile [Global Coordinate System]
  (-)       (flag)       (flag)       (flag)       (flag)       (flag)       (flag)       (string)
  61             1            1            1            1            1            1 "OC4_Jacket_SD_SSI.txt"
  62             1            1            1            1            1            1    "OC4_Jacket_SD_SSI.txt"
  63             1            1            1            1            1            1    "OC4_Jacket_SD_SSI.txt"
  64             1            1            1            1            1            1    "OC4_Jacket_SD_SSI.txt"
------- INTERFACE JOINTS: 1/0 for Locked (to the TP)/Free DOF @each Interface Joint (only Locked-to-TP implemented thus far (=rigid TP)) ---------
             8   NInterf     - Number of interface joints locked to the Transition Piece (TP):  be sure to remove all rigid motion dofs
IJointID   ItfTDXss     ItfTDYss     ItfTDZss     ItfRDXss     ItfRDYss     ItfRDZss     [Global Coordinate System]
  (-)       (flag)       (flag)       (flag)       (flag)       (flag)       (flag)
  24             1            1            1            1            1            1
  28             1            1            1            1            1            1
  32             1            1            1            1            1            1
  36             1            1            1            1            1            1
  53             1            1            1            1            1            1
  54             1            1            1            1            1            1
  55             1            1            1            1            1            1
  56             1            1            1            1            1            1
---------------------------------- MEMBERS --------------------------------------
           112   NMembers    - Number of frame members
MemberID   MJointID1   MJointID2   MPropSetID1   MPropSetID2     COSMID
  (-)         (-)          (-)          (-)           (-)           (-)
   1            1            2            2             2
   2            2            3            2             2
   3            3            4            2             2
```

Figure C.14: OpenFAST SubDyn input file for OC4 jacket analysis - P.2

```
  4          4          5          2          2
  5          6          7          2          2
  6          7          8          2          2
  7          8          9          2          2
  8          9         10          2          2
  9         11         12          2          2
 10         12         13          2          2
 11         13         14          2          2
 12         14         15          2          2
 13         16         17          2          2
 14         17         18          2          2
 15         18         19          2          2
 16         19         20          2          2
 17          5         21          3          3
 18         21         22          3          3
 19         22         23          3          3
 20         23         24          3          3
 21         10         25          3          3
 22         25         26          3          3
 23         26         27          3          3
 24         27         28          3          3
 25         15         29          3          3
 26         29         30          3          3
 27         30         31          3          3
 28         31         32          3          3
 29         20         33          3          3
 30         33         34          3          3
 31         34         35          3          3
 32         35         36          3          3
 33          8          3          1          1
 34         13          8          1          1
 35         13         18          1          1
 36         18          3          1          1
 37          4         37          1          1
 38         37         20          1          1
 39         19         37          1          1
 40         37          5          1          1
 41          9         38          1          1
 42         38         15          1          1
 43         14         38          1          1
 44         38         10          1          1
 45          4         39          1          1
 46         39         10          1          1
 47          9         39          1          1
 48         39          5          1          1
 49         19         40          1          1
 50         40         15          1          1
 51         14         40          1          1
 52         40         20          1          1
 53          5         41          1          1
 54         41         33          1          1
 55         20         41          1          1
 56         41         21          1          1
 57         10         42          1          1
 58         42         29          1          1
 59         15         42          1          1
 60         42         25          1          1
 61          5         43          1          1
 62         43         25          1          1
 63         10         43          1          1
 64         43         21          1          1
 65         20         44          1          1
 66         44         29          1          1
 67         15         44          1          1
 68         44         33          1          1
 69         21         45          1          1
 70         45         34          1          1
 71         33         45          1          1
 72         45         22          1          1
 73         25         46          1          1
 74         46         30          1          1
 75         29         46          1          1
 76         46         26          1          1
 77         21         47          1          1
 78         47         26          1          1
 79         25         47          1          1
 80         47         22          1          1
 81         33         48          1          1
 82         48         30          1          1
 83         29         48          1          1
 84         48         34          1          1
 85         22         49          1          1
 86         49         35          1          1
 87         34         49          1          1
 88         49         23          1          1
 89         26         50          1          1
 90         50         31          1          1
 91         30         50          1          1
 92         50         27          1          1
 93         22         51          1          1
 94         51         27          1          1
 95         26         51          1          1
 96         51         23          1          1
 97         34         52          1          1
 98         52         31          1          1
 99         30         52          1          1
100         52         35          1          1
101         24         53          4          4
102         28         54          4          4
103         32         56          4          4
104         36         55          4          4
105         58          1          5          5
106         57         16          5          5
107         60          6          5          5
108         59         11          5          5
109         62         58          6          6
110         61         57          6          6
111         64         60          6          6
112         63         59          6          6
---------------- MEMBER X-SECTION PROPERTY data 1/2 [isotropic material for now: use this table for circular-tubular elements] ------------------------
          6   NPropSets   - Number of structurally unique x-sections (i.e. how many groups of X-sectional properties are utilized throughout all of the
members)
```

Figure C.15: OpenFAST SubDyn input file for OC4 jacket analysis - P.3

```
PropSetID     YoungE          ShearG          MatDens          XsecD           XsecT
  (-)         (N/m2)          (N/m2)          (kg/m3)           (m)             (m)
   1        2.10000e+11     8.07690e+10       7850.00         0.800000        0.020000
   2        2.10000e+11     8.07690e+10       7850.00         1.200000        0.050000
   3        2.10000e+11     8.07690e+10       7850.00         1.200000        0.035000
   4        2.10000e+11     8.07690e+10       7850.00         1.200000        0.040000
   5        2.10000e+11     8.07690e+10       3339.12         2.082000        0.491000
   6        2.10000e+11     8.07690e+10       7850.00         2.082000        0.060000
------------------ MEMBER X-SECTION PROPERTY data 2/2 [isotropic material for now: use this table if any section other than circular, however provide COSM(i,j)
below] ------------------------
            0   NXPropSets  - Number of structurally unique non-circular x-sections (if 0 the following table is ignored)
PropSetID     YoungE          ShearG          MatDens          XsecA          XsecAsx       XsecAsy       XsecJxx       XsecJyy        XsecJ0
  (-)         (N/m2)          (N/m2)          (kg/m3)          (m2)            (m2)          (m2)          (m4)          (m4)          (m4)
---------------------- MEMBER COSINE MATRICES COSM(i,j) ------------------------
            0   NCOSMs      - Number of unique cosine matrices (i.e., of unique member alignments including principal axis rotations); ignored if NXPropSets=0
or 9999 in any element below
COSMID    COSM11    COSM12    COSM13    COSM21    COSM22    COSM23    COSM31    COSM32    COSM33
 (-)       (-)       (-)       (-)       (-)       (-)       (-)       (-)       (-)       (-)
------------------------ JOINT ADDITIONAL CONCENTRATED MASSES--------------------------
            0   NCmass      - Number of joints with concentrated masses; Global Coordinate System
CMJointID       JMass             JMXX             JMYY             JMZZ
  (-)            (kg)          (kg*m^2)         (kg*m^2)         (kg*m^2)
---------------------------- OUTPUT: SUMMARY & OUTFILE ------------------------------
True            SSSum       - Output a Summary File (flag).It contains: matrices K,M  and C-B reduced M_BB, M-BM, K_BB, K_MM(OMG^2), PHI_R, PHI_L. It can also
contain COSMs if requested.
True            OutCOSM     - Output cosine matrices with the selected output member forces (flag)
False           OutAll      - [T/F] Output all members' end forces
            2   OutSwtch    - [1/2/3] Output requested channels to: 1=<rootname>.SD.out;  2=<rootname>.out (generated by FAST);  3=both files.
True            TabDelim    - Generate a tab-delimited output in the <rootname>.SD.out file
            1   OutDec      - Decimation of output in the <rootname>.SD.out file
"ES11.4e2"      OutFmt      - Output format for numerical results in the <rootname>.SD.out file
"A11"           OutSFmt     - Output format for header strings in the <rootname>.SD.out file
------------------------ MEMBER OUTPUT LIST ------------------------------------------
            8   NMOutputs   - Number of members whose forces/displacements/velocities/accelerations will be output (-) [Must be <= 9].
MemberID   NOutCnt    NodeCnt [NOutCnt=how many nodes to get output for [< 10]; NodeCnt are local ordinal numbers from the start of the member, and must be >=1
and <= NDiv+1] If NMOutputs=0 leave blank as well.
  (-)        (-)        (-)
   4          2          1 2 3   ! M1
  16          2          1 2 3   ! M2
   8          2          1 2 3   ! M3
  12          2          1 2 3   ! M4
  17          2          1 2 3   ! M5
  29          2          1 2 3   ! M6
  21          2          1 2 3   ! M7
  25          2          1 2 3   ! M8
------------------------ SSOutList: The next line(s) contains a list of output parameters that will be output in <rootname>.SD.out or <rootname>.out. ------
"M1N2FKZe" - Member 1 forces
"M2N2FKZe" - Member 2 forces
"M3N2FKZe" - Member 3 forces
"M4N2FKZe" - Member 4 forces
"M5N2FKZe" - Member 5 forces
"M6N2FKZe" - Member 6 forces
"M7N2FKZe" - Member 7 forces
"M8N2FKZe" - Member 8 forces
"M1N2FKZe" - Member 1 forces
"M2N2FKZe" - Member 2 forces
"M3N2FKZe" - Member 3 forces
"M4N2FKZe" - Member 4 forces
"M5N2FKZe" - Member 5 forces
"M6N2FKZe" - Member 6 forces
"M7N2FKZe" - Member 7 forces
"M8N2FKZe" - Member 8 forces
"M1N1MKXe, M1N2MKXe, M1N1MKYe, M1N2MKYe, M1N1MKZe, M1N2MKZe" - Member 1 moments
"M2N1MKXe, M2N2MKXe, M2N1MKYe, M2N2MKYe, M2N1MKZe, M2N2MKZe" - Member 2 moments
"M3N1MKXe, M3N2MKXe, M3N1MKYe, M3N2MKYe, M3N1MKZe, M3N2MKZe" - Member 3 moments
"M4N1MKXe, M4N2MKXe, M4N1MKYe, M4N2MKYe, M4N1MKZe, M4N2MKZe" - Member 4 moments
"M5N1MKXe, M5N2MKXe, M5N1MKYe, M5N2MKYe, M5N1MKZe, M5N2MKZe" - Member 5 moments
"M6N1MKXe, M6N2MKXe, M6N1MKYe, M6N2MKYe, M6N1MKZe, M6N2MKZe" - Member 6 moments
"M7N1MKXe, M7N2MKXe, M7N1MKYe, M7N2MKYe, M7N1MKZe, M7N2MKZe" - Member 7 moments
"M8N1MKXe, M8N2MKXe, M8N1MKYe, M8N2MKYe, M8N1MKZe, M8N2MKZe" - Member 8 moments
END of output channels and end of file. (the word "END" must appear in the first 3 columns of this line)
```

Figure C.16: OpenFAST ExtPtfm input file for OC4 jacket analysis

```
---------------------- EXTPTFM INPUT FILE -------------------------------------
Comment describing the model
---------------------- SIMULATION CONTROL --------------------------------------
False          Echo          - Echo input data to <RootName>.ech (flag)
"default"     DT           - Communication interval for controllers (s) (or "default")
   3          IntMethod     - Integration Method {1:RK4; 2:AB4, 3:ABM4} (switch)
---------------------- REDUCTION INPUTS ----------------------------------------
   1          FileFormat    - File Format {0:Guyan; 1:FlexASCII} (switch)
"ExtPtfm_SE.dat"   Red_FileName    - Path of the file containing Guyan/Craig-Bampton inputs (-)
"NA"         RedCst_FileName - Path of the file containing Guyan/Craig-Bampton constant inputs (-) (currently unused)
-1           NActiveDOFList - Number of active CB mode listed in ActiveDOFList, use -1 for all modes (integer)
1,2,3,4,5,6,7,8,9,10,11,12,13,14,15,16,17,18,19,20,21,22,23,24,25     ActiveDOFList  - List of CB modes index that are active, [unused if
NActiveDOFList<=0]
0          NInitPosList   - Number of initial positions listed in InitPosList, using 0 implies all DOF initialized to 0  (integer)
0,         InitPosList    - List of initial positions for the CB modes  [unused if NInitPosList<=0 or EquilStart=True]
0          NInitVelList   - Number of initial positions listed in InitVelList, using 0 implies all DOF initialized to 0  (integer)
0,         InitVelList    - List of initial velocities for the CB modes  [unused if NInitVelPosList<=0 or EquilStart=True]
---------------------- OUTPUT --------------------------------------------------
True          SumPrint      - Print summary data to <RootName>.sum (flag)
         3    OutFile       - Switch to determine where output will be placed: {1: in module output file only; 2: in glue code output file
only; 3: both} (currently unused)
True          TabDelim      - Use tab delimiters in text tabular output file? (flag) (currently unused)
"ES11.4e2"    OutFmt        - Format used for text tabular output (except time).  Resulting field should be 10 characters. (quoted string)
(currently unused)
          0   TStart        - Time to begin tabular output (s) (currently unused)
              OutList       - The next line(s) contains a list of output parameters.  See OutListParameters.xlsx for a listing of available
output channels, (-)
"KBBt"                      - Platform interface force  - Directed along the x-direction  (N)
"MBBt"                      - Platform interface force  - Directed along the x-direction  (N)
"MRB"                       - Mass Matrix
"IntrfFx"                   - Platform interface force  - Directed along the x-direction  (N)
"IntrfFy"                   - Platform interface force  - Directed along the y-direction  (N)
"IntrfFz"                   - Platform interface force  - Directed along the z-direction  (N)
"IntrfMx"                   - Platform interface moment - Directed along the x-direction  (Nm)
"IntrfMy"                   - Platform interface moment - Directed along the y-direction  (Nm)
"IntrfMz"                   - Platform interface moment - Directed along the z-direction  (Nm)
"InpF_Fx"                   - Reduced Input force at interface point - Directed along the x-direction  (N)
"InpF_Fy"                   - Reduced Input force at interface point - Directed along the y-direction  (N)
"InpF_Fz"                   - Reduced Input force at interface point - Directed along the z-direction  (N)
"InpF_Mx"                   - Reduced Input moment at interface point - Directed along the x-direction  (Nm)
"InpF_My"                   - Reduced Input moment at interface point - Directed along the y-direction  (Nm)
"InpF_Mz"                   - Reduced Input moment at interface point - Directed along the z-direction  (Nm)
"CBQ_001"                   - Modal displacement of internal Craig-Bampton mode number XXX  (-)
"CBQ_002"                   - Modal displacement of internal Craig-Bampton mode number XXX  (-)
"CBQ_003"                   - Modal displacement of internal Craig-Bampton mode number XXX  (-)
"CBQ_004"                   - Modal displacement of internal Craig-Bampton mode number XXX  (-)
"CBQ_005"                   - Modal displacement of internal Craig-Bampton mode number XXX  (-)
"CBQ_006"                   - Modal displacement of internal Craig-Bampton mode number XXX  (-)
"CBQ_007"                   - Modal displacement of internal Craig-Bampton mode number XXX  (-)
"CBQ_010"                   - Modal displacement of internal Craig-Bampton mode number XXX  (-)
"CBQ_011"                   - Modal displacement of internal Craig-Bampton mode number XXX  (-)
"CBQ_012"                   - Modal displacement of internal Craig-Bampton mode number XXX  (-)
"CBQ_013"                   - Modal displacement of internal Craig-Bampton mode number XXX  (-)
"CBQ_014"                   - Modal displacement of internal Craig-Bampton mode number XXX  (-)
"CBQ_015"                   - Modal displacement of internal Craig-Bampton mode number XXX  (-)
"CBQ_016"                   - Modal displacement of internal Craig-Bampton mode number XXX  (-)
"CBQ_017"                   - Modal displacement of internal Craig-Bampton mode number XXX  (-)
"CBQ_020"                   - Modal displacement of internal Craig-Bampton mode number XXX  (-)
"CBQ_021"                   - Modal displacement of internal Craig-Bampton mode number XXX  (-)
"CBQ_022"                   - Modal displacement of internal Craig-Bampton mode number XXX  (-)
"CBQ_023"                   - Modal displacement of internal Craig-Bampton mode number XXX  (-)
"CBQ_024"                   - Modal displacement of internal Craig-Bampton mode number XXX  (-)
"CBQ_025"                   - Modal displacement of internal Craig-Bampton mode number XXX  (-)
"CBF_001"                   - Modal force        on internal Craig-Bampton mode number XXX  (-)
"CBF_002"                   - Modal force        on internal Craig-Bampton mode number XXX  (-)
"CBF_003"                   - Modal force        on internal Craig-Bampton mode number XXX  (-)
"CBF_004"                   - Modal force        on internal Craig-Bampton mode number XXX  (-)
"CBF_005"                   - Modal force        on internal Craig-Bampton mode number XXX  (-)
"CBF_006"                   - Modal force        on internal Craig-Bampton mode number XXX  (-)
"CBF_007"                   - Modal force        on internal Craig-Bampton mode number XXX  (-)
"CBF_010"                   - Modal force        on internal Craig-Bampton mode number XXX  (-)
"CBF_011"                   - Modal force        on internal Craig-Bampton mode number XXX  (-)
"CBF_012"                   - Modal force        on internal Craig-Bampton mode number XXX  (-)
"CBF_013"                   - Modal force        on internal Craig-Bampton mode number XXX  (-)
"CBF_014"                   - Modal force        on internal Craig-Bampton mode number XXX  (-)
"CBF_015"                   - Modal force        on internal Craig-Bampton mode number XXX  (-)
"CBF_016"                   - Modal force        on internal Craig-Bampton mode number XXX  (-)
"CBF_017"                   - Modal force        on internal Craig-Bampton mode number XXX  (-)
"CBF_020"                   - Modal force        on internal Craig-Bampton mode number XXX  (-)
"CBF_021"                   - Modal force        on internal Craig-Bampton mode number XXX  (-)
"CBF_022"                   - Modal force        on internal Craig-Bampton mode number XXX  (-)
"CBF_023"                   - Modal force        on internal Craig-Bampton mode number XXX  (-)
"CBF_024"                   - Modal force        on internal Craig-Bampton mode number XXX  (-)
"CBF_025"                   - Modal force        on internal Craig-Bampton mode number XXX  (-)
"WavElev"                   - Wave elevation                                        (m)
END of input file (the word "END" must appear in the first 3 columns of this last OutList line)
---------------------------------------------------------------------------------------
```

Figure C.17: OpenFAST ExtPtfm superelement data (1/14 pages) for OC4 jacket analysis

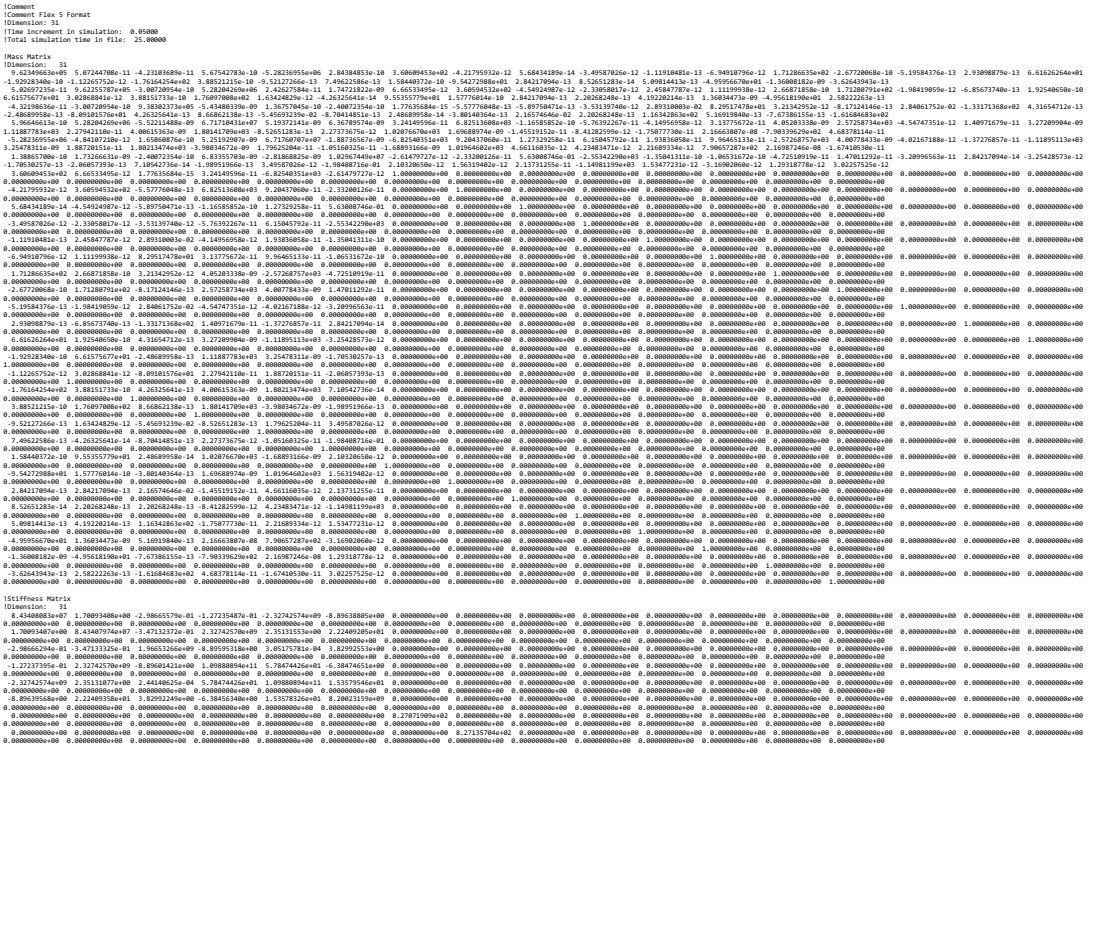

D

KK-joint mode shapes

D.1. Appendix description

In this appendix, the obtained mode shapes for the submodelled joints for the first 10 modes are shown. The welded alternative is compared to the wrapped composite alternative for each mode.

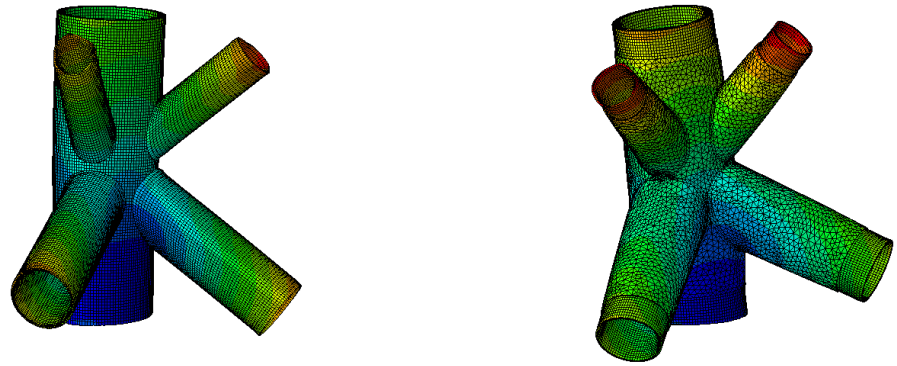

(a) Mode 1 - Welded **(b)** Mode 1 - Wrapped

Figure D.1: KK-Joint - Mode 1

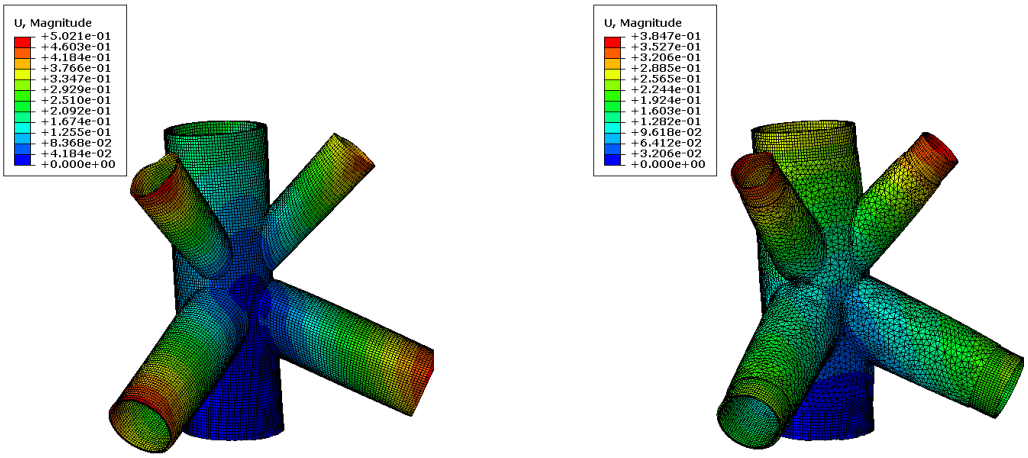

(a) Mode 2 - Welded **(b)** Mode 2 - Wrapped

Figure D.2: KK-Joint - Mode 2

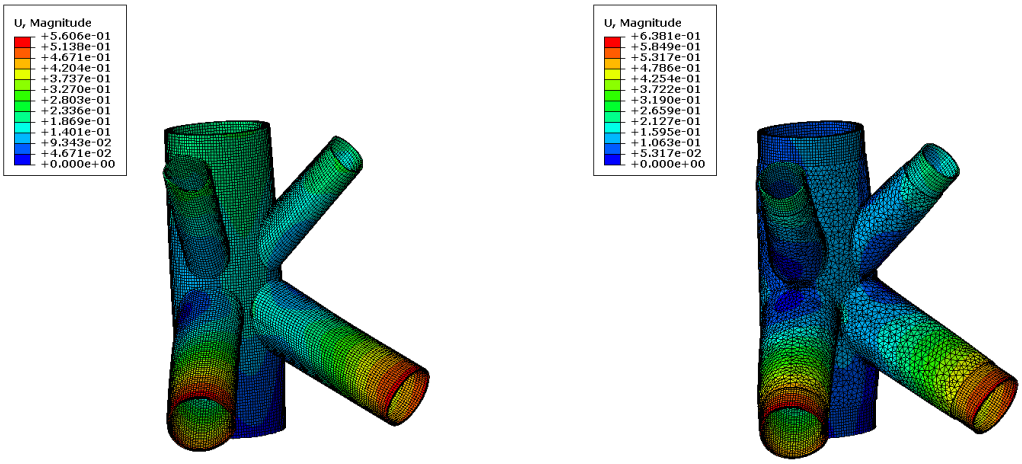

(a) Mode 3 - Welded **(b)** Mode 3 - Wrapped

Figure D.3: KK-Joint - Mode 3

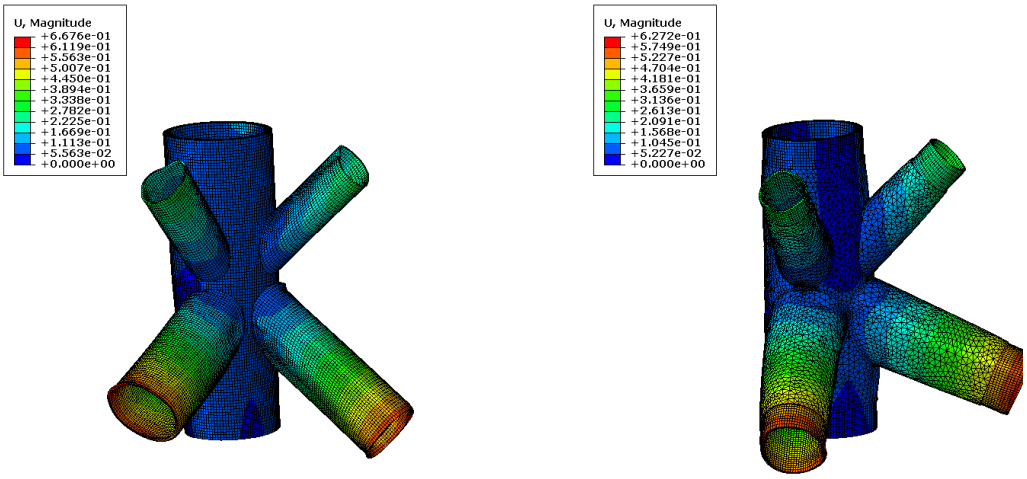

(a) Mode 4 - Welded **(b)** Mode 4 - Wrapped

Figure D.4: KK-Joint - Mode 4

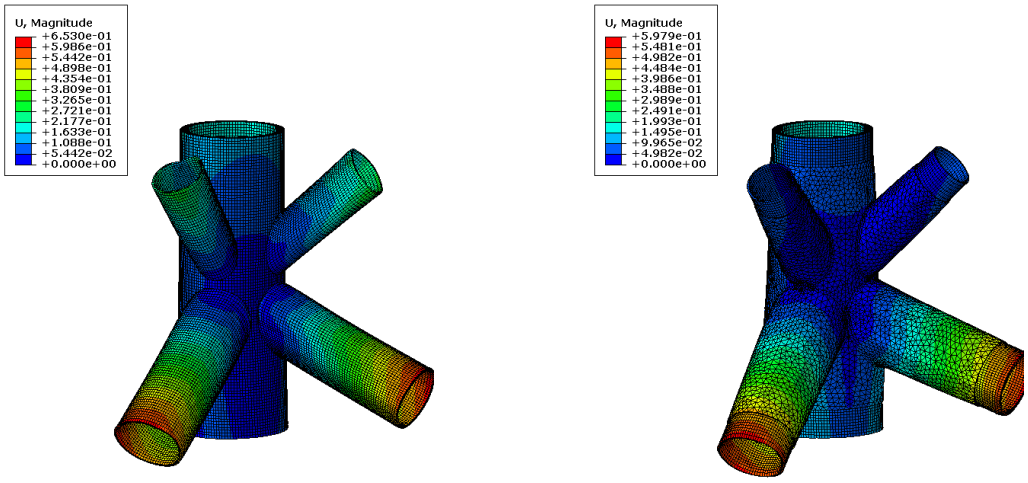

(a) Mode 5 - Welded **(b)** Mode 5 - Wrapped

Figure D.5: KK-Joint - Mode 5

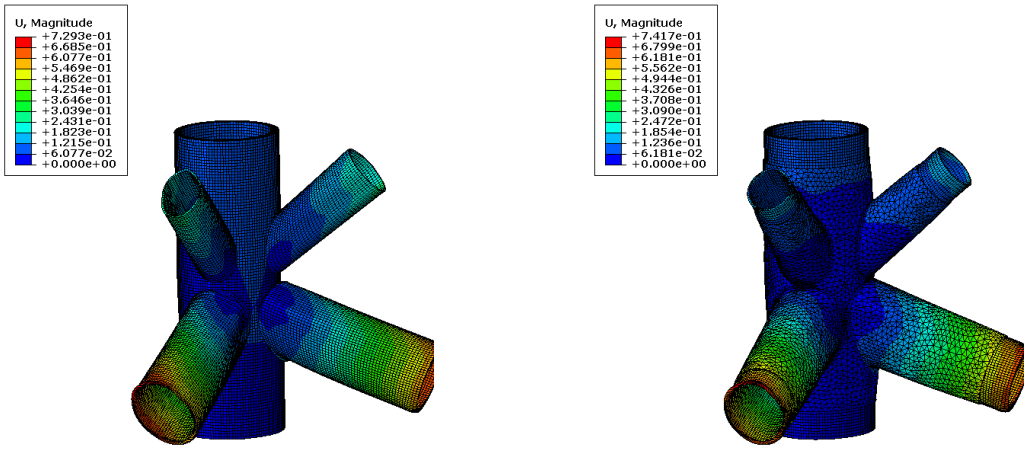

(a) Mode 6 - Welded **(b)** Mode 6 - Wrapped

Figure D.6: KK-Joint - Mode 6

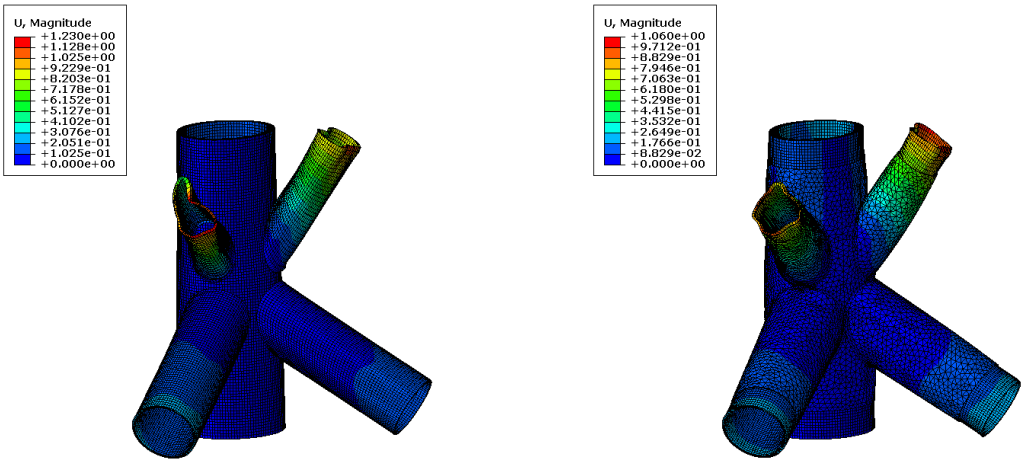

(a) Mode 7 - Welded **(b)** Mode 7 - Wrapped

Figure D.7: KK-Joint - Mode 7

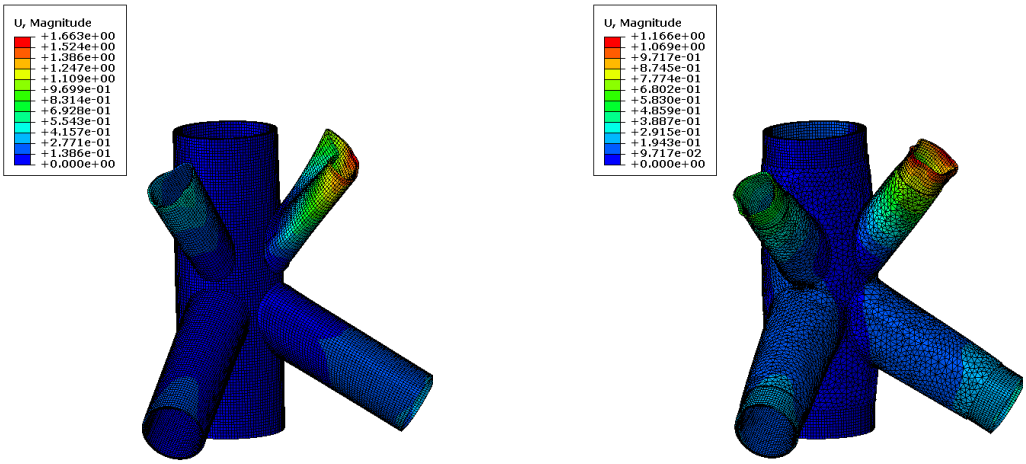

(a) Mode 8 - Welded **(b)** Mode 8 - Wrapped

Figure D.8: KK-Joint - Mode 8

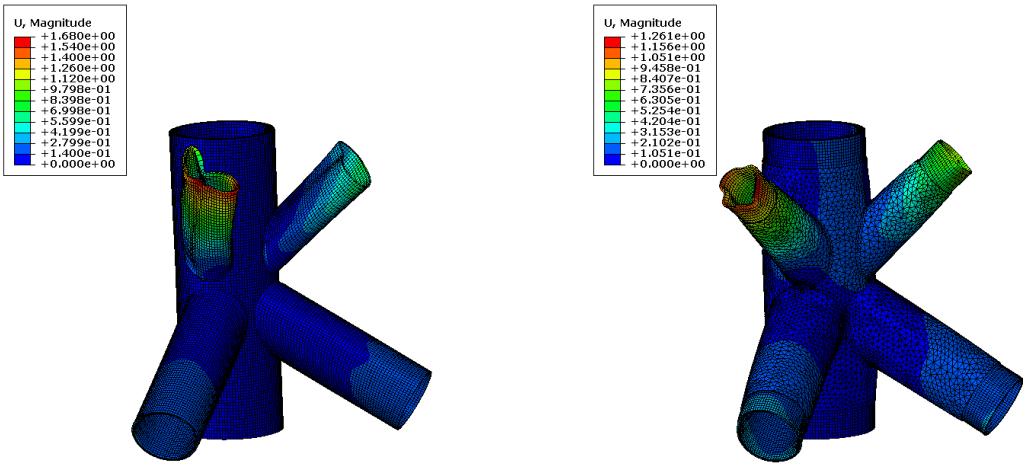

(a) Mode 9 - Welded **(b)** Mode 9 - Wrapped

Figure D.9: KK-Joint - Mode 9

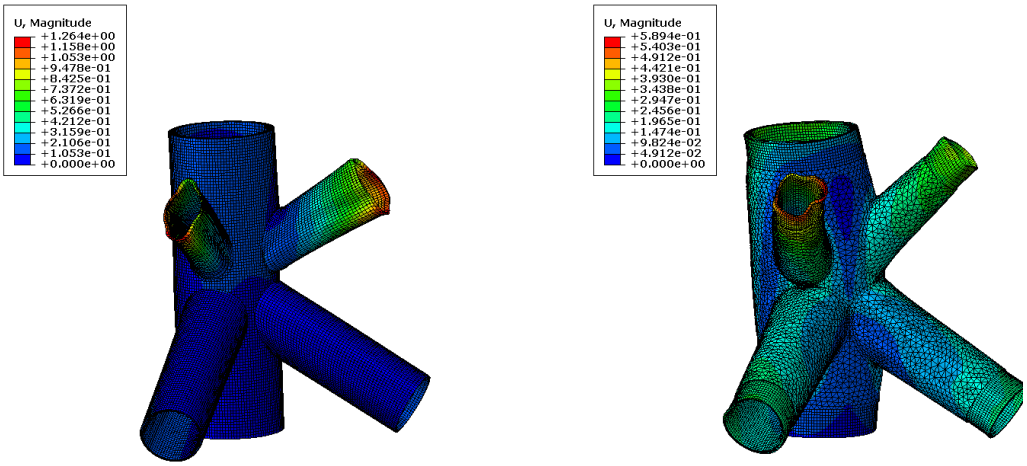

(a) Mode 10 - Welded **(b)** Mode 10 - Wrapped

Figure D.10: KK-Joint - Mode 10

E

10MW OWT - project description

E.1. 10MW - Turbine information

Properties of the RNA are held in table E.1. These properties serve to approximate the mass and inertia of the wind turbine. This includes the blades, hub, and nacelle.

Table E.1: RNA properties for INNWIND jacket

Lumped mass [kg]	676723
Moment of inertia I_x $[kg * m^2]$	1.66e+08
Moment of inertia I_y $[kg * m^2]$	1.27e+08
Moment of inertia I_z $[kg * m^2]$	1.27e+08

E.2. 10MW - Tower geometry

Figure E.1: INNWIND.EU, D4.34, Innovative design of 10MW steel jackets, Tower Dimensions (Stolpe et al., 2016)

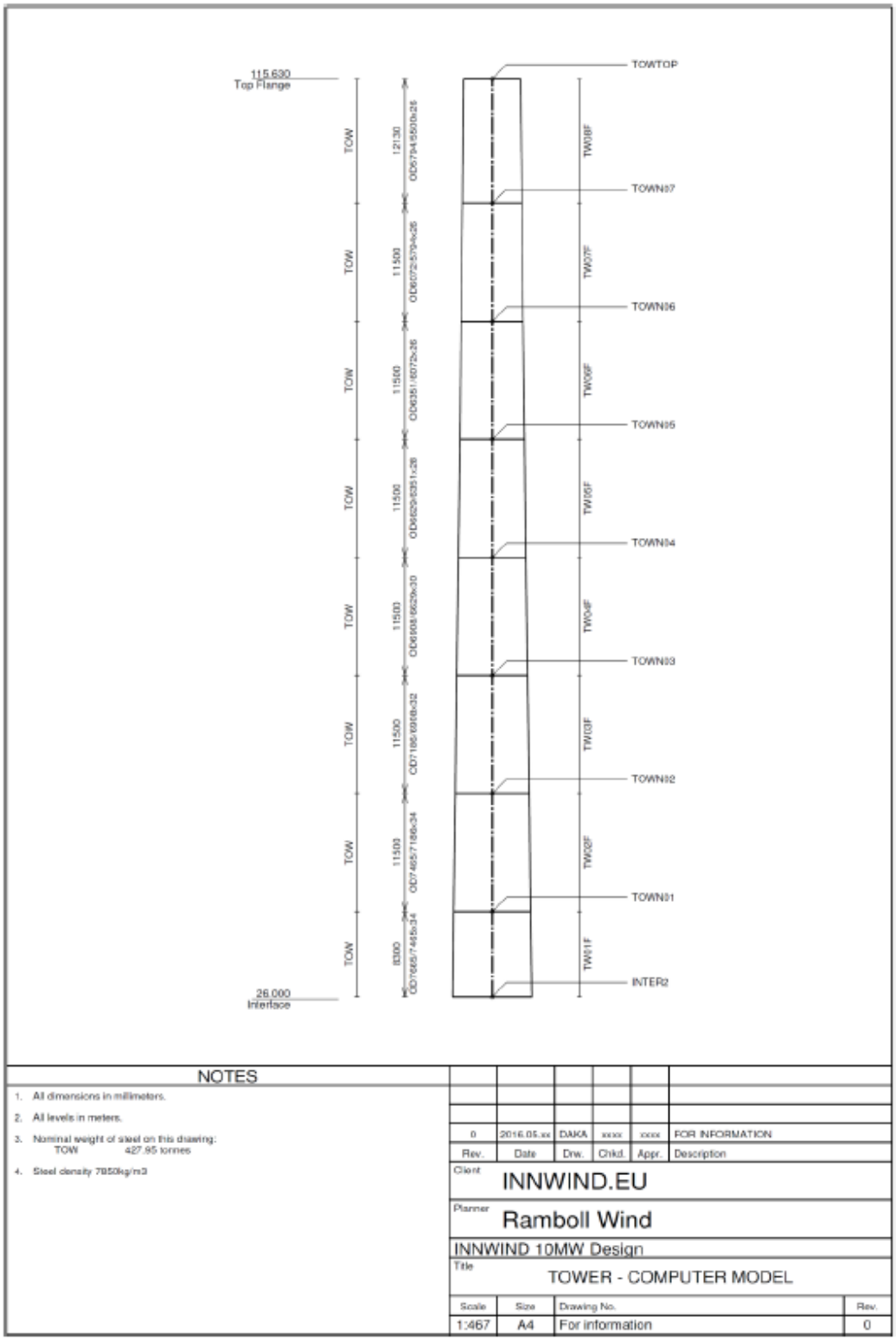

E.3. 10MW - Jacket geometry

Figure E.2: INNWIND.EU, D4.34, Innovative design of 10MW steel jackets, geometry of jacket - P.1 (Stolpe et al., 2016)

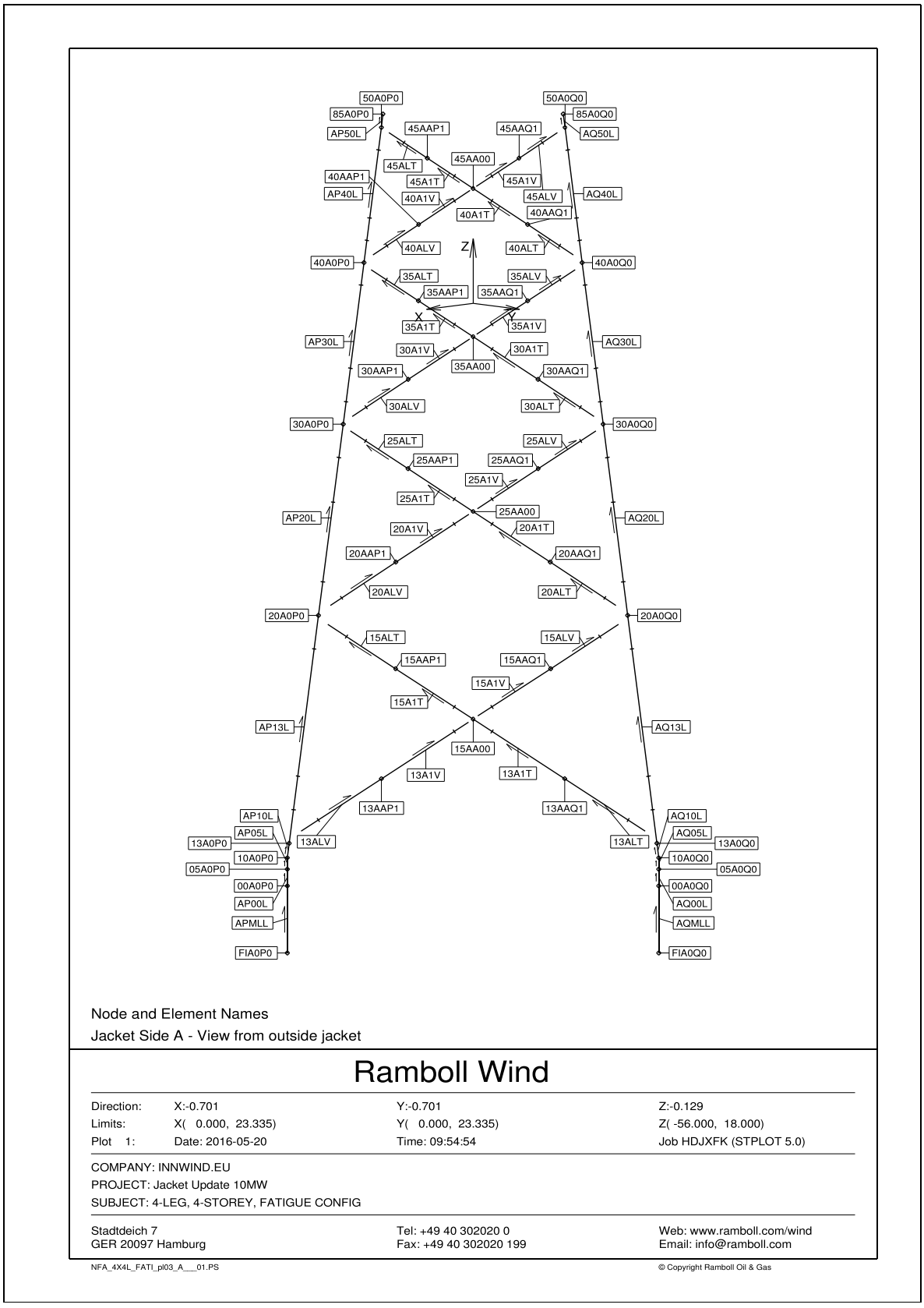

Node and Element Names
Jacket Side A - View from outside jacket

Ramboll Wind

Direction:	X:-0.701	Y:-0.701	Z:-0.129
Limits:	X(0.000, 23.335)	Y(0.000, 23.335)	Z(-56.000, 18.000)
Plot 1:	Date: 2016-05-20	Time: 09:54:54	Job HDJXFK (STPLOT 5.0)

COMPANY: INNWIND.EU
PROJECT: Jacket Update 10MW
SUBJECT: 4-LEG, 4-STOREY, FATIGUE CONFIG

Stadtdeich 7
GER 20097 Hamburg
Tel: +49 40 302020 0
Fax: +49 40 302020 199
Web: www.ramboll.com/wind
Email: info@ramboll.com

NFA_4X4L_FATI_pl03_A___01.PS

Figure E.3: INNWIND.EU, D4.34, Innovative design of 10MW steel jackets, geometry of jacket - P.2 (Stolpe et al., 2016)

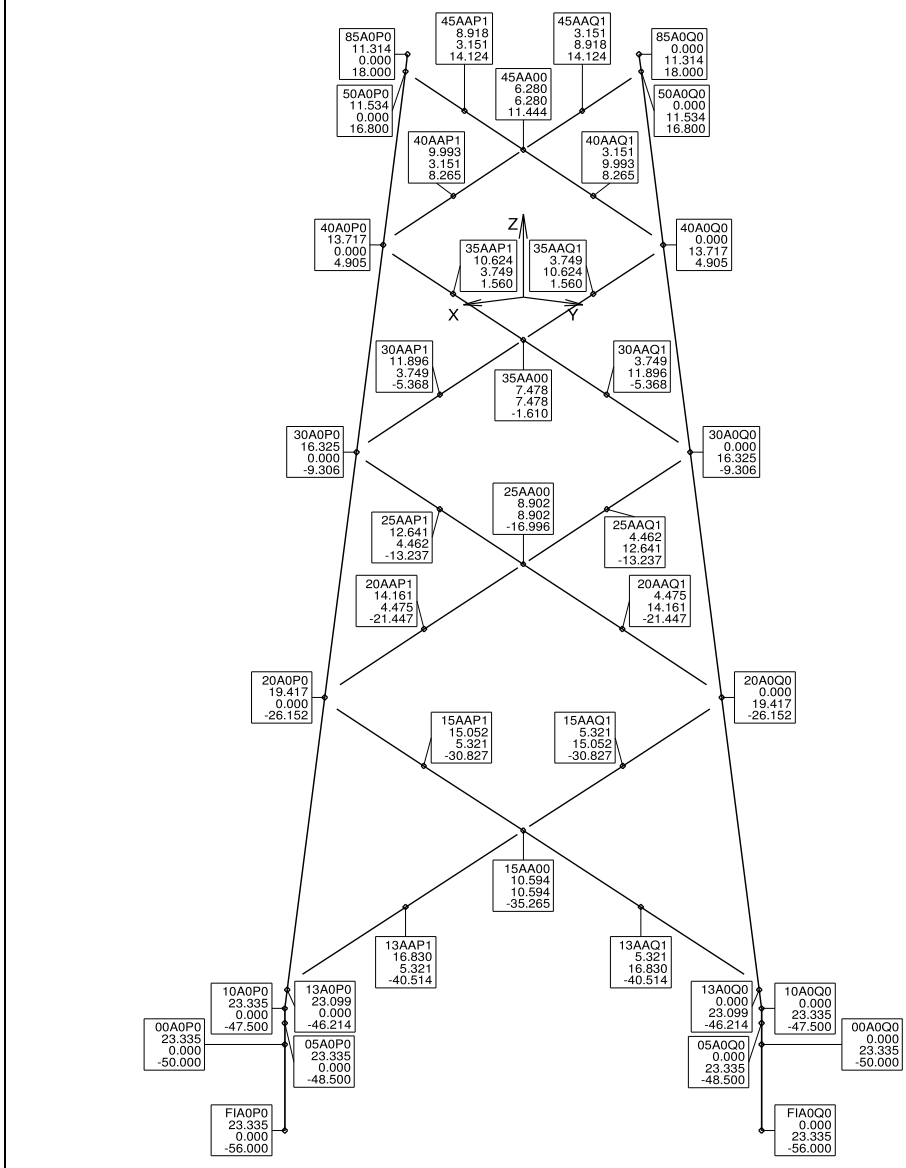

Node coordinates (m)

Jacket Side A - View from outside jacket

Ramboll Wind

Direction:	X:-0.701	Y:-0.701	Z:-0.129
Limits:	X(0.000, 23.335)	Y(0.000, 23.335)	Z(-56.000, 18.000)
Plot 1:	Date: 2016-05-20	Time: 09:54:54	Job HDJXFK (STPLOT 5.0)

COMPANY: INNWIND.EU

PROJECT: Jacket Update 10MW

SUBJECT: 4-LEG, 4-STOREY, FATIGUE CONFIG

Stadtdeich 7
GER 20097 Hamburg

Tel: +49 40 302020 0
Fax: +49 40 302020 199

Web: www.ramboll.com/wind
Email: info@ramboll.com

NFA_4X4L_FATI_pl03_NCO_02.PS

Figure E.4: INNWIND.EU, D4.34, Innovative design of 10MW steel jackets, geometry of jacket - P.3 (Stolpe et al., 2016)

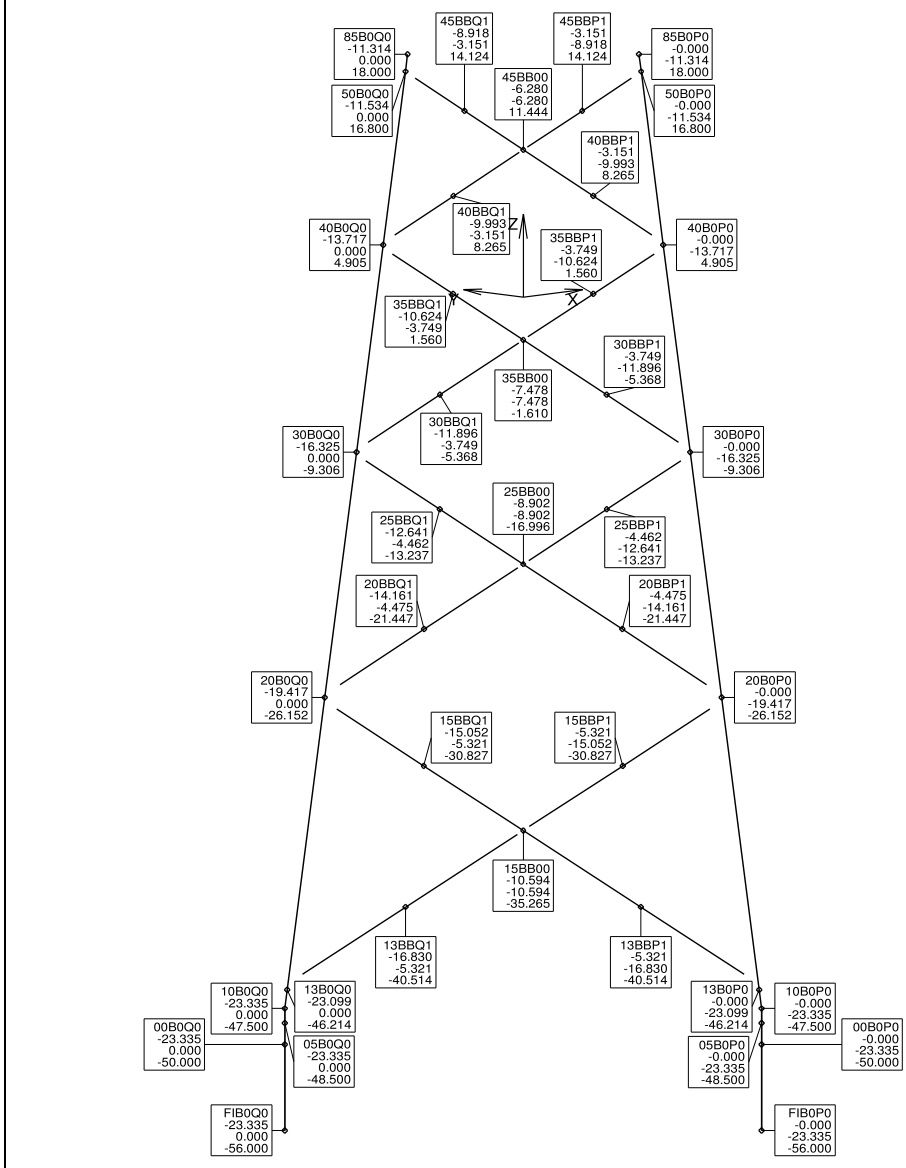

Node coordinates (m)

Jacket Side B - View from outside jacket

Ramboll Wind

Direction:	X: 0.701	Y: 0.701	Z:-0.129
Limits:	X(-23.335, -0.000)	Y(-23.335, 0.000)	Z(-56.000, 18.000)
Plot 2:	Date: 2016-05-20	Time: 09:54:54	Job HDJXFK (STPLOT 5.0)

COMPANY: INNWIND.EU
PROJECT: Jacket Update 10MW
SUBJECT: 4-LEG, 4-STOREY, FATIGUE CONFIG

Stadtdeich 7
GER 20097 Hamburg
Tel: +49 40 302020 0
Fax: +49 40 302020 199
Web: www.ramboll.com/wind
Email: info@ramboll.com

NFA_4X4L_FATI_pl03_NCO_02.PS

Figure E.5: INNWIND.EU, D4.34, Innovative design of 10MW steel jackets, geometry of jacket - P.4 (Stolpe et al., 2016)

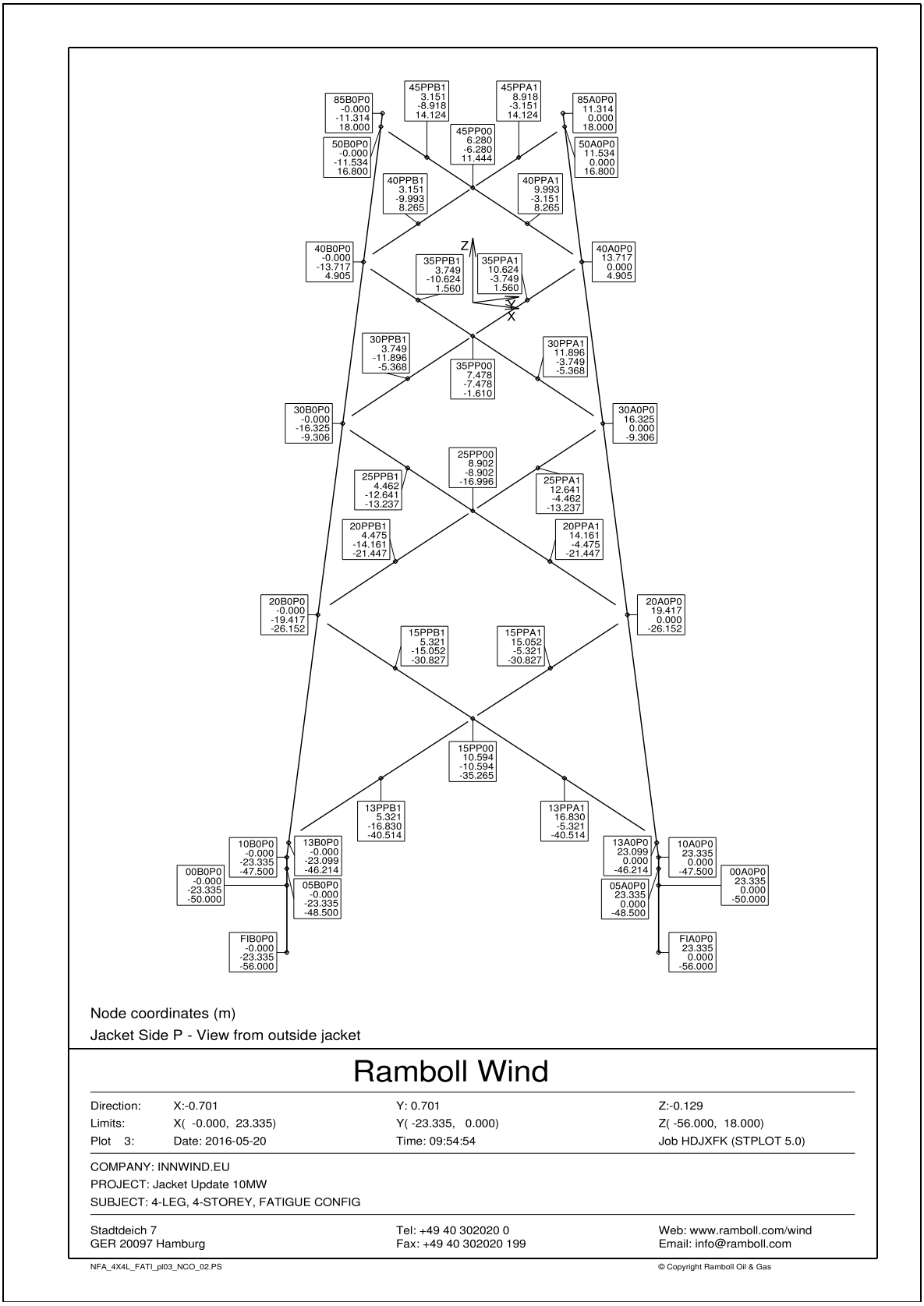

Figure E.6: INNWIND.EU, D4.34, Innovative design of 10MW steel jackets, geometry of jacket - P.5 (Stolpe et al., 2016)

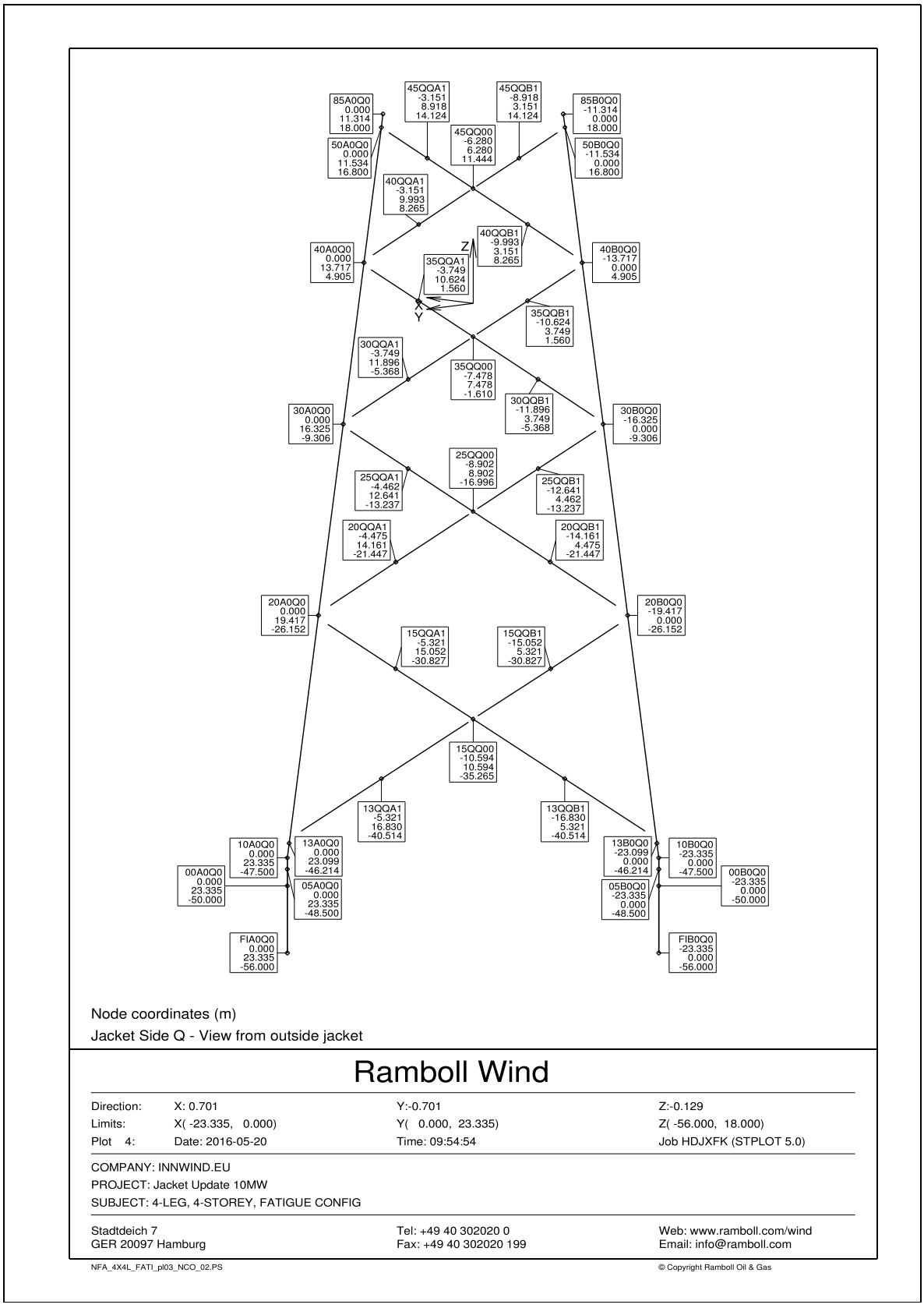

Figure E.7: INNWIND.EU, D4.34, Innovative design of 10MW steel jackets, geometry of jacket - P.6 (Stolpe et al., 2016)

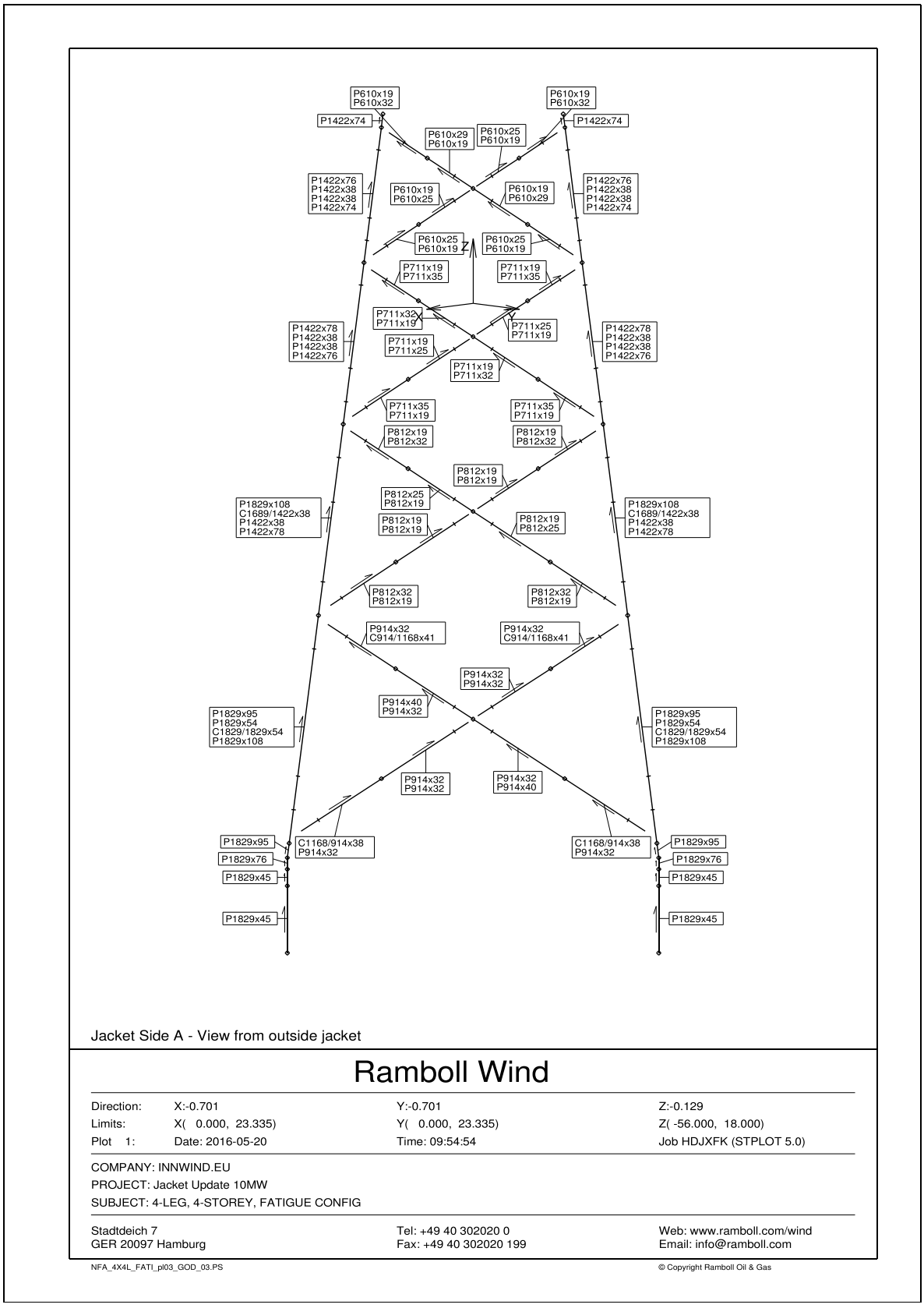

Figure E.8: INNWIND.EU, D4.34, Innovative design of 10MW steel jackets, geometry of jacket - P.7 (Stolpe et al., 2016)

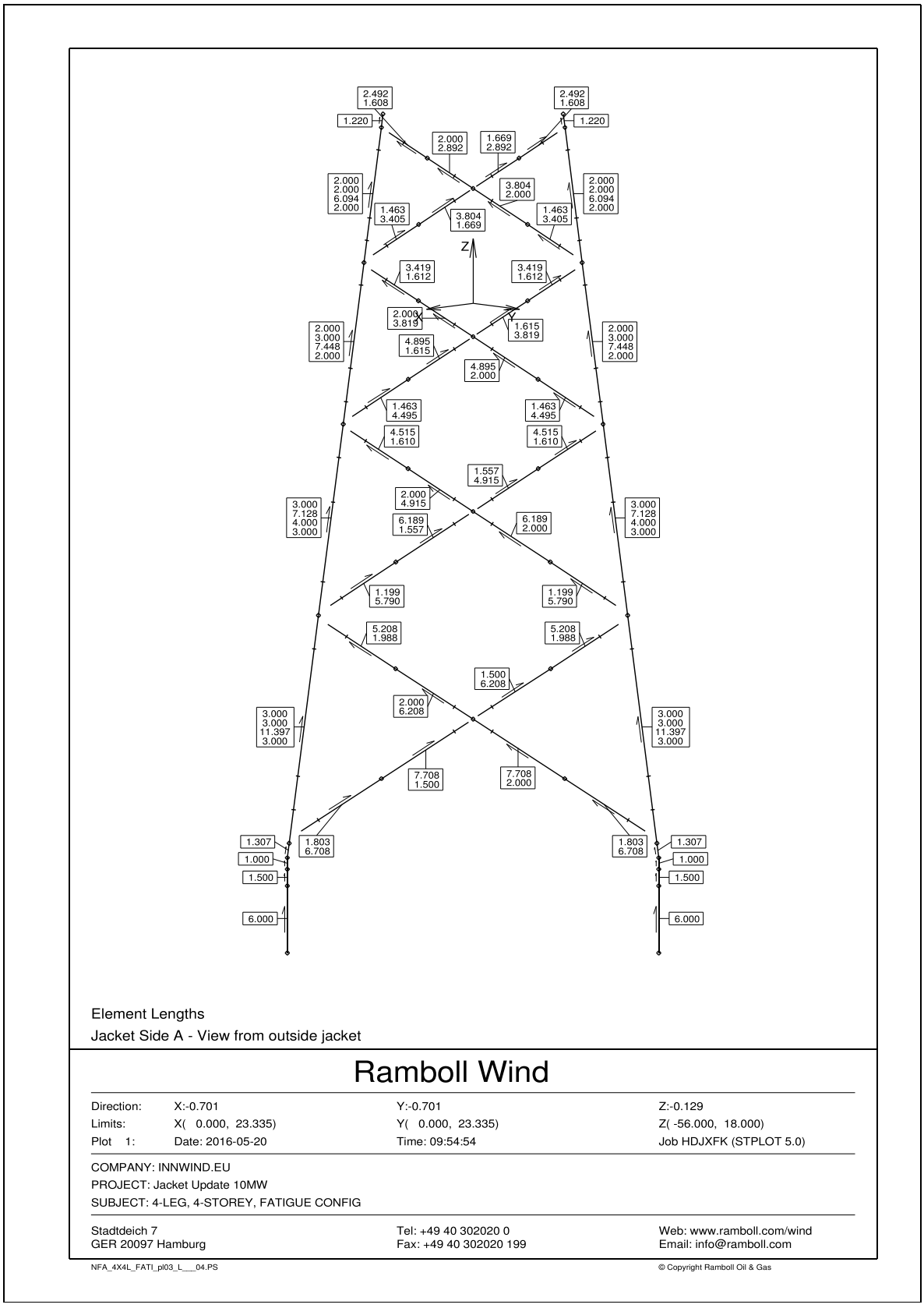

Figure E.9: INNWIND.EU, D4.34, Innovative design of 10MW steel jackets, geometry of jacket - P.8 (Stolpe et al., 2016)

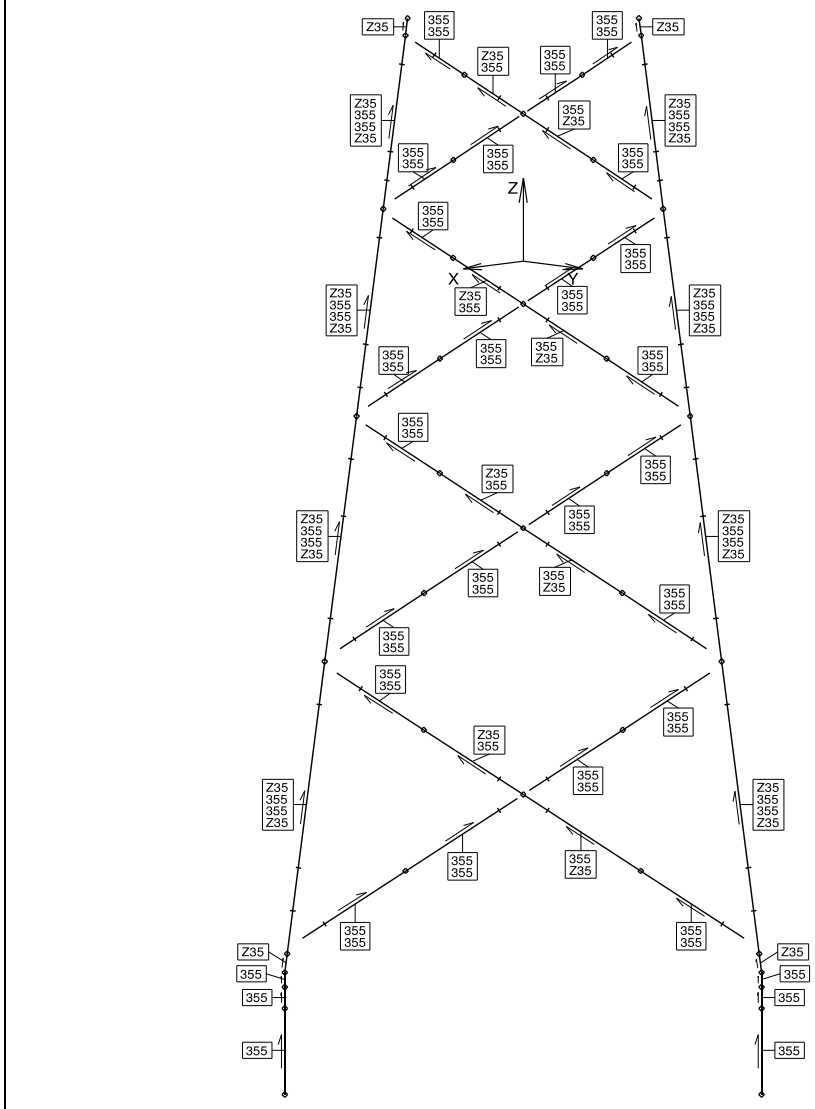

Material Names

Jacket Side A - View from outside jacket

Ramboll Wind

Direction:	X:-0.701	Y:-0.701	Z:-0.129
Limits:	X(0.000, 23.335)	Y(0.000, 23.335)	Z(-56.000, 18.000)
Plot 1:	Date: 2016-05-20	Time: 09:54:55	Job HDJXFK (STPLOT 5.0)

COMPANY: INNWIND.EU
PROJECT: Jacket Update 10MW
SUBJECT: 4-LEG, 4-STOREY, FATIGUE CONFIG

Stadtdeich 7
GER 20097 Hamburg
Tel: +49 40 302020 0
Fax: +49 40 302020 199
Web: www.ramboll.com/wind
Email: info@ramboll.com

NFA_4X4L_FATI_pl03_M___05.PS

F

10MW jacket mode shapes

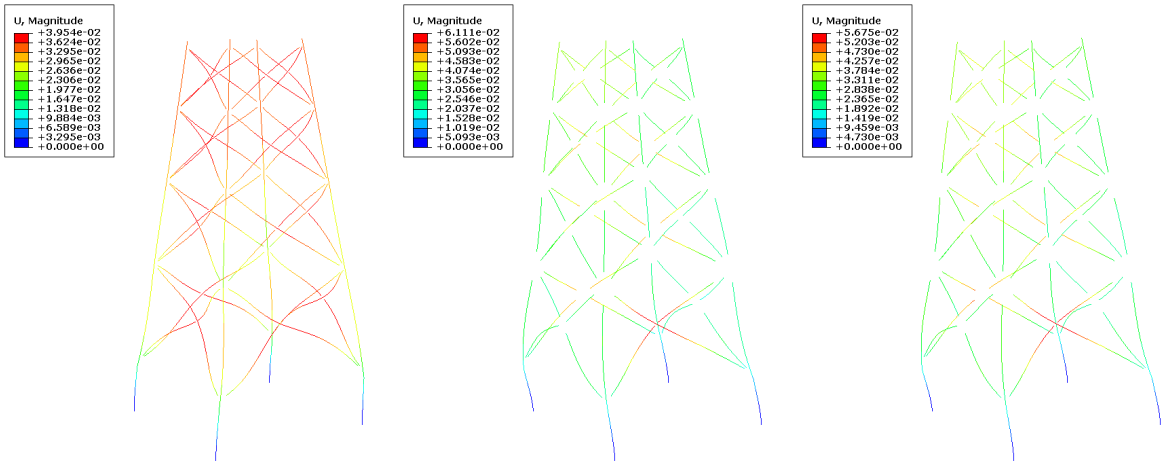

(a) Mode 1 - Rigid **(b)** Mode 1 - Welded **(c)** Mode 1 - Wrapped

Figure F.1: Jacket - Mode 1

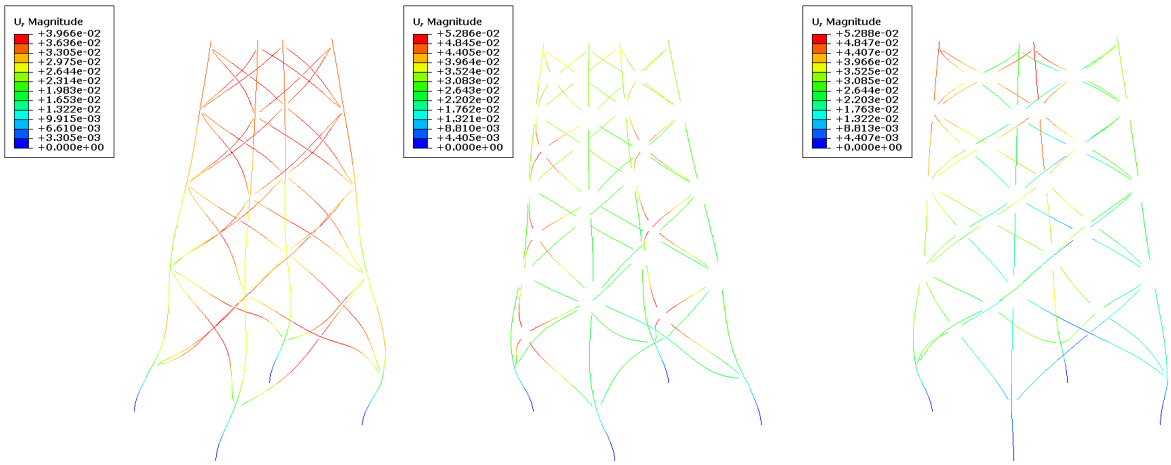

(a) Mode 2 - Rigid **(b)** Mode 2 - Welded **(c)** Mode 2 - Wrapped

Figure F.2: Jacket - Mode 2

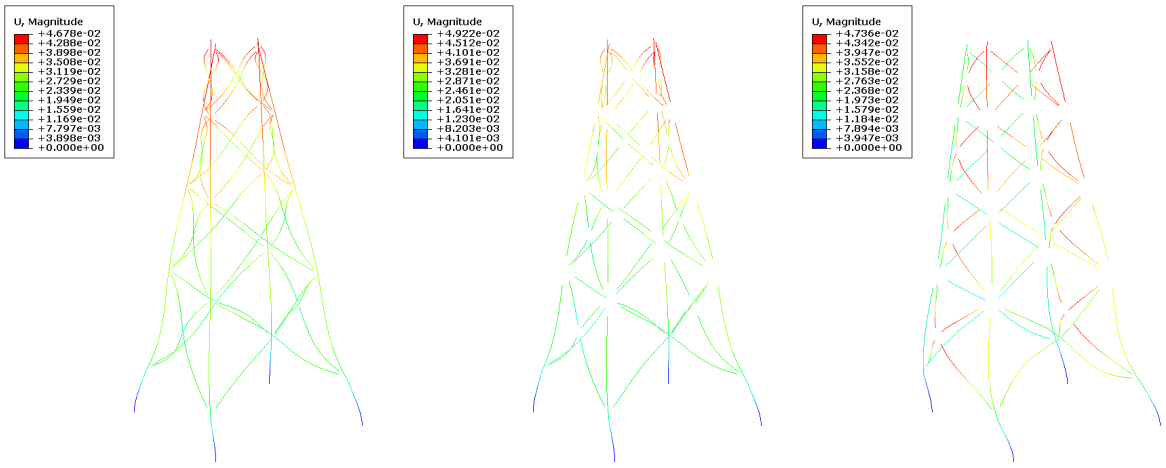

(a) Mode 3 - Rigid **(b)** Mode 3 - Welded **(c)** Mode 3 - Wrapped

Figure F.3: Jacket - Mode 3

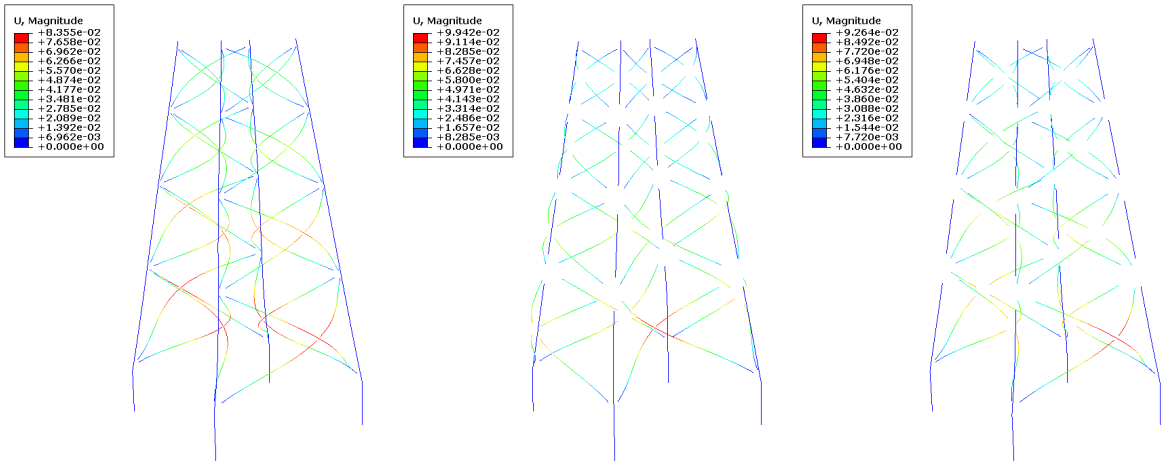

(a) Mode 4 - Rigid **(b)** Mode 4 - Welded **(c)** Mode 4 - Wrapped

Figure F.4: Jacket - Mode 4

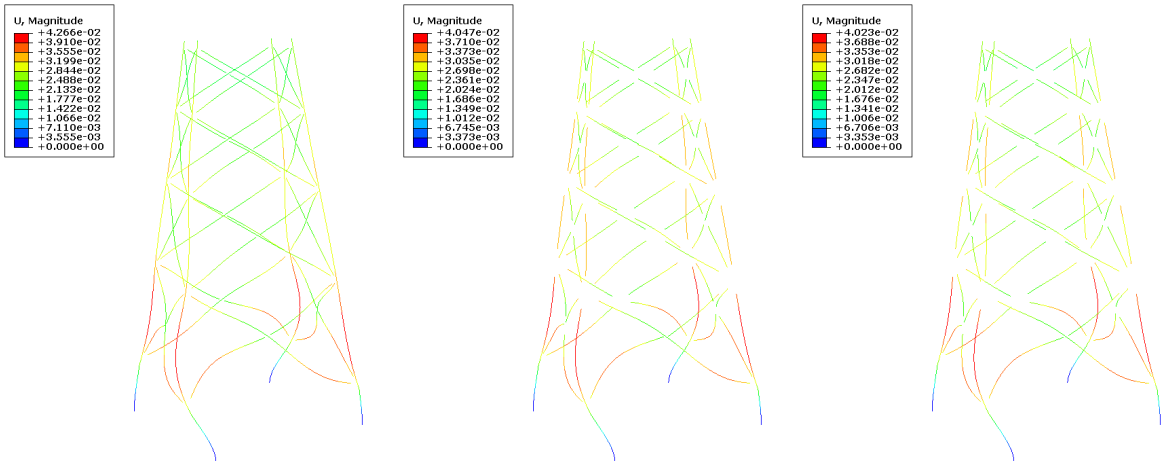

(a) Mode 5 - Rigid **(b)** Mode 5 - Welded **(c)** Mode 5 - Wrapped

Figure F.5: Jacket - Mode 5

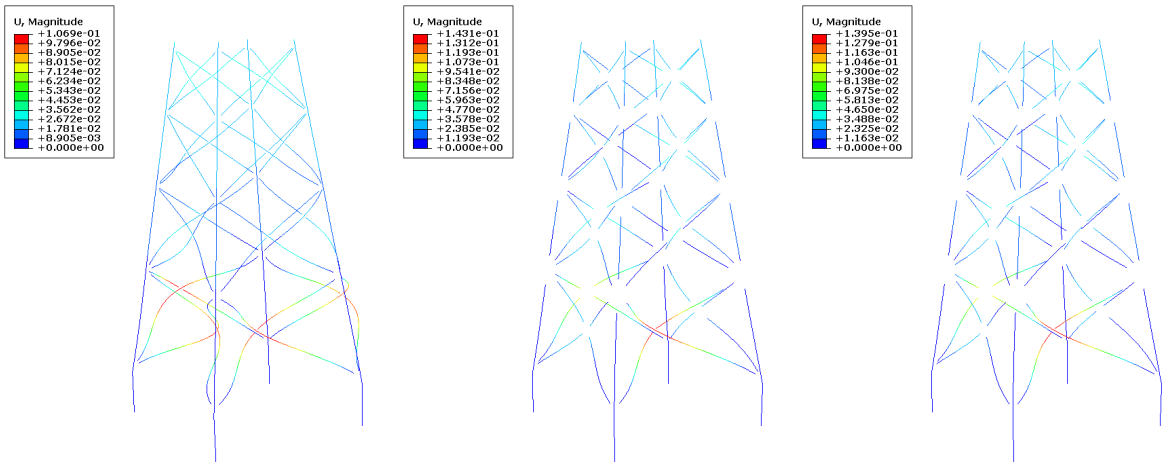

(a) Mode 6 - Rigid **(b)** Mode 6 - Welded **(c)** Mode 6 - Wrapped

Figure F.6: Jacket - Mode 6

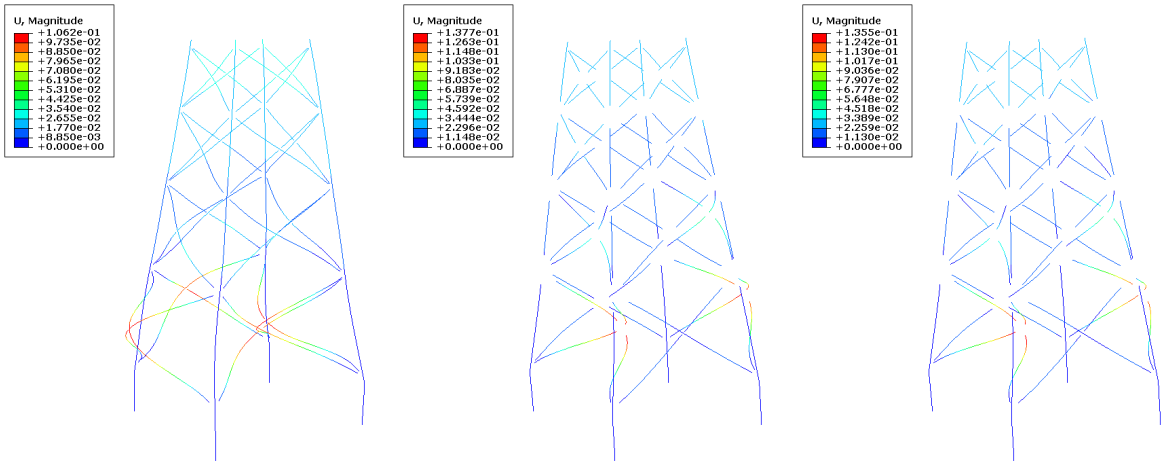

(a) Mode 7 - Rigid **(b)** Mode 7 - Welded **(c)** Mode 7 - Wrapped

Figure F.7: Jacket - Mode 7

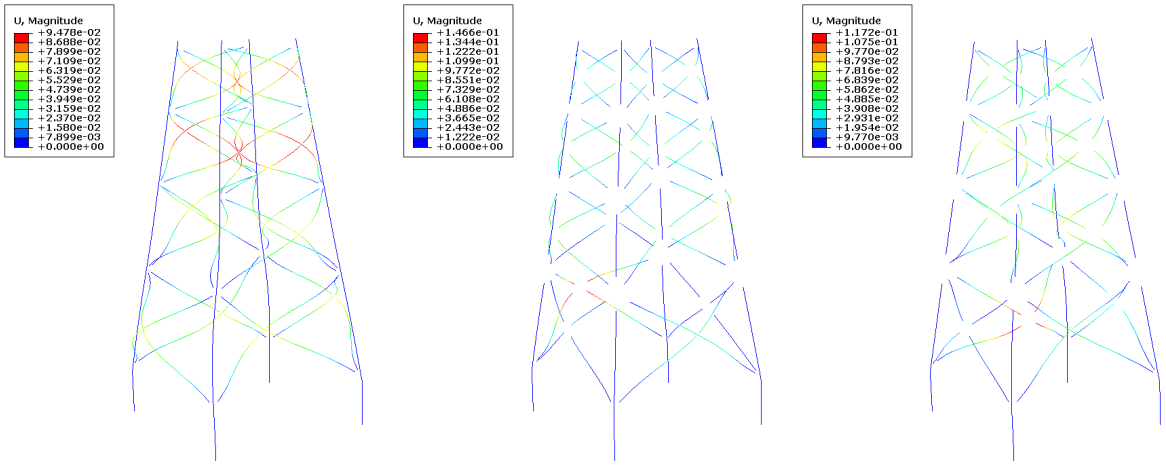

(a) Mode 8 - Rigid **(b)** Mode 8 - Welded **(c)** Mode 8 - Wrapped

Figure F.8: Jacket - Mode 8

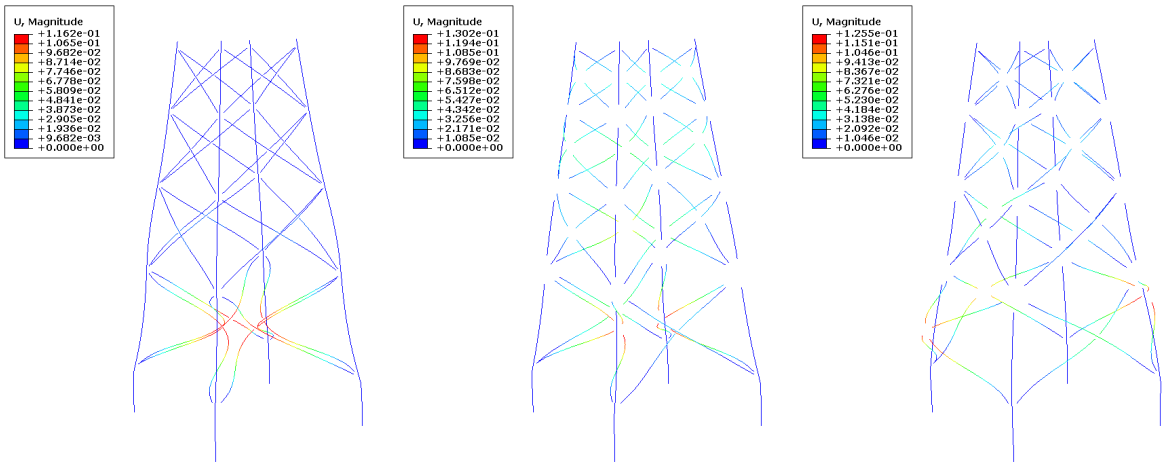

(a) Mode 9 - Rigid **(b)** Mode 9 - Welded **(c)** Mode 9 - Wrapped

Figure F.9: Jacket - Mode 9

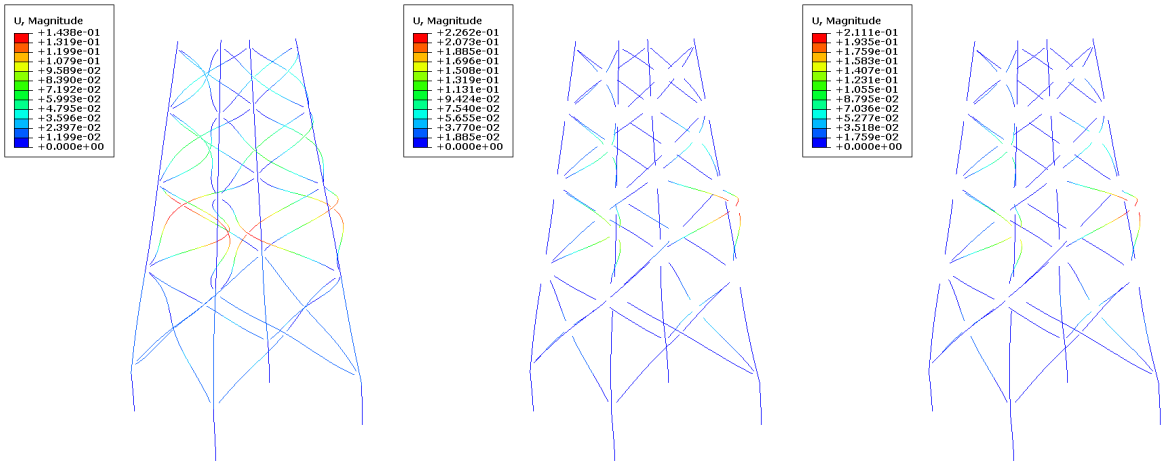

(a) Mode 10 - Rigid **(b)** Mode 10 - Welded **(c)** Mode 10 - Wrapped

Figure F.10: Jacket - Mode 10

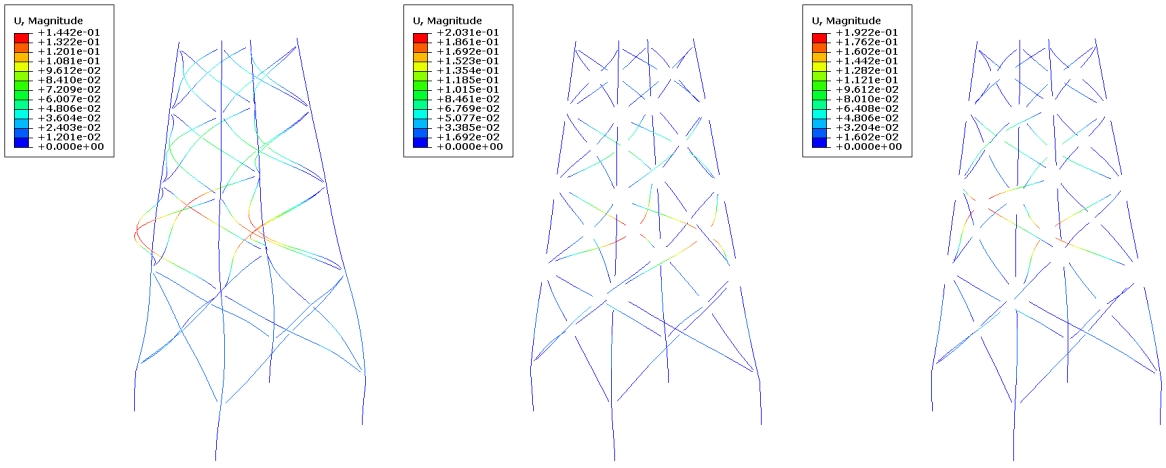

(a) Mode 11 - Rigid **(b)** Mode 11 - Welded **(c)** Mode 11 - Wrapped

Figure F.11: Jacket - Mode 11

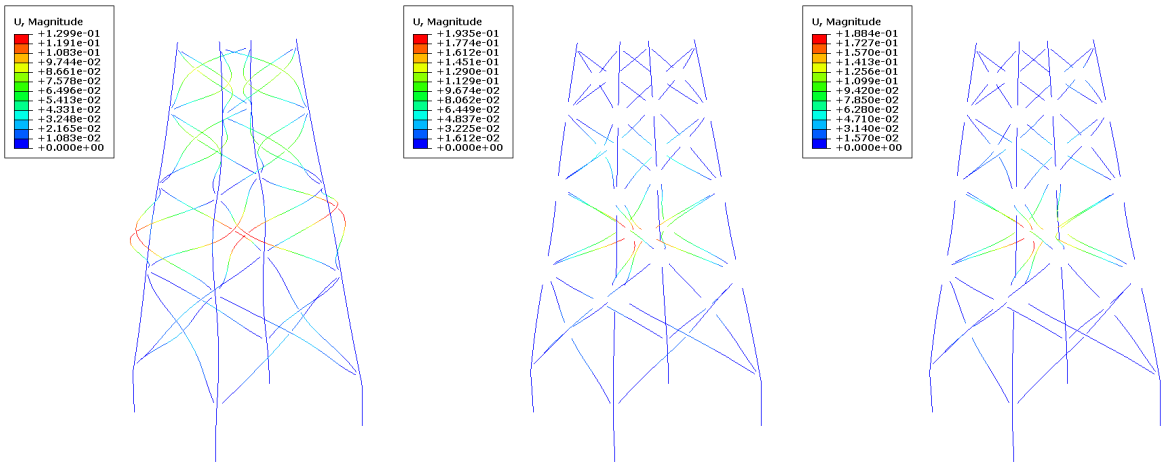

(a) Mode 12 - Rigid **(b)** Mode 12 - Welded **(c)** Mode 12 - Wrapped

Figure F.12: Jacket - Mode 12

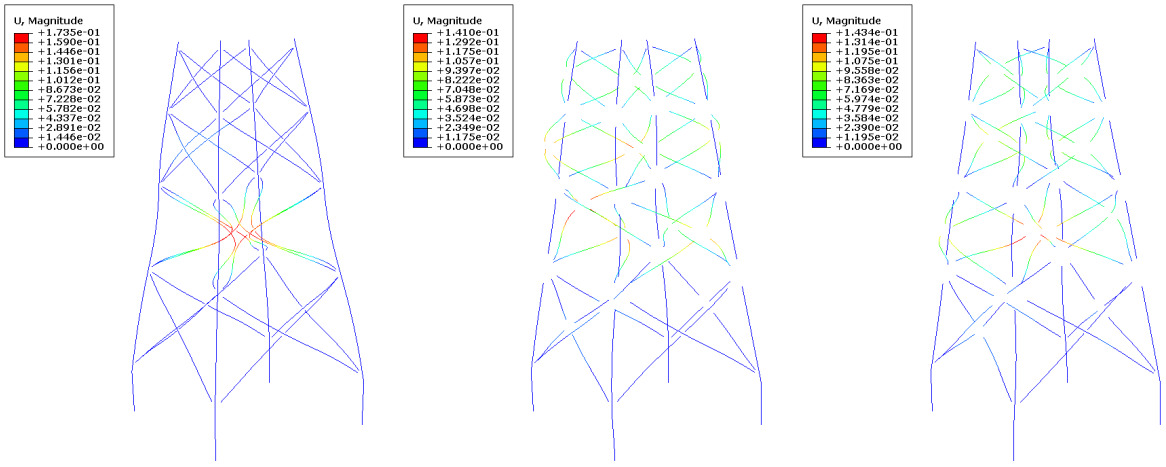

(a) Mode 13 - Rigid **(b)** Mode 13 - Welded **(c)** Mode 13 - Wrapped

Figure F.13: Jacket - Mode 13

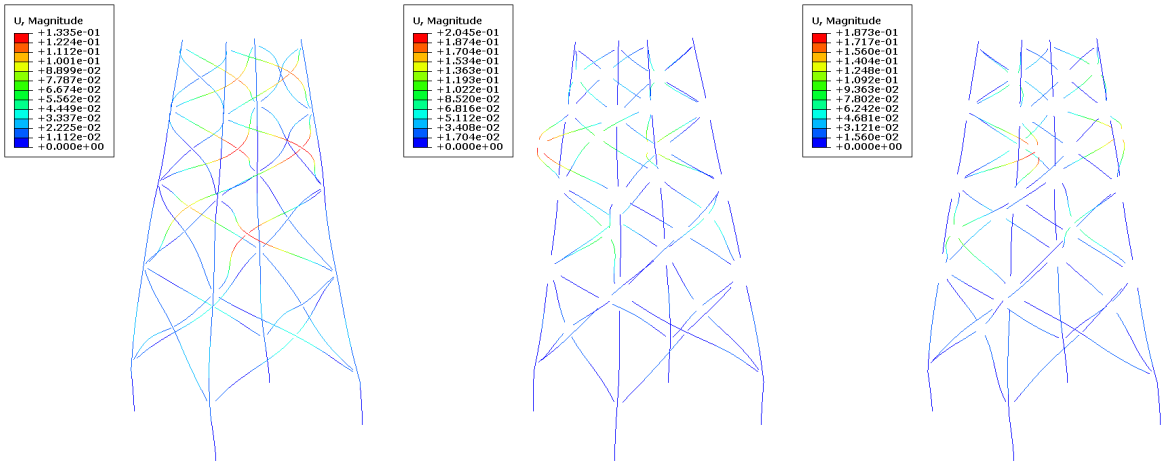

(a) Mode 14 - Rigid **(b)** Mode 14 - Welded **(c)** Mode 14 - Wrapped

Figure F.14: Jacket - Mode 14

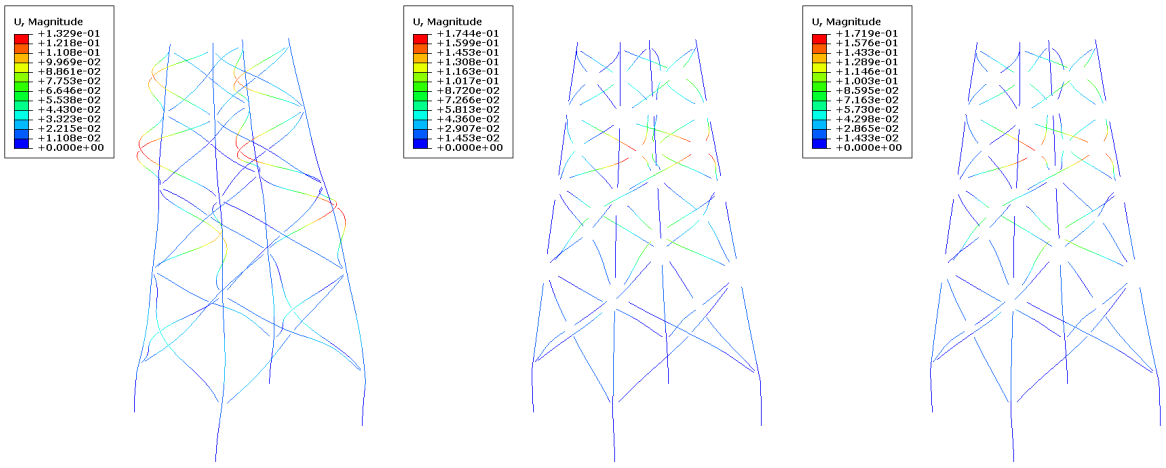

(a) Mode 15 - Rigid **(b)** Mode 15 - Welded **(c)** Mode 15 - Wrapped

Figure F.15: Jacket - Mode 15

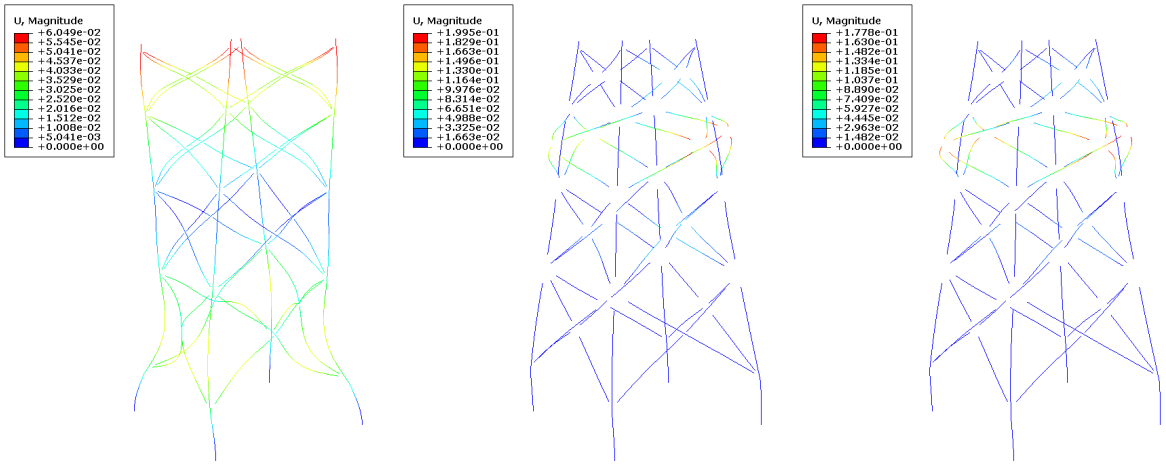

(a) Mode 16 - Rigid **(b)** Mode 16 - Welded **(c)** Mode 16 - Wrapped

Figure F.16: Jacket - Mode 16

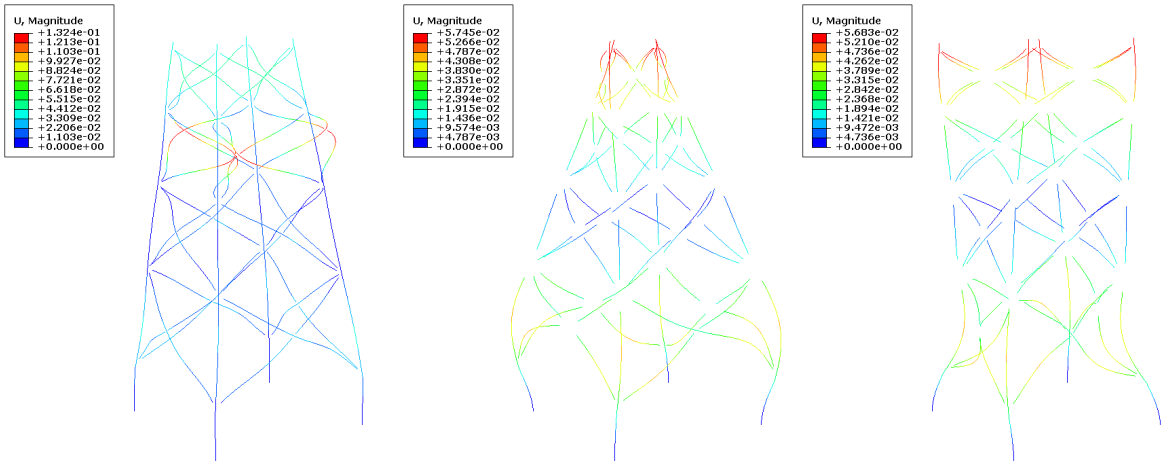

(a) Mode 17 - Rigid **(b)** Mode 17 - Welded **(c)** Mode 17 - Wrapped

Figure F.17: Jacket - Mode 17

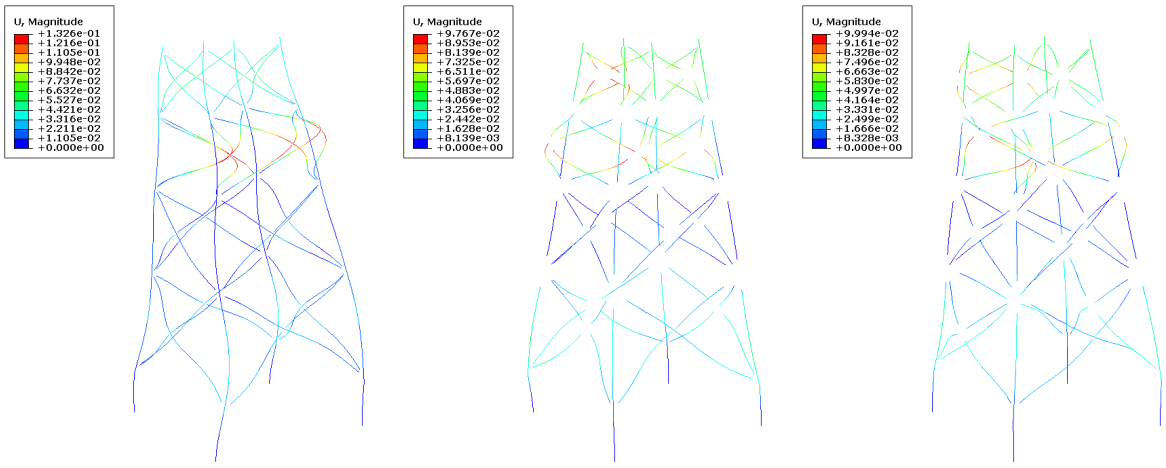

(a) Mode 18 - Rigid **(b)** Mode 18 - Welded **(c)** Mode 18 - Wrapped

Figure F.18: Jacket - Mode 18

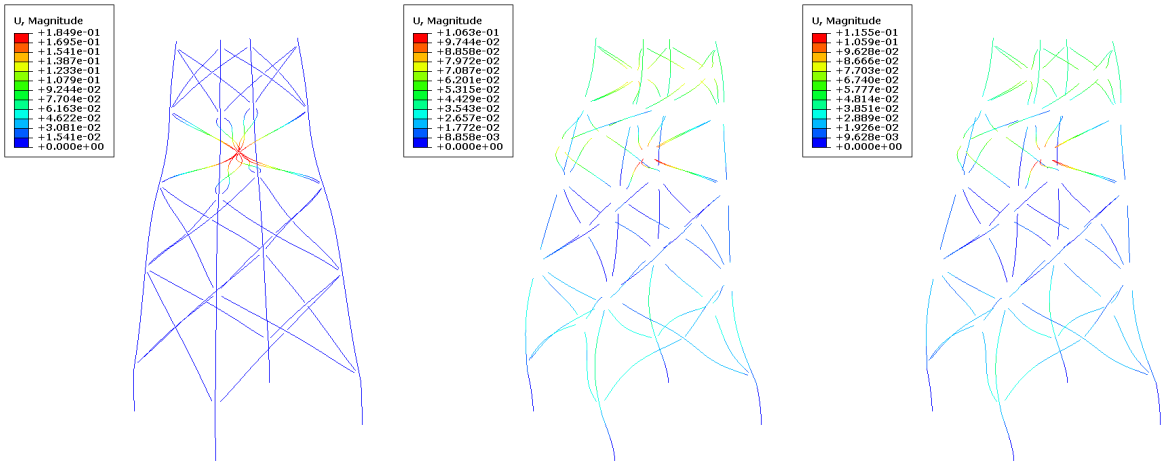

(a) Mode 19 - Rigid **(b)** Mode 19 - Welded **(c)** Mode 19 - Wrapped

Figure F.19: Jacket - Mode 19

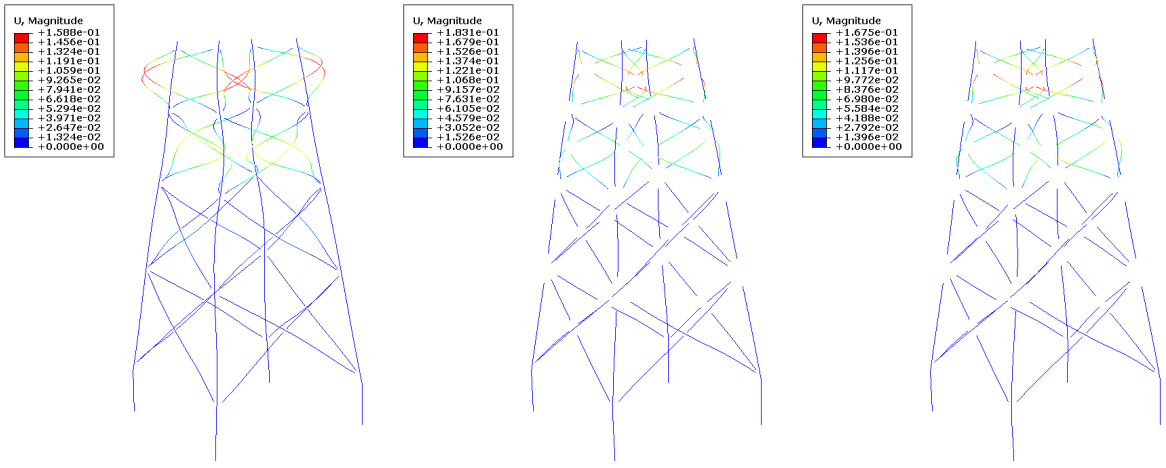

(a) Mode 20 - Rigid **(b)** Mode 20 - Welded **(c)** Mode 20 - Wrapped

Figure F.20: Jacket - Mode 20

G

10MW OWT mode shapes

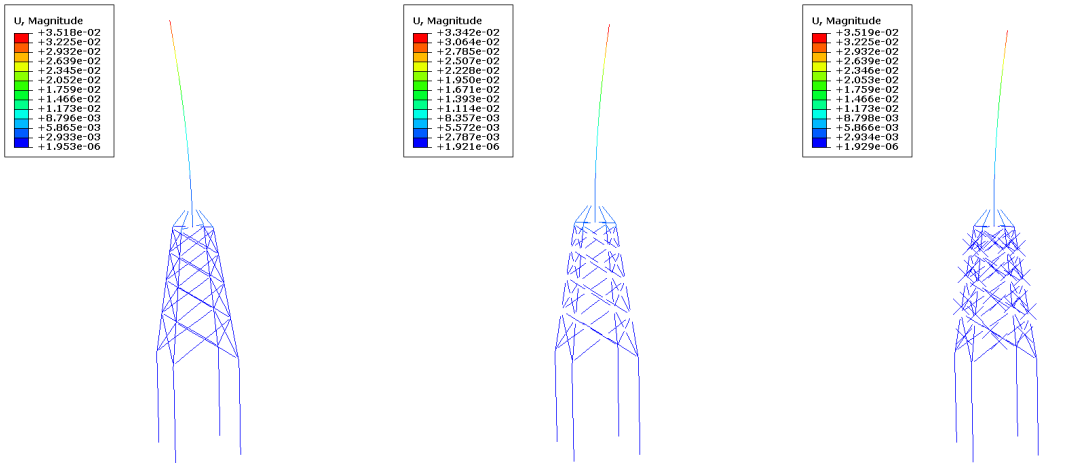

(a) Mode 1 - Rigid **(b)** Mode 1 - Welded **(c)** Mode 1 - Wrapped

Figure G.1: OWT - Mode 1

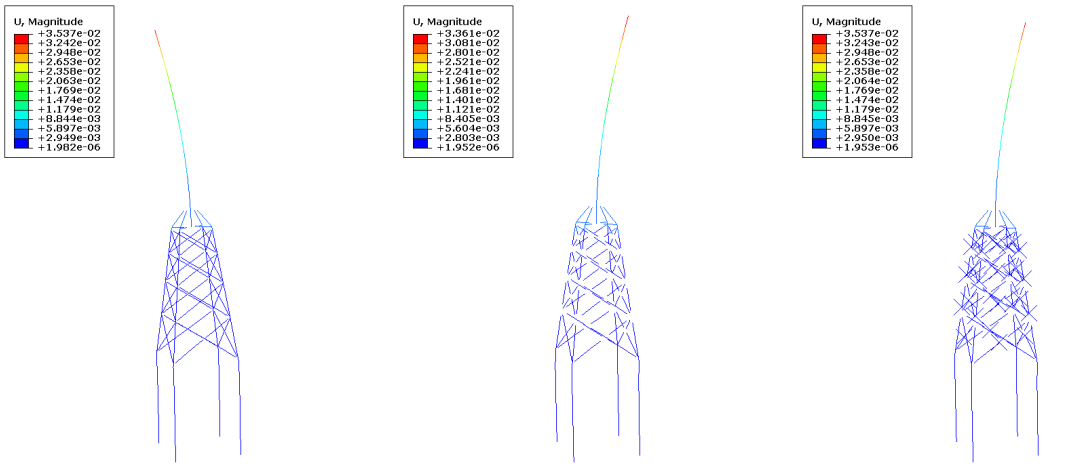

(a) Mode 2 - Rigid **(b)** Mode 2 - Welded **(c)** Mode 2 - Wrapped

Figure G.2: OWT - Mode 2

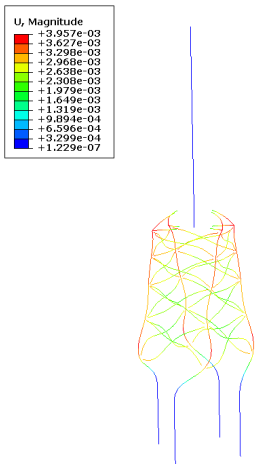

(a) Mode 3 - Rigid

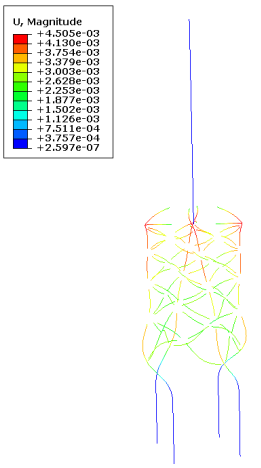

(b) Mode 3 - Welded

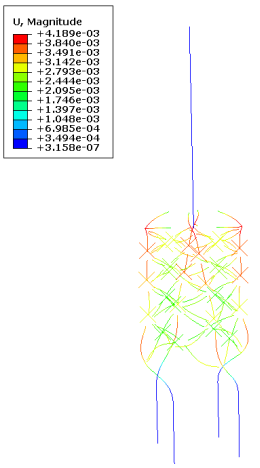

(c) Mode 3 - Wrapped

Figure G.3: OWT - Mode 3

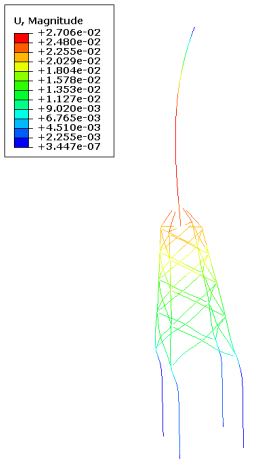

(a) Mode 4 - Rigid

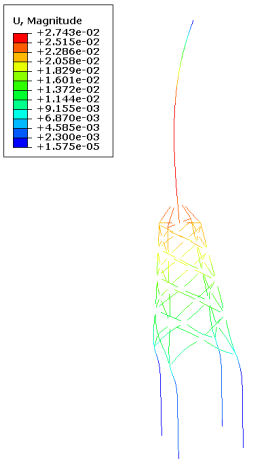

(b) Mode 4 - Welded

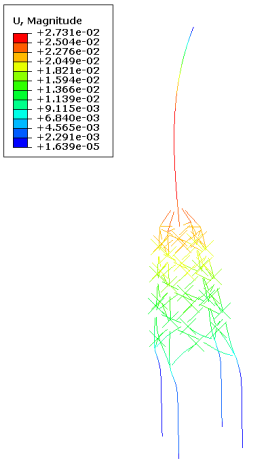

(c) Mode 4 - Wrapped

Figure G.4: OWT - Mode 4

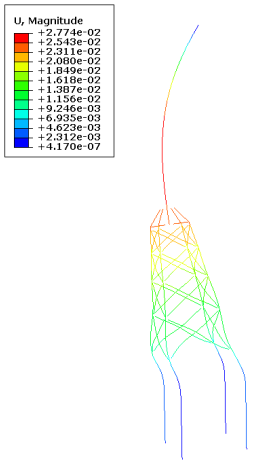

(a) Mode 5 - Rigid

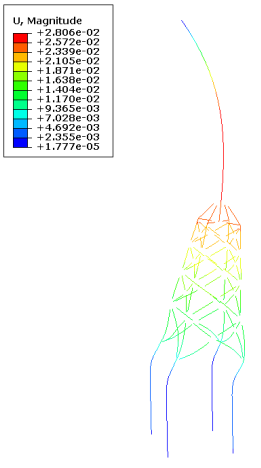

(b) Mode 5 - Welded

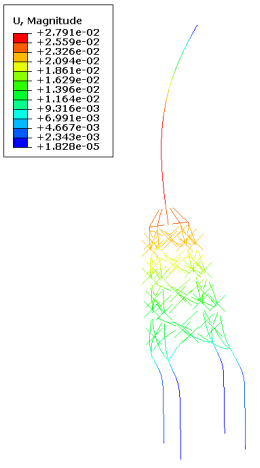

(c) Mode 5 - Wrapped

Figure G.5: OWT - Mode 5

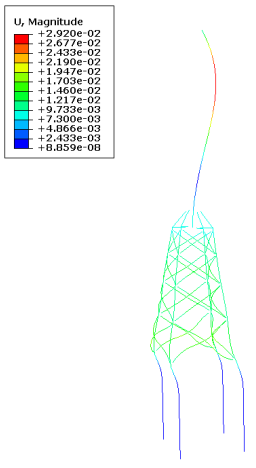

(a) Mode 6 - Rigid

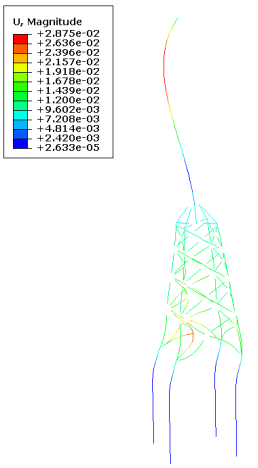

(b) Mode 6 - Welded

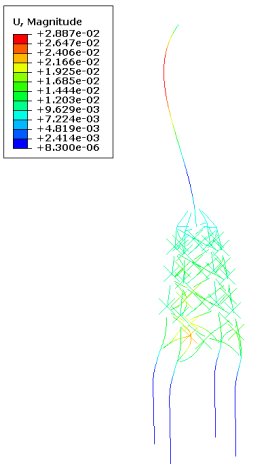

(c) Mode 6 - Wrapped

Figure G.6: OWT - Mode 6

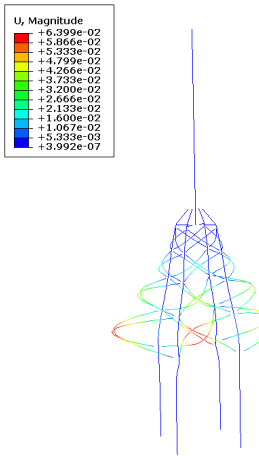

(a) Mode 7 - Rigid

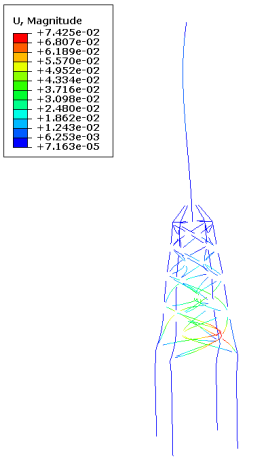

(b) Mode 7 - Welded

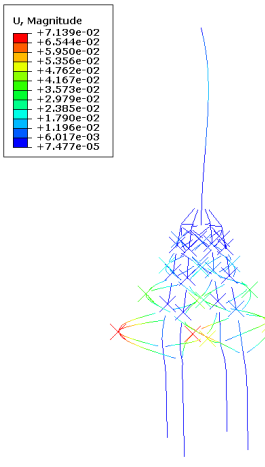

(c) Mode 7 - Wrapped

Figure G.7: OWT - Mode 7

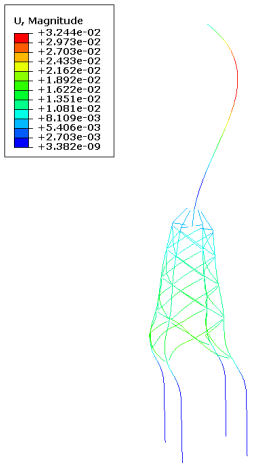

(a) Mode 8 - Rigid

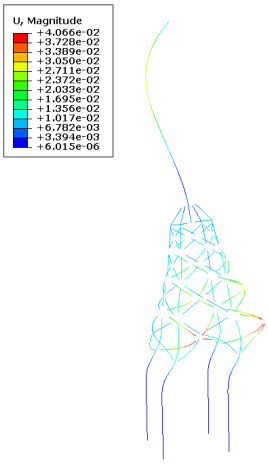

(b) Mode 8 - Welded

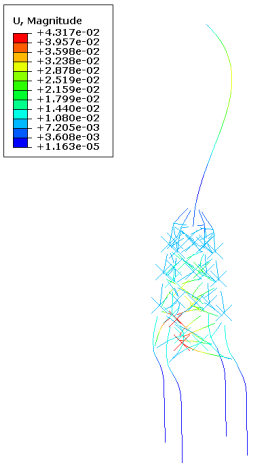

(c) Mode 8 - Wrapped

Figure G.8: OWT - Mode 8

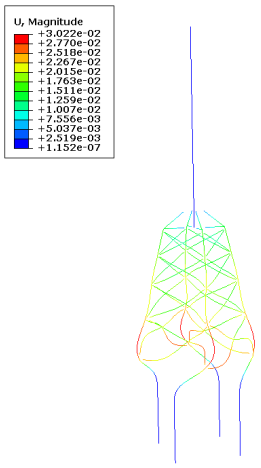

(a) Mode 9 - Rigid

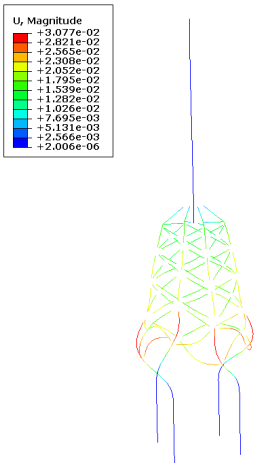

(b) Mode 9 - Welded

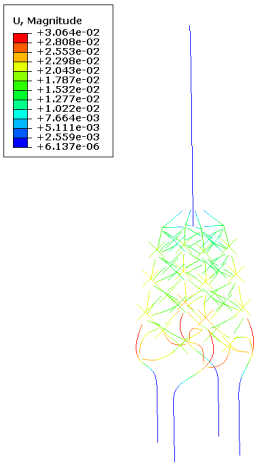

(c) Mode 9 - Wrapped

Figure G.9: OWT - Mode 9

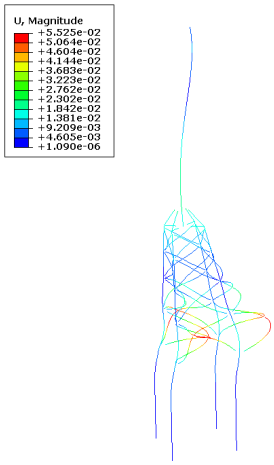

(a) Mode 10 - Rigid

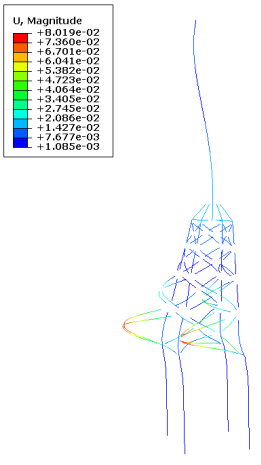

(b) Mode 10 - Welded

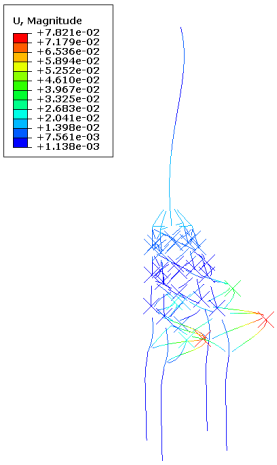

(c) Mode 10 - Wrapped

Figure G.10: OWT - Mode 10

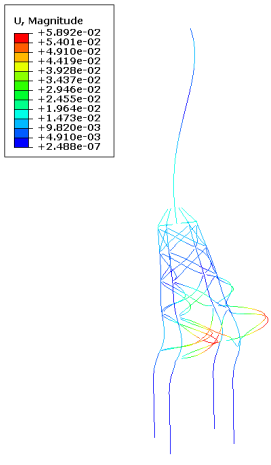

(a) Mode 11 - Rigid

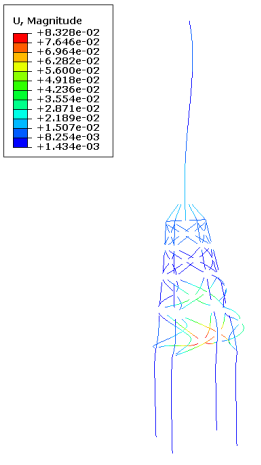

(b) Mode 11 - Welded

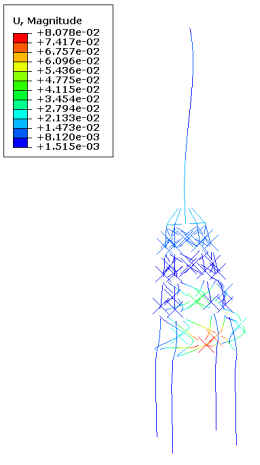

(c) Mode 11 - Wrapped

Figure G.11: OWT - Mode 11

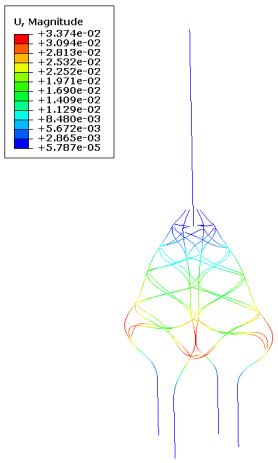

(a) Mode 12 - Rigid

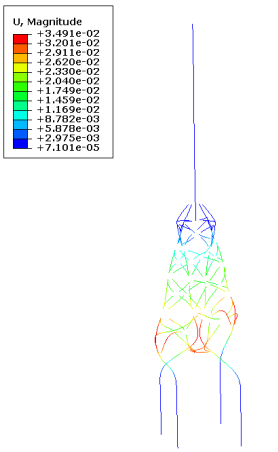

(b) Mode 12 - Welded

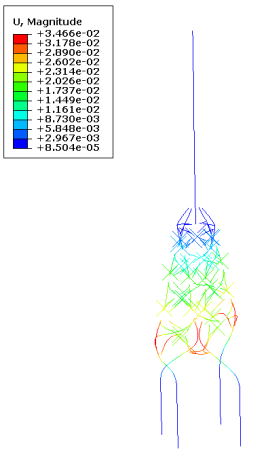

(c) Mode 12 - Wrapped

Figure G.12: OWT - Mode 12

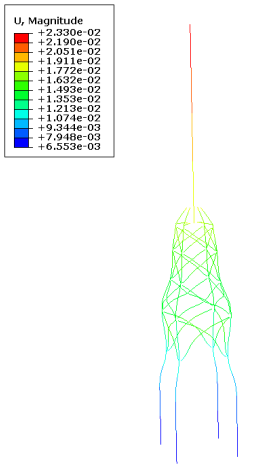

(a) Mode 13 - Rigid

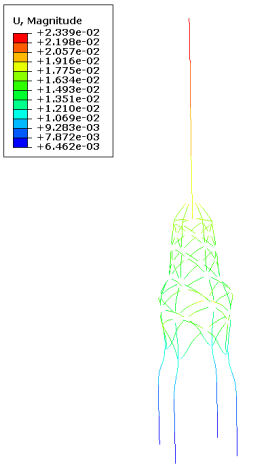

(b) Mode 13 - Welded

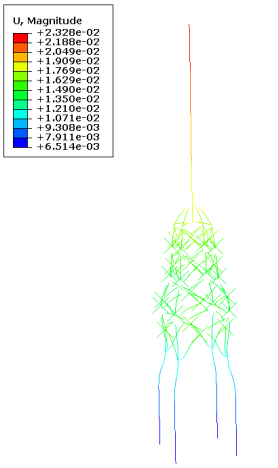

(c) Mode 13 - Wrapped

Figure G.13: OWT - Mode 13

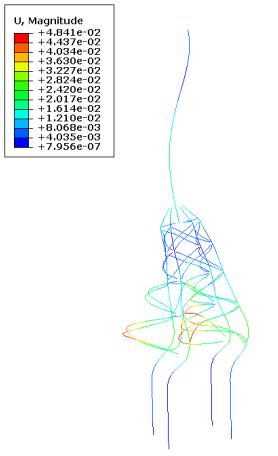

(a) Mode 14 - Rigid

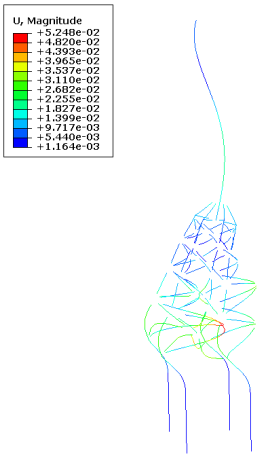

(b) Mode 14 - Welded

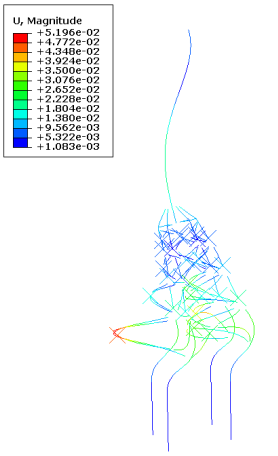

(c) Mode 14 - Wrapped

Figure G.14: OWT - Mode 14

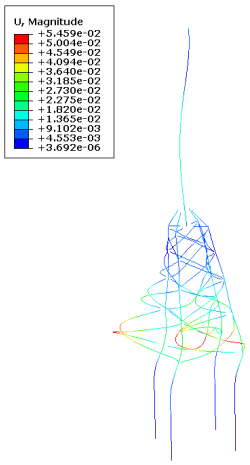

(a) Mode 15 - Rigid

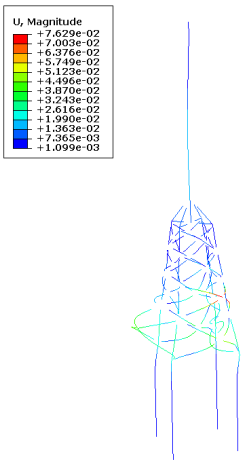

(b) Mode 15 - Welded

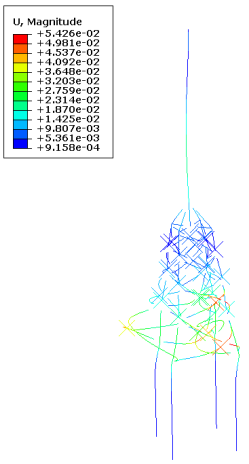

(c) Mode 15 - Wrapped

Figure G.15: OWT - Mode 15

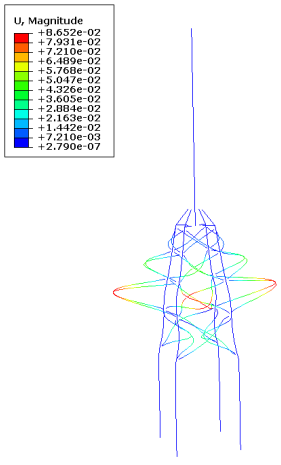

(a) Mode 16 - Rigid

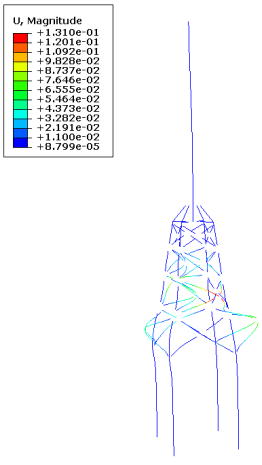

(b) Mode 16 - Welded

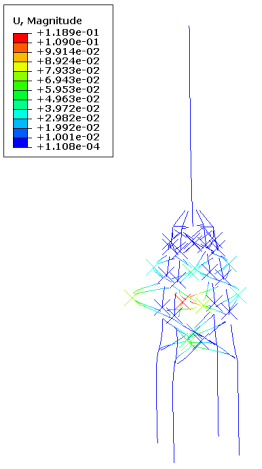

(c) Mode 16 - Wrapped

Figure G.16: OWT - Mode 16

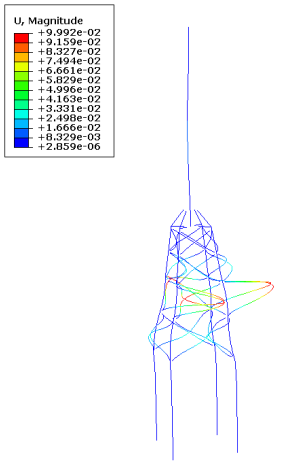

(a) Mode 17 - Rigid

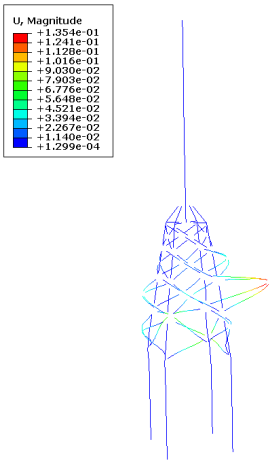

(b) Mode 17 - Welded

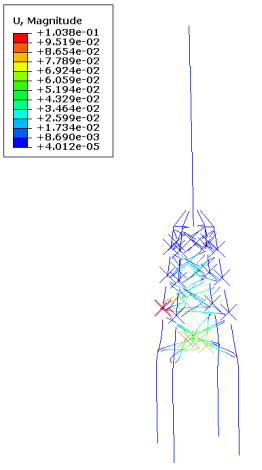

(c) Mode 17 - Wrapped

Figure G.17: OWT - Mode 17

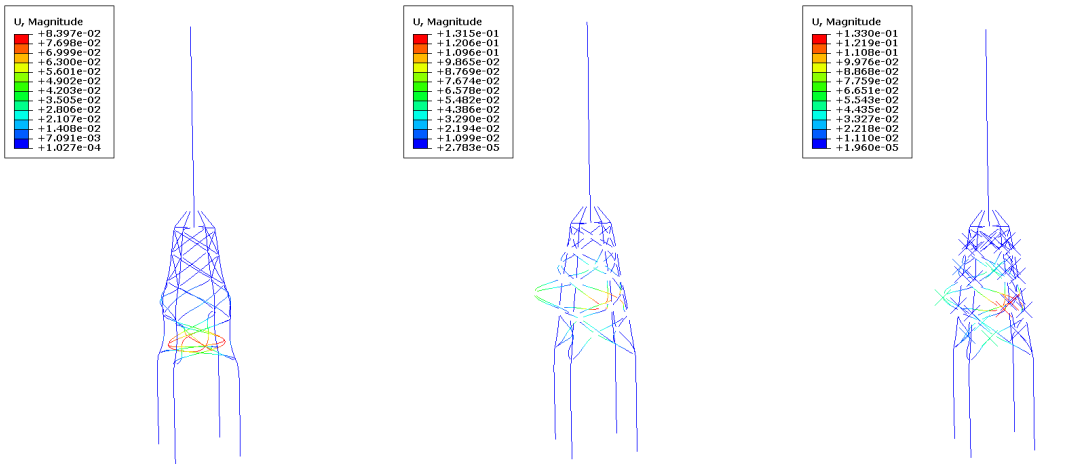

(a) Mode 18 - Rigid **(b)** Mode 18 - Welded **(c)** Mode 18 - Wrapped

Figure G.18: OWT - Mode 18

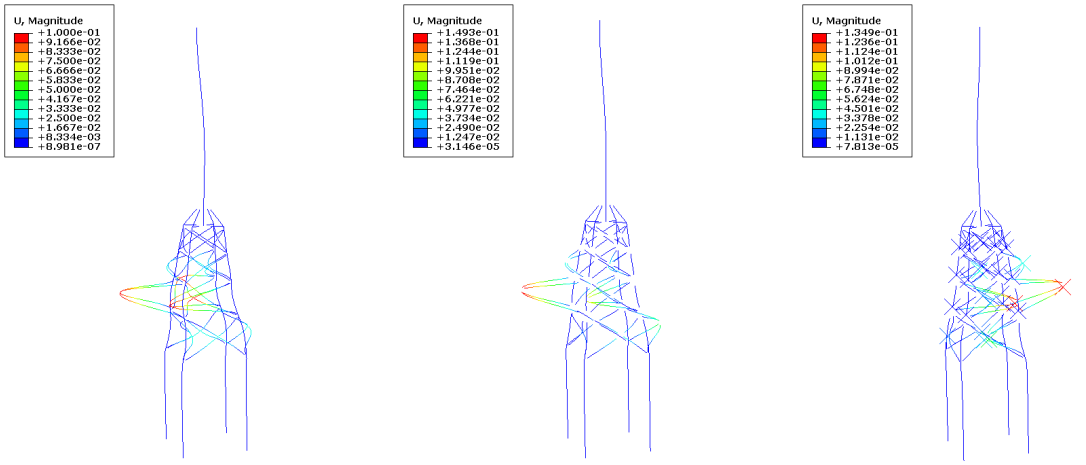

(a) Mode 19 - Rigid **(b)** Mode 19 - Welded **(c)** Mode 19 - Wrapped

Figure G.19: OWT - Mode 19

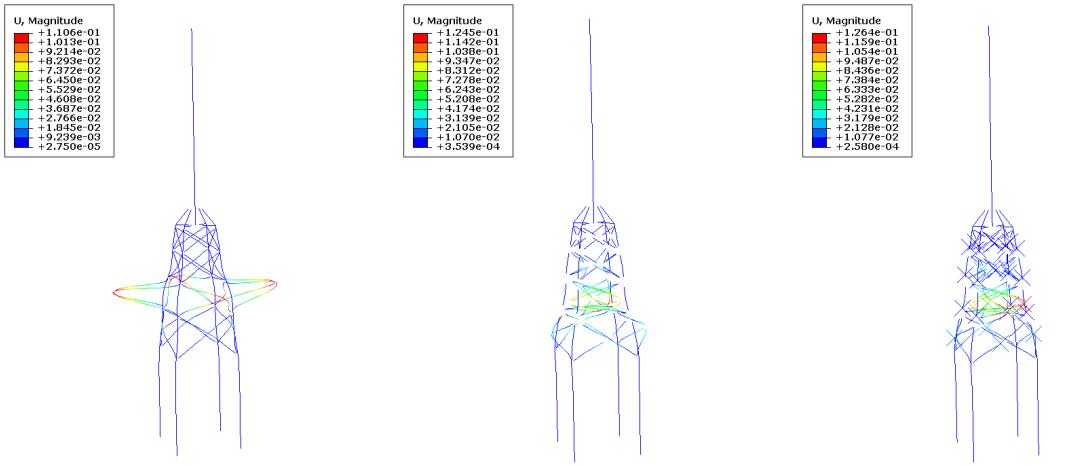

(a) Mode 20 - Rigid **(b)** Mode 20 - Welded **(c)** Mode 20 - Wrapped

Figure G.20: OWT - Mode 20